Microwave Remote Sensing Center

13th Specialist Meeting on Microwave Radiometry and Remote Sensing of the Environment

Pasadena, California

March 24-27, 2014

Final Program

Welcome to MicroRad 2014 in Pasadena!

On behalf of the Local Organizing Committee and the Scientific and Steering Committee, we are very pleased to welcome you to the 13th Specialist Meeting on Microwave Radiometry and Remote Sensing Applications, MicroRad 2014, in Pasadena, California. MicroRad is the latest in a series of specialist meetings held every 2 years since their inception in Rome in 1983.

The purpose of this meeting is to provide an open forum to report and discuss recent advances in microwave radiometry. MicroRad is a unique gathering where the microwave radiometry community has an opportunity to present new designs, research results, technological advances and unique innovations in the field of passive microwave remote sensing. The meeting will cover wide radiometry applications and fields such as soil moisture, ocean salinity, cryosphere, ocean dynamics, sounding, radiometer calibration, radio frequency interference issues and new technologies.

The MicroRad 2014 Call for Papers generated a very large response of 167 abstracts. As is the tradition of MicroRad, we will have a single track of oral sessions along with interactive sessions during the week. The papers were peer reviewed and organized into 16 oral sessions with 83 papers and 10 interactive sessions with 79 papers. We organized the technical topics over the week so that attendees will find topics directly related to their research spread over the entire meeting. In an attempt to place interactive papers in the center of the technical discussion, the MicroRad 2014 poster sessions are scheduled within two hour interactive sessions placed between the afternoon oral half sessions on Tuesday and Wednesday of the conference. Additionally, the coffee breaks and lunches will be held in the vicinity of the posters allowing for extended informal discussions. The long morning and afternoon breaks, along with the evening social events planned, will provide an opportunity to catch up with colleagues.

We hope you will find the depth and diversity of the MicroRad 2014 technical program very representative of the current art. Passive Microwave Radiometry is experiencing an unprecedented period with two major missions concentrating on L-band on-orbit, the recent launch of the Global Precipitation Measurement Mission, and the Global Change Operational Monitoring Mission. Microwave radiometers continue to observe every part of the globe multiple times a day providing critical measurements for weather forecasting, and climate studies. Still, we await the completion and launch of several more observing systems including the Soil Moisture Active Passive mission and MetOp Second Generation. In light of a growing and diverse specialty, our goal for MicroRad this year were not focused on building a program following the basic structure of our major space-based missions, but rather to address technical topics from a combined mission and research point of view. We hope that you find we have achieved our goals and that this approach also provides value in your experience at MicroRad.

Authors are encouraged to submit papers to the proceedings via the MicroRad 2014 website. The deadline for submitting a proceedings paper is April 14, 2014. In addition to the conference proceedings that will be available after the conference, there will be a Special Issue of the IEEE Journal of Selected Topics in Applied Earth Observations and Remote Sensing (JSTARS) for MicroRad 2014. The JSTARS Special Issue is open to all contributions in the field of microwave radiometry, with primary interest in MicroRad topics.

We would like to express our gratitude to the MicroRad 2014 local organizing committee, the scientific and steering committee and all session co-chairs for their assistance in the planning and execution of MicroRad. We gratefully acknowledge the support and cooperation of the IEEE Geoscience and Remote Sensing Society (GRSS), the California Institute of Technology, the Jet Propulsion Laboratory and the CeTeM.

In closing, we would also like to recognize the efforts of the reviewers appearing below and thank them for their contributions to MicroRad 2014. Their reviews, scoring and insightful comments provided a strong basis for organization of this meeting. We hope you enjoy your visit to Pasadena and your participation in MicroRad 2014!

We wish you an enjoyable and productive MicroRad 2014 in Pasadena, CA!

Best Regards,

Shannon Brown
General Chair, MicroRad 2014

David Kunkee
Technical Chair, MicroRad 2014

Organizing Committee

Shannon Brown (General Chair), Jet Propulsion Laboratory, CalTech, USA
David Kunkee (Technical Chair), Aerospace Corporation, USA
Sidharth Misra, Jet Propulsion Laboratory, CalTech, USA
Boon Lim, Jet Propulsion Laboratory, CalTech, USA
Andreas Colliander, Jet Propulsion Laboratory, CalTech, USA
Sharmila Padmanabhan, Jet Propulsion Laboratory, CalTech, USA
Alan Tanner, Jet Propulsion Laboratory, CalTech, USA
Todd Gaier, Jet Propulsion Laboratory, CalTech, USA
Simon Yueh, Jet Propulsion Laboratory, CalTech, USA
Eni Njoku, Jet Propulsion Laboratory, CalTech, USA

Scientific Committee

Paolo Ferrazzoli, Tor Vergata University of Rome, Italy
Leila Guerriero, Tor Vergata University of Rome, Italy
Roger Lang, The George Washington University, USA
David LeVine, NASA Goddard Space Flight Center, USA
Giovanni Macelloni, IFAC-CNR, Italy
Frank Marzano, La Sapienza University of Rome, Italy
Simonetta Paloscia, IFAC-CNR, Italy
Paolo Pampaloni, IFAC-CNR, Italy
Nazzareno Pierdicca, La Sapienza University of Rome, Italy
Steven Reising, Colorado State University, USA
Domenico Solimini, Tor Vergata University of Rome, Italy
Calvin T. Swift, University of Massachusetts, USA
Jothiram Vivekandanan, NCAR, Boulder, USA
Ed R. Westwater, University of Colorado, USA

Reviewers

Bill Blackwell, MIT LL
Shannon T. Brown, NASA Jet Propulsion Lab
Adriano Camps, Universitat Politecnica de Catalunya
Andreas Colliander, JPL
Chris Derksen, Environment Canada
Dara Entekhabi, MIT
Todd Gaier, Jet Propulsion Laboratory
Peter Gaiser, Naval Research Laboratory
Martti Hallikainen, Aalto University
Ye Hong, The Aerospace Corporation
Brian Hornbuckle, Iowa State University
Keiji Imaoka, Japan Aerospace Exploration Agency
Gail Jackson, NASA Goddard Space Flight Center
Thomas Jackson, ARS USDA HRSL
Joel Johnson, The Ohio State University
Yann Kerr, Centre d'Etudes Spatiales de la Biosphère
Ed Kim, NASA Goddard Space Flight Center
David B. Kunkee, The Aerospace Corporation
Roger Lang, George Washington University
David Le Vine, Goddard Space Flight Center
Boon Lim, Jet Propulsion Laboratory
Giovanni Macelloni, IFAC-CNR
Darren McKague, University of Michigan
Sidharth Misra, JPL
Eni Njoku, Jet Propulsion Laboratory
Sharmila Padmanabhan, JPL
Paolo Pampaloni, Institute of Applied Physics National research Council
Jeffrey Piepmeier, NASA's Goddard Space Flight Center
Nazzareno Pierdicca, Sapienza University of Rome
Paul Racette, NASA Goddard Space Flight Center
Niels Skou, Technical University of Denmark
Steve Swadley, Naval Research Laboratory
Calvin Swift, University of Massachusetts
Alan Tanner, JPL
Leung Tsang, University of Washington
Fuzhong Weng, NOAA/NESDIS/Center for Satellite Applications and Research
Simon Yueh, JPL

The official address of Caltech is 1200 East California Boulevard
Pasadena, CA 91125

The campus is between Del Mar Blvd and California Blvd to the north and south and Wilson Ave and Hill Ave to the east and west.

By foot: Pasadena is very accessible by foot, particuarly from the hotels near Old Town Pasadena and those along Colorado Blvd. Caltech can be reached by foot in less than 30 minutes from most of the hotels in Pasadena.

By car: Those with cars may wish to drive to Caltech. Parking is available for a daily fee. Parking at Caltech is described in more detail below.

By bus: The Pasadena ARTS allows low-cost access throughout the city and to JPL (end of line 52). Although, the bus to JPL only runs once in the morning and once in the afternoon.

ARTS Link: http://cityofpasadena.net/Transportation/Arts_Routes_and_Schedules/

The 10 bus accesses Caltech via Del Mar Blvd.

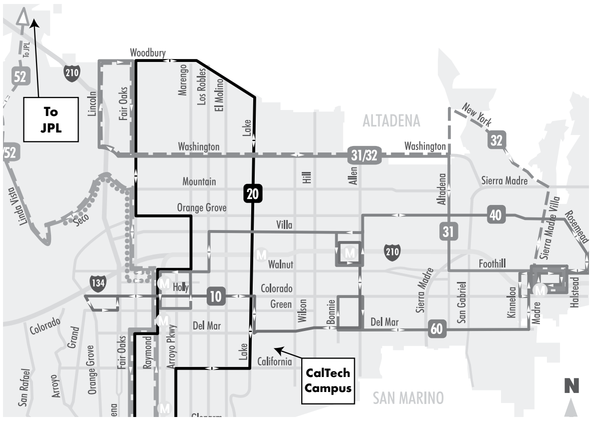

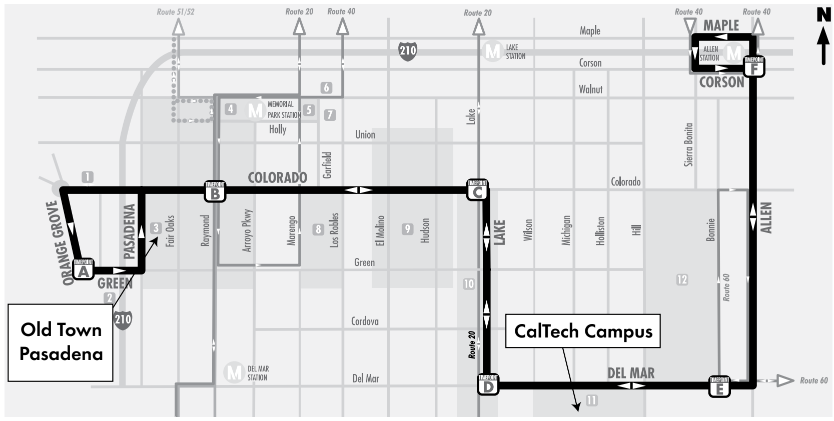

To arrive at the meeting location by 8am from the hotels near Old Town, one will need to catch the 7:15 or 7:40 am bus.

There are several buses that will return you to the Old Town area. Note, the last bus leaving Caltech departs at 7:50 pm.

Parking

The most convienient parking lot to the conference venue is the lot off of California Blvd indicated on the maps on the back cover of this publication and shown below. Other parking lots are off of Wilson Ave. Parking at the structure or lots requires parking permits that can be obtained at automated pay stations. Parking rates vary from $2 an hour, to $6 a day or $18 per week. The automatic pay stations accept cash or credit card. The permits obtained from the automatic pay stations should be placed on the dashboard of the car.

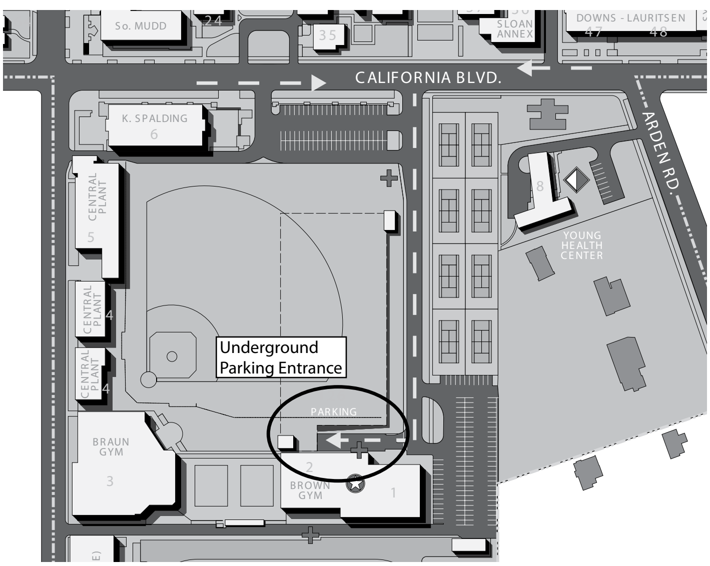

Venue

Oral Session

The oral sessions will be in Ramo Auditorium, located at building number 77 (see map on back page.) The entrance to the auditorium is indicated by the red circle. Presenters should load their presentation onto the computer at the lectern on the stage. Presentations before lunch should be loaded prior to the first session of the day. Presentations after lunch can be loaded in the morning or during the lunch break.

Poster Session

The poster session will take place in Dabney Hall adjacent to the Ramo Auditorium. Dabney Hall is located at building number 40 (see map on back page) and the entrance indicated by the red circle. The easiest way to get into Dabney Hall is to proceed through the garden and enter through one of the four double doors that open onto the garden.

Authors are requested to attend their poster during the official Poster Session time. Posters can also be viewed informally during the coffee breaks. Authors in the Tuesday session are asked to hang their posters by Monday afternoon and remove them by Wednesday morning. Authors in the Wednesday session are asked to hang them by lunch time on Wednesday and remove them by Thursday afternoon. Material for mounting the posters will be available at the registration desk.

Following the tradition of MicroRad, the best posters will receive a prize. A specific committee is be responsible for the evaluation.

Lunches and Coffee Breaks

Lunches and coffee during breaks are included with the conference registration. All lunches and coffee breaks will take place in Dabney Gardens adjacent to the poster hall.

Special Events

March 24: Opening Reception

An opening reception will be held in the Dabney Gardens directly after the last oral session of the day. The event will feature local cuisine along with wine and other beverages. The opening reception is open to everyone that has registered for MicroRad.

March 26: MicroRad Banquet

The MicroRad banquet will be held at the Athenaeum, located at building number 61 on the map (see map on back page) and circled in red. The event will be inside the Athenaeum in the Main Lounge and take place on March 26. A wine reception will be held in the Main Lounge prior to dinner. The banquet will include the world famous prime rib buffet, featuring a carving station, a selection of salads, sea food selection, bread and a desert bar. Wine and non-alcoholic beverages will also be included. The Golden Florin award will be presented at the banquet. The banquet requires a ticket which costs $60. A ticket can be purchased at the registration desk until the event sells out.

March 28: JPL Lab Tour

The JPL tour will take place on Friday, March 28 starting at 8:30 am and is open to those that previously registered for it. You should plan to arrive at JPL by 8:15 am. Due to JPL security restrictions, we cannot accept any additional registrants during the week. Visitor parking is available free of charge at JPL. The JPL tour includes a multimedia presentation on JPL entitled "Journey to the Planets and Beyond," which provides an overview of the Laboratory's activities and accomplishments a visit to the von Karman Visitor Center, the Space Flight Operations Facility, the Spacecraft Assembly Facility, and MicroRad delegates will have a unique opportunity to view the SMAP (Soil Moisture Active Passive) radiometer mission in final stages of integration.

JPL requires that all U.S. citizens, 18 years of age or older, present official, government issued photo identification (driver's license or passport) before being allowed entry. All non-U.S. Citizens 18 years of age or older must present a passport or resident visa (green card) before being allowed entry. Individuals without proper identification will not be admitted to the Laboratory. Please be advised that tours involve a considerable amount of walking and stair climbing. Wheelchair access can be accommodated with advance notice, however wheelchairs cannot be provided. Cameras are permitted on the facility.

Monday, March 24

07:00 - 08:15	Registration / Check-in	Ramo Auditorium, Bldg 77
08:15 - 08:30	Opening Remarks	Ramo Auditorium, Bldg 77
08:30 - 10:10	Soil Moisture and Vegetation	Ramo Auditorium, Bldg 77
10:10 - 10:40	Coffee Break	Dabney Gardens
10:40 - 12:20	Instruments and Techniques	Ramo Auditorium, Bldg 77
12:20 - 13:30	Lunch	Dabney Gardens
13:30 - 15:10	Atmospheric Retrieval Algorithms	Ramo Auditorium, Bldg 77
15:10 - 15:40	Coffee Break	Dabney Gardens
15:40 - 17:40	Calibration Theory and Techniques	Ramo Auditorium, Bldg 77
17:40 - 20:00	Opening Reception	Dabney Gardens

Tuesday, March 25

08:00 - 09:40	Ocean Salinity	Ramo Auditorium, Bldg 77
09:40 - 10:10	Coffee Break	Dabney Gardens
10:10 - 11:50	Current and Future Missions	Ramo Auditorium, Bldg 77
11:50 - 13:00	Lunch	Dabney Gardens
13:00 - 14:40	Snow and Ice	Ramo Auditorium, Bldg 77
14:40 - 16:00	Current and Future Missions	Dabney Hall, Bldg 40
	Instruments and Techniques I	Dabney Hall, Bldg 40
	Instruments and Techniques II	Dabney Hall, Bldg 40
	RFI and Spectrum Management	Dabney Hall, Bldg 40
	Soil Moisture and Vegetation	Dabney Hall, Bldg 40
16:00 - 17:40	Calibration for Climatology	Ramo Auditorium, Bldg 77

Wednesday, March 26

08:00 - 09:40	Airborne and Groundbased Instruments	Ramo Auditorium, Bldg 77
09:40 - 10:10	Coffee Break	Dabney Gardens
10:10 - 11:50	Passive/Active Soil Moisture Retrieval Algorithms	Ramo Auditorium, Bldg 77
11:50 - 13:00	Lunch	Dabney Gardens
13:00 - 14:40	Calibration for L-band Radiometers	Ramo Auditorium, Bldg 77
14:40 - 16:00	Calibration Techniques and Methods	Dabney Hall, Bldg 40
	Clouds and Precipitation	Dabney Hall, Bldg 40
	Oceans and Ice I	Dabney Hall, Bldg 40
	Oceans and Ice II	Dabney Hall, Bldg 40
	Theory and EM Models	Dabney Hall, Bldg 40
16:00 - 18:00	Theory and EM Models	Ramo Auditorium, Bldg 77
18:30 - 22:00	Banquet	Athenaeum, Bldg 61

Thursday, March 27

08:00 - 09:40	Instrument Technology	Ramo Auditorium, Bldg 77
09:40 - 10:10	Coffee Break	Dabney Gardens
10:10 - 11:50	Small Satellite Instruments and Missions	Ramo Auditorium, Bldg 77
11:50 - 13:00	Lunch	Dabney Gardens
13:00 - 14:40	RFI and Spectrum Management	Ramo Auditorium, Bldg 77
15:00 - 15:30	Coffee Break	Dabney Gardens
15:30 - 17:30	Snowfall Retrieval Algorithms and Snow Modeling	Ramo Auditorium, Bldg 77

Friday, March 28

08:30 - 10:30	JPL Lab Tour	

Proceedings Papers

Authors are encouraged to submit full-length manuscripts for the MicroRad 2014 proceedings by April 14, 2014. Only papers submitted, registered and presented at the conference will be included in the proceedings. These full-length articles will be reviewed by the technical committee and published in the IEEE Xplore as part of the conference proceedings. Manuscripts should be submitted electronically on the MicroRad 2014 website. Submissions must be between a minimum of 2 pages and maximum of 6 pages long. Templates for formatting can be found on the MicroRad 2014 website.

Session Co-Chairs: Tom Jackson, USDA; Haydee Karszenbaum, IAFE

Paper 1 **SMAP GLOBAL MODEL CALIBRATION USING SMOS MULTI-ANGLE TIME-SERIES OBSERVATIONS**
08:30 *Steven Chan, NASA Jet Propulsion Laboratory, California Institute of Technology, United States; Rajat Bindlish, USDA ARS Hydrology and Remote Sensing Laboratory, United States; Eni Njoku, NASA Jet Propulsion Laboratory, California Institute of Technology, United States; Peggy O'Neill, NASA Goddard Space Flight Center, United States; Tom Jackson, USDA ARS Hydrology and Remote Sensing Laboratory, United States*

With a launch date in late 2014, the Soil Moisture Active Passive (SMAP) mission is poised to provide global mapping of soil moisture and freeze/thaw state with high accuracy, resolution, and coverage. The resulting observations are expected to improved forecasts of weather, flood, drought, and agricultural productivity. Within the suite of SMAP's standard data products is the Level 2 Passive Soil Moisture Product, which is derived primarily from SMAP's brightness temperature (TB) observations. The baseline retrieval algorithm uses an established microwave emission model that had been extensively tested in many past field experiments. It was shown in these studies that the model, once properly calibrated, is able to provide a soil moisture retrieval accuracy of 0.04-0.06 cm3/cm3 over common land cover types. One approach to applying the same model at a global scale with SMAP's TB observations is to use the same calibration coefficients derived from past field experiments and apply them globally. Although this approach is a simplification of reality, it resulted in accurate retrieval in several geographically limited studies. Nevertheless, significant retrieval bias may occur in areas whose land cover types had not been considered in past field experiments. In this work, a time-series global model calibration approach is proposed and evaluated. One year of gridded L-band TB observations from the Soil Moisture and Ocean Salinity (SMOS) mission were used as the primary input. At each land pixel on the SMAP grid, the observed TBs were compared with the simulated TBs according to the model with unknown calibration coefficients to be determined. Because of the time-series nature of the input, the above comparison could be repeated for successive revisit dates as a system of equations until the number of known variables (TBs) exceeds the number of unknown variables (calibration coefficients and/or geophysical retrieval). Global nonlinear optimization techniques, subject to proper constraints imposed by ancillary data, were then applied to the equations to solve for the optimal model calibration coefficients for that pixel. Following global application of this approach and SMAP's baseline retrieval algorithm running on SMOS TBs, soil moisture estimates were extracted and compared with in-situ ground measurement at several USDA watershed sites. The resulting soil moisture estimates were shown to have an accuracy comparable to what was observed in past field experiments, confirming the versatility of this global model calibration approach.

Paper 2 **GLOBAL HIGH RESOLUTION SOIL MOISTURE PRODUCT AND ITS ASSOCIATED UNCERTAINTIES FROM THE SOIL MOISTURE ACTIVE PASSIVE (SMAP) MISSION**
08:50 *Narendra Das, Jet Propulsion Lab, United States; Dara Entekhabi, MIT, United States; Eni Njoku, Simon Yueh, Jet Propulsion Lab, United States*

The NASA Soil Moisture Active and Passive (SMAP) mission is due to launch in November 2014. The satellite carries an L-band radiometer and and L-band radar that share a reflector and feed. The radiometer measurements (H, V and third and fourth Stokes parameters) are sensitive to surface soil moisture with moderate (up to 5 kg/m2) vegetation cover. But the radiometer measurements are at coarse (about 40 km) resolution. The radar measurements (VV, HH and HV) are relatively less sensitive to surface soil moisture due to the impacts of surface roughness and vegetation canopy on the active signal. Nonetheless the SMAP radar measurements are at much higher resolution (3 km for 1 dB relative accuracy). The SMAP Project will use the higher-resolution radar data to disaggregate the brightness temperature observed with the radiometer. The parameters of the disaggregation are estimated using accumulated time-series of the radar and radiometer measurements. The disaggregated brightness temperature is then used to estimate surface soil moisture at 9 km based on the single-channel tau-omega model (baseline SMAP algorithm for soil moisture retrieval based on brightness temperature). The active-passive soil moisture product is subject to errors in both the disaggregation step and the tau-omega inversion step. In the disaggregation step the error sources include: 1) radiometer instrument noise, 2) radar instrument noise, 3) water-body fraction within the scene, and 4) disaggregation parameters estimation error. In the tau-omega inversion step the sources of error are: 1) vegetation opacity, 2) single-scattering albedo, 3) surface roughness statistics, 4) soil dielectric constant model soil texture, and 5) surface physical temperature. Taken together, the two steps introduce nine major sources of error. In this paper we present closed-form analytical solutions for the variance of disaggregated brightness temperature that accounts for each of these sources of error, term-by-term and taken together. The variance of the error is a function of the nominal (mean conditions) for each of these parameters. Therefore the variance will vary from location to location across the global land region. In this paper we present the analytical expressions for brightness temperature disaggregation and tau-omega model inversion. The uncertainty statistic is estimated for every data granule and hence can be mapped. We use one full seasonal cycle of the SMAP Algorithm Testbed end-to-end synthetic data set used to test error propagation in the SMAP algorithms. The derived expressions allow inclusion of quantitative uncertainty information in SMAP active-passive surface soil moisture science data products.

Paper 3 **OVERVIEW AND INTER-COMPARISON OF SELECTED GLOBAL SOIL MOISTURE RETRIEVAL APPROACHES THAT UTILIZE PASSIVE-BASED OBSERVATIONS**
09:10 *Iliana Mladenova, Thomas Jackson, USDA-ARS, United States; Eni Njoku, NASA, United States; Rajat Bindlish, USDA-ARS, United States; Steven Chan, NASA, United States; Michael Cosh, Thomas Holmes, USDA-ARS, United States; Richard de Jeu, VU, Netherlands; Lucas Jones, John Kimball, UMT, United States; Simonetta Paloscia, Emanuele Santi, IFAC, Italy*

Accurate and routine knowledge of the amount of water in the soil column is essential for numerous applications. Many of these applications, including drought monitoring and water resource management, demand regional and global coverage. In situ measurements cannot provide this information due to problems involving inadequate spatial representativeness, restricted global coverage. Advances in satellite-based remote sensing instrumentation have opened up a path to overcoming these limitations. The launch of the Advanced Microwave Scanning Radiometer on the Earth Observing System Aqua satellite (AMSR-E) marked the beginning of routinely generated and publicly accessible global soil moisture products. The official Aqua/AMSR-E soil moisture product is provided through the National Snow and Ice Data Center (NSIDC). This product is derived using a Normalized Polarization Difference (NPD) approach and has been extensively evaluated since the launch of AMSR-E in 2002. These previous evaluations have demonstrated some significant limitations of the NPD AMSR-E product associated with its temporal response and range of the retrieved soil moisture values. Other algorithms have also been used to retrieve soil moisture globally from AMSR-E data, and these products show varying levels of differences between each other and with in situ data. This is the case even though all the algorithm approaches are based fundamentally on the same microwave principles and use similar radiative transfer equations. Our efforts in this study were aimed at identifying the causes of differences between the products and improving the Aqua/AMSR-E NPD soil moisture product, based on more recent analyses and availability of additional ancillary data. Also under consideration is a reprocessing of the entire mission AMSR-E dataset that would include a second soil moisture algorithm, the Single Channel Algorithm (SCA), so that both the improved NPD and SCA retrieved soil moisture values would be made available as part of an upgraded official Aqua/AMSR-E soil moisture product at NSIDC. Here we present the first part of this study which includes a detailed theoretically-based inter-comparison between published global soil moisture retrieval algorithms along with results from a sensitivity analysis aimed at assessing the impact of the various simplifications and assumptions made by the individual algorithms. Approaches for the algorithm improvements are reviewed and evaluated. USDA is an equal opportunity provider and employer.

Paper 4 **SMOS SOIL MOISTURE ALGORITHM: RETRIEVAL ACCURACY AND INTERCOMPARISON WITH OTHER SENSORS**
09:30 *Yann Kerr, Ahmad Al Bitar, CESBIO, France; Amen Alyaari, INRA, France; Rajat Bindlish, USDA, United States; Maria-José Escorihuela, IsardSAT, Spain; Thomas Jackson, USDA, United States; Delphine Leroux, CESBIO, France; Joaquin Munoz-Sabater, ECMWF, United Kingdom; Philippe Richaume, CESBIO, France; Thierry Pellarin, LTHE, France; Christoph Rudiger, Monash University, Australia; Jean-Pierre Wigneron, INRA, France*

The Soil Moisture and Ocean Salinity (SMOS) mission was launched by European Space Agency (ESA) in November 2009 to measure soil moisture and ocean surface salinity. SMOS is a synthetic aperture L-band radiometer and provides global coverage in 3 days. The level 2 soil moisture products are distributed by ESA's DPGS (European Space Agency's Data Processing Ground Segment) for each half orbit since January 2010. The Centre National d'Etudes Spatiales (CNES) has developed the CATDS (Centre Aval de Traitement des Données SMOS) ground segment that now provides spatial and temporal synthesis products (referred to as Level 3 products) of soil moisture, ocean salinity and brightness temperatures at multiple incidence angles over the entire operational of SMOS. The AMSR –E sensor on board NASA's AQUA satellite and its successor, JAXA's AMSR-2, has been providing soil moisture estimates since 2002 either through the NASA DAAC at the National Snow and Ice Data Center (NSIDC) or through the Vrije Universiteit of Amsterdam. Similarly, the ERS-1 and -2 scatterometers, followed by ASCAT on board METOP have been delivering soil wetness indices through the Eumetsat H-SAF project with a very long climatological record since 1991. Also available now the new Aquarius SM retrievals which are now available and will soon be distributed through NSIDC. The goal of this presentation is three folds: 1 - provide an estimate of the SMOS retrieval accuracy using a large set of ground data 2 - intercompare the different products to assess the pros and cons of each mission and their relative merits as a function of land cover, season etc.. 3 - establish how one could build up a long term environmental data record of soil moisture from these data sets in order to study the impact of climate change on the global water cycle.

Paper 5 **A BAYESIAN APPROACH FOR AN SAC-D/AQUARIUS SOIL MOISTURE PRODUCT**
09:50 *Cintia Alicia Bruscantini, Francisco Grings, Matias Barber, Pablo Perna, Haydee Karszenbaum, Instituto de Astronomía y Física del Espacio (IAFE-CONICET-UBA), Argentina*

Several retrieval algorithms were developed to retrieve soil moisture from passive remote sensing data. The most commonly used are the Single Channel Algorithm (SCA), the Dual Channel Algorithm (DCA) and LPRM. All these algorithms rely on the omega-tao model to link brightness temperature (Tb) and surface dielectric and geometric properties, and differ among them on the polarization channels they use and the minimization scheme implemented [1]. LPRM and DCA make use of TbH and TbV to retrieve soil moisture and optical depth. One disadvantage of both previous algorithms is their sensitivity to noise in both TbH and TbV. On the other hand, SCAH (SCAV) uses only TbH (TbV) to retrieve soil moisture using optical depth as an auxiliary input to the retrieval algorithm (usually derived from an optical proxy). The main disadvantage of relying on optical depth to retrieve soil moisture is that if optical depth is not well known, SCA will have poor performance. In practice, accurate knowledge of optical depth is tricky. In general, optical depth is obtained through the vegetation parameter b (a land cover dependent parameter, empirically derived, not unique values found on literature) and vegetation water content, VWC (derived from different proxies and models that result in different VWC values). All these retrieval implementations also need ancillary parameters as necessary auxiliary inputs. In this paper, a novel retrieval algorithm (BRA, Bayesian Retrieval Algorithm) is developed, which uses Bayesian inference to retrieve soil moisture and optical depth from both H & V channels. Bayesian likelihood is derived in a non parametric manner, in such a way to be a function of ancillary parameters uncertainties (uncertainties in the parameters needed for the retrieval). As a major advantage, prior knowledge for soil moisture and optical depth can be directly included as inputs to BRA to improve the retrieval. The advantages of BRA compared to previously mentioned retrievals are: i) errors on the retrieved variables can be estimated in an univocal way, ii) it gives the possibility to use prior information about the retrieved variables (provided by other sensors or in situ historical data), iii) it can handle uncertainties on the ancillary parameters. The comparison of the retrieval performance of the different algorithms was carried out using an Observing System Simulation Experiment developed for the Aquarius/SAC-D L-band radiometer [2]. A first version of the operative algorithm is under evaluation. This version is customized for Pampas Plains (Argentina), and includes specific ancillary data for the area (landcover, local VWC information priors). Moreover, several proxies to vegetation

optical depth are being tested (RVI, NDVI and SMOS optical depth). Argentinean radiometer MWR data is used as proxy of skin temperature over vegetated areas. This work is carried out in the framework of the SAC-D/Aquarius announcement of opportunity (CONAE-NASA-Mincyt), "La Plata Basin floods and droughts: Contribution of microwave remote sensing in monitoring and prediction", and the first author is one of the PhD candidates financed by the project. References [1] Jackson, T.J.; Cosh, M.H.; Bindlish, R.; Starks, P.J.; Bosch, D.D.; Seyfried, M.; Goodrich, D.C.; Moran, M.S.; Jinyang Du, "Validation of Advanced Microwave Scanning Radiometer Soil Moisture Products," Geoscience and Remote Sensing, IEEE Transactions on , vol.48, no.12, pp.4256,4272, 2010. [2] Bruscantini, C.; Perna, P.; Ferrazzoli, P.; Grings, F.; Karszenbaum H.; Crow, W.T.; "Effect of forward/inverse model asymmetries over retrieved soil moisture assessed with an OSSE for the Aquarius/SAC-D," IEEE Journal of Selected Topics in Applied Earth Observations and Remote Sensing, 2013.

Monday, March 24 | **Instruments and Techniques** | **10:40 - 12:20**

Lecture Session | **Ramo Auditorium, Bldg 77**

Session Co-Chairs: Steven C. Reising, Colorado State University; Boon Lim, NASA - Jet Propulsion Laboratory

Paper 1 **A LOW-POWER 5X5 DIGITAL CORRELATOR PROTOTYPE FOR GEOSTAR**
10:40 *David Austerberry, Darren McKague, Christopher Ruf, University of Michigan, United States*

The capacity to retrieve all-weather temperature and humidity soundings on the global scale with nearly continuous sampling has been identified as a priority in the National Research Council's Earth Science Decadal Survey. Size, weight, power, and pointing constraints make synthetic aperture radiometry the most feasible way to achieve this goal with a microwave sounder in geostationary orbit. A Geostationary Synthetic Thinned-Aperture Radiometer (GeoSTAR) has been proposed by NASA's Jet Propulsion Laboratory to achieve this goal. Two-dimensional synthesis of a digital aperture entails sampling statistical correlations among many thousands of receiver pairs at very high frequencies. Existing FPGA technology can accomplish this in ground-based systems, but has prohibitively high power requirements for spacecraft. Algorithm-specific integrated circuit (ASIC) technology is capable of reducing the operating power to a level available from a spacecraft bus. A small-scale prototype ASIC with 5x5 coarse (2-bit) digital correlated inputs was designed and fabricated with the goal of enabling the technology for a full-scale correlator with hundreds of receiver inputs. Thus, our objective is to determine whether the prototype's performance characteristics are sufficient to meet the science requirements for GeoSTAR. The 5x5 ASIC correlator prototype was tested to measure characteristics pertinent to interferometric performance and instrument power draw. Noise levels in synthesized images depend strongly upon uncertainties in digital correlations and uncertainties in the mapping of digital correlations to analog correlations. These properties in turn depend upon the sampling rate, digital correlation efficiency, and other characteristics. The variation of correlation efficiency with input power determines the amplification required for input signals, which contributes substantially to operating power. The 5x5 correlator was operated with inputs controlled via an arbitrary waveform generator to measure correlation efficiency, isolation, and frequency response using correlated or partially correlated signals. Digital correlation efficiencies above 90% were achieved for input powers of -15 dBm. Correlation efficiency was found to be symmetric and independent of clock speed up through the correlator's nominal 1 GHz clock. Uniformity of correlation efficiency across correlator cells could be improved through clock trimming specific to each cell. Coupling of input channels was low, with isolation between adjacent channels no greater than -40 dB. Overall noise and power characteristics are sufficient to meet GeoSTAR science requirements. Testing of the 5x5 prototype's performance has substantially informed the design of the 64x64 correlators for use in a full-scale GeoSTAR prototype.

Paper 2 **DESIGN AND DEVELOPMENT OF THE SMAP MICROWAVE RADIOMETER ELECTRONICS**
11:00 *Jeffrey Piepmeier, NASA GODDARD SPACE FLIGHT CENTER, United States; James Medeiros, Kevin Horgan, Cliff Brambora, Robert Estep, NASA's Goddard Space Flight Center, United States*

The SMAP microwave radiometer will measure land surface brightness temperature at L-band (1413 MHz) in the presence of radio frequency interference (RFI) for soil moisture remote sensing [1]. The radiometer design was driven by the requirements to incorporate internal calibration, to operate synchronously with the SMAP radar, and to mitigate the deleterious effects of RFI. The system design includes a highly linear super-heterodyne microwave receiver with internal reference loads and noise sources for calibration and an innovative digital signal processor and detection system. The front-end comprises a coaxial cable-based feed network, with a pair of diplexers and a coupled noise source, and radiometer front-end (RFE) box. Internal calibration is provided by reference switches and a common noise source inside the RFE. The RF back-end (RBE) downconverts the 1413 MHz channel to an intermediate frequency (IF) of 120 MHz. The IF signals are then sampled and quantized by high-speed analog-to-digital converters in the radiometer digital electronics (RDE) box. The RBE local oscillator and RDE sampling clocks are phase-locked to a common reference to ensure coherency between the signals. The RDE performs additional filtering, sub-band channelization, cross-correlation for measuring third and fourth Stokes parameters, and detection and integration of the first four raw moments of the signals. These data are packetized and sent to the ground for calibration and further processing [2]. Here we discuss the novel features of the radiometer hardware particularly those influenced by the need to mitigate RFI. The radio-frequency (RF) electronics subsystem comprises the RBE, RFE, diplexers, and external noise source and directional couplers. The purpose of the RF electronics is to select the desired frequency spectrum and amplify the signal sufficiently to be sampled by the RDE. Testing shows the noise figure is approximately 1.5 dB. The calibration circuits and basic design of the L-band portion was adapted from the Aquarius radiometer [3]. While Aquarius was a direct detection radiometer, SMAP uses the RBE to downconvert the signals to an IF suitable for digital sampling and detection in the RDE. Given the high gain of the system (~80 dB) and expected presence of RFI, particular attention was paid to specifying the system linearity and shape of the frequency response. Measurements of the RFE show the system operates at most 25-dB below 1-dB compression, resulting in <0.2K of non-linearity error before correction. The excellent linearity coupled with aggressive out-of-band filtering ensures that high-power neighboring interferers will not drive the radiometer nonlinear and cause undetected calibration errors. The RDE applies signal processing to the IF channels to produce detected data in all four Stokes parameters and the first four raw moments integrated across the fullband channel and 16 subband channels. A polyphase filter bank (PFB) is used to separate the 24-MHz full bandwidth in to 16x1.5-MHz channels. Testing shows there is greater than 40-dB isolation between every other adjacent channel, which provides the ability to isolate RFI in individual channels while successfully making science measurements in others. The SMAP radiometer spaceflight electronics are designed in multiple aspects to meet science requirements in the presence of RFI. The architecture is a channelized digital radiometer/polarimeter with superheterodyne front-end. To handle RFI in the ground algorithm, the system outputs 8 packets each with 360 samples with time, frequency, polarization, and statistical diversity. Currently, the electronics have completed environmental testing and ground calibration, were integrated with the spin mechanism this past summer and will be delivered to the next higher level of assembly in January 2014.

Paper 3 **A NOVEL RECONSTRUCTION ALGORITHM FOR THE IMPROVEMENT OF SMOS BRIGHTNESS TEMPERATURES**
11:20 *Antonio Turiel, Verónica González-Gambau, Estrella Olmedo, CSIC, Spain*

Due to its interferometric design, the direct measurements acquired by the SMOS payload, MIRAS, are the visibilities sampled on a hexagonal grid. These visibilities are transformed into a 2D brightness temperature map by means of a Fourier-like integral transformation. Therefore, retrieving brightness temperatures (which is in fact the variable used in the geophysical parameters retrieval) from visibilities requires an appropriate image reconstruction algorithm. Different approaches have been proposed so far, trying to improve the quality of the signal and to reduce side lobes and other effects associated to incorrect spatial phases. One important difficulty in the image reconstruction is that for a Y-shape instrument such as MIRAS the spatial frequency coverage has a star-shape, so no tiling can be defined and hence any inverse Fourier transform will require introducing zero coefficients at high frequencies. Those lacking coefficients may generate Gibbs-like phenomena and spread side lobes from any sharp transition in the brightness temperature scene. The simplest reconstruction algorithm consists in calculating the inverse Fourier coefficients associated to the minimum hexagon embedding the MIRAS spatial frequency coverage by direct application of the Fourier series formulas. However, this approach is very sensitive to the presence of high amplitude, small spatial extent sources in the image, since a strong punctual source is seen by the instrument as a strong point together with some tails at ±30º, ±90º and ±150º that may corrupt the entire scene. Even if the coefficients for the full hexagon were known, and even if the version of Fourier series adapted to hexagonal grids to avoid introducing spurious zeros at high frequencies were applied, any delta-like high-amplitude signal in the original scene will significantly corrupt the scene retrieved with this algorithm. This makes Radio-Frequency Interference (RFI) sources, Sun signal and even land-sea transitions very disturbing, as they may generate large side lobes that corrupt large areas and therefore degrade the quality of the geophysical parameter retrieval. A new reconstruction algorithm to reduce side lobes associated to delta-like sources is proposed by accepting some degradation in the spatial resolution. This approach is based on the observation that when the visibility star is embedded in hexagons of larger scales and the inverse Fourier coefficients are calculated, the nodal points - those at which the oscillating interference passes through zero, and the signal has the minimum distortion by tails- remain invariant under changes in scale. As scale is increased nodal points are representative of pixels with smaller footprints, so they become less and less representative of the associated geographical area; but if the geophysical signal to retrieve has a slow-enough spatial pattern of variation the retrieved value is still very representative of the actual geophysical average on the coarser grid. Direct application of uniform nodal grids on SMOS visibilities corrupted by high levels of RFI-induced noise leads to highly attenuated side lobes, too. However, mutual dephasing between SMOS antennas lead to a certain mispointing and nodal grid associated to MIRAS is not completely uniform. This implies that an adaptive grid is needed. In order to diminish the effect of the misfit between the actual nodal points and the resolved ones, an averaging of the signal around the nodal points is performed maintaining the hexagonal symmetry. This averaging combined with the non-uniform adaptive nodal sampling lead to the highest reduction of side lobes while preserving a good enough representativity of the retrieved geophysical signal.

Paper 4 **THE NEW DEMONSTRATION OF GIMS WITH MODULAR DESIGN: TOWARDS TYPHOON MONITORING FROM GEOSTATIONARY EARTH ORBIT**
11:40 *Hao Liu, Ji Wu, Ying Zhang, Cheng Zhang, Lijie Niu, National Space Science Center, Chinese Academy of Sciences (CAS/NSSC), China*

Typhoon is mature tropical cyclone generated in northwestern Pacific Ocean. Typhoon-related disasters caused lots of damages in the East and Southeast Asia every year, imposing significant negative effects on the social & economic developments in this region. In China, there are almost 20 typhoons that can cause damages to the eastern coastal area per year, about 7~8 out of them landed on the continent. The existing typhoon observations from space are largely depended on the optical/infrared sensors onboard GEO meteorological satellite and also the optical/infrared and microwave sensors onboard LEO meteorological satellites. Microwave observation from GEO is demanding due to its cloud-penetration capability, which can continuously provide the inner thermal/humidity structure of typhoon. However, this tool is still missing because of the technical challenges. The largest obstacle of GEO microwave sounding is the required spatial resolution, since the GEO altitude increases 60 times as compared to LEO. GEM/GOMAS concept was proposed in 1990's, based on 2.5~3m real aperture reflector, covering frequencies from 53~424GHz. Manufacturing, testing and scanning such a large antenna aperture at sub-millimeter wave band in space are difficult. Interferometric aperture synthesis is another possible solution to this problem, by using a thinned antenna array to replace the single large aperture antenna, especially for the relative low sounding frequency (50~56GHz). Based on this technology, NASA/JPL and ESA proposed GEOSTAR and GAS concept, and developed ground-based demonstrators respectively. The Geostationary Interferometric Microwave Sounder (GIMS) is a new concept imaging radiometer proposed by CAS/NSSC, aiming for China's next generation geostationary meteorological satellite (FY-4M). The concept of GIMS is based on MIR(Microwave Interferometric Radiometer) technology with a rotating circular thinned array. A ground-based 50~56GHz GIMS demonstrator with 28 elements has been developed in 2011. Imaging experiments and systematic performance tests had been carried out on the demonstrator. Although the instrument concept (MIR with rotating thinned circular array) and performance (50km spatial resolution, 0.8K radiometric resolution, 3000*3000km FOV and 5 minutes imaging period per channel) has been successfully demonstrated by the proof-of-concept demonstrator, there are still several technical issues should be solved before the instrument eligible for a real mission, including: (1) the instrument FOV is expected to extend to full-disk coverage, which implies the least antenna spacing to be 3.5 wavelengths. The number of overall antenna units will increase to around 70; (2) power consumption and mass should be further reduced for space application, which implies the design of the sub-system should be improved by using MMIC and ASIC technology; (3) adding humidity sounding capability: 183GHz channel is on high priority. A new demonstration plan has been approved to address above technical issues. Compared with the proof-of-concept demonstrator with 28 elements, the new demonstrator will have more elements (~70), larger circular array diameter (~3.5m), smaller element antenna aperture size (~3.5 wavelength). More important, the new demonstrator will be built based on modular system design and customized 50~56GHz LNA/IQ Mixer MMIC and 3-level quantization ADC, which can largely reduce the mass/power/volume of the system and ensure the inter-element consistency and in-orbit performance. In this paper, the system design of the new GIMS demonstrator will be introduced. Preliminary performance of the taped out chips will also be introduced. In addition to the hardware development, imaging algorithm and system simulation study has been carried out in parallel, which is focus on the evaluation of the imaging capability on the dynamic target like typhoon. Preliminary simulation results will also be introduced.

Paper 5 PSEUDO-CORRELATION RADIOMETERS FOR EARTH SCIENCE INSTRUMENTS
12:00 *Todd Gaier, Hamid Javadi, Pekka Kangaslahti, Jet Propulsion Laboratory, United States; Kieran Cleary, Rodrigo Reeves, Rohit Gawande, California Institute of Technology, United States*

A growing need for lower-cost radiometers systems, has led to a renewed interest in self-calibrating receivers. This is particularly true for spaceborne receivers, where the need for external calibration can drive the mission cost through bearing and motor assemblies which must carry the mass and power for large portions of the instrument. At lower frequencies, Dicke radiometers with switched internal loads are used to stabilize radiometric gain and/or offsets, but the lossy front-end switches become problematic at higher frequencies and performance is significantly degraded. The radioastronomy community has had great success with pseudo-correlation receivers at millimeter wavelengths with notable space mission successes in WMAP and Planck-LFI [1,2]. The technique is similar to correlation radiometry where the input signals from a signal and reference port, are summed and differenced with a low-loss passive hybrid coupler, amplified, phase switched and multiplied. The resulting multiplied signal, when phase demodulated, tracks the signal and reference inputs respectively, where both signals have experienced the same gain path. The noise figure of the receiver is minimally impacted because the loss of the input hybrid is low and the phase switching occurs after gain. Pseudo-correlation differs from correlation only in that the multiplication is performed by an output hybrid coupler and two detector diodes. We have been evaluating the use of pseudo-correlation radiometry for Earth science applications. Radiometers have been fabricated at 36 and 90 GHz , providing a crossover from microwave to millimeter-wavelengths. The receivers use waveguide hybrid networks at the input and output. The gain stages are InP MMIC amplifiers with noise figure of 1.5 dB and 2.5 dB at 36 and 90 GHz respectively. Phase switching uses MMIC 0/180 degree switches . At 36 GHz the receiver uses tunnel diode detectors, similar to those on other cm-wavelength radiometers. At 90 GHz, the detectors are zero bias Schottky diodes, maximizing the detected voltage. The radiometers will be evaluated in a testbed, which is also being used to characterize traditional Dicke radiometers. The testbed allows testing over a range of ambient temperatures with a wide range of stable input signal brightness temperatures. This allows a direct comparison of the two techniques for such systematics at gain-temperature coefficient, offset stability, gain stability and residual 1/f noise. We will present the performance characteristics of the 36 and 90 GHz radiometers as well as a comparison of the pseudo-correlation and Dicke radiometer performance in the testbed. References [1] "The Microwave Anisotropy Probe Mission" C. L. Bennett et al. 2003 ApJ 583 1 [2]"Planck pre-launch status: Design and description of the Low Frequency Instrument" M. Bersanelli, N. Mandolesi, R. C. Butler, A. Mennella, F. Villa, B. Aja, E. Artal, E. Artina, C. Baccigalupi, M. Balasini et al. (103 more)A&A 520, A4 (2010)

Monday, March 24 — Atmospheric Retrieval Algorithms — 13:30 - 15:10

Lecture Session — Ramo Auditorium, Bldg 77

Session Co-Chairs: Domenico Cimini, IMAA; Boon Lim, NASA - Jet Propulsion Laboratory

Paper 1 TOWARDS IMPROVED OVER-LAND PRECIPITATION ESTIMATION FOR THE GLOBAL PRECIPITATION MEASUREMENT (GPM) MISSION
13:30 *F. Joseph Turk, Jet Propulsion Laboratory, United States; Christa Peters-Lidard, Goddard Space Flight Center, United States*

The joint National Aeronautics and Space Administration (NASA) and Japanese Aerospace Exploration Agency (JAXA) Global Precipitation Mission (GPM) will provide considerably more observations over complex and dynamically changing land backgrounds. The centerpiece is the GPM core satellite, carrying a 13-channel (10-183 GHz) passive microwave (PMW) radiometer and a narrower swath, dual-frequency (Ku/Ka-band) precipitation radar. A major challenge for the physically based radiometer-only and combined radar/radiometer retrieval algorithms is to identify precipitation profiles whose simulated PMW and radar observations agree with the GPM satellite observations, and are also representative of the underlying surface conditions. As a constellation mission, the retrieval framework should function as seamlessly as possible across the different constituent PMW sensors, each of which may have a different channel set, incidence angles, and orbital parameters. In preparation, the GPM Land Surface Working Group (LSWG) was organized to coordinate research amongst the various microwave emissivity models, radar surface backscatter cross section variability, as well as strategies to test and evaluate these techniques in the radiometer and combined radar/radiometer precipitation retrieval algorithms. Various observationally-based emissivity methods have been developed that estimate the emissivity mean and covariance at the typical 10, 19, 37 and 85 GHz PMW window channels, and the higher-frequency (183 GHz water vapor) channels. For the combined algorithm, the current Tropical Rainfall Measuring Mission (TRMM) Ku-band radar and TMI radiometer are useful to examine the joint variability between the surface emissivity and the radar surface cross section. Since the ultimate goal of these efforts is to improve the quality of the over-land precipitation products, the validation of the PMW radiometer algorithm (GPM Profiling Algorithm, GPROF) is currently being carried out over warm and cold seasons in the United States and Canada, using high quality ground radar-based precipitation for verification. This presentation will summarize the LSWG activities and efforts in preparation for the deployment of the GPM core satellite in 2014.

Paper 2 SIMULATION OF GPM OBSERVATIONS, FROM COMBINED RADIOMETER AND RADAR OBSERVATIONS FROM TRMM AND CLOUD MODELS
13:50 *V. Chandrasekar, Srinivasa Ramanujam Kannan, Minda Le, Colorado State University, United States*

Abstract A methodology to combine Tropical Rainfall Measuring Mission (TRMM) based TRMM's Microwave Imager (TMI), TRMM's Precipitation Radar (TRMM PR) and a community developed mesoscale numerical weather prediction model, namely Weather Research and Forecast (WRF) are used to simulate the Global Precipitation Measurement (GPM) radar and radiometer observations. TRMM is a collaborative program between the National Aeronautics and Space Administration (NASA) of USA and Japanese Space Exploration Agency (JAXA) of Japan. Launched in August 1997, the satellite has a radar-radiometer combination that scans precipitating atmosphere simultaneously [Kummerow et. al. (1998)]. The success of TRMM observations has inspired the international scientific community to launch a network of satellites as part of the Global Precipitation Measurement (GPM) mission. The GPM core satellite is due to be launched in 2014, which will have a GPM's Microwave Imager (GMI) and a dual – frequency precipitation radar (DPR). The GMI takes observations at 10.7, 18.7, 89.0, 165.5 GHz in vertical and horizontal polarizations, and 23.8, 183.3 ± 7, 183.3 ± 3 GHz channels in vertical polarization only. The DPR senses the precipitation at 14 GHz and 35 GHz. The goal of the present study is to combine the TMI, TRMM PR and a mesoscale WRF model to simulate the DPR reflectivity profiles and GMI brightness temperatures. The paper is divided into two parts. The first part describes a methodology to retrieve self consistent hydrometeor profiles from a combination of TMI, PR observations as well as WRF model, whereas the second part uses the retrieved hydrometeor profiles to simulate DPR and GMI observations. In addition a direct neural network approach is also investigated to obtain the same solution.The TMI retrieved hydrometeor profiles are used to simulate GPM's observations. The precipitating water and ice contents retrieved from TMI are used to simulate the DPR reflectivity profile. The vertical atmosphere is divided into three regions for the radar profile simulations; the rain region, melting layer region and ice region. Prior simulation methodologies have used direct frequency translation of radar reflectivities as well as attenuation. However the impact of cloud attenuation was missing in those simulations (Chandrasekar et al 2003). Radar reflectivity profile that are measured in Ku and Ka band is subjected to heavy attenuation from non – raining particles such as cloud water content, atmospheric oxygen and water vapor. This paper addresses the issue of cloud attenuation. In addition this paper also addresses the reflectivity frequency scaling for the melting layer separately.In addition to the standard frequency scaling methods, retrieved DSD will also be used to simulate precipitation profiles from radars. In summary, this paper provides an integrated framework to investigate the combined radar and radiometer observations.For the simulation of GMI observations, the retrieved cloud water, cloud ice, precipitating water, and precipitating ice are converted to radiation interaction parameters to solve a plane parallel polarized radiative transfer. Sample simulations of past observed storms from the TRMM program are generated, to study the variability of the GPM type observations. One example of the potential GPM observation of a tropical storm is presented. References: 1. Kummerow C., Barnes. W., Kozu. T., Shiue. J., and Simpson. J., 1998, The Tropical Rainfall Measuring Mission (TRMM) sensor package, Journal of Atmosphere and Oceanic Technology, Vol. 15, 809–817. 2. Chandrasekar, V.; Fukatsu, H.; Mubarak, K., 2003, Global mapping of attenuation at Ku- and Ka-band, IEEE Transactions on Geoscience and Remote Sensing, Vol. 41, 10, 2166–2176.

Paper 3 INVESTIGATING SATELLITE MICROWAVE OBSERVATIONS OF PRECIPITATION IN DIFFERENT CLIMATE REGIMES
14:10 *Nai-Yu Wang, University of Maryland, United States; Ralph Ferraro, NOAA, United States*

Microwave satellite remote sensing of precipitation over land is a challenging problem due to the highly variable land surface emissivity, which, if not properly accounted for, can be much greater than the precipitation signal itself, especially in light rain/snow conditions. Additionally, surfaces such as arid land, deserts and snow cover have brightness temperature characteristics similar to precipitation Ongoing work by GPM microwave radiometer team is constructing databases through a variety of means, however, there is much uncertainty as to what is the optimal information needed for the wide array of sensors in the GPM constellation, including examination of regional conditions. The original data sets will focus on stratification by emissivity class, surface temperature and TPW. We'll perform sensitivity studies to determine the potential role of ancillary data (e.g., land surface temperature, snow cover/water equivalent, etc.) to improve precipitation estimation over land in different climate regimes, including rain and snow. In other words, what information outside of the radiances can help describe the background and subsequent departures from it that are active precipitating regions? It is likely that this information will be a function of the various precipitation regimes. Statistical methods such as Principal Component Analysis (PCA) will be utilized in this task. Databases from a variety of sources are being constructed. They include existing satellite microwave measurements of precipitating and non-precipitating conditions, ground radar precipitation rate estimates, surface emissivity climatology from satellites, surface temperature and TPW from NWP reanalysis. Results from the analysis of these databases with respect to the microwave precipitation sensitivity to the variety of environmental conditions in different climate regimes will be discussed.

Paper 4 **RETRIEVAL OF WATER VAPOR AND LIQUID WATER FROM GROUND-BASED MICROWAVE RADIOMETER MEASUREMENTS USING THE CLOUDY SKY RATIO**
14:30

Swaroop Sahoo, Xavier Bosch-Lluis, Steven C. Reising, Colorado State University, United States; Jothiram Vivekanandan, National Center for Atmospheric Research, United States; Paquita Zuidema, University of Miami, United States; Scott M. Ellis, National Center for Atmospheric Research, United States

The DYNAMO/CINDY2011 Experiment was conducted in the central equatorial Indian Ocean between September 1, 2011 and January 5, 2012 to improve understanding of the Madden-Julian oscillation (MJO) in that region. Observations of vertical moisture profiles, cloud structure, precipitation processes and the planetary boundary layer are necessary to improve understanding of MJO initiation. A number of remote sensing instruments, including NCAR's S-PolKa (dual-wavelength S- and Ka-band) radar and the University of Miami's microwave radiometer, were deployed to estimate water vapor and cloud structure. These instruments were collocated and scanned a common volume of the troposphere over a range of azimuth and elevation angles. The University of Miami's microwave radiometer performed brightness temperature measurements at 23.8 GHz, affected mostly by water vapor, and at 30.0 GHz, primarily sensitive to cloud liquid water. These measurements were performed continuously to estimate slant water path and liquid water path during various weather conditions, including clear and cloudy skies, as well as precipitation of various intensities. This work focuses on classifying clear and cloudy skies as well as precipitating conditions using ground-based brightness temperature measurements during DYNAMO. To perform this classification, the cloudy sky ratio (CSR) was defined as the ratio of the brightness temperature at 23.8 GHz to that at 30.0 GHz. This technique uses the principle that during clear sky conditions brightness temperatures at 23.8 GHz are larger than those at 30.0 GHz, and the ratio varies slightly depending on the atmospheric water vapor density. However, this relationship changes when liquid water is present in the atmosphere. As the amount of liquid water in the atmosphere increases, the brightness temperatures at 23.8 GHz and 30.0 GHz converge to a similar value, yielding a CSR near unity. CSR is sensitive to variability in liquid water and to some extent to the water vapor as well as the elevation angle of brightness temperature measurement. This sensitivity of CSR will be used to develop relationships for retrieval of integrated water vapor and liquid water in the atmosphere. The performance and sensitivity of the CSR will be evaluated based on quantitative comparisons with simultaneous measurements of reflectivity by the collocated S-PolKa radar.

Paper 5 **A DATA ASSIMILATION EXPERIMENT OF TEMPERATURE AND HUMIDITY PROFILES FROM AN INTERNATIONAL NETWORK OF GROUND-BASED MICROWAVE RADIOMETERS**
14:50

Domenico Cimini, National Research Council of Italy, Italy; Olivier Caumont, CNRM-GAME, France; Ulrich Löhnert, University of Cologne, Germany; Lucas Alados-Arboledas, University of Granada, Spain; Rènè Bleisch, University of Bern, Switzerland; Jèsùs Fernández-Gálvez, University of Granada, Spain; Thierry Huet, Onera, France; Massimo Enrico Ferrario, ARPA Veneto, Italy; Fabio Madonna, National Research Council of Italy, Italy; Olaf Maier, Meteoswiss, Switzerland; Francesco Nasir, Istituto Nazionale di Astrofisica, Italy; Giandomenico Pace, ENEA, Italy; Rafael Posada, University of Leon, Spain

Nowadays, ground-based microwave radiometers (MWR) are robust instruments providing continuous unattended operations and real time accurate atmospheric observations under nearly all-weather conditions. However, the use of MWR data for assimilation into Numerical Weather Prediction (NWP) models has been limited to a few sporadic cases. For example, 4-Dimensional Variational Assimilation (4DVAR) of data from a single ground-based MWR has been attempted for a winter fog event (Vandenberghe and Ware, 2002). More recently, an Observing System Simulation Experiment (OSSE) considering a simulated network of some 200 MWR has been carried out for a winter storm case (Otkin et al., 2011; Hartung et al., 2011). To our knowledge, the assimilation of data from a real network of ground-based MWR has never been attempted before. Thus, in the framework of the international Hydrological cycle in the Mediterranean Experiment (HyMeX), temperature and humidity retrievals from an international continental-scale network of ground-based microwave radiometers (MWR) have been collected and synchronized to exploit the potential for data assimilation into Numerical Weather Prediction (NWP) modeling. This activity was carried on in preparation to the HyMeX Special Observing Period, held from September to November 2012. The domain under analysis is the HyMeX West Mediterranean (WMed) target area, using data assimilation tools developed for the Météo-France Arome-WMed NWP system. Arome-WMed has a horizontal resolution of 2.5 km, a non-hydrostatic dynamical core, detailed physics inherited from a research model, and is coupled with the global Arpege NWP system. As a first step towards the assimilation of MWR products, observation-minus-background (O-B) statistics have been computed for temperature and relative humidity to check the consistency between MWR products and 3-h Arome forecasts. Results show that the standard deviations of MWR retrievals are generally consistent with those of radiosondes, while biases are generally much larger than for radiosondes. These large biases are due to a combination of model bias, instrument bias, and retrieval bias, and will be further investigated. Results from the first data assimilation experiments of MWR products show that the impact on forecasts is rather limited. While these results are still under investigation, possible reasons for low impact include the aforementioned biases and a relatively low amount of data with respect to other assimilated data. In this regard, activities have been started within the EU COST Action TOPROF (TOwards operational ground based PROFiling with ceilometers, doppler lidars and microwave radiometers for improving weather forecasts), towards the optimization of MWR data assimilation into NWP models and the evaluation of their impact on analyses and forecasts. Thus, in this presentation we introduce the data set, discuss the O-B statistics, show some preliminary results of data assimilation experiments, and present the TOPROF activities. References: - Hartung et al., Assimilation of Surface-Based Boundary Layer Profiler Observations during a Cool-Season Weather Event Using an Observing System Simulation Experiment. Part II: Forecast Assessment", Mont. Weather Rev, 2011. - Otkin et al., Assimilation of Surface-Based Boundary Layer Profiler Observations during a Cool-Season Weather Event Using an Observing System Simulation Experiment. Part I: Analysis Impact", Mont. Weather Rev., 2011. - Vandenberghe F. and R. Ware, 4-Dimensional Variational Assimilation of Ground-Based Microwave Observations during a Winter Fog Event, International Symposium on Atmospheric Sensing with GPS, Tsukuba, Japan, 2004.

Monday, March 24 — Calibration Theory and Techniques — 15:40 - 17:40

Lecture Session — **Ramo Auditorium, Bldg 77**

Session Co-Chairs: Niels Skou, Technical University of Denmark; Andreas Colliander, NASA - Jet Propulsion Laboratory

Paper 1 **RECEIVER PASSBAND EFFECTS ON WINDSAT BRIGHTNESS TEMPERATURE CALIBRATION**
15:40

Michael Bettenhausen, Peter Gaiser, Naval Research Laboratory, United States

Receiver frequency passband characteristics can have significant effects on the brightness temperatures measured by microwave imaging radiometers. We briefly describe a method to estimate these effects for space-based radiometers such as SSMI, SSMIS, WindSat and the AMSR instruments. We show results which demonstrate that the effects are primarily due to variations in atmospheric absorption of radiation over the passband. The effects are greatest for channels near the 22.235 GHz water vapor resonance and increase with receiver bandwidth. WindSat was launched in January 2003 with the primary mission to evaluate the use of a polarimetric microwave radiometer to provide measurements of the ocean surface wind vector. The importance of the receiver passband characteristics was not fully recognized in the WindSat test plans and only a limited set of measurements of the passband characteristics was taken prior to launch. We will present radiative trans- fer analysis results using the WindSat passband measurements. We will also present results of our analysis of WindSat data to investigate whether the pre-launch characterization of the passbands is representative of the on-orbit performance of the receivers. We analyze the impact of the receiver passband characteristics on WindSat brightness temperature calibration with emphasis on the polarimetric frequency bands at the nominal center frequencies of 10.7, 18.7 and 37 GHz. We also discuss the implication of the brightness temperature effects for retrieval of environmental parameters including ocean surface vector winds, sea surface temperature, precipitable water vapor and soil moisture. In general, the impact is larger for ocean scenes than for land scenes due to differences in the effect of the atmospheric absorption on the measured brightness temperatures. Consequently, our analysis primarily focuses on the impact for ocean scenes.

Paper 2 **GLOBAL PRECIPITATION MEASUREMENT (GPM) MICROWAVE IMAGER (GMI) PRE-FLIGHT NOISE SOURCE CALIBRATION**
16:00

David Draper, David Newell, Ball Aerospace & Technologies Corp., United States

The Global Precipitation Measurement (GPM) Microwave Imager (GMI) program delivered the GMI Instrument to Goddard Space Flight Center early 2012. Goddard Space Flight Center plans to launch the GMI in 2014 aboard the GPM spacecraft with the Dual-frequency Precipitation Radar, affording better correlation of active and passive measurement techniques. The GMI will fly in a 65 degree inclination orbit and is intended to become the calibration standard for radiometer precipitation measurements. The GMI employs a unique dual calibration system. As other scanning microwave imagers, the GMI provides primary calibration uses a hot load blackbody and cold sky views. The GMI also employs a secondary calibration system with noise sources on the lower frequency channels, providing four calibration points rather than two. The dual calibration system enables on-board trending of non-linearity, as well independent cross-checking of each calibration element for stability and anomalous behavior. One important benefit of the dual calibration system is the direct evaluation of noise source behavior on-orbit. For systems that depend on noise sources for absolute calibration, noise source performance has to be done vicariously, using the earth as the reference. Using GMI, noise source radiometric trending can be done directly using the hot load and cold sky views. This paper presents the pre-flight calibration performance of the noise diodes based on thermal vacuum measurements taken during GMI testing. We address stability of the noise sources and their usefulness in detecting anomalous behavior in the primary calibration system. We draw conclusions of on-orbit noise source performance based on the ground measurements.

Paper 3 **RADIOMETRIC BIASES IN AMSU-A RESULTING FROM LOCAL OSCILLATOR DRIFTS AND SHIFTS: IMPROVED RADIATIVE TRANSFER MODELLING AND IMPACTS IN THE MET OFFICE**
16:20 **NWP MODEL**

Katie Lean, William Bell, Met Office, United Kingdom; Qifeng Lu, National Satellite Meteorological Center/China Meteorological Administration, China

For key temperature sounding channels on AMSU-A, background errors mapped into radiance space are typically 50–100 mK leading to a requirement for residual biases in the observations to be at least as small in magnitude. However, observations from channels sensing in the 50-58 GHz range have been shown to exhibit biases of several tenths of a Kelvin relative to NWP model fields. Improvements in the radiative transfer modelling for the lower tropospheric channels of AMSU-A (channels 6-8) have been achieved through developing more accurate estimates of the centre frequencies for the channel passbands. Shifts and drifts in the centre frequencies caused by instability in the local oscillator have been diagnosed for NOAA-15, -16, 18, -19 and Metop A. The effect of accounting for these deviations is assessed through analysis of departure statistics using the Met Office global model. Corrections to the centre frequency were often found to be greater than 20 MHz (in some cases more than 50 MHz) leading in many cases to significant reductions (greater than 10%) in the standard deviation of the departures and improvements in the mean departure of up to a few tenths of a Kelvin. The form and magnitude of the residual bias in AMSU-A before and after implementation of the improvements to the radiative transfer model are investigated. The errors in the centre frequency manifest as air mass and scan position dependent biases which are shown to be reduced once the corrections have been applied. Further to this, the effectiveness of the current bias correction scheme after taking into account the shifts is considered. Assimilation experiments are also carried out in order to determine the impact of the frequency correction on the Met Office NWP analyses and forecasts.

Paper 4 **IMAGE SYNTHESIS FOR THE GEOSTAR ARRAY**
16:40 *Alan Tanner, Todd Gaier, Pekka Kangaslahti, Bjorn Lambrigtsen, Isaac Ramos, Jet Propulsion Laboratory, California Institude of Technology, United States*

GeoSTAR is a large interferometric "Y" array that will observe the Earth's atmosphere from geostationary earth orbit in bands from 50 GHz to 183 GHz. The array provides uniform hexagonal sampling of the visibility function which can be converted to images by Fourier Transform. Yet the array will be subject to non-ideal distortions and other alignment and antenna fabrication errors- as well as electrical anomalies caused by mutual coupling or leakage of RF and IF signals in the back end electronics, fringe wash, et cetera- which will require some corrections. In past earth sensing interferometer arrays, the so called G-matrix approach lumps all these irregularities into one large numerical array which, based on antenna range measurements for example, provides the full forward model of the interferometric system. This model is then inverted using the Projection Theorem (which can be considered a generalization of the Fourier Transform). This approach has worked reasonably well for small to medium sized arrays of up to 60 antenna elements, but the basic inversion formula becomes unstable for larger arrays where small measurement errors are amplified by the matrix inversion. An updated G-matrix algorithm will be presented, and demonstrated using GeoSTAR data, which greatly simplifies and stabilizes the inversion while retaining the essential capabilities that the G-matrix offers--which is the ability to correct measured array anomalies. The approach reduces the dimensions of the inversion by breaking it up into a series of smaller inversions which individually include only a small cluster of nearest neighbors in the UV plane. The idea is to form a linear combination of visibility samples from the non-ideal array to produce a visibility sample with an ideal response. This re-mapped response can then be inverted with the standard Fourier Series.

Paper 5 **CALIBRATION EFFORTS FOR MWR ON-BOARD SAC-D/AQUARIUS MISSION**
17:00 *Cintia Alicia Bruscantini, Martin Maas, Francisco Grings, Haydee Karszenbaum, Instituto de Astronomía y Física del Espacio (IAFE-CONICET-UBA), Argentina*

The Microwave Radiometer (MWR) on board the SAC-D/Aquarius mission, launched on June 2011, is a Dicke radiometer operating at 23.8 GHz (H-Pol) and 36.5 GHz (H/V-Pol). MWR channels are useful to provide ancillary data for the various retrievals to be performed with Aquarius regarding ocean and land applications. In this study we report some of the calibration results obtained with two different techniques: a land cross-calibration with Windsat and the Vicarious Cold calibration [1]. In both cases, results were generated for the 2011-2012 period and using the version V5.0S of the MWR data. Radiometer inter-comparison over selected homogeneous targets is widely used for calibration assessment and data quality evaluation. The methodology lays on the temporal stability of the selected targets and their homogeneity in terms of brightness temperature (Tb), so that radiometers with similar characteristics (frequency, polarization, incidence angle) should observe the same Tb when passing over the target within a short temporal window. Differences on observed Tbs are associated to a poor calibration of the instrument under study. The cross-calibration is an adjustment of the Tb data of the radiometer under study to match the Tb data of the calibrated radiometer. In this study, linear adjustments are applied for each MWR beams of its three channels to match Windsat observations. In order to examine the entire dynamic range of land observations, 19 homogeneous targets were selected for cross-calibration. These targets have been previously selected for quality assessment of AMSR-E data [2]. Targets include tropical and boreal forests, desert, grassland and Sahel. In addition, we performed the Vicarious Cold Calibration Method which yields complementary results and it is applicable even in the absence of data from other satellites. We briefly discuss some issues in this methodology, regarding the most convenient time-window and extrapolation method to employ. A 30-day time window and linear extrapolation has been shown to be more stable than 14-day time windows and cubic extrapolation, but our experiments show that, for linear extrapolation, long time windows are roughly equivalent to taking a moving average of shorter 2-day or 4-day windows, thus we can interpret this 30-day moving average as a post-processing step, rather than an essential feature of the method. This methodology has allowed us to characterize drifts in various beams and channels throughout its lifetime. In particular, beam 7 of the 23H channel drifted for several months after the launch but finally became stable. We also detected a difference between the ascending and descending passes of 1.5 K which yet has to be addressed. Overall, it was found that the instrument presents good stability properties and compares favorably to Windsat over land targets. Nevertheless, certain issues to be resolved are identified and corrections are proposed. References [1] Ruf, C. S., "Vicarious Calibration of an Ocean Salinity Radiometer from Low Earth Orbit", Journal of atmospheric and oceanic technology, vol. 20, pp. 1656-1670, 2003. [2] Njoku, E.G.; Chan, T.; Crosson, W.; Limaye, A; "Evaluation of the AMSR-E Data Calibration Over Land", Italian Journal of Remote Sensing, vol. 29, pp. 19 – 37, 2004.

Paper 6 **GPM X-CAL INTER-CALIBRATION OF AMSR2**
17:20 *Darren McKague, University of Michigan, United States; Wesley Berg, Colorado State University, United States; Spencer Farrar, Linwood Jones, University of Central Florida, United States; Rachael Kroodsma, University of Michigan, United States; Thomas Wilheit, Texas A&M University, United States; John Yang, University of Michigan, United States*

Presenting Author: Darren McKague Dept. Atmospheric, Oceanic and Space Sciences University of Michigan The Advanced Microwave Scanning Radiometer 2 (AMSR2) instrument is an important element of the joint NASA/JAXA Global Precipitation Mission (GPM), which seeks to provide global estimates of precipitation with high temporal resolution [1]. The AMSR2 instrument provides data in the important A-Train orbital slot. In order to create a self-consistent global record of precipitation, the data from the GPM constellation of microwave radiometers must be inter-calibrated. The process of inter-calibration accounts for any radiometer-to-radiometer observational differences that cannot be traced back to some root cause for which a calibration adjustment can be made. The X-Cal group within GPM is responsible for developing the inter-calibration methods [2]. This presentation will discuss the X-Cal analysis and inter-calibration of AMSR2. The X-Cal process consists of two main steps: pre-screening of the data, and computation of inter-calibration differences. With the pre-screening step, the radiometer data are scrubbed of physically un-reasonable measurements (brightness temperatures outside the range of what can be expected to be observed on Earth) and the data are examined for any calibration issues not already addressed by the data provider for which a correction can be developed and applied (e.g., sun intrusion on the on-board warm load, an emissive main reflector, scan biases due to edge-of-scan interference, uncorrected radiometer non-linearity). Using the pre-screened data from the first step, the relative differences between the observations of each radiometer in the GPM constellation with respect to a reference radiometer are computed in the second step. The end product is a set of brightness temperature adjustments as that can be applied to a given radiometer to achieve consistency with the reference radiometer together with an associated uncertainty estimate for the adjustment. Preliminary results show that AMSR2 data are quite clean (very few un-physical outliers) and stable with little scan position dependent bias. The AMSR2, TMI relative differences computed by the various groups within X-Cal agree well with one another (within ~.2 K). Channel by channel relative differences between AMSR2 and the rest of the GPM constellation will be presented at the conference. References: [1] A. Y. Hou, G. Skofronick-Jackson, C. D. Kummerow, and J.M. Shepherd, "Global precipitation measurement" in Precipitation: Advances in Measurement, Estimation and Prediction, S. Michaelides, Ed., Springer, 2008, pp. 131-170. [2] T. Wilheit, W. Berg, L. Jones, R. Kroodsma, D. McKague, C. Ruf, and M. Sapiano, "A consensus calibration based on TMI and WindSat," Proc. 2011 IEEE International Geoscience and Remote Sensing Symposium, 2011, pp. 2641-2644.

Tuesday, March 25	Ocean Salinity	08:00 - 09:40
Lecture Session		Ramo Auditorium, Bldg 77

Session Co-Chairs: David Le Vine, NASA - Goddard Space Flight Center; Emmanuel Dinnat, Chapman University

Paper 1 **A ROUGHNESS CORRECTION ALGORITHM FOR AQUARIUS USING MWR**
08:00 *Yazan Hejazin, Linwood Jones, Salem El-Nimri, University of Central Florida, United States*

Aquarius/SAC-D is a collaborative earth science satellite mission between NASA and the Argentine Space Agency, CONAE. The two microwave radiometers on the satellite are the NASA Aquarius (AQ, L-band 1.4 GHz) and the CONAE MicroWave Radiometer (MWR, Ka-band 36.5 GHz V- & H-pol and K-band 24.8 GHz H-pol). The mission science objective is to provide high-resolution global sea surface salinity (SSS) maps every 7-days, which are derived using the AQ combined L-band radiometer/scatterometer. The remote sensing of SSS is extremely challenging because there are many corrections that must be made to obtain the smooth ocean surface brightness temperature (Tb) from which SSS is retrieved. The major sources of Tb contamination include: cosmic noise from the galaxy, solar emissions, mixing of polarized ocean emissions when propagating through the ionosphere and ocean surface warming due to wave and wind roughness. All of these effects produce unwanted brightness contributions, which must be estimated and subtracted from the AQ antenna brightness temperature to yield the desired smooth ocean surface Tb. After correction, the root sum square residual error budget for all terms is 0.38 K, and the major error source is the effect of ocean roughness at 0.28 K. The baseline approach to provide roughness correction uses the AQ scatterometer ocean radar backscatter to infer excess ocean emissivity. In this paper, an alternative sea surface roughness correction algorithm will be presented that uses a new semi-empirical Radiative Transfer Model (RTM) to estimate the ocean emissivity. This RTM has been tuned using 2-years of observed AQ and MWR Tb's and corresponding atmospheric and oceanic environmental conditions from numerical weather and oceanographic models. Inputs to this model are collocated MWR Ka-band Tb's and available ancillary data (e.g., sea surface temperature, surface wind vector, and SSS); and the outputs are the corresponding roughness corrections for each AQ footprint. Results of independent comparisons (not used in the RTM tuning process) will be presented between the AQ scatterometer derived ocean roughness correction and the MWR roughness correction algorithm. Also SSS retrievals using these two independent approaches will be compared to an oceanographic salinity model known as Hybrid Coordinate Ocean Model (HYCOM) salinity and collocated AQ Validation Data System (AVDS) buoy SSS measurements.

Paper 2 **RECENT PROGRESS IN THE AQUARIUS SALINITY RETRIEVALS**
08:20 *Thomas Meissner, Frank Wentz, Kyle Hilburn, Joel Scott, Remote Sensing Systems, United States*

The Aquarius L-band radiometer/scatterometer system is designed to provide ocean surface salinity at an accuracy of 0.2 psu. This poses a challenge for the instrument design and calibration as much as for the salinity retrieval algorithm. Many sizeable spurious signals have to be removed to a high level of accuracy. The first part of our presentation summarizes and discusses the most recent steps that were implement-ed within the Aquarius L2 processing for the Version 3 release. 1. Correcting effects of the wind roughened ocean surface. The Aquarius L-band scatterometer has proven to be an invaluable tool, as it allows an accurate measurement of the ocean surface wind speed at the instance of the Aquarius radiometer observation. We discuss the steps of the Aquarius wind speed measurement and how it is incorporated in the surface roughness correction algorithm. 2. Correcting intruding celestial radiation. The largest signal comes from the galactic radiation that is reflected from the ocean surface into the main lobes of the antenna. Its size varies with season and latitude of the observation and it can be as large as 5 K. If left uncorrected this would translate into a salinity error of about 10 psu. The Version 2 Aquarius Level 2 algorithm corrects for this effect using a physical geometric optics model for the reflection of the galactic radiation from the ocean surface, which has been derived pre-launch. Data analysis shows removes the unwanted galactic signal to about 90%. The remaining 10% error shows up in the data as bias between the salinity values from the ascending (evening) and descending (morning) swaths. In order to remove this spurious bias we have derived an empirical correction that is applied in addition to the geometric optics correction. These two steps play a crucial role in achieving the aforementioned mission accuracy requirement of 0.2 psu. In the second part of our presentation we presents a validation study for the new salinity product, which consists in an intercomparison between

Aquarius, in-situ buoy salinity measurements and the HYCOM model salinity field. The Aquarius salinity shows a fresh bias in the tropics when compared to HYCOM and ARGO buoy measurements. This indicates that the Aquarius instrument can pick up rain freshening of the ocean surface.

Paper 3 **AQUARIUS' COMBINED ACTIVE PASSIVE ALGORITHM FOR OCEAN SURFACE SALINITY AND WIND RETRIEVAL**
08:40 *Simon Yueh, Wenqing Tang, Alexander Fore, Akiko Hayashi, Yueh Song, Tong Lee, Jet Propulsion Laboratory, California Institute of Technology, United States*

Aquarius is a combined passive/active L-band (~1 GHz) microwave instrument developed to map the sea surface salinity (SSS) field from space. This paper describes Aquarius' Combined Active-Passive (CAP) retrieval algorithm, which uses Aquarius' brightness temperature and radar backscatter for sea surfaces for simultaneous retrieval of surface salinity and wind. Unlike the algorithm developed by the Remote Sensing System (RSS), which has been implemented in the Aquarius Data Processing system, the JPL CAP algorithm does not require monthly climatology SSS maps to constrain the salinity retrieval. Furthermore the RSS algorithm fully uses the NCEP winds for data correction, while the CAP algorithm uses NCEP winds only near the crosswind directions. The CAP product is available through the JPL Physical Oceanography Distributed Active Archive Center. The major recent updates to the CAP algorithm include the galactic reflection correction, Faraday rotation (FR) and Antenna Pattern Correction (APC) as well as the geophysical model functions (GMF) of wind, wave and rain impacts. We use a series expansion with Gaussian basis functions to approximate the scattering coefficients of ocean surfaces; this results in more accurate modeling of the reflection of galactic radiation and consequently significantly reduces the ascend-descending bias in the salinity retrievals. This improvement along with the FR and APC corrections greatly reduces the errors of Aquarius CAP salinity retrievals. We assess the accuracy of Aquarius CAP wind by performing comparison with the SSMI/S wind and triple collocation analysis. The root-mean-square (RMS) difference with respect to the SSMI/S wind speed is about 1 m/s. The triple collocation analysis using the SSMI/S, CAP and ECMWF winds indicates that the accuracy of CAP wind speed is about 0.7 m/s, essentially the same as that of SSMI/S wind speed and less than the 0.9 m/s error for the ECMWF. We assess the accuracy of CAP's salinity by comparison with ARGO's monthly gridded salinity obtained from the Asia-Pacific Data-Research Center (APDRC). The RMS differences between CAP and APDRC-ARGO salinities on 1x1 degree latitude and longitude grid are less than 0.2 psu for most parts of global oceans, except the regions in the Inter-tropical Convergence Zone (ITCZ), near the outflow of major rivers and high latitudes. We find that the amplitude of monthly anomaly in the Aquarius CAP salinity is highly correlated with that in the ARGO data products in the ITCZ. The high correlation suggests that the difference between Aquarius' CAP and Argo salinities could be a result of surface stratification, leading to differences between the salinity in the top few cm observed by Aquarius and a few meters below the surface measured by ARGO. Thus, Aquarius and ARGO could provide complimentary information about the stratification in the ocean mixed layer.

Paper 4 **INTER-COMPARISON OF SMOS AND AQUARIUS SEA SURFACE SALINITY, AND EFFECT OF THE DIELECTRIC CONSTANT AND VICARIOUS CALIBRATION**
09:00 *Emmanuel Dinnat, NASA-GSFC/Chapman University, United States; Jacqueline Boutin, Xiaobin Yin, IPSL-LOCEAN, France; David Le Vine, NASA-GSFC, United States*

Two ongoing space missions share the scientific objective of mapping the global Sea Surface Salinity (SSS), yet their observations show significant discrepancies. ESA's Soil Moisture and Ocean Salinity (SMOS) and NASA's Aquarius use L-band (1.4 GHz) radiometers to measure emission from the sea surface and retrieve SSS. Significant differences in SSS retrieved by both sensors are observed, with SMOS SSS being generally less than Aquarius SSS, except for very cold waters where SMOS SSS is the largest overall. We assess the impact on the retrieved SSS of the differences in vicarious calibration and retrieval algorithm used by both mission. Differences in SSS retrieved by SMOS and Aquarius are mostly between -1 practical salinity unit (psu) and +1 psu, with a significant regional and latitudinal dependence. Part of this difference is due to the different sea water permittivity models used for both missions. The permittivity model is used at two stages of the data processing: 1/ to calibrate the instruments by comparing radiometric measurements to forward model simulations, and 2/ to invert SSS from surface brightness temperature (Tb). In order to assess the impact of the permittivity model on the SSS difference between SMOS and Aquarius, we reprocess the Aquarius data using the model used for SMOS: We adjust the calibration of Aquarius and perform the inversion in SSS with the SMOS model. Various permittivity models exhibit differences of less than a percent, but this uncertainty results in differences in Tb of the order of a few tenths of a Kelvin. The difference in retrieved salinity between these models is up to ~1 psu, but it varies regionally and seasonally according to changes in environmental conditions (mostly temperature). The differences between Aquarius original data and data reprocessed with SMOS permittivity model vary mostly within 0.5 psu at global scale, with a few larger regional variations (for example in cold waters). Seasonal variations occur at mid and high latitudes. Aquarius and SMOS differences exhibit a dependence in temperature, which is reduced when Aquarius data are reprocessed with SMOS's permittivity model. We find that the permittivity model explains part of the differences between both instruments, particularly in cold waters, but some significant disagreements remain. Another difference between the two missions concerns the vicarious calibration. SMOS Ocean Target Transformation (OTT) uses comparisons between measured Tb's and forward model simulations over a limited region in the Pacific Ocean. Aquarius performs a similar comparison at global scale. The reference SSS for the simulations is the World Ocean Atlas (2009) for SMOS, the HYbrid Coordinates Ocean Model (HYCOM) for Aquarius. For the surface roughness, SMOS uses data from the European Center for Medium range Weather Forecasting (ECMWF) model and Aquarius uses a combination of the National Centers for Environmental Prediction (NCEP) model and the onboard scatterometer. We will discuss the differences between the different calibration targets and their impact on the SSS inter-comparison.

Paper 5 **THE RAIN EFFECT ON AQUARIUS SEA SURFACE SALINITY RETRIEVAL**
09:20 *Wenqing Tang, Simon Yueh, Jet Propulsion Laboratory, United States; Gary Lagerloef, Earth and Space Research, United States; Alexander Fore, Akiko Hayashi, Jet Propulsion Laboratory, United States*

Rain has instantaneous impact on the sea surface salinity (SSS), but also interfere with the microwave remote sensing signals, making the task to retrieve SSS under rainy conditions difficult. The current version of Aquarius Geophysical Model Functions (GMF) was built using data under rain free condition. The impact of rain on L-band radar and radiometer have been examined using the Aquarius data and the SSM/I rain rate based on analysis of the residual signals after accounting for roughness due to wind and flat surface emissivity. The presence of rain increases the radar backscatter and excess emissivity at low wind speeds, but the effects decrease with increasing wind speed. Based on residual analysis, a rain correction scheme is developed to modify Aquarius radar and radiometer GMFs and implemented in the operational combined active-passive (CAP) processor for Aquarius. Two years of level 2 data is retrieved in parallel, with (SSSCAP_RC) or without (SSSCAP) rain correction. Aquarius retrieved SSS is evaluated using a global monthly dataset of ARGO float observations objectively interpolated to 1°x1° grid and standard pressure levels from surface to 2000 dbar. The global monthly RMSE for SSSCAP_RC with respect to SSSARGO is reduced from that of SSSCAP by about 0.1 PSU. The error distribution in the 2-D space of wind-rain shows that a large domain with significant large negative biases observed in SSSCAP is eliminated in SSSCAP_RC. Regional biases between SSSARGO, SSSCAP and SSSCAP_RC are examined in areas with frequent rain events. Results show ΔSSS (=SSSCAP_RC-SSSCAP) is highly correlated with the seasonal precipitation pattern and reduces surface freshening by about 0.2-0.3 PSU under heavy rain. However, ΔSSS shows no correlation with the difference pattern between SSSARGO and either SSSCAP_RC or SSSCAP. The associated upper layer stratification depicted by ARGO profiles suggests this may reflect the true difference between skin and near surface salinity in high-stratified regions, for example, around the edge of freshwater pools. The advantage of satellite data in spatial sampling is demonstrated in the much-detailed structure detected by Aquarius around SSS fronts. The impact of ΔSSS on the global water cycle is estimated in terms of the normalized mixed-layer salt storage tendency, F, defined as [h dSSS/dt / SSS] where the mixed layer depth h is obtained from ARGO monthly profiles. The large scale feature of the amplitude of annual cycle of F calculated from SSSARGO, SSSCAP_RC and SSSCAP are comparable with that of the surface fresh water flux E-P, while shows about 20% difference between FA(SSSCAP_RC) and FA(SSSCAP) in areas with strong freshwater flux.

Tuesday, March 25 | **Current and Future Missions** | **10:10 - 11:50**

Lecture Session | **Ramo Auditorium, Bldg 77**

Session Co-Chairs: Yann Kerr, CESBIO; Al Gasiewski, University of Colorado

Paper 1 **AQUARIUS RADIOMETER STATUS**
10:10 *David Le Vine, Emmanuel Dinnat, Jeffrey Piepmeier, Paolo de Matthaeis, Saji Abraham, Goddard Space Flight Center, United States; Gary Lagerloef, Earth and Space Research, United States; Thomas Meissner, Frank Wentz, Remote Sensing Systems, United States*

Aquarius was launched on June 10, 2011 as part of the Aquarius/SAC-D observatory and the instrument has been operating continuously since being turned on in August of the same year. The initial map of sea surface salinity was released the following September and the quality of the retrieval has continuously improved since then. The Aquarius radiometers include several special features such as internal calibration and temperature control for stability, measurement of the third Stokes parameter to correct for Faraday rotation, and fast sampling to mitigate the effects of Radio Frequency Interference (RFI). This paper presents an overview of the instrument performance and the status of Faraday rotation and RFI detection algorithms. From the beginning, the Aquarius radiometers have performed close to predictions based on the forward model assembled to predict the expected antenna temperatures. Once a bias was removed, the performance has been within specifications, but with a slight drift. The drift impacts the salinity retrieval and is currently being removed with a periodic re-calibration. In addition, a seasonally dependent difference between ascending and descending orbits has been traced to a roughness-dependent error in the correction for the reflected galactic radiation, and an empirical correction has been implemented. Two important problems for remote sensing at L-band are Faraday rotation and RFI. To measure the Faraday rotation, Aquarius uses the ratio of the third Stokes parameter to the first Stokes parameter. This has worked well over ocean and produces results in agreement with IGS models and has been verified with coincident measurements of the JASON-II altimeter. To help mitigate the effects of RFI, Aquarius implemented rapid sampling and a time-domain "glitch" detector. This has worked well over ocean, where RFI is generally small. Over land, Aquarius RFI maps are consistent with those of SMOS, suggesting that the detector is working well. Research continues to refine the retrieval of Faraday rotation and improve the RFI mitigation. For example, it has been suggested that noise in the retrieval of salinity in a few coastal areas in the North Atlantic might be related to undetected RFI. Finally, precautions were taken in the design of Aquarius to avoid contamination by the Sun. This appears to have been successful, but research is underway to test the approach using radiation during solar flares with large Tb at L-band and which are known to have a large effect as confirmed, for example, by the impact on SMOS.

Paper 2 **ICE CLOUD IMAGER INSTRUMENT FOR METOP SECOND GENERATION**
10:30 *Ville Kangas, Salvatore D'Addio, Marc Loiselet, Graeme Mason, European Space Agency, Netherlands; Raquel Gonzalez, Marc Bergada, EADS CASA Espacio, Spain; Jean-Claude Orlhac, EADS ASTRIUM, France; Bertrand Thomas, Michael Brandt, Radiometer Physics GmbH, Germany*

Since 2006, the European contribution to operational meteorological observations from polar orbit has been provided by the Meteorological Operational (MetOp) satellites, which is the space segment of the EUMETSAT Polar System (EPS). As part of the next generation EUMETSAT Polar System (EPS-SG), the MetOp Second Generation (MetOp-SG) satellites will provide continuity and enhancement of these observations in the 2020 – 2040 timeframe.

The MetOp-SG will consists of two series of satellites ("Satellite A" and "Satellite B"), with a nominal baseline of two or three satellites of each series. The payload complement of MetOp-SG was confirmed by EUMETSAT Council in 2012 and, out of ten instruments, it includes three microwave radiometers, namely Microwave Sounder (MWS), Microwave Imager (MWI) and Ice Cloud Imager (ICI). This payload complement provides a unique suite of high performance, operational microwave radiometers covering a total of 63 channels over a very wide frequency range from 18.7 GHz up to 664 GHz. These three radiometers will provide continuous and simultaneous operation for more than 20 years, representing an invaluable opportunity for cross-calibration of future spaceborne radiometer systems. After the confirmation of the payload complement, the European Space Agency issued a request for proposals for the microwave radiometers of MetOp-SG in 2012 and made the final selection in early 2013.For the ICI instrument, ESA selected EADS CASA Espacio (E) as the prime contractor. The main objective of the ICI is to provide measurements of cloud ice, cirrus clouds and water vapour profile. The ICI is a conically scanning total-power sub-millimetre wave radiometer, providing calibrated and geo-located measurements in a total of 13 channels ranging from 183 GHz up to 664 GHz, offering dual polarisation measurements for 243 GHz and 664 GHz channels. The frequency range provided by ICI is unique and ICI will be the first instrument of its kind to fly in space. The ICI is composed of one rotating part and one fixed part. The rotating part includes the main antenna, the feed assembly and the receivers electronics. The fixed part contains the hot calibration target, the reflector for viewing the cold-sky and the electronics for the instrument control and interface with the platform. In order to achieve very good radiometric accuracy and stability, the ICI instrument is designed with sun-shields in order to minimize sun-intrusion at all possible sun angles. The ICI instrument rotates at a constant speed of 45 rpm, providing earth scene measurements over an azimuth range of +/-65 degrees, with a footprint of 15 km for all channels. This ensures a nyquist sampling along-track and across track. Hot and Cold calibration is performed periodically at each rotation. In addition to performance, ICI also provides a robust design as required for an operational instrument. The ICI instrument is designed to guarantee very good reliability and availability for the whole lifetime of 7.5 years and is specifically designed to provide a high failure detection and recovery autonomy. This paper will present the ICI instrument key design features and predicted performance, as well as an overview of associated key technology developments. This paper will be accompanied by two other papers, presenting the Microwave Sounder and Microwave Imager instruments for MetOp Second Generation.

Paper 3 STATUS OF SOIL MOISTURE ACTIVE PASSIVE MISSION DEVELOPMENT
10:50 *Simon Yueh, Kent Kellogg, Curtis Chen, Jet Propulsion Laboratory, California Institute of Technology, United States; Jeffrey Piepmeier, Goddard Space Flight Center, United States*

NASA's Soil Moisture Active Passive (SMAP) mission uses an L-band radar and an L-band radiometer for concurrent, coincident measurements integrated as a single observation system. The radiometer and radar share one common antenna reflector, which is a 6-m mesh deployable antenna. The antenna design is based on the offset parabola reflector design with one antenna feed to produce the antenna beam pointing at an incidence angle of about 40 degrees on the earth surface. The mesh antenna together with the feed will be positioned on a spinning assembly with a conical scanning rate of about 14 rotations per minute. The resulting swath width is about 1000 km, which will allow a global coverage every 3 days. The SMAP mission is being developed by NASA's Jet Propulsion Laboratory, which is building the spacecraft, the instrument (except for the radiometer), and the science processing system. NASA's Goddard Space Flight Center is providing the L-band radiometer along with the level 4 processing. SMAP's radiometer is a fully polarimetric radiometer with onboard digital processor producing data over 16 sub-bands for the mitigation of radio frequency interference. The SMAP L-band radar is a Synthetic Aperture Radar (SAR), and will provide linearized polarized (VV, HH, and HV) backscatter measurements at higher resolution (~ 1 to 3 km) than the coarser-resolution (~ 40 km) radiometer measurement. SMAP will be launched from Vandenberg Air Force Base in California on a Delta II launch vehicle in November 2014, and will be placed into a polar sun synchronous orbit with a 685 km altitude. The radiometer build was completed by GSFC, and was delivered to JPL in mid-2013 for instrument integration and test. The radar electronics development was also completed, and has been integrated with the radiometer for a series of functional, performance and compatibility tests. The antenna performance has been modeled by using the GRASP model and range testing using a scale model with results indicating that all the requirements can be met. It is expected that the deployable reflector-boom-antenna will be delivered to JPL in January 2014 for integration and test with the radar/radiometer electronics and feed. We will present available test results to indicate the performance of SMAP's instrument. We will also describe the status of mission development, including mission operation, science data processing, data archive/distribution and planned activities for post launch calibration/validation.

Paper 4 GPM MISSION OVERVIEW AND U.S. SCIENCE STATUS
11:10 *Arthur Hou, Gail Skofronick-Jackson, NASA Goddard Space Flight Center, United States*

Water is fundamental to life on Earth. Knowing where and how much rain and snow falls globally is vital to understanding how weather and climate impact both our environment and Earth's water and energy cycles, including effects on agriculture, fresh water availability, and responses to natural disasters. The Global Precipitation Measurement (GPM) Mission, scheduled to launch from Japan in early 2014, just prior to MicroRad 2014, is an international satellite mission to unify and advance precipitation measurements from a constellation of research and operational sensors to provide "next-generation" precipitation products. Since rainfall and snowfall vary greatly from place to place and over time, satellites can provide more uniform observations of rain and snow around the globe than ground instruments, especially in areas where surface measurements are difficult. The cornerstone of the GPM mission is the deployment of a NASA-JAXA Core Observatory in a unique 65o non-Sun-synchronous orbit to serve as a physics observatory and a calibration reference to improve precipitation measurements by a constellation of 8 or more dedicated and operational, U.S. and international passive microwave sensors. The Core Observatory will carry a Ku/Ka-band Dual-frequency Precipitation Radar (DPR) and a multi-channel (10-183 GHz) GPM Microwave Radiometer (GMI). The DPR will provide measurements of 3-D precipitation structures and microphysical properties, which are key to achieving a better understanding of precipitation processes and improving retrieval algorithms for passive microwave radiometers. The combined use of DPR and GMI measurements will place greater constraints on possible solutions to radiometer retrievals to improve the accuracy and consistency of precipitation retrievals from all constellation radiometers. The GPM instruments are capable of detecting falling snow, measuring light rain, and providing, for the first time, quantitative estimates of microphysical properties and size distributions of precipitation particles. As a science mission with integrated application goals, GPM is designed to (1) advance precipitation measurement capability from space through combined use of active and passive microwave sensors, (2) advance the knowledge of the global water/energy cycle and freshwater availability through better description of the space-time variability of global precipitation, and (3) improve weather, climate, and hydrological prediction capabilities through more accurate and frequent measurements of instantaneous precipitation rates and time-integrated rainfall accumulation. An overview of the GPM mission concept and science activities in the United States, together with an update on international collaborations in radiometer inter-calibration and ground validation, will be presented. Pre-launch activities and launch information will also be presented.

Paper 5 S-NPP ATMS INSTRUMENT PERFORMANCE EVALUATION
11:30 *Edward Kim, NASA, United States; Cheng-Hsuan Joseph Lyu, NASA/ IMSG, United States; Kent Anderson, Northrop Grumman Aerospace Systems, United States; Vince Leslie, Bill Blackwell, MIT Lincoln Laboratory, United States*

The first of a new generation of weather and climate sensors was launched aboard the Suomi-NPOESS (National Polar-orbiting Operational Environmental Satellite System) Preparatory Project (S-NPP) satellite two and a half years ago in October, 2011. S-NPP joined the fleet of international polar-orbiting satellites that provides observations for operational weather forecasting as well as for continuing and improving the long-term environmental data records provided by operational and research missions over the last 40 years. A key member of the new sensor suite, the Advanced Technology Microwave Sounder (ATMS), combines the capabilities and channel sets of three predecessor microwave sounders into a single package. ATMS observations are combined with measurements from the Cross-track Infrared Sounder (CrIS) to provide two Key Performance Parameters (KPPs)–atmospheric vertical moisture profile (AVMP) and atmospheric vertical temperature profile (AVTP). From these two products a third Environmental Data Record (EDR, equivalent to NASA "Level 2" data), the Atmospheric Vertical Pressure Profile (AVPP), is also calculated. AVTP and AVMP are needed in both clear and cloudy conditions. While the infrared measurements from CrIS provide high vertical resolution they are blocked when clouds are in the field of view. The microwave measurements from ATMS are much more immune to clouds, but provide measurements at a lower vertical resolution. In areas of dense cloud cover, the microwave measurements are used exclusively to derive the AVTP and AVMP products. AVTP and AVMP are the most critical observations needed for numerical weather forecast models. ATMS sensor enhancements include size/mass/power approximately one third of the previous total, new sounding channels, the first space-based, Nyquist-sampled cross-track microwave temperature soundings for improved fusion with infrared soundings, plus improved temperature control and reliability. This paper will describe the ATMS sensor characteristics in comparison with its predecessor, the Advanced Microwave Sounding Unit (AMSU), and present the first comprehensive evaluation of key pre-launch and on-orbit performance parameters. A thorough evaluation of the performance of ATMS is especially important for this first flight unit of what will eventually be a series of ATMS sensors providing operational sounding capability for the US and its international partners well into the next decade.

Tuesday, March 25	Snow and Ice	13:00 - 14:40
Lecture Session		Ramo Auditorium, Bldg 77

Session Co-Chairs: Joel Johnson, Ohio State University; Martti Hallikainen, Aalto University

Paper 1 SNOW LAYERING EFFECTS ON L-BAND PASSIVE MEASUREMENTS AT DOME C - ANTARCTICA
13:00 *Marco Brogioni, Simone Pettinato, Francesco Montomoli, Giovanni Macelloni, IFAC -CNR, Italy*

Back in 2004 the Microwave Remote Sensing Group at IFAC-CNR started the ground-based Domex experiment at Concordia Station (Antarctica, 75°06'06'S 123°24'43'E) for monitoring the L- band microwave emission of the plateau. The experiment, founded by the European Space Agency and by the Italian Research Program in Antarctica, was aimed at charactering the emission of the Dome C region in order to use it as an external calibrator for low-frequency microwave space-borne radiometers and the ESA's SMOS satellite in particular. The research started in 2004 with a pilot-project of a one month duration, had a second period of acquisition from 2009 to 2010, prosecuted in December 2012 and it is still on-going. It is expected that the experiment will stop in December 2015. The L-band radiometer (RADOMEX) was installed on a observation tower at an height of 15 m above the surface and data were collected at a fixed incidence angle of 42 degs during winter period while observation at different incidence angle and sky observation were performed in summer. Together to microwave data, snow physical properties were collected along the experiment. The acquired data confirm that the microwave emission of the Dome C site at L-band can be considered stable (especially at V polarization) for periods several months long. A very good correlation with SMOS data is also noticed. Beside this major result, a deeper analysis of the microwave time series revealed that L band data at H polarization are quite sensitive (1-2 K) to the changes in the firsts layers of the snowpack mainly caused by the wind ablation and deposition. Moreover, during the summer season, it was observed that H polarization reveals a significant Tb fluctuation which is due to the contribution of the Sun emission reflected by the snowpack into the radiometer antenna. Whereas this effect is largely expected, what is of a particular interest is that the increases and decreases of the Tb is not monotonic according to the relative position of the star with respect to the instrument, and it presents significant oscillations due to the multiple-reflection occurred in the interfaces of the ice-sheet layers. In order to assess the dependency of L-band microwave emission on geophysical properties of the Antarctic snowpack, in particular of the upper layers, a dedicated multi-layer microwave emission model was developed. Since the size of the scatterers with respect to the wavelength is very small, we choose to simulate the scattering under the Rayleigh approximation in order to keep the code simple and fast. The inputs of the model were obtained from ground measurements (collected during the Domex and EPICA experiments) and by physical ice-sheet models (e.g. for the snow temperature or density profiles). Model simulations are in good agreement with RADOMEX measurements and can explain how the snow-layering is able to produce the observed results.

Paper 2 **ON THE RELATIONSHIPS BETWEEN THE GEOPHYSICAL PROPERTIES OF THE ICE-SHEET AND L-BAND RADIOMETRIC DATA IN ANTARCTICA**
13:20 *Giovanni Macelloni, Marco Brogioni, IFAC -CNR, Italy*

In the last decade different Space Agencies have promoted L-band radiometric missions with the purpose of investigating on two Essential Climate Variable: ocean salinity and soil moisture. While the ESA's SMOS mission is devoted to the investigation on both physical quantities the NASA dedicates a single mission for each: Aquarius for the ocean salinity, and SMAP for soil moisture which will be launched in 2014. Beyond these specific topics, the global scale availability of low-frequency data has opened to the investigation in other research fields including the cryosphere. Because of the low losses, the penetration depth in dry snow and ice at L-band is estimated to range from several hundred up to one thousands of meters. While on one hand this fact limits the use of this frequency for investigating on snow on land, on the other side this is very attractive for the analysis of the deep ice caps and Antarctica in particular. In the last years several works were devoted to study the spatial variability and temporal stability of brightness temperature over the East Antarctic plateau especially around Dome C [1]. These studies demonstrated that this region exhibits a high temporal stability on annual scale, showing a Tb variation lower than 1 K at V polarization, but also revealed several areas where the brightness temperature is particularly homogeneous and differs appreciably from the surrounding ones. Although several attempts were performed to explain these data, a systematic analysis was not yet performed. In the present work we try to explain such Tb features by relating them to the geophysical properties of the Antarctic ice cap and also by using an electromagnetic model for assessing the obtained results. In order to investigate on these aspects, a comprehensive analysis was carried out here by using SMOS data collected in the 2010 – 2013 period. The area of interest was between 0° and 180° of Longitude, south of 66° Latitude. We considered only data acquired in the Alias Free - Field of View (AF-FOV) of the sensor. In particular we average all the data within the angular ranges 22.5°< ' < 27.5° and 52.5°< ' < 57.5°, resulting in mean observation angles of 25° and 55° respectively. Data collected in the whole time period were averaged and maps of Tb mean and Tb standard deviation were realized at H and V polarization. In particular, regions where the temporal standard deviation was lower than 1 K were considered for the next analysis. As first step the Tb maps were co-registered to bedrock and surface heights obtained from the Bedmap2 project [2]. In the analyzed regions it was found that at the same latitude (i.e. at similar surface temperature and accumulation rate) the Tb was clearly correlated to the bedrock height and to the ice thickness. With the aim of understand these results an electromagnetic model which uses as input real data and geo-physical models of ice sheet physical properties, appropriate for the interior of East Antarctic Ice Sheet, was developed. Model simulations are able to explain the obtained results and open to the possibility to derive the physical properties of deep layers of the ice sheet from low frequency measurements. [1] Macelloni, G., Brogioni, M., Rahmoune, R., "Characterization of the spatial and temporal stability of the east-antarctic plateau in the low-microwave bands", (2012), 12th Specialist Meeting on Microwave Radiometry and Remote Sensing of the Environment, MicroRad 2012 - Proceedings, art. no. 6185251, 2012. [2] Fretwell, P., et al. "Bedmap2: improved ice bed, surface and thickness datasets for Antarctica", The Cryosphere, 7, 375-393, doi:10.5194/tc-7-375-2013, 2013.

Paper 3 **REMOTE SENSING OF ICE SHEET SUBSURFACE TEMPERATURES**
13:40 *Mustafa Aksoy, Joel Johnson, Kenneth Jezek, The Ohio State University, United States*

Understanding the behavior of polar ice sheets and predicting their future changes are very important goals for improving understanding of weather, climate, and the water cycle on Earth. Currently many geophysical quantities about ice sheets such as ice sheet surface topography, ice surface velocity, mass change, ice sheet thickness, seaward bathymetry, surface accumulation rate and basal geology can be retrieved via airborne and spaceborne remote sensing instruments. Internal ice sheet temperature is absent from this list although it is a primary factor to determine the internal ice deformation and ice flow across the base. Therefore, remote sensing of subsurface temperature of ice sheets is crucial for better understanding polar ice sheet dynamics. Microwave radiometry offers potential opportunities to remotely sense internal ice sheet temperatures. Using models for ice sheet internal temperatures, electromagnetic permittivity, and other physical parameters such as density and particle grain size, the microwave emission from an ice sheet can be computed. Such studies utilize the dense media radiative transfer theory for multi-layered media (DMRT-ML). In this presentation, microwave emission from ice sheets with varying physical and electromagnetic properties computed using DMRT-ML will be examined for different frequencies. Results which indicate that emissions at different frequencies correspond roughly to different depths of the ice sheet will be shown. Extension of this concept into the possibility of remote sensing of subsurface temperatures via a wideband microwave radiometer will also be discussed. Finally, an ultra-wideband software defined microwave radiometer design will be proposed for future experiments in ice sheet subsurface temperature sensing.

Paper 4 **BRIGHTNESS TEMPERATURE OF SNOW ON LAKE ICE IN THE 1.4 TO 36.5 GHZ RANGE**
14:00 *Martti Hallikainen, Matti Vaaja, Jaakko Seppänen, Anssi Hakkarainen, Juha Kainulainen, Aalto University, Finland*

Space-borne microwave radiometers are presently the only sensors that provide information on the water equivalent (SWE) of dry snow. In northern lake-rich regions the effect of lakes to the satellite-derived brightness temperature must be accounted for in order to obtain adequate accuracy in SWE retrieval. Due to the modest spatial resolution of space-borne data, detailed investigation of the brightness temperature behavior of snow on lake ice can be only done with airborne radiometers. We have investigated the brightness temperature behavior of snow on lake ice by conducting airborne radiometer measurements over two lakes in southern Finland since 2004 and with a more intense schedule since 2011. The flight path includes two lakes of different sizes and, additionally, a forested area and an open, mostly agricultural area. This allows us to compare the behavior of the brightness temperature of snow on lake ice with that of snow on terrain. The main airborne instrument is our HUTRAD system, which operates at 6.8, 10.7, 18.7, 23.8, and 36.5 GHz, providing data for both vertical and horizontal polarization at an incidence angle of 50 degrees off nadir. The antenna beamwidth is 3 to 5 degrees depending on frequency. Additional data have been collected with our HUT-2D interferometric imaging radiometer, which operates at 1.4 GHz and looks straight down covering an incidence angle range up to ±25 degrees with a swath of 95 % of the flight altitude. The radiometers are accommodated on our Skyvan research aircraft. In-situ measurements have been made simultaneously with airborne data collection. We have covered a variety of conditions including dry snow/ice, occasional water on top of ice, moist snow surface, and the melting season. In order to study the effect of diurnal temperature variations during the melting season we have collected data both in the morning (dry refrozen snow) and afternoon (moist topmost snow layer). Our results indicate that radiometer response to the snow/ice system depends mainly on snow surface grain size at 36.5 GHz. A 15-cm layer of snow on lake ice may cause volume scattering effects equal to those caused by a 50-cm snowpack on terrain. At 6.8 GHz the occasional presence of water on top of ice may cause the brightness temperature to vary substantially from that for dry conditions. We include for the first time the behavior of the 1.4 GHz brightness temperature behavior of snow on lake ice in our analysis and compare it to that of snow on terrain, including open and forested areas next to the two lakes.

Paper 5 **SNOW MICROSTUCTURE SIMULATIONS USING THERMODYNAMIC SNOW MODEL SNOWPACK – APPLICATION TO HUT SNOW EMISSION MODEL**
14:20 *Anna Kontu, Juha Lemmetyinen, Leena Leppänen, Juho Vehviläinen, Jouni Pulliainen, Finnish Meteorological Institute, Finland*

The microstructure of snow particles (size, shape and cohesion of ice grains), as well as distinct layered structures, are known to affect the microwave emission from natural snowpacks [1], [2], [3]. A priori information and forward modelling capability of these characteristics is a prerequisite for successful retrieval of key snowpack characteristics, such as Snow Water Equivalent, from passive microwave radiometry. Recent efforts in the field of modelling the propagation of microwaves in snow have been focussed on these effects. Detailed in situ observations can be applied to extract the necessary information to drive snow models; however, an acknowledged problem in this respect is the actual measure sensitive to microwave propagation, and methods to measure these characteristics objectively in the field. Moreover, considering the practical retrieval of snow characteristics on a global scale by means of model inversion, the use of in situ information is not feasible. The application of physical snow models to predict snow structure has been demonstrated to improve model predictions (e.g. [4]) and thus show promise of being applicable in retrieval schemes. In this study, we present recent results of using the SNOWPACK model [5], coupled with the HUT snow emission model [3], [6], in estimating the microwave emission from snow. SNOWPACK simulations are compared to in situ data on snow properties; moreover, estimates of the coupled SNOWPACK and HUT models are compared to a time series of snow brightness temperature observations. The collected experimental data from Sodankylä, Finland comprises of tower-based microwave brightness temperature observations, detailed measurements of snow properties and of ancillary data required to successfully drive the SNOWPACK model. Manual measurements on snow structure are made weekly, including objective measurements of snow microstructure [7]. The experimental data currently covers four winter seasons from 2009 to 2013. Results show that the coupled response of the SNOWPACK and HUT models can be used to simulate the brightness temperature response with accuracy better or comparable to that of directly applying in situ measurements. However, the snow microstructure parameters predicted by SNOWPACK show good correlation with measured in situ information on snow, provided that appropriate scaling factors are applied. [1] Wiesmann, A., and C. Mätzler, 1999. Microwave emission model of layered snowpacks. Remote Sens. Environ., 70(3) 307 - 316. [2] Liang, D., X. Xu, L. Tsang, K. M. Andreadis, and E. G. Josberger, 2008. The effects of layers in dry snow on its passive microwave emissions using dense media radiative transfer theory based on the quasicrystalline approximation (QCA/DMRT). IEEE Trans. Geosci. Remote Sens., 46(11): 3663–3671. [3] Pulliainen, J., J. Grandell, and M. T. Hallikainen, 1999. HUT snow emission model and its applicability to snow water equivalent retrieval. IEEE Trans. Geosci. Remote Sens., 37, 1378–1390. [4] Brucker, L., A. Royer, G. Picard, A. Langlois, and M. Fily, 2011. Hourly simulations of the microwave brightness temperature of seasonal snow in Quebec, Canada, using a coupled snow evolution–emission model. Remote Sens. Env., (155): 1966-1977. [5] Lehning, M., P. Bartelt, B. Brown, C. Fierz, and P. Satyawali, 2002. A physical snowpack model for the Swiss avalanche warning part 2. snow microstructure. Cold Reg. Sci. Technol., 35, 147-167. [6] Lemmetyinen, J., J. Pulliainen, A. Rees, A. Kontu, Y. Qiu, and C. Derksen, 2010. Multiple layer adaptation of the HUT snow emission model: comparison with experimental data. IEEE Trans. Geosci. Remote Sens., 48, 2781-2794. [7] Gallet, J.C., F. Dominé, C. S. Zender, and G. Picard, 2009. Measurement of the specific surface area of snow using infrared reflectance in an integrating sphere at 1310 and 1550 nm. The Cryosphere, 3, 167-182.

Session Co-Chairs: Sharmila Padmanabhan, NASA - Jet Propulsion Laboratory; Andreas Colliander, NASA - Jet Propulsion Laboratory

Paper 1 SMOSNEXT MISSION: STATUS OF THE PROJECT

Yann Kerr, Bernard Rougé, CESBIO, France; Eric Anterrieu, IRAP, France; François Cabot, Ali Khazaal, Younes Moujid, Yan Soldo, CESBIO, France

During the last decades the need for a global estimation with high temporal resolution of key environmental variables such as soil moisture and ocean salinity has grown greatly (Robock et al. 2000; Dai et al. 2004; Roemmich et al. 2000). Satellites represent the best mean for satisfying such need, and several instruments have been launched onboard European and American satellites with the intent of retrieving large-scale soil moisture and ocean salinity maps. These instruments are based on different principles. They may involve radiometers (Njoku et al. 2003), scatterometers (Bartalis et al. 2007), interferometric radiometers (Kerr et al. 2001), or they may rely on both passive and active elements (LeVine et al. 2007; Entekhabi et al. 2010). Although different technologies were adopted, all these instruments are limited by a spatial resolution of few tens of kilometers. In order to be able to make use of these data in hydrological models, and for many other applications, like the survey of water resources at the scale of irrigated zones, a better spatial resolution must be achieved, typically it should be improved by an order of magnitude. To assure continuous monitoring of soil moisture and ocean salinity, while attaining an unprecedented fine spatial resolution, an original concept was proposed in Kerr et al. 2010, which aims at achieving a spatial resolution of few kilometers while maintaining roughly the same radiometric resolution. This presentation will give an overview of the new concept : SMOS next, together with project status and the main accomplishments in terms of theoretical modelling of the instrument hardware principle validation and next steps.

Paper 2 SCANNING L-BAND ACTIVE PASSIVE (SLAP)—A NEW AIRBORNE SOIL MOISTURE SENSOR

Edward Kim, NASA, United States; Tammy Faulkner, NASA/ ASRC, United States; Albert Wu, NASA/Emergent Space Technologies, United States; Cornelis du Toit, NASA/ AS&D, United States; Victor Marrero, Mark Wong, Damon Bradley, Lynn Miles, NASA, United States; Jinzheng Peng, NASA/ Morgan State Univ., United States; Steve Seufert, NASA, United States

Two recent satellite missions feature L-band microwave observations at their core: the Soil Moisture Ocean Salinity (SMOS) mission from ESA (Kerr, et al, 2001) and the Aquarius sea surface salinity mission from NASA (Lagerloef, et al 1995). In the near future, NASA plans to launch the Soil Moisture Active Passive (SMAP) mission (Entekhabi, et al., 2010), to provide global soil moisture products with resolutions in the 10–40 km range. SMAP and SMOS, with their focus on soil moisture, are particularly sensitive to the natural heterogeneity of land surface conditions (vegetation, topography, soil texture, surface roughness, open water). Their soil moisture retrieval algorithms are relatively complex (Wigneron, et al, 2007), particularly SMAP's combined active-passive algorithm—the key to achieving the highly-desired 10 km spatial resolution by combining the higher-resolution but noisy active radar observations with the lower-resolution but more accurate passive radiometer observations. Airborne simulators have played a critical role related to these missions. A partial list would include the ESTAR instrument (Swift et al, 1995) used to develop and demonstrate early soil moisture retrievals at large scales using passive-only observations, the PLMR and EMIRAD instruments (Panciera, et al, 2008; Skou, et al, 2005) used extensively for calibration/ validation of SMOS, and the PALS instrument (Wilson, et al, 2001)—one of the few combined radar-radiometers. Recently, the demand for L-band airborne simulators has increased in the USA as new applications beyond just SMAP have appeared, leading to the development of a new airborne simulator named Scanning L-band Active Passive (SLAP) built by NASA's Goddard Space Flight Center. SLAP is expected to be available for algorithm refinement work prior to SMAP launch, for post-launch calibration/validation activities, as well as other applications that rely on L-band sensing. SLAP's principal features are a) a new thin aerodynamic antenna to permit simple accommodation on multiple aircraft, b) a real-aperture radar at 1.26 GHz and a radiometer at 1.4 GHz, c) a dual-frequency dual-polarized antenna enabling quad-pol radar and 4-Stokes radiometer operation with the same antenna at the SMAP incidence angle of 40 degrees, d) conical scanning via a rotating antenna to simulate the conical scanning of SMAP, e) use of identical or nearly-identical RF front end parts as the SMAP radiometer, for high-fidelity simulation of SMAP performance, f) a digital backend that exactly mimics the SMAP digital backend, including RFI processing code, This paper will present the details of the design of SLAP as well as performance evaluations of the antenna, radiometer, radar, and digital backend. Performance results from SLAP's initial test flights will be described.

Paper 3 FARADAY ROTATION ANGLE RETRIEVAL USING SMOS RADIOMETRIC DATA

Lin Wu, Ignasi Corbella, Francesc Torres, Nuria Duffo, Universitat Politecnica de Catalunya, Spain; Manuel Martín-Neira, European Space Agency, Netherlands

SMOS is an European Space Agency (ESA) mission designed to provide global maps of soil moisture over land and sea surface salinity over oceans. It has a single payload named MIRAS (Microwave Imaging Radiometer with Aperture Synthesis) responsible of measuring the polarimetric brightness temperature of the Earth surface, wich in turn is injected into scientific models for estimating both geophysical parameters. At the instrument operating frequency (1.4 GHz), Faraday rotation is not negligible and must be corrected for accurate retrievals. The Faraday rotation effect is summarized as follows: As microwave radiation from earth propagates through the ionosphere, the field components are rotated by an angle that depends on the total ionospheric electron content (TEC), the frequency, the Earth magnetic field and geometrical parameters. From the point of view of SMOS data processing, all these parameters are known, either from external sources or from the instrument configuration and attitude. Particularly, the so-called "consolidated TEC" is available globally for each day with a delay typically of 15 days since radiometric data acquisition. For faster processing, an estimation of the TEC is also available, although with much less quality. For improved data processing it is desirable to get the Faraday rotation angle directly from the SMOS radiometric data in a continuous way. This is possible using the full polarimetric capability of the SMOS data. The rotation matrix of the polarimetric brightness temperature from ground to antenna frame depends on the total rotation angle, with is the sum of the geometrical and the Faraday contributions. If at ground frame the third and fourth Stokes parameters are assumed to have negligible values compared to horizontal and vertical brightness temperature, the total rotation angle can be computed by phi=0.5*atan(U/Q) where Q and U are the second and third Stokes parameters at antenna frame respectively. Substracting the geometrical angle from this result, the Faraday rotation angle is estimated. Using this procedure out of current SMOS data is not as straightforward as it may seem. MIRAS has relatively poor radiometric sensitivity (thermal noise) and accuracy (spatial bias), and this makes it difficult to estimate the Faraday rotation angle with the required quality. Improved data procesing and error correction techniques have been developed in order to obtain better polarimetric brightness temperature with respect to the current version of the SMOS data. This, toghether with smart filtering methods has resulted in good estimations of Faraday rotation angle, which compare very well with the ones computed using the consolidated TEC. Furthermore, rotation angle obtained ony from radiometric data has been used to estimate the ionospheric TEC. Except in the areas where the Earth magnetic field is perpendicular to the line of sight (in which the rotation angle is zero), the result matches quite well with the values provided in the consolidated TEC in SMOS auxiliary data files. The MicroRad presentation will describe in detail the procedures designed for the successful estimation of Faraday rotation angle using SMOS radiometric data.

Paper 4 ANALYSIS AND CHARACTERIZATION OF THE NOISE FLOOR IN MICROWAVE INTERFEROMETRIC RADIOMETERS

Raúl Díez-García, Manuel Martín-Neira, European Space Agency, Netherlands

The European Space Agency (ESA) Soil Moisture and Ocean Salinity mission (SMOS) is intended to provide continuous global maps of soil moisture and ocean surface salinity. Its payload MIRAS (Microwave Imaging Radiometer with Aperture Synthesis) is an L-band interferometric radiometer which achieves unprecedented low-frequency resolution. It was successfully launched on November 2009 under the European Space Agency Earth Explorers program, and is now acquiring high precision data which shows sufficient orbital stability. Although the analysis presented here has been done in the framework of SMOS, the conclusions are also valid for other types of missions using Synthetic Aperture Radiometers for observing planetary surfaces from space. This paper assesses and analyses the observed noise floor in SMOS brightness temperature images, to improve further the accuracy of the data, which would allow new scientific breakthroughs. The noise floor is defined as that the time-averaged residual spatial ripple that remains after an image reconstruction process, assuming perfect knowledge of the instrument and no calibration errors. The noise error is therefore completely independent to the radiometric noise or the presence of modelling errors, being then solely related with the reconstruction process, summarized by the matrix G. It is known that a condition which makes the noise floor to appear is to have small differences between the antenna patterns. In the case of SMOS, antenna patterns differ by up to 0.57% (0.05 dB) of the nominal peak value. This differences, among other smaller contributions (like the fringe-washing function), introduce the undesired spatial ripple in the processed images, which cannot be improved using Gibbs-reducing techniques. In the present work, the reconstruction error, formulated using linear algebra theory, shown to be linked with the fundamental metrics of G. The presented approach on the representation of the reconstruction error provides a fundamental tool to understand the origin of the noise floor and to attempt to minimize it. To validate the theoretical results, several simulations have been performed, cross-comparing the conclusions with actual SMOS level 1 processed data. In addition, the performance of some correction strategies is assessed.

Paper 5 ADVANCED MULTIPLE-BEAM RADIOMETER SYSTEMS FOR FUTURE SPACEBORNE OCEAN MISSIONS.

Niels Skou, Sten Søbjærg, Technical University of Denmark, Denmark; Cecilia Cappelin, Knud Pontoppidan, TICRA, Denmark

The next generation of spaceborne microwave radiometer missions, aiming at measuring sea surface temperature and the wind vector, will require very good radiometric sensitivity around 0.25 K and at the same time good spatial resolution approaching 20 km at C and X bands and 10 km at Ku band. For a representative 800 km orbit and 53 deg incidence angle, the footprint requirement calls for antennas with 5 m electrical aperture, and the useful swath is 1500 km. Since the bandwidths are limited to a few hundreds of MHz, even the most optimistic receiver noise properties cannot ensure the required radiometric sensitivity when considering a single beam scanning system. The only way forward for scanners is to employ several independent antenna beams per frequency, and achieve sensitivity by integration of the several footprints. This calls for a host of feeds and associated receivers – in the present case up to 30 beams at Ku band. An alternative to a scanner is the push-broom system, in which a large number of antenna beams simultaneously sense the Earth. Each antenna beam is associated with a feed and a receiver, and sensitivity is achieved due to the fact that all across track footprints do not have to be multiplexed through one single receiver, but each footprint is measured by it's own receiver. Sensitivity is no longer a problem, but a more complicated antenna design is needed as well as many receivers – in the present case up to 390 at Ku band. A trade-off can, however, be made between number of receivers, hence swath width, and time to cover the globe. The many beams makes it impractical to consider traditional feed horns due to congestion in the feed area. Instead, a dense array of a large number of smaller antenna elements will be used, and by summing the outputs from clusters of those, properly in phase and amplitude, the individual beams are generated. Each element has its associated receiver followed by a suitable A to D converter and the beam forming takes place in a computing system (FPGA). The large antennas in question, 5 m parabolic dish for the scanner, and an even larger torus reflector for the push-broom, calls for the use of a knitted metal mesh supported by a peripheral ring. This technology provides relatively low weight, and the antenna can be folded for launch. Three viable systems will be discussed and compared: a 5 m aperture scanner with many beams per frequency / a 5 x 8 m torus push-broom having 154 beams at Ku band (and a reduced swath of 600 km corresponding to a ± 20 deg "scan") / a system using 2 "standard" 5 m reflectors each using a ± 10 deg "scan" in a push-broom mode. The beam forming method described above makes it possible to illuminate the reflector suitably and achieve very good beam performance even when going 10 deg off boresight. Also issues like receiver architecture, calibration, RFI detection and mitigation will be discussed.

Paper 6 PASSIVE AND NOISE ILLUMINATED IMAGING OF W-BAND RADIOMETER

Ki-In Kim, Gwangju Institute of Science and Technology, Republic of Korea; Jun-Ho Choi, Agency for Defense Development, Republic of Korea; Joon-Ho So, Agency for Defense Developement, Republic of Korea; Yon-Hoon Kim, Gwangju Institute of Scienec and Technology, Republic of Korea

The imaging radiometer from microwave to sub-millimeter wave can be used not only for remote sensing, but also target identification in indoor environment. Unlike to visible and IR sensor, the image contrast of millimeter-wave radiometer in indoor is very poor because of the image background thermal noise is very high compare with target brightness temperature. To improve the image quality contrast, an incoherent wideband noise source is used to illuminate the target and acquired the high contrast microwave image. In this paper, a wideband noise source of ENR 15 dB, 50 cm aperture size of lens antenna, direct detection radiometer of 45 dB gain and focal plane receiver at W-band are described. Before image capture of the targets, two points calibration using hot and cold source was done to fix the brightness temperature resolution of designed imaging radiometer. The passive images captured by designed total power type radiometer and the noise illuminated images from noise source using same receiver are presented and compared the different characteristics of two case images. The brightness temperature images of target are acquired by change illumination level of noise source, illumination angle between noise source and target. Also the images affected by vertical (V), horizontal (H) polarization at receiver side is observed and analyzed the polarization effect briefly. The illumination effects of image by noise source is modeled and analyzed to understand the characteristics of noise illuminated image. To identify the target only in the image, the background of target is normalized to remove the background thermal noise. The detail experiments and captured image characteristics of passive and noise illumination will be described in the paper.

Paper 7 CLOCK SCANNING MICROWAVE INTERFEROMETRIC RADIOMETER AND ITS POTENTIAL APPLICATIONS AT GEOSTATIONARY ORBIT

Cheng Zhang, Ji Wu, Hao Liu, Jingye Yan, National Space Science Center,Chinese Academy of Sciences, China

Microwave (MW) radiometry is a well-established passive technology for remote sensing of the environment. MW radiometers have been flown, so far, on Low Earth Orbiting (LEO) satellites in order to achieve a required spatial resolution. This, however, produces low temporal resolution data since the satellite usually generates two snapshots per day for any given location over the earth at middle latitudes and less for equatorial areas. Applying passive microwave sensor in GEO earth observations are of special interest because it has the advantages of temporally continuous and spatially large coverage compared to the LEO systems. Unfortunately the required horizontal resolution leads to a rather large antenna size in GEO which is unpractical for the traditional real aperture radiometers especially in low frequency bands. Several attempts are made to evaluate launching a GEO satellite carrying MW radiometers. These attempts consist of both real aperture technique with a large parabolic reflector and aperture synthesis technique with an array composed by a large number of small antenna elements. All these GEO concepts are operating at high frequencies of millimeter or sub-millimeter waves to reduce the antenna size. Low frequency bands specifically lower than 50GHz are deemed as unpractical to obtain the required horizontal resolution from GEO for the reason of over-endurable large antenna size, even though these low frequencies are very important for numerical weather prediction (NWP) and climate research. The new concept of clock scanning microwave interferometric radiometer (CS-MIR) using aperture synthesis provides an opportunity to resolve this problem. The array of CS-MIR is composed by two groups of coplanar antenna elements, which are laid on two concentric circles and connected to a fixed central axis by two groups of arms. The two groups of antenna elements are rotating at two different speeds. This kind of rotation is similar in spirit to the clock hands rotation, and is named as clock scan. The array configuration of CS-MIR is quite feasible for folding during launch and deploying after entering orbits. In this paper we specifically focus on an array configuration of 2+2 arm with multi-endpoint, which is deemed as the best choice for the space borne instruments, by far, because it is easy to actualize rotation balance with the least arm number. By utilizing counter-rotation, i.e. the two antenna groups rotate in the opposite directions, the moment of inertias of the two antenna groups can be easy to compensate each other, which is very important for maintaining the platform balance during rotating scan. Multi antenna elements arranged at the endpoint of each arm are helpful to increase the radiometric resolution. Some approaches of CS-MIR, specifically on the items of array configuration, sampling patterns and imaging algorithm, are described in this paper. The potential applications at GEO are also presented. The user requirements for some geophysical variable observations where CS-MIR at GEO is potentially applicable are described, which are consistent to WMO observational requirements for global numerical weather prediction (GNWP) and Regional NWP (RNWP). According to these user requirements, the preliminary design of MW CS-MIR operating on the MW channels below 50GHz and recommended by EUMETSAT are presented.

Paper 8 EFFICIENT DECONVOLUTION AND SPATIAL RESOLUTION ENHANCEMENT FROM CONTINUOUS AND OVERSAMPLED OBSERVATIONS IN MICROWAVE IMAGERY

Igor Yanovsky, Bjorn Lambrigtsen, Alan Tanner, Jet Propulsion Laboratory, United States

In this paper, we propose a novel and efficient image and signal processing methodologies and apply these techniques to reduce PATH image blurring and distortion inherent in an aperture synthesis system as well as enhance spatial resolution from continuous and oversampled observations. Hurricanes and other physically deforming phenomena will soon be continuously imaged using geostationary microwave sensors, which are designed to penetrate through thick clouds to see the structure of a storm. Such images may represent distribution of temperature, water vapor, and cloud liquid water and are valuable for evaluating the storm's internal processes and its strength. However, imagery generated using microwave sensors is blurry, noisy, and of low resolution. Multi-frame super-resolution reconstruction produces a high-resolution image from a sequence of low-resolution images. Our proposed super-resolution methodologies are based on current research in sparse optimization and compressed sensing, which lead to unprecedented efficiencies for solving image reconstruction problems. An important step in multi-frame super-resolution is deconvolution, which reverses effects of a blurring sensor point spread function on observed data. We minimize the deconvolution problem within the Split Bregman minimization framework and demonstrate a factor of a hundred computational time improvement generating deconvolved results using the new approach over already robust total-variation energy minimization techniques. As recommended by the National Research Council (NRC) in the Decadal Survey, PATH should be implemented as a "MW array spectrometer", which has been interpreted as an aperture synthesis system. One such system is the Geostationary Synthetic Thinned Aperture Radiometer (GeoSTAR) that has been developed at JPL under the NASA Instrument Incubator Program. A characteristic of such a system, which functions as a spatial interferometer observing in the spatial Fourier domain, is that the point spread function (PSF) is a 2-dimensional sinc-like function that produces ringing at sharp edges and other transitions in the observed field. The conventional approach to suppressing interferometric sidelobes is to apply apodization, which has the side effect of degrading spatial resolution by a factor of 1.5 - 2. Our approach simultaneously reduces image ringing substantially while sharpening the image and preserving information content. In contrast to apodization, preliminary results indicate that our approach to sidelobe suppression leads to an improvement in spatial resolution by a factor of 4 over the conventional apodization method. Furthermore, proposed multi-frame super-resolution method is robust to image noise and noise in the point spread function and leads to additional improvements in spatial resolution. With the developed methods for improving spatial resolution of satellite sensors through image processing techniques, it will be possible to reduce the physical aperture size of satellite instruments without sacrificing spatial resolution as is normally the case.

Paper 9 INTEGRATION AND TEST VALIDATION OF GEOSTAR II: INITIAL RESULTS

Isaac Ramos, Todd Gaier, Alan Tanner, Pekka P. Kangaslahti, JPL, United States

The Geostationary Synthetic Thinned Array Radiometer (GeoSTAR) demonstrator [1] has been successfully developed under NASA's Instrument Incubator Program over the last years. Following the NASA Earth Science Decadal Survey [2] recommendations in the Precipitation and All-weather Temperature and Humidity (PATH) mission [3], a second version, GeoSTAR II [4], is under development. GeoSTAR II is a Y-shaped array interferometric radiometric sounder of 144 elements operating at the millimeter-wave water vapor absorption line (165-183 GHz region). This work presents the most recent GeoSTAR II integration activities including alignment of antenna array assemblies in a ground plane structure. Array assemblies consist of nine manifolds of 4x4 elements, each of which incorporates local oscillator (LO) distribution for 16 receivers. Each manifold has four intermediate frequency (IF) circuit boards, each of which supports four Monolithic Microwave Integrated Circuit (MMIC) receiver modules. The main function of the MMIC module is to amplify the input signal with two InP FET Low Noise Amplifier (LNA) in series and down-convert it with an harmonic I/Q mixer [5] to IF (10-500 MHz). A previous step to assemble the subsystems is to validate electrical performance, including crosstalk in the IF boards, noise figure, gain, and I/Q phase quadrature error of all the MMICS. To provide relevant tests over the full IF bandwidth (500 MHz), a Field Programmable Gate Array (FPGA) correlator with a sampling frequency of 1 GHz has been applied. Other integration and testing tasks include alignment of the gate and drain voltages in the MMIC amplifiers. Furthermore, a temperature test has been carried out on the MMICs, IF board and manifold over a temperature range from -15 ˚C to +50 ˚C observing lineal decreasing gain of 0.043 dB/˚C close to the thermal drift of the output power 0.033 dBm/˚C. REFERENCES [1] A. Tanner, W. Wilson, B. Lambrigtsen, S. Dinardo, S. Brown, P. Kangaslahti, T. Gaier. C. Ruf, S. Gross, B. Lim, S. Musko, S. Rogacki, and J. Piepmeier, "Initial results of the Geostationary Synthetic Thinned Array Radiometer (GeoSTAR) demonstrator instrument" IEEE Trans Geoscience Remote Sens., vol. 45, pp 1947-1957, 2007. [2] R. Anthes, and B. Moore (ed.) "Earth science and applications from space national imperatives for the next decade and beyond", National Academies Press, Washington, D.C. 2007. [3] B. Lambrigtsen, S. Brown, T. Gaier, L. Herrell, P. Kangaslahti, A. Tanner, "Monitoring the hydrologic Cycle with the PATH mission", Proceeding of the IEEE vol. 98, No 5, May 2010. [4] T. Gaier, et al, "GeoSTAR-II: A prototype water vapor imager/sounder for the PATH mission", Geoscience and Remote Sensing Symposium (IGARSS), 2011 IEEE International, pp 3626 – 3628, 2011. [5] P. Kangaslahti, D. Pukala, T. Gaier, A. Tanner, I O'Dwyer, B. Lambrigtsen, X. Mei, R. Lai "Miniature low noise G-band I-Q Receiver", Microwave Symposium Digest (MTT), 2010 IEEE MTT-S International , vol., no., pp.497,500, 23-28 May 2010

Tuesday, March 25	Instruments and Techniques II	14:40 - 16:00
Poster Session		Dabney Hall, Bldg 40

Session Co-Chairs: Sharmila Padmanabhan, NASA - Jet Propulsion Laboratory; Andreas Colliander, NASA - Jet Propulsion Laboratory

Paper 1 A 4 METER 180 TO 680 GHZ ANTENNA FOR THE SCANNING MICROWAVE LIMB SOUNDER

Richard Cofield, Samuel C. Bradford, Alyn Lambert, Paul Stek, Jet Propulsion Laboratory, United States; Eldon P. Kasl, Vanguard Space Technologies, Inc., United States

"A 4 Meter 180 to 680 GHz antenna for the Scanning Microwave Limb Sounder" Richard E. Cofield Jet Propulsion Laboratory 4800 Oak Grove Drive, MS 183-701 Pasadena, CA 91109-8099, USA Tel.:(818) 354-2501, Fax (818) 393-5065, email: Richard.E.Cofield@jpl.nasa.gov Presenting Author Affiliation: Richard E. Cofield Jet Propulsion Laboratory, California Institute of Technology. Co-authors: Samuel C. Bradford (1) Alyn Lambert (1) Paul C. Stek (1) Eldon P. Kasl (2) 1. Jet Propulsion Laboratory, California Institute of Technology. 2. Vanguard Space Technologies, Inc. The Scanning Microwave Limb Sounder (SMLS) is a space-borne heterodyne radiometer which will measure pressure, temperature and atmospheric constituents from thermal emission between 180 and 680 GHz. SMLS, planned for the Global Atmospheric Composition Mission of the NRC Decadal Survey, uses a novel toric Cassegrain antenna to perform both elevation and azimuth scanning. These provide better horizontal and temporal resolution and coverage than were possible with elevation-only scanning at the orbit spacings of two previous MLS satellite instruments. We report on a 2010 Instrument Incubator Program (IIP) to develop the SMLS antenna. This program continues a 2006 Small Business Innovative Research (SBIR) program whose phase II culminated in the fabrication and thermal stability testing of a composite demonstration model of the SMLS primary reflector. That reflector had the full 4m height and 1/3 the width planned for flight. The current project, titled "A deployable 4

Meter 180 to 680 GHz antenna for the Scanning Microwave Limb Sounder", contains 5 tasks: 1) detailed mathematical modeling of antenna patterns from which we simulated geophysical parameter retrievals in order to establish FOV performance requirements; 2) Correlation of finite-element model predictions with measurements made on the SBIR reflector. We also measure this reflector's deformations under more flight-like thermal gradients, using higher precision metrology techniques available in a large-aperture test facility at JPL; 3) fabrication of a full-width breadboard primary reflector followed by measurements and model correlation of its deformations during similar thermal gradient testing; 4) integration of the primary with other reflectors, and with residual front ends from a 2007 IIP, in a breadboard antenna; and finally 5) RF testing of the breadboard on a Near Field Range at JPL. This paper describes results in all 5 areas of the current IIP. Keywords: microwave limb sounding, composite reflectors, toroidal, thermal distortion, physical optics

Paper 2 POST-DETECTOR DIGITIZERS AND DIGITAL SPECTROMETERS. LESSONS LEARNED, TIPS AND TRICKS, AND THE FUTURE OF SPECTROMETERS FOR MICROWAVE RADIOMETERS

Robert Jarnot, Ryan Monroe, Sharmila Padmanabhan, Paul Stek, JPL, United States; Dan Werthimer, Borivoje Nikolic, UCB, United States

In this presentation we discuss traditional filterbank spectrometers and the newer digital implementations which will eventually replace them in all but the simplest applications. The current state of the art in digital spectrometers will be presented, as well as ongoing developments for lower power and wider bandwidth implementations. A popular form of post-detector digitizer for filter channels in simple microwave radiometers is the Voltage to Frequency Converter (VFC), as this provides a low noise (integrating) digitizer with a simple interface to an FPGA. This simple scheme is not without its drawbacks however, including limited resolution in broad bandwidth channels with short integration times, and flat spots in the VFC transfer function. Both of these issues, together with potential solutions and alternative digitizer schemes, are discussed. It appears that the future of spectrometers for microwave radiometers lies in the digital domain. Field results from broad bandwidth FPGA-based digital spectrometers, and ongoing developments in both FPGA-based and low power ASIC digital spectrometers are presented. In addition to replacing the older analog implementations, the digital implementations provide improved performance, stability, repeatability, manufacturability, and lower fabrication costs. The most common architectures for digital spectrometers are discussed, together with their relative strengths and weaknesses. Digital spectrometers also bring new opportunities, with the ability to detect RFI, and to provide digital corrections for sideband separation, and digital implementations for polarimetric systems. These digitally assisted implementations not only offer higher performance that the traditional analog approaches, but often simplify the analog portions of the implementation as well.

Paper 3 NOISE SOURCES FOR INTERNAL CALIBRATION OF MILLIMETER-WAVE RADIOMETERS

Chaitali Parashare, Pekka Kangaslahti, Shannon Brown, Douglas Dawson, Todd Gaier, Sharmila Padmanabhan, Alan Tanner, Oliver Montes, Jet Propulsion Laboratory, California Institute of Technology, United States; Victoria Hadel, Thaddeus Johnson, Xavier Bosch-Lluis, Steven C. Reising, Colorado State University, United States

We are developing a High-Frequency Wide-Band Airborne Microwave Radiometer to provide increased spatial resolution of wet-tropospheric path delay correction for coastal regions and inland water. In addition to the conventional low-frequency microwave radiometers at 18.7, 23.8 and 34.0 GHz, this airborne radiometer will include high-frequency millimeter-wave radiometers centered at 90, 130, and 166 GHz, in atmospheric window bands. The high-frequency millimeter-wave radiometers use a direct- detection architecture based on MMIC low-noise amplifiers (LNAs), a waveguide band-definition filter, and a diode detector. Nadir-viewing radiometers require internal calibration sources to permit a fixed radiometer viewing angle and avoid the need for any moving parts. We implement internal calibration using coupled noise diodes and Dicke-switched matched loads. We have developed a noise source using a beam-lead noise diode with a high excess noise ratio (ENR) of 17 dB, 9.6 dB and 6 dB at 90 GHz, 130 GHz and 166 GHz, respectively. This is the highest ENR ever measured at these frequencies for a noise diode meeting the radiometric stability, mass and size requirements, which enables us to achieve internal calibration for the high-frequency millimeter-wave channels. Furthermore, we have developed a novel approach that utilizes a MMIC LNA as a noise source in the 166 GHz frequency band. Both of these noise sources have demonstrated excellent stability of 0.07% per hour. This translates to < 0.1K per hour TA stability for cold ocean scene. We will present the preliminary stability analysis results obtained using the testbed developed at JPL and discuss the development of the millimeter-wave radiometers to be deployed on an airborne platform.

Paper 4 TECHNOLOGY DEVELOPMENT FOR A HYPERSPECTRAL MICROWAVE ATMOSPHERIC SOUNDER

Bill Blackwell, MIT Lincoln Laboratory, United States

The MIT Lincoln Laboratory and NASA Goddard Space Flight Center have partnered to develop a Hyperspectral Microwave Atmospheric Sounder (HyMAS). Funded through ESTO's Advanced Component Technology program, the hyperspectral radiometer will use six receivers and a compact Low Temperature Co-fired Ceramic (LTCC) Intermediate Frequency Processor (IFP) to sample 52 channels about the 118.75-GHz Oxygen and 183.31-GHz Water Vapor absorption lines. The channel passbands are selected to correspond to closely spaced temperature and humidity weighting functions. Simulations indicate this 'hyperspectral' microwave set of channels will yield all-weather sounding capability comparable to hyperspectral infrared sounders in clear air with vertical resolution up to 1 km. Surface precipitation rate and water path retrievals for small hail, soft hail, or snow pellets, snow, etc. with accuracies comparable to those of the Advanced Technology Microwave Sounder are possible. Further improvements in retrieval methodology (for example, polarization exploitation) are expected. This project aims to develop compact filter and receiver technologies for demonstrating microwave hyperspectral sounding. HyMAS comprises four 118 GHz and two 183 GHz receivers, three dual-polarized lens antennas, the IFP, power supply, thermal control, and data handling system. Each receiver includes a dielectric resonator oscillator, single-sideband mixer, and an integrated IF amplifier. Each IF passband spans 18 – 29 GHz and is passed to the IFP. The IFP with its LTCC Substrate Integrated Waveguide (SIW) filter banks, is a key technological advancement enabling the novel hyperspectral capability of HyMAS in a super compact design. The IFP amplifies, filters, detects and digitizes the six IF passbands into the 52 channels of aggregated data. The IFP will use a Serial Peripheral Interface (SPI) for passing the digitized data to the scanhead computer. The entire IFP is packaged within a volume of 10 x 10 x 1 cm^3. HyMAS will be the third in a series of radiometer scanheads that share a common scanning pedestal with the Conical Scanning Microwave Imaging Radiometer (CoSMIR) and Compact Scanning Submillimeter-wave Imaging Radiometer (CoSSIR). The instrument pedestal uses an azimuth over elevation mechanism to achieve across track and conical scanning with period calibration using two blackbody references. The instrument package is compatible with NASA's DC-8, WB-57, and ER-2 high-altitude aircraft that are well suited for atmospheric research. Successful completion of this project will result in the HyMAS scanhead ready flight demonstration.

Paper 5 NEW POSSIBILITIES FOR GEOPHYSICAL PARAMETER RETRIEVALS OPENED BY GCOM-W1 AMSR2

Elizaveta Zabolotskikh, Russian State Hydrometeorological University, Russian Federation; Leonid Mitnik, V.I. Il'ichev Pacific Oceanological Institute, Russian Federation; Nicolas Reul, Bertrand Chapron, IFREMER, France

The Advanced Microwave Scanning Radiometer 2 (AMSR2) onboard the GCOM-W1 satellite was launched on 18 May 2012, starting the new round of Japan well calibrated and technologically advanced radiometers in space. As its predecessor, AMSR-E, the new radiometer has the same channels in C, X, K, Ka and W bands, measuring the radiation at both polarizations, which makes it possible to provide estimates of many oceanic and atmospheric geophysical parameters, including such important ones as total atmospheric water vapor content (WVC), total cloud liquid water content (CLW), sea surface wind speed (SWS) and sea surface temperature (SST). Parameter retrievals are possible independent on day time and over not only clear-sky but also over cloud covered oceans. The new AMSR2 instrument has two additional channels in C-band intended for removing from data the pixels, contaminated by radio-frequency interference. It is demonstrated in this paper that measurements at these additional channels can be effectively used for rain pixel identification. Moreover, rain rate (RR) estimation, based on C-band measurements, can be used also to detach the rain emission constituent from the total microwave radiation measured at X-band channels. After the rain constituent having been excluded from the brightness temperature (BT), other parameters (SWS, SST), retrievals of which are based on C and X band measurements, can be retrieved as if there were no rain, using the retrieval algorithms, developed for non-rain conditions. The analysis presented in the paper is based on the usage of numerical simulation of BT over the open oceans under conditions of non-scattering atmospheres. Measurements at C and X bands are not influenced by rain drop scattering up to high RR values (> 30 mm/h), hence BT can be calculated under assumption that rain drop only emit the radiation. Numerical simulations have been fulfilled for the database of simultaneous data for atmospheric meteorological parameter profiles and oceanic parameters, using advanced models for ocean emission and atmospheric emission/absorption. The algorithms for parameter retrievals have been developed using calculated values of BT and Neural Networks as an inversion function. The suggested approach for rain handling has been applied to several case studies associated with hurricanes and extratropical cyclones for the period of 2012-2013. RR estimation has been verified through the comparison with TMI RR fields. Geophysical parameter fields have been built after application of the algorithms to AMSR2 data, and comparison of the results with independent data (satellite products and in-situ measurement data) allowed concluding the great potential of the suggested approach.

Paper 6 HIGH STABILITY MICROWAVE INTERFEROMETRIC RADIOMETER FOR OCEAN SALINITY MEASUREMENT

Hao Liu, Lijie Niu, Ji Wu, Cheng Zhang, National Space Science Center, Chinese Academy of Sciences (CAS/NSSC), China

In recent years, the application of L-band radiometry on soil moisture and ocean salinity measurement attracts common interests within geoscience community. Two space missions, SMOS and Aquarius, have already been successfully implemented. In near future, SMAP mission will also be in operation in space. With the experiences achieved by current two missions (SMOS and Aquarius), several factors, such as the on-orbit accuracy & stability of the instrument, the availability of the axillary data, and the correctness of the model used for retrieving, etc., have been identified having significant influences on the realization of scientific goals. With all these experiences and lessens, the authors proposed a new mission concept based on a novel combined L-band active/passive instrument. The passive part of the combined instrument is a 8-element1-D microwave interferometricradiometer(MIR, working at 1.4135GHz), while the active part is a 7-elementdigital beamformingscatterometer(DBF, working at 1.26GHz). Both the radiometer and scatterometer share a parabolic cylinder reflector antenna (~4.5*3m) with linear patch array feeds. The motivations of this design are: 1) Comparing with 2-D system, 1-D MIR is much less complex, then it could be very carefully temperaturecontrolled and calibrated, ensuring good stability and accuracy (0.1K level); Comparing with real-aperture system, 1-D MIRhas larger swath and better spatial resolutionperformance; 2) By using DBF, the swath of the scatterometer can be very well fitted with the FOV of radiometer; 3) With the parabolic reflector, it is also possible to add more frequency band (S, C-band or X-band) MIR systems with additional patch feed array; 4) Although the reflector is relative large, it's still technical feasible to manufacture a 4.5m size reflector at L-band and deploy it in space; if mesh reflector can be used, the size of the reflector could be even larger. A ground-based prototype has been planned to demonstrate the concept and performance, which is foreseen to be finished in middle of 2014. In this paper, the authors will focus on the technical issues related with design and development of the high stability correlation receivers for the L-band MIR system. The correlation receivers are consisted with patch feeds, front-ends, IF modules and digital correlators. In order to achieve high stability (0.1K within 10 days), following measures are used for the system: 1) Noise injection architecture is used, including a common noise source, andan individual noise source and a match load for each single receiver channel. The so-called "running average" technical is used to achieve balance between the stability and sensitivity. 2) Thefront-end unit is installed on the back of the patch feed as a compact module, which is very well temperature controlled. 3) The temperature performances of some critical components have been characterized, such as coupler, switch, LNA, etc. Before the integration and tests of the L-band MIR system, following long-term stability tests on the correlation receivers are planned to be carried out 1) Total power stability test So far, an 8-day total power stability test has been finished under indoor ambient temperature environment (with open window). 0.1K radiometric resolution (4s integration time, 343K target) and 0.05K stability have been achieved over whole 8-day test period. During this test, 0.05K stability and 0.3K gradient have also been achieved with the front-end thermal control system. 2) Interferometric stability test This test is planned to be carried out in anechoic chamberand foreseen to be accomplished before the end of 2013. The stability of the correlation measurement, including amplitude, phase and offset, will be evaluated through this test. The results will also be presented in this paper.

Session Co-Chairs: Joel Johnson, Ohio State University; Sidharth Misra, NASA JPL

Paper 1 ACCURATE GEOLOCATION OF RFI SOURCES IN SMOS IMAGERY BASED ON SUPERRESOLUTION ALGORITHMS

Hyuk Park, Universitat Politècnica de Catalunya (UPC), Spain; Veronica Gonzalez-Gambau, ICM-CSIC, SMOS BEC, Spain; Adriano Camps, Universitat Politècnica de Catalunya (UPC), Spain

The SMOS mission from the European Space Agency (ESA) was launched in November the 2nd, 2009, and it is providing accurate soil moisture and ocean salinity maps. However, sometimes the quality of the retrievals is limited, or even the retrieval itself is prevented, due to the presence of radio-frequency interference (RFI). Thanks to coordinated efforts led by ESA, about 42 % of the RFI sources have been identified and suppressed, however, many RFI sources are still contaminating the SMOS brightness temperature images. The ultimate solution to overcome the impact of the RFI consists of switching off illegal transmitters. Previous RFI detection methods are based on L1C images: geolocated brightness temperatures. However, despite all the efforts to turn them off, the coarse resolution of the MIRAS sensor aboard SMOS (~35-50 km) has proven to be an added difficulty in their geolocation. Angular resolution can be improved based on a statistical approach using multiple snapshots, but there are still inherent limitations given by the angular resolution, such as the fact that RFI sources located closely to each other cannot be resolved, and very strong RFI sources mask weaker sources. In this work, a new RFI geolocation method is proposed to improve the achievable angular resolution by using beamforming and Direction Of Arrival (DOA) estimation techniques used in Signal Processing and Information Theory. To understand the procedure, we must first recall that the MIRAS sensor is a 2D synthetic aperture interferometric and its observables are the so-called visibility samples, which are computed from the cross-correlation of the outputs of antenna pairs. Using array beamforming theory terminology, the visibility samples can then be understood as elements of the covariance matrix of the signals collected by the array elements, and therefore high-performance DOA estimation techniques in sensor arrays can be employed to accurately detect RFI sources. In this case, RFI sources are treated as signals, while the emission from the Earth is a background noise. Based on this idea, the feasibility of using DoA beamforming algorithms for RFI detection in SMOS imagery has been studied, and their performance compared among them and with respect to the original SMOS L1C imagery. Prelimary results using single snapshots, show an improved angular resolution as compared to previous methods, and the capability to resolve individual sources of RFI in clusters, which were not resolved using previous methods. This improved performance in single snapshots leads more efficient RFI detection in multiple snapshot process. Results will be shown at the conference.

Paper 2 DETECTION OF RFI USING COMPLEX KURTOSIS IN MICROWAVE RADIOMETRY

Damon Bradley, Joel M. Morris, Tulay Adali, University of Maryland Baltimore Counry, United States; Mustafa Aksoy, Joel Johnson, Ohio State University, United States

Radio-frequency interference (RFI) is a persistent threat to the utility of radiometric measurements as it corrupts the thermal noise signal received by the radiometer. Use of these measurements containing undetected RFI leads to erroneous geophysical parameter retrievals. Various test statistics such as the kurtosis are currently used to detect RFI based on the non-Gaussianity of the probability density function (pdf) of the received radiometer signal. Though the kurtosis was shown to be the best test statistic for detecting a wide variety of RFI signal types to date, only the real-valued kurtosis has been applied to the problem of RFI detection. In this paper, we interpret two signal pairs that occur in a fully polarimetric digital radiometer as complex-valued signals, and apply the complex-valued kurtosis test statistic to the problem of detecting RFI. The signal pairs are: (1) the in-phase and quadrature component signals of a single, complex, downconverted, polarimetric channel and (2) the horizontal and vertical polarization component signals. By interpreting these signals as single complex-valued random signals, rather than two separate real-valued random signals we can take advantage of new results for complex non-Gaussianity detection. We argue that the complex-valued interpretation provides a more meaningful and useful representation of internal radiometer signals since these signals appear naturally in total-power, polarimetric, and interferometric radiometers. For example, in a total-power radiometer, the input signal can be downconverted to complex baseband. The complex kurtosis can be applied to the complex signal formed from the in-phase and quadrature component signals, as opposed to applying the real kurtosis separately to the in-phase and quadrature component signals. We address the issue of circularity of the complex radiometric signal pairs and show improved detection performance over the real-valued case for the two signal pairs considered. Finally, we discuss implications of these results regarding the signal processing architecture of future digital radiometers.

Paper 3 A STUDY OF RADIO FREQUENCY INTERFERENCE DETECTION FOR THE SMAP RADIOMETER

Mustafa Aksoy, Joel Johnson, The Ohio State University, United States; Jeffrey Piepmeier, Priscilla Mohammed, NASA Goddard Space Flight Center, United States

NASA's SMAP mission will be launched in November 2014 to measure soil moisture over Earth's surface. SMAP includes a microwave radiometer that produces 16 frequency sub-channels each of which has 1.5MHz bandwidth occupying the 1400-1424MHz frequency band. The SMAP radiometer also produces a single "fullband" channel for the entire operational bandwidth that is resolved more finely in time. Although the 1400-1424 MHz portion of the microwave spectrum is solely allocated for passive remote sensing, earlier studies have shown that radio frequency interference (RFI) in this band is a major problem causing erroneous retrievals of physical parameters. Therefore, SMAP implements a comprehensive RFI detection procedure formed by a combination of previously developed pulse-detection, cross-frequency, kurtosis, and polarimetric algorithms. The received power in the full-band channel is reported for 350μs intervals, and kurtosis values are also computed for each 350μs interval. Time domain pulse detection and kurtosis algorithms are then applied to flag RFI in this data for every footprint. The reporting interval for sub-channel products is 1.2ms, and cross-frequency and kurtosis algorithms are applied in each sub-channel. Polarization detection is also applied in both full-band and sub-band channels by thresholding the 3rd and 4th Stokes parameters of the measured power. RFI detection algorithms are implemented over each footprint formed by 44 full-band and 11x16 sub-band measurements, but final brightness temperature products are computed only from sub-band measurements. If a 350μs full-band sample is flagged as containing RFI, all 16 1.2 ms sub-band channels corresponding to that time interval are also flagged. To produce final brightness temperature products, all measurements in the 11 time interval x16 sub-channel spectrogram not flagged by any of the detection algorithms are averaged. This approach may lead to high false alarm rates in the case of narrowband pulsed interference. Such interference occupies only a few sub-channels, but detections by the full-band pulse and kurtosis detection algorithms cause all 16 sub-band channels in the corresponding time interval to be discarded. Two solutions to this problem will be examined in the presentation. The first approach involves computing brightness temperature products both from the fullband data and the sub-band data. The lower brightness temperature from these two approaches is then reported. The second approach allows full-band flagging of all 16 channels only during time intervals when no interference was detected in any sub-channel. The presentation will report the performance of the current SMAP RFI detection procedure and the proposed improvements for different RFI scenarios. The implications of these results for SMAP radiometer analysis will also be discussed.

Paper 4 CHARACTERISTICS OF THE SPATIO-TEMPORAL VARIABILITY IN SEA SURFACE SALINITY AND RADIOFREQUENCY INTERFERENCE OVER THE EAST CHINA SEA SHOWN BY THE AQUARIUS DATA

Seung-bum Kim, CALTECH Jet Propulsion Laboratory, USA, United States; Paolo de Matthaeis, NASA Goddard Space Flight Center, USA, United States; Jae-Hak Lee, Korea Ocean Institute of Science and Technology, South Korea, Republic of Korea; Ik-Chan Pang, Jeju university, South Korea, Republic of Korea

The northern East China Sea (ECS) occupies an area of 800 km × 500 km to the east of Shanghai, China. The observed surface salinity of the ECS changes by 3 psu and larger due to river runoff. However, the shallow ECS is not sampled by the Argo floats, and therefore is an area where satellite remote sensing may become a vital tool for monitoring sea surface salinity (SSS) variability. The area is adjacent to the strong sources of radiofrequency interference (RFI) at L-band. This paper aims at understanding the characteristics of the RFI contamination on Aquarius SSS and assessing the fidelity of the retrieved SSS. An analysis of the Aquarius product (version 2.0) in this region provides two interesting findings. First, the Aquarius SSS is much lower (often by more than 3 psu) on descending passes than on ascending counterparts (the main beam points towards China on the descending pass). Second, even on the ascending passes, the Aquarius SSS is too low: compared with in situ observations taken at mostly 0.5 m depth at three locations in 2011 and 2012, the mean biases are all negative and almost -0.8 psu in the worst case; compared with regional numerical model outputs, the mean bias derived over a two-year period is almost -1 psu. These differences are suspected to originate mostly from unfiltered RFI, since the study area is away from the coastline by at least one Aquarius radiometer pixel (~150 km) to limit any uncertainties in the correction of land contamination. To understand the above results on Aquarius SSS validation, first the percentage of RFI-flagged samples was examined: the percentage is 10 to 20% of RFI for the ascending track while it is much smaller for the descending. The RFI enters the sidelobes of the radiometer antenna (but it was detected and removed). Since the antenna gain of the portion of the sidelobe that points to the RFI source regions (i.e., land rather than ocean) is higher with the ascending geometry than with the descending one, the RFI contamination would be more severe for the ascending track, even if the boresight points away from the sources of RFI on the track. A spatial map of ascending minus descending in terms of the percentage will be examined to further confirm this explanation. Second, a plausible explanation of the much lower (by more than 3 psu) SSS for the descending track than for the ascending SSS is that the RFI enters the main beam (null-to-null area with ~15 degree beam-width). When the boresight points to the sources of RFI during the descending pass, the RFI power will be averaged by the gain and reduced to below the detection threshold level, which would result in the detection failure and eventually the lower salinity reported earlier. This explanation will be verified using the Goddard simulator of Aquarius observation. The apparent discrepancy (that is, the ascending data have higher percentage of filtered-RFI than the descending data but the ascending SSS is more reliable) may be found in the other parts of the world ocean.

Paper 5 AN IMAGING ALGORITHM FOR SYNTHETIC APERTURE INTERFEROMETRIC RADIOMETERS WITH BUILT-IN RFI MITIGATION

Adriano Camps, Hyuk Park, Universitat Politecnica de Catalunya and IEEC, Spain; Veronica Gonzalez-Gambau, Institut de Ciencies del Mar/CSIC, Spain

The Soil Moisture and Ocean Salinity (SMOS) mission from the European Space Agency (ESA) was launched in November 2nd, 2009, carrying the Microwave Imaging Radiometer by Aperture Synthesis (MIRAS). MIRAS is a synthetic aperture interferometric radiometer (SAIR) that provides full-polarimetric multi-angular L-band brightness temperature imagery. MIRAS operates in a protected band (1400–1427 MHz), but from the very begining, radio-frequency interference (RFI) has present in many areas of the world, preventing quality retrievals. Many efforst have been devoted to the development of algorithms for the detection and -eventually- mitigation of RFI sources [1-5], and algorithms must take into account a number of considerations: 1.Strong RFI sources are easy to detect, but the instrument's impulse response "tails" are large as well, and extend over large parts of the image. Their cancellation is a challenge because it strongly depends on the geo-localization accuracy of the RFI source. 2.Weak RFI sources are more difficult to detect, and therefore, more difficult to cancel properly. 3.RFI sources are usually time- and polarization-dependent, and algorithms must operate on a snap-shot basis, independently for each polarization. 4.Finally, since most RFI sources appear in the alias regions, but their impact extends over the "alias-free" field-of-view (FOV), algorithms must operate in the whole hexagonal period in which the Fourier imaging process takes place, not just in the alias-free FOV. With the above considerations in mind, and making use of the interpretation of the SAIR as an antenna array with an "equivalent array factor" [6] determined by the (u,v) points sampled by the SAIR, null steering beamforming techniques [7] can be applied to form the image by "focusing" each pixel, while at the same time "nulls" are introduced in the directions in which the RFI sources have been previously detected [8]. This work will describe the proposed technique. Then, simulation results will be presented as a function of the error in the estimation of the RFI source location, using the Root Mean Square and Peak Errors as performance metrics. Finally, the proposed technique will be applied to several SMOS snap- shots with

different number and types of RFIs in the image, showing its goodness and its limitations. References: [1] A. Camps et al., "Radio-frequency interference detection and mitigation algorithms for synthetic aperture radiometers," Algorithms 4(3),pp.155–182,2011. [2] E. Anterrieu, "On the detection and quantification of RFI in L1a signals provided by SMOS," IEEE-TGRS 49(10),pp.3986–3992,2011. [3] R. Castro et al., "A first set of techniques to detect radio frequency interferences and mitigate their impact on SMOS data," IEEE-TGRS 50(5),pp.1440–1447,2012. [4] S. Misra and C.S. Ruf, "Analysis of radio frequency interference detection algorithms in the angular domain for SMOS," IEEE-TGRS 50(5),pp.1448–1457,2012. [5] E. Daganzo-Eusebio et al., "SMOS radiometer in the 1400-1427-MHz passive band: Impact of the RFI environment and approach to its mitigation and cancellation," IEEE-TGRS 51(10),pp.4999–5007,2013. [6] A. Camps, "Aplication of Interferometric Radiometry to Earth Observation," Ph. D. Dissertation, Universitat Politecnica de Catalunya, 1996 (Chapter 3): http://www.tdx.cat/handle/10803/6885 [7] L. C. Godara, "Application of Antenna Arrays to Mobile Communications, Part II: Beam-Forming and Direction-of-Arrival Considerations," Proceedings of the IEEE 85(8),pp.1195-245,1997 [8] H. Park et al., High Angular Resolution RFI Detection in Synthetic Aperture Interferometric Radiometers Using Direction of Arrival Estimation, IEEE Geoscience and Remote Sensing Letters (submitted),October 2013

Paper 6 **RFI MITIGATION IN MICROWAVE RADIOMETRY USING INDEPENDENT COMPONENT ANALYSIS**

Englin Wong, Damon Bradley, Lynn Miles, Edward Kim, National Aeronautics and Space Administration, United States

As wireless, radar, and communications technologies proliferate, there is a growing potential for radio frequency interference (RFI) to corrupt important radiometric measurements taken by spaceborne microwave radiometers. This leads to significant amount of unusable data which degrades the quantity but also the quality of the science. The potential impact led to the development of the RFI detection digital radiometer backend in the recent NASA's Soil Moisture Active and Passive mission (SMAP) [Entekhabi, D et. al, 2010 proceedings 98-5] which will launch in late 2014. More importantly, the digital signal processing that been implemented in SMAP's digital radiometer has proven that more complex algorithms can be implemented a spaceflight applications, particularly statistical signal processing. In this paper, we explore the potential of using a well-known algorithm, Independent Component Analysis (ICA) [Hyvarinen 1997, Adaptive Signal Processing 2010], on the Goddard Radio-frequency EXplorer (GREX) system to mitigate the RFI. ICA is proven in [Hyvarinen] to separate the non-Gaussian signal in the mixture. This is an advantage for detecting interference in microwave radiometer signals since most of the known RFI are non-Gaussian. The GREX system is the NASA Goddard owned airborne high speed L-Band microwave radiometer system. Its digital backend consists of a dual-channel 400MHz, 14-bit ADC, Xilinx V5 FPGA and 23TB of RAID data storage. The ICA algorithm is implemented inside the Xilinx V5 of the GREX digital backend to process the radiometer signal. The processed data is stored directly in storage for further analysis. The idea is to perform a real-time RFI airborne survey of the Chesapeake Bay in spring 2014 with the complete ICA based airborne RFI surveyor. With the success of this effort, a potential ground breaking RFI digital processing instrument can be implemented in future space flight missions. A study that shows the potential of the ICA based RFI detection using simulated radiometer data as well as the actual GREX test flight data, collected back in 2012 is presented in this paper.

Tuesday, March 25	Soil Moisture and Vegetation	14:40 - 16:00
Poster Session		Dabney Hall, Bldg 40

Session Co-Chairs: Eni Njoku, NASA - Jet Propulsion Laboratory; Rajat Bindlish, USDA-ARS

Paper 1 **ADVANTAGES OF MULTIFREQUENCY MICROWAVE SATELLITE SENSORS: WHAT DO MICROWAVE INDICES SHOW IN ARGENTINA AND AUSTRALIA ECOSYSTEMS?**

Veronica Barraza, Francisco Grings, Institute of Astronomy and Space Physics, Argentina; Paolo Ferrazzoli, Tor Vergata University, Italy; Natalia Restrepo-Coupe, Alfredo Huete, University of Technology Sydney, Australia; Haydee Karszenbaum, Institute of Astronomy and Space Physics, Argentina

This study analyzes time series of passive microwave and optical data collected in Southern Hemisphere ecosystems of Australia and Argentina. The subtropical regions selected are located in the north and southeast of Australia and in the northwest of Argentina. These sites are located across a wide range of land cover types including deciduous open forests, evergreen forests, woody savannas, shrublands and grasslands. To this end, we used two microwave indices (Frequency Index (FI) and Polarization Index (PI)) and one optical index (NDVI), to link canopy variables with soil properties. We analyzed AMSR-E and WINDSAT data at X and Ka bands, considering up to four observations per day at different local times (2:30, 7:00, 14:.30 and 19:.00) for 2007 to 2009. We have found that microwave indices provide complementary information to classical greenness indices, since they present a crucial sensitivity to soil properties and to vegetation moisture and structure. Both seasonal and hourly variations of both microwave indices were observed. For the seasonal and hourly trend the results obtained for deciduous open forests in Argentina are not easily extensible to Australian sites, where NDVI appears to have completely different relations with microwave indices. We provide interpretations for these differences in terms of vegetation structure, soil moisture changes under partial vegetation cover and deep soil emission. An exception among the Australian locations is the evergreen forest, where the magnitude of both indices is in the same range of values that the ones at deciduous open forests in Argentina, showing that the contribution of the vegetation component could be important. Furthermore, FI and PI show a similar hourly behavior as deciduous open forests, but without the seasonal component. In different ecosystems microwave indices are affected by different processes, so we presented the FI vs. PI scheme which is a useful and easy tool to understand the biophysical processes involved. In our analysis, we have found that positive correlations and low average FI and PI values are associated to land covers in which the observations are related to vegetation properties (leaf area index (LAI) and canopy water content (CWC)); positive correlations and higher average FI and PI values are associated to soil properties (soil moisture and thermodynamic temperature); no correlations and higher average FI and PI values are associated to vegetation properties (LAI) and soil properties (thermodynamic temperature).These results are relevant since vegetation and soil conditions are component of the overall water balance and surface radiation budget, which effectively modulates evapotranspiration. The implications of these results for a possible regional evapotranspiration application are evaluated using flux data in two Australian OzFlux sites. We selected two OzFlux sites where FI is affected mainly by the soil component (SW and S). The resulting ET was calculated for the four times and at different composition periods (1-day, 8-days and 16-day). As expected, the coefficient of determination increases as increase the aggregation due to the smoothing effect of the high frequency noise in both eddy covariance flux data and microwave time series. The better accuracy has been obtained after midday (R2 (8-days) SW= 0.55 and R2 (8-days) S= 0.91) for these two areas. While correlation does not imply a causal relationship, our result indicates that available energy and moisture are the two main external drivers of ET in this two study area. Further work is needed in order to evaluate more in deeply the relation between FI and ET in forest areas and in order to assimilate these vegetation and/or soil moisture correlations into a sound soil/vegetation/atmosphere process model to estimate water vapor fluxes.

Paper 2 **SMOS AND ASCAT SOIL MOISTURE RETRIEVALS: A COMPARISON OVER EUROPE AND NORTHERN AFRICA**

Nazzareno Pierdicca, Fabio Fascetti, Sapienza University, Italy; Luca Pulvirenti, Cima Research Foundation, Italy; Raffaele Crapolicchio, Serco SpA, Italy

Microwave remote sensing represents a very useful tool to monitor soil moisture at different spatial and temporal scales. The microwave band presents a direct sensitivity to volumetric soil moisture content (SMC) because SMC directly influences the soil dielectric permittivity; moreover, the atmosphere can be considered fairly transparent in the low-frequency portion of the microwave spectrum (1-5 GHz). Microwave remote sensing encompasses both active and passive forms depending on the sensor and its mode of operation, with different swath widths and temporal and spatial resolutions. Microwave radiometers (passive sensors) and scatterometers (active sensors) measure the surface emission and the radar backscattering, respectively. Those quantities are sensitive to common parameters as soil permittivity, vegetation conditions and roughness, although the influence of these parameters on emission and backscattering is not identical. This paper describes a comparison study between two remotely sensed surface soil moisture datasets: one from the L-band Soil Moisture and Ocean Salinity (SMOS) radiometer (available through an ESA Category 1 project) and one from the C-band Advanced Scatterometer ASCAT onboard METOP (available through the Eumetsat H-SAF project). The study has been performed in the frame of the Eumetsat activity managed by the Italian Civil Protection Department, aimed at validating the H-SAF soil moisture products. Both Europe and Northern Africa have been considered and data acquired during years 2010, 2011 and partially 2012 have been analyzed. As for the SMOS-derived SMC, the data produced by two processors (version 501 and version 551, the latter implementing a different permittivity model) will be used. As for ASCAT-derived SMC, since each data represents a soil moisture relative index between 0 and 100% (i.e., driest and wettest conditions), the ASCAT retrievals have been converted into volumetric soil moisture by a specific strategy to obtain a reasonable comparison. For this purpose, ASCAT products have been rescaled taking as references SMC max/minimum maps obtained both by SMOS retrievals and also by an independent modeled dataset (the ERA/Interim LAND). Results demonstrate that ASCAT and SMOS products show a fairly good degree of correlation, but their consistency has some dependence on season, geographical zone and surface land cover. The capacity to capture both temporal and spatial variability of the soil moisture field has been also analyzed and compared for the two systems. Additionally, for specific sites which belonging to the International Soil Moisture Network, satellite products have been compared to the ground measurements of moisture gauges, implementing several normalization approaches and analysis as the triple collocation (TC) technique, useful to estimate the relative amount of error affecting three different sources of soil moisture products. For this purpose, one dataset has been chosen as reference and scaling constants have been introduced and calculated for the other two systems. Then, since SMC can be considered as a space-temporal random function of space and time with zero mean plus a space-time drift, the drift has been evaluated by combining space dependent and time dependent functions. Assuming uncorrelated noise with zero mean, the TC technique has been implemented and the noise variances of the products has been estimated (in the order of 5% for all three systems).

Paper 3 **PARANA RIVER DELTA 2013 FLOOD AS SEEN BY AMSR-2, SMOS, AQUARIUS AND SAR SYSTEMS**

Mercedes Salvia, Francisco Grings, Cintia Alicia Bruscantini, Veronica Barraza, Pablo Perna, Institute Of Astronomy and Space Physics (IAFE), Argentina; Paolo Ferrazzoli, DICII - Tor Vergata, Italy; Haydee Karszenbaum, Institute Of Astronomy and Space Physics (IAFE), Argentina

Over the past decade, several flood monitoring/forecasting methodologies based on remote sensing data have been proposed. Among them, the ones based on microwave observations are the most successful, since large flood events and intense cloud covers are often encountered simultaneously. This is a severe limitation of flood monitoring based on optical instruments. In general, flooding increases the moisture of the soil and decreases its roughness. For higher water levels and in presence of vegetation cover, flooding also reduces the height of the emerged vegetation. In extreme cases, water level submerges vegetation. All these processes produce a decrease of the surface emissivity and an increase of the difference between the emissivity measured in the vertical and horizontal polarizations. Therefore, passive microwave polarization index (PI) has the potential to detect the fraction of inundated area and to monitor the increase of water level. These issues have been discussed in several papers (Prigent et al., 2007, Sippel et al 1994, Salvia et al., 2011). Furthermore, the backscattering coefficient is also sensitive to flooding and vegetation condition. In summary, the combination of microwave remote sensing (active and passive) constitutes a good option, in which the best of both systems (high spatial resolution from SAR and high temporal resolution from passive systems) can be exploited for large river basins monitoring. This led us to the development of a methodology to retrieve flooded area in herbaceous wetlands, based on active/passive microwave data (Salvia et al., 2011). Currently there are several passive systems available, which present different characteristics (resolutions, frequencies, and incidence angles). In this study, we analyze the multi-frequency temporal trends of available radiometers (Aquarius (L Band), SMOS (L Band) and AMSR2 (C, X, Ka Band)) to estimate the fraction of flooded area inside a wetland floodplain. The influence of resolution, frequency and incidence angles are discussed using model simulations. In this case Cosmo Skymed data acquired once every ~20 days is used to compute high resolution flooding maps that are used to re-calibrate the parameters (mainly the Polarization difference of flooded area) in order to enhance the accuracy of passive data flooded area fraction estimation performed with a temporal resolution of a few days to a week. The Parana River Delta was selected as test site. In April-June, 2013, strong rains fell over the upper Parana Basin (South of Brazil and North-East of Argentina), leading to the occurrence of a moderate flood wave that reached the lower Parana Basin (including Parana River Delta) on July, 2013. In this context, the objective of this paper is to estimate flooded area fraction from passive microwave data. The general approach is based on the exploitation of the PI from a complete series of passive data, and the use of high resolution flooding maps based on Cosmo Skymed data in specific dates for parameter calibration (Salvia et al., 2011). We show the feasibility to monitor flood condition with the combination of active and passive microwave data, and the effects of spatial resolution, frequency and incidence angle of passive data in the algorithm performance. Sippel, S.K., et al.. "Determination of inundation area in the Amazon River floodplain using the SMMR 37 GHz polarization difference". Remote Sensing Environment, 48: 70-76, 1994. Prigent, C., F. Papa, F. Aires, W. B. Rossow, and E. Matthews (2007), Global inundation dynamics inferred from multiple satellite observations, 1993- 2000, J. Geophys. Res., 112, D12107, doi:10.1029/2006JD007847. Salvia,M., Grings,F., Ferrazzoli,P., Barraza,V., Douna,V., Perna,P., Bruscantini,C., Karszenbaum,H. "Estimating flooded area and mean water level using active and passive microwaves: the example of Parana River Delta floodplain". Hydrol. Earth Syst. Sci., vol. 15, 2679–2692, 2011.

Paper 4 FREEZE/THAW DETECTION USING AQUARIUS' L-BAND PASSIVE/ACTIVE DATA

Xiaolan Xu, Simon Yueh, Jet Propulsion Laboratory, United States

The landscape freeze/thaw state dominates the seasonal cycle in high latitudes and provides a sensitive indicator of global climate change. The timing of the freeze/thaw transition influences critical processes such as land surface energy balance and carbon cycle dynamics related to vegetation growth. In this paper, we produce the daily freeze/thaw state classification map of 2011~2012 water year based on L-band radar and radiometer data from Aquarius. The Aquarius satellite carries a combined passive/active L-band microwave instrument that observes the Earth surface globally in a week. Data from Aquarius acquired over land are made use of in this study to extend the Aquarius applications to observations of large-scale land hydrologic and ecological phenomena. The spatial resolution of Aquarius swath is approximately 100 km and all three beams have been re-gridded into 36km resolution of Equal-Area Scalable Earth Grid (EASE-Grid) with incidence angle normalized to 40 degree. The daily freeze/thaw maps are averaging over 7 day moving window. The active freeze/thaw detection algorithm described here is based on a seasonal threshold approach being developed for application to higher-resolution (3 km) radar measurements that will be provided by NASA's Soil Moisture Active/Passive (SMAP) mission (to be launched in October 2014). When the ground state changes between frozen and thawed states the soil and vegetation permittivities change significantly, and these changes are reflected in changes in microwave emissivity and backscattering from the surface. The passive algorithm is also based on the similar seasonal threshold but using the polarization difference of the two co-polarization brightness temperature. Surface air temperatures from a distributed network of weather stations and the in situ data from SNOTEL stations are used as ground validation data to assess algorithm performance. The analysis of the Aquarius data will also support SMAP freeze/thaw algorithm development by providing a capability to assess L-band data in advance of the SMAP launch.

Paper 5 ANALYSIS OF SOIL MOISTURE RETRIEVAL FROM AIRBORNE PASSIVE/ACTIVE L-BAND SENSOR MEASUREMENTS IN SMAPVEX 2012

Liang Chen, Xiaojun Yin, Qian Xuesen Laboratory of Space Technology, China Academy of Space Technology, China

Soil moisture is a key component in the hydrologic cycle and climate system. It is an important input parameter for many hydrologic and meteorological models. NASA'S upcoming Soil Moisture Active Passive (SMAP) mission, to be launched in October 2014, will address this need by utilizing passive and active microwave measurements at L-band, which will penetrate moderately dense canopies. In preparation for the SMAP mission, the Soil Moisture Validation Experiment 2012 (SMAPVEX12) was conducted from 6 June to 17 July 2012 in the Carment-Elm Creek area in Manitoba, Canada. Over a period of six weeks diverse land cover types ranging from agriculture over pasture and grassland to forested sites were re-visited several times a week. The Passive/Active L-band Sensor (PALS) provides radiometer products, vertically and horizontally polarized brightness temperatures, and radar products. Over the past two decades, successful estimation of soil moisture has been accomplished using passive and active L-band data. However, remaining uncertainties related to surface roughness and the absorption, scattering, and emission by vegetation must be resolved before soil moisture retrieval algorithms can be applied with known and acceptable accuracy using satellite observations. This work focuses on analyzing the Passive/Active L-band Sensor observations of sites covered during SMAPVEX12, investigating the observed data, vegetation covered surface model, inversion algorithm and analyzing observed soil moisture changes over the time period of six weeks. The data and analysis results from this study are aimed at increasing the accuracy and range of validity of SMAP soil moisture retrievals via enhancing the accuracy for soil moisture retrieval.

Paper 6 COMPARISON OF SMOS AND SMAP OPTICAL THICKNESS DATA

Jason Patton, Brian Hornbuckle, Daniel Fortin, Iowa State University, United States

L-band radiometers used for the purpose of soil moisture retrieval require information about vegetation in order to make accurate retrievals. Specifically, the vegetation optical thickness, represented by tau in the zeroth-order "tau-omega model", must be known or retrieved. Tau characterizes the attenuation of soil emitted and surface reflected microwave radiation, and also characterizes the emission of radiation from the vegetation itself. Water held in vegetation (vegetation water content, VWC) has been found to be the primary contributor to tau. L-band soil moisture sensing satellites, such as Soil Moisture Ocean Salinity (SMOS) and Soil Moisture Active Passive (SMAP), obtain tau through different methods. SMOS is able to simultaneously retrieve tau and soil moisture by using multi-angular measurements of brightness temperature. The influence of tau depends on the incidence angle at which radiation is measured, e.g. at larger incidence angles, tau has a larger influence as radiation emitted from the soil must travel through more vegetation. Using the multi-angular data, the SMOS retrieval algorithm finds the soil moisture and tau values that best fit the tau-omega model to observations. SMOS's method has advantages of not requiring any outside sources of vegetation data, and of not requiring any knowledge of phenology (i.e. the timing of vegetative growth stages). SMAP will only measure at a single incidence angle, and so information for tau must come from a different method, e.g. multi-polarization or ancillary vegetation data. Currently, the SMAP team plans on using the latter: a climatology of MODIS NDVI has been developed, and an empirical model will estimate daily values of tau from the NDVI climatology. SMAP's method has an advantage of not requiring (often slow to acquire) "real-time" data from other satellites. It should work well where vegetation "greenness" tracks VWC and where vegetation phenology is fairly constant year-to-year. Our study will compare SMOS and SMAP's estimates of tau in the United States Corn Belt region over the years 2010 to 2013. This region's vegetation is dominated by row crops, primarily maize and soybean. The Corn Belt is a challenging region to characterize tau and VWC for because vegetation phenology is tied strongly to the local weather conditions. For example, phenology may be determined by soil moisture conditions in the spring; farmers cannot use machinery if fields are too muddy, and the soil must be adequately moist for seed germination. Once crops begin to grow, phenology is determined by temperature (i.e. growing degree days) and VWC is partially determined by soil moisture conditions. Our comparison will use the latest version of SMOS level 2 data and MODIS NDVI data (climatology if available, direct if not). We will also use farm-level measurements of VWC to demonstrate the year-to-year variability in timing and magnitude of crop growth. We will not have VWC measurements at the scale of a SMOS/SMAP satellite pixel (~40 km) as it is nearly economically impossible to make such measurements, however we will discuss other means (e.g. by using county-level crop yields) by which we have attempted to analyze and validate SMOS tau data. Our hypothesis is that SMAP's NDVI climatology method of deriving tau will not match SMOS's measurements of tau over the US Corn Belt in both timing and magnitude. If the methods do not match, we will discuss some of the reasons why they may not match (e.g. NDVI saturation, annual weather variability) and and conclude with implications. For example, using a forward model, we will estimate the impact of various tau error scenarios on soil moisture retrievals.

Paper 7 GLOBAL-SCALE EVALUATION OF TWO SATELLITE-BASED PASSIVE MICROWAVE SOIL MOISTURE DATA SETS (SMOS AND AMSR-E) WITH RESPECT TO MODELLED ESTIMATES

Amen Alyaari, Jean-Pierre Wigneron, INRA, France; Agnes Ducharne, CNRS, UMR Sisyphe, France; Yann Kerr, Ahmad Al Bitar, CESBIO, France; Richard de Jeu, VU University, France; Ajit Govind, INRA, France; Patricia Rosnay, Clement Albergel, Joaquin Munoz, ECMWF, United Kingdom; Shu Wang, INRA, France

Global Level-3 surface soil moisture (SSM) maps from the passive microwave Soil Moisture and Ocean Salinity satellite (SMOSL3) have been released. To further improve the Level-3 retrieval algorithm, evaluation of the accuracy of the spatio-temporal variability of the SMOS Level 3 products (referred to here as SMOSL3) is necessary. In this study, a comparative analysis of SMOSL3 with a SSM product derived from the observations of the Advanced Microwave Scanning Radiometer (AMSR-E) computed by implementing the Land Parameter Retrieval Model (LPRM) algorithm, referred to here as AMSRM, is presented. The comparison of both products (SMSL3 and AMSRM) were made against SSM products produced by a numerical weather prediction system (SM-DAS-2) at ECMWF (European Centre for Medium-Range Weather Forecasts) for the 03/2010-09/2011 period at global scale. The latter product was considered here a "reference" product for the inter-comparison of the SMOSL3 and AMSRM products. Three statistical criteria were used for the evaluation, the correlation coefficient (R), the root-mean-squared difference (RMSD), and the bias. Global maps of these criteria were computed, taking into account vegetation information in terms of biome types and Leaf Area Index (LAI). We found that both the SMOSL3 and AMSRM products captured well the spatio-temporal variability of the SM-DAS-2 SSM products in most of the biomes. In general, the AMSRM products overestimated (i.e., wet bias) while the SMOSL3 products underestimated (i.e., dry bias) SSM in comparison to the SM-DAS-2 SSM products. In term of correlation values, the SMOSL3 products were found to better capture the SSM temporal dynamics in highly vegetated biomes ("Tropical humid", "Temperate Humid", etc.) while best results for AMSRM were obtained over arid and semi-arid biomes ("Desert temperate", "Desert tropical", etc.). When removing the seasonal cycles in the SSM time variations to compute anomaly values, better correlation with the SM-DAS-2 SSM anomalies were obtained with SMOSL3 than with AMSRM, in most of the biomes with the exception of desert regions. Eventually, we showed that the accuracy of the remotely sensed SSM products is strongly related to LAI. Both the SMOSL3 and AMSRM (slightly better) SSM products correlate well with the SM-DAS2 products over regions with sparse vegetation for values of LAI < 1 (these regions represent almost 50% of the pixels considered in this global study). In regions where LAI>1, SMOSL3 outperformed AMSRM with respect to SM-DAS-2: SMOSL3 had almost consistent performances up to LAI = 6, whereas AMSRM performance deteriorated rapidly with increasing values of LAI.

Session Co-Chairs: Boon Lim, NASA - Jet Propulsion Laboratory; Ville Kangas, ESA

Paper 1 **SMOS LEVEL3 AND 4: NEW PRODUCTS FOR NEW SCIENCE**

Yann Kerr, Ahmad Al Bitar, Simone Bircher, CESBIO, France; Jacqueline Boutin, LOCEAN, France; Audrey Choné, CESBIO, France; Jennifer Grant, Lund University, Sweden; Olivier Merlin, Arnaud Mialon, Beatriz Molero, CESBIO, France; Thierry Pellarin, LTHE, France; Kimmo Rautiainen, FMI, Finland; Nicolas Reul, Ifremer, France; Philippe Richaume, Nemesio Rodriguez, CESBIO, France; Mike Schwank, WSL, Switzerland; Jean-Pierre Wigneron, INRA, France

The SMOS mission was launched in November 2009 and allows for measuring of the surface soil moisture and vegetation optical depth over continental land areas, covering the entire globe every 3 days. The ESA's DPGS (European Space Agency's Data Processing Ground Segment) has been delivering the so called Level 2 products, consisting in ½ orbits data. The CNES (Centre National d'Etudes Spatiales) has developed the CATDS (Centre Aval de Traitement des Données SMOS) ground segment that now provides spatial and temporal synthesis products (referred to as Level 3 products) of soil moisture, vegetation optical depth, ocean salinity and brightness temperature, which now cover the whole SMOS operation period, from January 2010 onwards. After developing the level 3 products over land and oceans, a wealth of new science applications started to appear and are being put into the level 4 scheme after validation. These products are currently in their validation stage, with some being more mature than others. Some products are currently being implemented. These encompass root zone soil moisture and drought indices over land, dis-aggregated (i.e., high resolution) soil moisture fields in local areas, and hurricane monitoring over the oceans. A near real time soil moisture product for Numerical Weather Prediction) (NWP) and risk assessment is also being tested. Other products are currently being studied or finalized such as flood monitoring and risk assessment over land, rain fall estimates over specific areas (land and in some specific cases ocean), hydrology in organic rich soils, freeze-thaw cycle in boreal areas, and vegetation water content/monitoring. During the presentation, we will give an overview of the different products and an assessment of their maturity and validation together with their scientific relevance.

Paper 2 **MIRATA: A NEW CUBESAT MISSION FOR HIGH-RESOLUTION EARTH ATMOSPHERIC SENSING USING COMBINED MICROWAVE RADIOMETRY AND GNSS RADIO OCCULTATION**

Bill Blackwell, MIT Lincoln Laboratory, United States

We introduce a new technique for absolute "through-the-antenna" calibration of cross-track- scanning passive microwave radiometers viewing earth from a low-earth orbit. This method offers significant advantages, in that neither internal calibration targets nor noise diodes are needed to calibrate the radiometer. The algorithm does require periodic updates of the atmospheric state, which can be readily provided by GNSS radio occultation observations, for example. An iterative algorithm retrieves the radiometer gain given a sequence of observations of the earth's limb. The algorithm uses a parameterized radiative transfer model of a spherically- stratified atmosphere. We will present results showing that this method yield calibration accuracies similar to those that could be obtained with ideal internal calibration targets. This analysis is based on global Monte Carlo simulations using the NOAA88b profile set. An analysis will also be presented showing how calibration performance degrades as the radiometer characteristics deviate from the ideal case. Among the factors considered are: 1) antenna pattern, 2) spectral passband, 3) pointing errors, 4) atmospheric state variability, 5) the number of limb observations required, and 6) sensitivity to sensor noise. There are several key benefits to the use of the earth's limb for calibration: 1) nearly the entire dynamic range of the radiometer is covered with each scan of the limb; 2) the largest sources of validation error in the non-opaque radiometer channels are surface emissivity and boundary layer temperature variability, and these are minimized to negligible levels because of increased absorption due to the longer line-of-sight associated with the limb viewing geometry; 3) the shape of the limb brightness temperature distribution with angle can be used to estimate radiometer boresight direction with very high accuracy. To demonstrate the concept described above, the Microwave Radiometer Technology Acceleration (MiRaTA) CubeSat mission will launch in 2015 into an orbit with ~400-km initial altitude and 52-degree inclination. The MiRaTA CubeSat will carry out mission objectives over a 90-day mission, including the on-orbit checkout and validation period. MiRaTA is a 3U CubeSat comprising V- and G- band radiometers (52-58 GHz, 175-191 GHz, and 206.4-208.4 GHz), the Compact TEC/Atmosphere GPS Sensor (CTAGS) with five-element patch antenna array to permit radio occultation atmospheric profiles, and relatively standard CubeSat spacecraft subsystems for attitude determination and control, communications, power, and thermal control. The spacecraft dimensions are 10 × 10 × 34 cm, total mass is 4.0 kg, and total average power consumption is 6W. The cross-track scanning capabilities to be demonstrated by the MicroMAS cubesat mission (Dec 2013 launch) together with the multi-band radiometer and GPS radio occultation capabilities of MiRaTA could be combined into a 6U CubeSat to offer unprecedented performance at very low cost.

Paper 3 **MICROWAVE LIMB SOUNDING OF EARTH'S ATMOSPHERE – ACCOMPLISHMENTS FROM AURA AND UARS MLS, AND PLANS FOR FUTURE INSTRUMENTS**

Nathaniel Livesey, Michelle Santee, Paul Stek, William Read, Lucien Froidevaux, Robert Jarnot, Jet Propulsion Laboratory, California Institute of Technology, United States

Passive microwave limb sounding of Earth's atmosphere offers unique insights into frontline issues in Earth science affecting climate, ozone layer stability and air quality. We present an overview of the Microwave Limb Sounder (MLS) instruments on the Aura spacecraft (launched in 2004) and the earlier Upper Atmosphere Research Satellite (UARS, launched in 1991). Issues of instrument design and performance will be reviewed and the data analysis methodology described. The MLS instruments observe Earth's atmosphere from the upper troposphere (~10 km altitude) to the mesosphere (~90 km altitude). Measurements include abundances of key molecules such as water vapor (the strongest greenhouse gas), ozone (a pollutant and a greenhouse gas in the lower atmosphere and, in the stratosphere, an absorber of harmful solar ultraviolet radiation), markers of air pollution from a variety of sources, tracers of atmospheric motions, and many species critical for stratospheric ozone layer stability. The MLS instruments also measure atmospheric temperature, geopotential height and cloud ice water content. Key findings from MLS will be highlighted, including the observation of unprecedented loss of stratospheric ozone over the Arctic in 2011; evaluation of the realism of state-of-the-art climate models, which show much poorer performance in the upper troposphere than at lower altitudes; and a study of the impact of air pollution on cloud properties – a cutting-edge issue in climate research. There are currently no plans, from NASA or any other agency, to continue the observation record from MLS (or any other sensor making similar measurements). Declining budgets for Earth atmospheric science missions, and a planned revisit of NASA's Earth science priorities in the next few years, dictate a nimble approach to meeting the urgent needs for both a compact low-cost limb sounder to continue and augment the critical MLS observation record, and for more advanced high spatial-resolution limb sounders that are uniquely placed to address key outstanding questions in atmospheric science, including the impact of deep convection and convective outflow on atmospheric composition and hence climate. Accordingly, we present a new vision for the implementation of these kinds of instruments, capitalizing upon recent advances in microwave amplifier and receiver technology, along with new capabilities in digital spectrometers.

Paper 4 **MICROWAVE SOUNDER INSTRUMENT FOR METOP SECOND GENERATION**

Ville Kangas, Salvatore D'Addio, Marc Loiselet, Graeme Mason, European Space Agency, Netherlands; Mike Buckley, George Tennant, Peter Campbell, Astrium Ltd, United Kingdom

Since 2006, the European contribution to operational meteorological observations from polar orbit has been provided by the Meteorological Operational (MetOp) satellites, which is the space segment of the EUMETSAT Polar System (EPS). As part of the next generation EUMETSAT Polar System (EPS-SG), the MetOp Second Generation (MetOp-SG) satellites will provide continuity and enhancement of these observations in the 2020 – 2040 timeframe. The MetOp-SG will consists of two series of satellites ("Satellite A" and "Satellite B"), with a nominal baseline of two or three satellites of each series. The payload complement of MetOp-SG was confirmed by EUMETSAT Council in 2012 and, out of ten instruments, it includes three microwave radiometers, namely Microwave Sounder (MWS), Microwave Imager (MWI) and Ice Cloud Imager (ICI). This payload complement provides a unique suite of high performance, operational microwave radiometers covering a total of 63 channels over a very wide frequency range from 18.7 GHz up to 664 GHz. These three radiometers will provide continuous and simultaneous operation for more than 20 years, representing an invaluable opportunity for cross-calibration of future spaceborne radiometer systems. After the confirmation of the payload complement, the European Space Agency issued a request for proposals for the microwave radiometers of MetOp-SG in 2012 and made the final selection in early 2013.For the MWS instrument, ESA selected Astrium Ltd (UK) as the prime contractor. The main objective of the MWS is to provide temperature and humidity profiles in clear sky and cloudy conditions, and cloud water total column measurements. MWS is a cross-track scanning microwave radiometer, providing total number of 24 channels from 23 GHz up to 230 GHz. All measurements are done at single polarisation (QV or QH). MWS has a single rotating antenna (35 cm projected aperture) providing a very good spatial resolution. MWS is calibrated using an internal hot target and a cold sky, which is viewed through the main antenna. A single antenna concept allows to the MWS instrument to remain compact, but requires a complex quasi-optical network capable of splitting the different channels in the instrument. MWS includes a mixture of direct detection and heterodyne receivers and a signal processing electronics unit that does gain/offset adjustment and digitises the signal. MWS provides a scan angle range of +/-49° around the nadir. The antenna rotates at non-uniform speed in order to maximise the scene and calibration targets integration times. Footprints are ranging from 40 km at the lowest frequency to 17 km at the highest frequencies. In addition to performance, MWS also provides a robust design as required for an operational instrument. MWS includes an input filtering at lowest channels to provide protection against radio frequency interference. The temperature sounding channels (50 GHz – 58 GHz) are fully redundant and also the instrument has an internal failure detection and high recovery autonomy. The MWS instrument is designed to guarantee very good reliability (0.84) and availability for the whole lifetime of 7.5 years. This paper will present the MWS instrument key design features and predicted performance, as well as an overview of associated key technology developments. This paper will be accompanied by two other papers, presenting the Microwave Imager and Ice Cloud Imager instruments for MetOp Second Generation.

Paper 5 **MICROWAVE IMAGER INSTRUMENT FOR METOP SECOND GENERATION**

Salvatore D'Addio, Ville Kangas, Marc Loiselet, Graeme Mason, European Space Agency, Netherlands; Andrea Sacchetti, Tito Lupi, CGS S.p.A. Compagnia Generale per lo Spazio, Italy; Christian Tabart, Carine Bredin, Franck Bayle, Astrium SAS, France; Enrico Vetrano, Nikolas Sidiropoulos, Space Engineering S.p.A., Italy

Since 2006, the European contribution to operational meteorological observations from polar orbit has been provided by the Meteorological Operational (MetOp) satellites, which is the space segment of the EUMETSAT Polar System (EPS). As part of the next generation EUMETSAT Polar System (EPS-SG), the MetOp Second Generation (MetOp-SG) satellites will provide continuity and enhancement of these observations in the 2020 – 2040 timeframe. The MetOp-SG will consists of two series of satellites ("Satellite A" and "Satellite B"), with a nominal baseline of two or three satellites of each series. The payload complement of MetOp-SG was confirmed by EUMETSAT Council in 2012 and, out of ten instruments, it includes three microwave radiometers, namely Microwave Sounder (MWS), Microwave Imager (MWI) and Ice Cloud Imager (ICI). This payload complement provides a unique suite of high performance, operational microwave radiometers covering a total of 63 channels over a very wide frequency range from 18.7 GHz up to 664 GHz. These three radiometers will provide continuous and simultaneous operation for more than 20 years, representing an invaluable opportunity for cross-calibration of future spaceborne radiometer systems. After the confirmation of the payload complement, the European Space Agency issued a request for proposals for the microwave radiometers of MetOp-SG in 2012 and made the final selection in early 2013. For the MWI instrument, ESA selected CGS S.p.A. Compagnia Generale per lo Spazio (Italy) as the prime contractor. The

Microwave Imager (MWI) instrument has the objective of providing cloud and precipitation observations, snow and sea-ice coverage as well as gross profiles of water vapour and temperature. The Microwave Imager (MWI) is a conical scanning total-power microwave radiometer, providing calibrated and geo-located measurements in a total of 26 channels ranging from 18.7 GHz up to 183.31 GHz, offering dual polarisation measurements for all the low-frequency channels up to 89 GHz. The MWI is composed of one rotating part and one fixed part. The rotating part includes the main antenna, the feed assembly and the receivers electronics. The fixed part contains the hot calibration target, the reflector for viewing the cold-sky and the electronics for the instrument control and interface with the platform. In order to achieve very good radiometric accuracy and stability, the MWI is designed with sun-shields in order to minimize sun-intrusion. The MWI instrument rotates at a constant speed of 45 rpm, providing earth scene measurements over an azimuth range of +/-65 degrees, with footprints ranging from 10 km to 50 km (depending on frequency) and ensuring an along-track overlap between consecutive footprints of 30%. Hot and Cold calibration is performed periodically at each rotation (4-point calibration is used for the lowest frequency channels). MWI also provides a robust design as required for an operational instrument. It includes a stringent input filtering at the lowest channels to provide protection against radio frequency interference. An RFI processor at 18.7GHz is also included in order to detect and mitigate interference on-board. The MWI instrument is designed to guarantee very good reliability and availability for the whole lifetime of 7.5 years and is specifically designed to provide a high failure detection and recovery autonomy. This paper will present the MWI instrument key design features and performance, as well as an overview of associated key technology developments. It will be accompanied by two other papers, presenting the Microwave Sounder and Ice Cloud Imager instruments for MetOp-SG.

Paper 6 THE JASON-3 RADIOMETER

Frank Maiwald, Oliver Montes, Sharmila Padmanabhan, Darren Michaels, Amarit Kitiyakara, Robert Jarnot, Shannon Brown, Douglas Dawson, William Hatch, Paul Stek, Todd Gaier, Jet Propulsion Laboratory, California Institute of Technology, United States

The Advanced Microwave Radiometer (AMR) for the Jason-3 mission is a radiometer instrument in support of ocean altimetry measurements to study the ocean topography over multiple decades by the National Oceanic and Atmospheric Administration (NOAA). Jason-3 continues the line of radiometer instruments on the TOPEX/Poseidon, JMR, Jason-1, and OSTM/Jason-2 missions. In support of NOAA's mission of continuous coverage of ocean height measurements at low instrument cost, AMR for Jason-3 was evolved from Jason-2 hardware by incorporating lessons learned to improve radiometer stability and calibration. The AMR development was cost effective requiring less than 24 months. The AMR instrument consists of noise sources and Dicke switching for calibration of the three radiometer channels at 18, 24, and 34 GHz. In contrast to a conventional approach in which the RF and DC are combined very early in the assembly phase, a more flexible approach was chosen for AMR where RF and DC are separated. This allows early screening during the assembly and test phases before the integration into a single receiver chassis. In addition, parallel work on multiple RF and DC subassemblies can be enabled along with high temperature burn-in of all RF components. The measured RF performance of all radiometer channels exceeded most of the project requirements over a wide temperature range. Special attention was given to radiometric stability and calibration repeatability, as well as low input return loss of the Dicke switch circuit and isolator. The purpose of this presentation is to provide details on the radiometer development and its RF performance for Jason-3.

Tuesday, March 25	Calibration for Climatology	16:00 - 17:40
Lecture Session		Ramo Auditorium, Bldg 77

Session Co-Chairs: Al Gasiewski, University of Colorado; Francesc Torres, UPC

Paper 1 ASSESSMENT OF THE LONG-TERM RADIOMETRIC CALIBRATION STABILITY OF THE TRMM MICROWAVE IMAGER AND THE WINDSAT SATELLITE RADIOMETERS

16:00 *Ruiyao Chen, Andrea Santos-Garcia, Spencer Farrar, Linwood Jones, Central Florida Remote Sensing Laboratory, United States*

The NASA's Global Precipitation Measurement (GPM) mission uses a constellation of international satellites with microwave radiometers to provide the next-generation of global observations of precipitation. The GPM core observatory with its Dual-frequency Precipitation Radar (DPR) and the GPM Microwave Imager (GMI) will function as a transfer standard to provide inter-satellite radiometric calibration between the constellation members. The GPM Intersatellite Calibration Working Group (aka XCAL) has the responsibility to perform this radiometric calibration process. Since GPM has not been launched yet, the Tropical Rainfall Measurement Mission (TRMM) Microwave Imager (TMI) has been used as a proxy for the GMI to develop procedures and data analysis algorithms for inter-comparing two similar, but not identical, radiometers. In this regard, this paper assesses the long-term radiometric calibration stability of TMI relative to the WindSat polarimetric radiometer. We conducted two independent inter-comparisons over oceans in 2005 and 2011, and results are presented, which demonstrate deciKelvin relative stability over this greater than five-year period. Since both TMI and WindSat are externally calibrated total power radiometers, the long-term brightness temperature (Tb) stability depends primarily upon the stability of the external hot-load and cold sky calibration targets. Secondary considerations are the stability of front-end losses, receiver electronics and square-law detectors. To assess these parameters, we compare near-simultaneous, collocated, ocean observations of TMI and WindSat Tb's. To account for differences in the radiometer systems that affect the measured Tb (e.g., center frequency, bandwidth and earth incidence angle), we have developed a double-difference radiometric inter-comparison technique. First, the theoretical Tb difference between radiometer channels is calculated using an ocean radiative transfer model. Next, the observed differences are calculated in 1° Lat/Lng boxes with filtering to assure homogeneous clear-sky oceanic scenes. Finally, double-difference (observed – theoretical) radiometric biases are determined by channel for two one-year periods, which are separated by more than five years (2005 and 2011). The relative change in these calibration biases over five years is used to estimate the long-term stability of one radiometer with respect to the other.

Paper 2 THE FUNDAMENTAL CLIMATE DATA RECORD OF SSM/I BRIGHTNESS TEMPERATURES FROM CM SAF

16:20 *Karsten Fennig, Marc Schröder, Axel Andersson, Deutscher Wetterdienst, Germany*

The satellite based HOAPS (Hamburg Ocean Atmosphere Parameters and Fluxes from Satellite Data; http://www.hoaps.org/) climatology provides climate data records of precipitation, evaporation and the resulting freshwater flux over the global ice-free ocean between 1987 and 2008. The latest version of HOAPS has been released by CM SAF and is available from the CM SAFs web user interface (http://wui.cmsaf.eu/). The HOAPS climate data records are primarily based on passive microwave measurements from the SSM/I (Special Sensor Microwave/Imager) sensor family. In order to derive reliable long term trend estimates of the global water cycle parameters it is strictly necessary to carefully correct for all known problems and deficiencies of the SSM/I radiometers as well as to inter-calibrate and homogenise the different instruments. Moreover, all applied corrections need to be clearly documented to provide a complete calibration traceability for a Fundamental Climate Data Record (FCDR). Following these recommendations, CM SAF has released the first version of the FCDR of SSM/I brightness temperatures, available from the web user interface (DOI:10.5676/EUM_SAF_CM/FCDR_SSMI/V001, http://dx.doi.org/10.5676/EUM_SAF_CM/FCDR_SSMI/V001). Three different FCDRs of SSM/I brightness temperatures are currently available, released by CM SAF, Colorado State University, and Remote Sensing Systems. All groups developed different approaches to homogenize the SSM/I sensor family. This presentation will focus on the main calibration issues identified for the SSM/I instruments and compare the different intercalibration procedures implemented to homogenise the time series of all 6 different SSM/I instruments. A validation of the brightness temperatures is a challenging task as there are no ground-truth reference measurements available for the microwave band. Hence, the homogeneity of the FCDR is evaluated by an analysis of the relative biases between the different instruments before and after the intercalibration offsets are applied. Finally, all three FCDRs are compared to identify strengths and weaknesses of the intercalibration approaches. This is a first step toward a consensus SSM/I Fundamental Climate Data Record. Significant differences between the diverse inter-calibration approaches must be identified and, if possible, traced back to the physical reason.

Paper 3 INTER-CALIBRATION AND VALIDATION OF OBSERVATIONS FROM MODERN SATELLITE MICROWAVE HUMIDITY SOUNDERS

16:40 *Isaac Moradi, University of Maryland, United States; Ralph Ferraro, National Oceanic and Atmospheric Administration, United States*

Atmospheric water vapour significantly contributes to the Earth's radiation budget and is a critical variable for climate studies. It is the dominant natural greenhouse gas and the largest known feedback mechanisms for amplifying global warming. Tropospheric humidity both directly and indirectly affects the hydrological cycle as well as strongly contributes to the water vapour feedback, especially in mid-upper troposphere, owing to the low temperatures at those altitudes. Two main sources of tropospheric humidity data include radiosonde measurements as well as observations from space-borne microwave instruments operating at the frequencies close to the water vapour absorption line at 183 GHz. Radiosonde data are available for a long-period and have a high vertical resolution compared to the microwave satellite data. On the other hand, satellite data provide global coverage, but radiosonde stations are very sparse. Both space-based and radiosonde observations are prone to different errors. Radiosonde data are affected by several factors including sensor contamination, daytime radiation bias, sensor icing in mid-upper troposphere, and discontinuity in the data because of the difference between observations from different sonde sensors. Microwave satellite data are also prone to several errors including calibration drift, geolocation error, sensor degradation, and inter-satellite biases. We present the results of evaluating observations from microwave instruments aboard recently launched the Suomi National Polar-orbiting Partnership (NPP, ATMS instrument) and Megha-Tropiques (SAPHIR instrument) satellites. The study includes inter-comparison and inter-calibration of observations of similar humidity channels from the two satellites, evaluation of the satellite data using high-quality radiosonde data from Atmospheric Radiation Measurement Program as well as geolocation error correction. Besides, we employ GPS Radio Occultaion Observations from the COSMIC mission to evaluate the measurements from the ATMS temperature sounding channels. The results of this study are valuable for generating climate data records from these instruments as well as for extending current climate data records from similar instruments such as AMSU-B and MHS to the ATMS and SAPHIR instruments.

Paper 4 LONG-TERM STABILITY AND CALIBRATION OF THE MLS INSTRUMENT ON THE AURA SATELLITE

17:00 *Robert Jarnot, Richard Cofield, Lucien Froidevaux, Alyn Lambert, Nathaniel Livesey, JPL, United States; Gloria Manney, Northwest Research Associates, United States; William Read, Michelle Santee, Michael Schwartz, Paul Stek, JPL, United States; Hugh Pumphrey, University of Edinburgh, United Kingdom*

The Microwave Limb Sounder (MLS) on the A-Train Aura satellite has been operational for almost nine years, making measurements in bands centered at 118, 190, 240, 640 and 2522 GHz. MLS uses a limb-viewing geometry, using a switching mirror for radiometric calibration with periodic views to cold space and to one of two internal calibration targets. Spectral analysis is performed using nineteen 25-channel filterbanks, five 11-channel filterbanks, 12 individual broad filter channels, and four narrow band 128-channel digital autocorrelators. The 2522 GHz radiometer was implemented separately from the lower frequency ones, with its own scanning mirror which served as both the telescope to view the atmospheric limb, and as the switching mirror for radiometric calibration. Unlike the lower frequency radiometers which used solid state local oscillators (LO), the 2522 GHz radiometer used a novel gas laser LO in which a CO_2 laser pumped a passive methanol laser. In this presentation we discuss pre- and post-launch calibrations, long-term stability, and systematic error sources which provide the ultimate limitations on accuracy. Extensive pre-launch calibrations covered radiometric and spectral characteristics, and FOV parameters. The FOV calibrations in the 118 GHz through 640 GHz bands were performed using a near-field range. Because of the relatively long timescale of MLS operations, understanding the limitations of the measurements becomes very important, especially when they are used for trend monitoring, particularly for Stratospheric HCl, O3, ClO and HNO3. As well as routine measurement data quality and properties, the results from special on-orbit calibration-specific measurements are presented. Lessons learned, and ways of improving measurement accuracy in future instruments of this type, are also discussed.

Paper 5 AQUARIUS WHOLE RANGE CALIBRATION: CELESTIAL SKY, OCEAN, AND LAND TARGETS
17:20 *Emmanuel Dinnat, NASA-GSFC/Chapman University, United States; David Le Vine, NASA-GSFC, United States; Rajat Bindlish, USDA-ARS, United States; Jeffrey Piepmeier, NASA-GSFC, United States*

Aquarius is a NASA instrument comprising three radiometers at L-band (1.4 GHz) dedicated to the remote sensing of global sea surface salinity. It has been operating nominally since the end of August 2011. Despite good performance over the ocean in the retrieval of salinity, residual biases have been identified when comparing Aquarius measurements to simulation over the Celestial Sky (CS) and well instrumented land sites. We discuss results of work to establish an accurate calibration of the Aquarius radiometers over the whole dynamic range of antenna temperatures (Ta) from the low Ta of the CS to the high Ta of land and ice surfaces. During the baseline processing, Aquarius' radiometers are calibrated using an internal hot target; An additional empirical adjustment is performed by comparing measured and simulated Ta's over oceans (Ta ~ 100K). The simulation utilizes a radiative transfer model that integrates contributions from all directions around the antenna and weights them by the antenna gain patterns [1]. The ocean calibration was used to correct biases of a few Kelvin at the beginning of the mission, and a drift of -1K during the first year of the mission. This resulted in measured Ta being within +/-0.2K of the simulations over oceans. However, when the spacecraft is rotated to point Aquarius beams toward the CS (Ta~5K), biases of the order of -2K are identified. On the opposite end of the Ta range (~250K), biases of the order of 5K–8K are identified over land surfaces. A significant source of bias is the uncertainty on the antenna gain pattern. Several version of Aquarius gain pattern models exist (derived from numerical simulations and measurements on a scale model of the spacecraft) and there is significant disagreement regarding the spillover ratio (SR). The SR is the off-Earth fraction of antenna power when the antenna is in its normal mode pointing toward the Earth. SRs differ by ~1.5% between various models, enough to create a ~1.5K/4K Ta bias over ocean/land. A first step in our Whole Range Calibration (WRC) is to validate the SR as accurately as possible. For that purpose, we use measurements performed when the spacecraft was in the CS-mode (i.e. inverted) and crossing an ocean/land transition: The very large change in scene temperature makes the uncertainty on the emissivity model negligible when estimating the SR. With the new estimate of SR, the existing gain pattern is adjusted to create a hybrid model for use in calibration. To accomplish the calibration, we compute a linear regression of Ta measured versus simulated, using only the data over the CS and ocean. Then, data over land are used as a validation of the new calibration. For the validation over land, we use in situ data from the USDA Little Washita watershed site, where measurements of soil moisture and surface temperature are available, in order to reduce the uncertainty on land emissivity. The use of the hybrid pattern and adjusted calibration results in significant improvements in the agreement between measurement and simulated TA at the cold (CS) and warm (land) ends and a more robust calibration of the Aquarius radiometers. [1] D. M. Le Vine, E. P. Dinnat, S. Abraham, P. de Matthaeis, F. J. Wentz, (2011), The Aquarius Simulator and Cold-Sky Calibration, IEEE Transactions on Geoscience and Remote Sensing, 49(9): 3198-3210; DOI:10.1109/TGRS.2011.2161481.

Wednesday, March 26 — Airborne and Groundbased Instruments — 08:00 - 09:40

Lecture Session — **Ramo Auditorium, Bldg 77**

Session Co-Chairs: Andreas Colliander, NASA - Jet Propulsion Laboratory; Sharmila Padmanabhan, NASA - Jet Propulsion Laboratory

Paper 1 MICROWAVE SCINTILLOMETERS FOR LATENT HEAT FLUX MEASUREMENTS
08:00 *Harald Czekala, Gerrit Maschwitz, Martin Philipp, Thomas Rose, RPG Radiometer Physics GmbH, Germany; Oscar Hartogensis, Wageningen University, Netherlands*

The use of Scintillometry for measurements of turbulent fluxes is a well-established technique in planetary boundary layer meteorology: One transmitter and one receiver are used to set up a horizontal line-of-sight Tx/Rx line which measures the modulation of a constant signal due to turbulence-induced changes of the refractive index along the path. Optical scintillometers for sensible heat flux (H) measurements are commercially available. In order to measure the latent heat flux (evapotranspiration, LvE) directly, a combination of and optical scintillometer and a microwave scintillometer can be used. The time series of intensity fluctuations have to be recorded simultaneously to permit the evaluation of not only the optical and microwave signal alone, but also the co-spectrum of both instruments. The co-spectrum gives a third measurement variable, when observing the natural eddy spectrum at two different wave lengths. This allows for an independent calculation of sensible and latent heat fluxes at the same time, without having to rely on assumptions about the two signals' covariance, or any other parameterization. RPG and the Wageningen University have – in a STW funded development project – developed a prototype microwave scintillometer instrument: This RPG-MWSC-160. This MWSC is working as a transmit/receive system at 160.8 GHz. We show test results from two very different environment conditions (irrigated crops in Mexico, and the Meteorological Observatory Lindenberg, Germany), which confirm the systems stability and sensitivity. RPG has now re-designed the prototype for series production. This series type is modified for 12 V power supply and significantly reduced in weight and size. The receiver internal data acquisition provides additional external connectors for real-time co-sampling of the raw-data signals of optical scintillometers of most vendors. An internal control computer takes care of the data evaluation and calculates the sensible and latent heat fluxes. All processes data is delivered to the user by an Ethernet/LAN interface. Keywords: scintillation, latent-heat-flux, microwave, remote sensing, millimetre wave propagation

Paper 2 ISMAR: A NEW SUBMILLIMETER AIRBORNE RADIOMETER
08:20 *Stuart Fox, Clare Lee, Ian Rule, Robert King, Stuart Rogers, Chawn Harlow, Met Office, United Kingdom*

ISMAR (International SubMillimeter Airborne Radiometer) is a new passive remote-sensing radiometer which has been jointly funded by the UK Met Office and the European Space Agency (ESA). It contains a number of heterodyne receivers operating at frequencies between 118 and 664GHz, some with dual polarisation. The design is modular and will allow further channels to be added in future, including 874GHz. Submillimeter waves are very sensitive to scattering by ice particles, and the channels have been selected to allow the direct retrieval of various ice-cloud properties, including Ice Water Path (IWP) which is an important parameter in General Circulation Models (GCMs). ISMAR can also be used for surface emissivity and radiative transfer studies as it can view in multiple nadir and zenith directions. ISMAR has been developed as a satellite demonstrator for ICI (Ice Cloud Imager) due for launch in 2022 on the EUMETSAT Polar System - Second Generation satellites (EPS-SG). It can be used for testing and developing retrieval algorithms prior to launch, as well as for calibration/validation post-launch and specific scientific case studies. It is designed to operate on board the FAAM BAe-146 atmospheric research aircraft, which also carries a wide range of complementary remote-sensing and in-situ instrumentation including microwave radiometers, infra-red and visible spectrometers and cloud physics probes. The instrument is self-contained, allowing simple ground-based operation as well as the potential for installation on other aircraft. ISMAR is currently undergoing integration testing, and flight testing will take place from April 2014. An ISMAR science campaign is currently planned to take place in Goose Bay, Canada in 2015 to study the submillimeter signature of cirrus cloud.

Paper 3 THE NCAR MICROWAVE TEMPERATURE PROFILER: DATA APPLICATIONS FROM RECENT DEPLOYMENTS
08:40 *Julie Haggerty, National Center for Atmospheric Research, United States; Michael J. Mahoney, Boon Lim, Jet Propulsion Laboratory, California Institute of Technology, United States; Kelly Schick, Chris Davis, National Center for Atmospheric Research, United States*

A newly-designed Microwave Temperature Profiler (MTP) was developed at JPL for the NSF-NCAR Gulfstream-V (Mahoney and Denning, 2009). MTP is a scanning microwave radiometer that measures thermal emission at spectral lines in the 50-60 GHz oxygen complex. MTP scans from near-zenith to near-nadir angles, measuring brightness temperatures forward, above, and below the aircraft at 17 s intervals. A statistical retrieval method derives vertical temperature profiles from the measurements, using radiosonde profiles in the vicinity of the aircraft as a priori information. Data products from MTP include atmospheric temperature profiles above and below the aircraft, as well as estimates of tropopause height, cold-point, and thermal lapse rate. Since 2008 this MTP has been deployed in numerous field experiments for a variety of scientific applications. Results based on MTP measurements from two recent experiments are summarized in this paper. The Tropical Ocean Troposphere Exchange (TORERO) project (Jan-Feb, 2012) employed MTP to support observations of the release, transport and fate of reactive halogen gases and oxidized volatile organic compounds in the Eastern Pacific (Wang et al., 2013). During this project, MTP provided measurements of the tropical tropopause layer (TTL) structure, evidence of double tropopause layers at higher latitudes, and examples of stratospheric intrusion. Thermal structure as derived from MTP demonstrates consistency between the lapse rate tropopause and other indicators of tropopause height such as ozone mixing ratio. Temperature anomalies at constant altitudes are currently being examined for evidence of convectively-induced gravity waves. The Mesoscale Predictability (MPEX) project (May-June, 2013) investigated the utility of sub-synoptic observations to extend convective-scale predictability and otherwise enhance skill in regional numerical weather prediction over short forecast periods. This project relied on MTP and dropsonde temperature profiles to characterize atmospheric structure on fine spatial scales. Comparison of MTP profiles with an independent set of dropsonde and rawinsonde profiles from MPEX demonstrates the accuracy of the MTP temperature profile retrievals. Ongoing work with MTP data will examine double tropopause structure in association with the sub-tropical jet, mountain lee waves, and variance of temperature in the lower stratosphere compared with the troposphere. Results based on analyses of MTP data from TORERO and MPEX will be presented at the meeting. References: M.J. Mahoney and R. Denning, "A State-of-the-Art Airborne Microwave Temperature Profiler (MTP)", Proceedings of the 33rd International Symposium on the Remote Sensing of the Environment, Stresa, Italy, May 4-8, 2009. Wang, S., R. Volkamer, B. Dix, S. Baidar, E. Apel, D. Bowadalo, T. Campos, R. Gao, J. Haggerty, S. Hall, R. Hornbrook, B. Pierce and P. Romashkin, "Large-scale ozone destruction due to halogen chemistry in the southern hemisphere free troposphere", Nature Geoscience, submitted Oct 2013.

Paper 4 THE AIRBORNE SCANNING MICROWAVE LIMB SOUNDER (A-SMLS): DESIGN, CAPABILITIES, AND INITIAL FLIGHTS
09:00 *Paul Stek, Richard Cofield, Anthony Guarnera, Jet Propulsion Laboratory, California Institute of Technology, United States; Howard Hui, California Institute of Technology, United States; Robert Jarnot, Lance Milligan, Ryan Monroe, Nathaniel Livesey, Sharmila Padmanabhan, Robert Stachnik, David Webb, Jet Propulsion Laboratory, California Institute of Technology, United States*

The Airborne Scanning Microwave Limb Sounder (A-SMLS) is a new airborne atmospheric composition sensor developed through the Earth Science Technology Office (ESTO) Instrument Incubator Program (IIP). A-SMLS was developed as a prototype and component test bench for advanced microwave limb sounders such as the one proposed for the Global Atmospheric Composition Mission (GACM) in the 2007 Earth Science Decadal Survey. It also can serve as a valuable tool for focused field campaigns measuring composition and transport in the upper troposphere/lower stratosphere (UTLS). Mounted in a spear pod on the wing of NASA's high altitude WB-57 aircraft, A-SMLS measures thermal molecular emission in the 220 to 250 GHz frequency band horizontally in front of the aircraft. A hemispherical HDPE radome with an antireflective Porex coating replaces the standard spear pod nose cone. A

20 cm gimbaled mirror scans the instrument's field of view ±5° in elevation and ±30° in azimuth. The incoming beam is then focused into a sideband separating superconducting insulator superconducting (SIS) mixer where it is downconverted to a band from 6-18 GHz. A chopper, scan mirror, and a partially reflecting beam splitter within the optical path allow the receiver to be calibrated using a zenith cold sky view, an 80 dB return loss calibration load, and a swept calibration tone. The bands of interest are then selected with a bandpass filter, downconverted to baseband, and analyzed using two 3 GHz wide polyphase spectrometers. Four engineering flights were conducted in the summer of 2012. The instrument design, data from the test flights, on ground calibration measurements, and future plans will be presented.

Paper 5 **WIDE-BAND AIRBORNE MICROWAVE AND MILLIMETER-WAVE RADIOMETERS TO IMPROVE THE SPATIAL RESOLUTION OF WET-TROPOSPHERIC PATH DELAY CORRECTIONS FOR**
09:20 **COASTAL AND INLAND WATER ALTIMETRY**

Steven C. Reising, Colorado State University, United States; Pekka Kangaslahti, Shannon Brown, Sharmila Padmanabhan, Chaitali Parashare, Oliver Montes, Jet Propulsion Laboratory, California Institute of Technology, United States; Xavier Bosch-Lluis, Thaddeus Johnson, Victoria Hadel, Colorado State University, United States; Douglas Dawson, Todd Gaier, Behrouz Khayatian, Jet Propulsion Laboratory, California Institute of Technology, United States; Behzad Razavi, University of California at Los Angeles, United States

Current satellite ocean altimeters include nadir-viewing, co-located 18-34 GHz microwave radiometers to measure wet-tropospheric path delay. Due to the area of the surface instantaneous fields of view (IFOV) at these frequencies, the accuracy of wet path retrievals is substantially degraded near coastlines, and retrievals are not provided over land. Retrievals are flagged as not useful within 40 km of the world's coastlines. A viable approach to improve their capability is to add wide-band millimeter-wave window channels from 90 to 170 GHz, yielding finer spatial resolution for a fixed antenna size. In addition, NASA's Surface Water and Ocean Topography (SWOT) mission in formulation (Phase A) is planned for launch in late 2020. The primary objectives of SWOT are to characterize ocean sub-mesoscale processes on 10-km and larger scales in the global oceans, and to measure the global water storage in inland surface water bodies and the flow rate of rivers. Therefore, an important new science objective of SWOT is to transition satellite radar altimetry into the coastal zone. The addition of millimeter-wave channels near 90, 130 and 166 GHz to current Jason-class radiometers is expected to improve retrievals of wet-tropospheric delay in coastal areas and to enhance the potential for over-land retrievals. The Ocean Surface Topography Science Team Meeting recommended in 2012 to add these millimeter-wave channels to the Jason Continuity of Service (CS) mission. To reduce the risks associated with wet-tropospheric path delay correction over coastal areas and fresh water bodies, we are completing the development of an airborne radiometer that combines millimeter-wave window channels at 90, 130 and 166 GHz with 18.7, 23.8 and 34.0 GHz microwave channels, as well as temperature and water vapor sounding channels near 118 and 183 GHz for validation of wet-path delay. For nadir-viewing space-borne radiometers with no moving parts, two-point internal calibration sources are necessary, and we have demonstrated packaged noise diodes with low mass as well as sufficient noise power and stability in the 90 to 170 GHz millimeter-wave frequency range. The instrument also includes Dicke-switched matched loads as well as an ambient black-body calibration target to provide a calibration reference independent of the internal noise sources. This instrument development and airborne flight demonstration will (1) assess wet-tropospheric path delay variability on 10-km and smaller spatial scales, (2) demonstrate millimeter-wave radiometry using both window and sounding channels to improve both coastal and over-land retrievals of wet-tropospheric path delay, and (3) provide an instrument for calibration and validation in support of the SWOT mission. The instrument has been tested in an outdoor environment for end-to-end calibration of the microwave channels. Fabrication and integration of the millimeter-wave channels will be completed by January 2014, with initial test and remote sensing flights aboard a Twin Otter aircraft planned during the spring of 2014.

Wednesday, March 26 — Passive/Active Soil Moisture Retrieval Algorithms — 10:10 - 11:50

Lecture Session — **Ramo Auditorium, Bldg 77**

Session Co-Chairs: Simonetta Paloscia, IFAC-CNR; Eni Njoku, NASA - Jet Propulsion Laboratory

Paper 1 **A PROTOTYPE ANN BASED ALGORITHM FOR THE SOIL MOISTURE RETRIEVAL FROM L- BAND IN VIEW OF THE INCOMING SMAP MISSION**
10:10 *Emanuele Santi, Simonetta Paloscia, Simone Pettinato, Giacomo Fontanelli, IFAC - CNR, Italy*

The moisture of soil (SMC) is one of the most important factors affecting the hydrological cycle, and therefore a systematic and timely monitoring of this parameter at both local and global scales is of primary importance in obtaining a better understanding of geophysical processes and in managing environmental resources as well as natural disasters. Frequent and spatially distributed soil moisture measurements are advisable for the most part of the applications related to the environmental disciplines, such as climatology, meteorology, hydrology and agriculture. Dedicated satellites for the SMC retrieval (e.g. SMOS) have been launched in recent years and some new initiatives are in progress. Among the others, the incoming SMAP mission is characterized by the unique feature of carrying on board both radar and radiometer, operating at the same frequency (L- band) but at a different spatial resolution. An algorithm for retrieving the SMC from SMAP acquisitions is presented here. The algorithm is based on Artificial Neural Networks (ANN) techniques and takes advantage by the synergy of the active and passive SMAP acquisitions. It considers the radiometric data at low resolution for estimating a 'first guess' of SMC that is then used for retrieving the SMC at high resolution, through the inversion of the radiative transfer model, that was implemented in the simplified form of the "water-cloud" model (Attema and Ulaby,1978) for radar data and the "tau - omega" model (Mo et al., 1982) for radiometric acquisitions. The inversion is performed by two ANNs that have been trained with extended datasets of microwave data (brightness and backscatter) simulated by using the above models. The ANNs were classical feedforward multilayer perceptron, trained with the back propagation (BP) learning rule. The best architecture of each net, in terms of number of hidden layers and neurons, was defined after an optimization process, in order to obtain a satisfactory accuracy, avoiding the problems related to a potential overfitting. The training set was obtained by iterating the model simulation for random values of the input parameters, in a range that is representative of the real observed targets. Experimental acquisitions from the PALS aircraft based SMAP simulator, along with the corresponding ground truth, have been considered for setting the range of the model inputs and calibrating the model in order to assess the validity of the simulated data. Training was obtained by feeding each net with the simulated electromagnetic parameters, while the output was the SMC. The algorithm was tested on the large dataset of SMAP simulated data that was delivered in the framework of the cal/val activities, obtaining results in line with the reference data and the climatic areas of the Earth's surface.

Paper 2 **PASSIVE AND ACTIVE FOREST SIMULATIONS AND COMPARISONS WITH SMAPEX-3 DATA**
10:30 *Cristina Vittucci, Leila Guerriero, Paolo Ferrazzoli, Rachid Rahmoune, University of Rome Tor Vergata, Italy; Mihai Tanase, Rocco Pancera, University of Melbourne, Australia; Alessandra Monerris, Christoph Rudiger, Y Gao, Jeff Walker, Monash University, Australia*

The Soil Moisture Active and Passive Experiment (SMAPEx) consisted of three airborne campaigns held in the Yanco Region within the Murrumbidgee River Catchment (New South Wales, Australia) between 2010 and 2011, in order to encompass seasonal variations of soil moisture and vegetation. The SMAPEx airborne facility consisted of the Polarimetric L-band Multibeam Radiometer (PLMR, operating at 1.41 GHz) and the Polarimetric L-band Imaging Scatterometer (PLIS, operating at 1.26 GHz). When used simultaneously on the same aircraft, these instruments simulate the SMAP (Soil Moisture Active Passive) mission data, with 1km passive microwave footprints and 10m active microwave footprints resolution, for a flight altitude of 3km. The present study focuses on the analysis of airborne passive and active data collected during eight flights over the Gillenbah and Boona State forests during the third SMAPEx campaign (SMAPEx-3), which took place during the beginning of the austral spring in September 2011. Concurrent ground measurements of soil moisture content and tree biophysical parameters, such as diameter at breast height and plant density, were also performed. In a first step, maps of emissivity e and backscattering '° have been processed for each flight and polarization. Then, a sensitivity analysis with respect to the bio-geophysical parameters measured at the ground sampling areas has been carried out. The dynamic range shown by the maps, as well as the emissivity and '° temporal trends, show that passive measurements have a better sensitivity to soil moisture variations over forested areas. On the other hand, the backscattering coefficient seems to be more influenced by tree characteristics that tend to hide the soil moisture effects, so that '° enhances discrimination between forests and non-forested areas better than emissivity. The effects of soil and vegetation parameters on the SMAPEX-3 data have been interpreted through model simulations. The theoretical electromagnetic model developed at Tor Vergata University is a discrete scatterer model which allows simulations of both emissivity and backscattering coefficient of forests under a unified approach. Specific allometric equations and tree density distribution functions, which were available for the case studies of Gillenbah and Boona forests, have been used. Both model simulations and experimental data confirm that an ideal triangle can be traced in the '°-e plane. The three vertexes correspond to the emission and backscattering of a dry surface, a wet surface and vegetation volume. Data collected during SMAPEX-3 are also located within this ideal triangle, although in a limited extent because of the quite dry environment of the Gillenbah and Boona forests. Nevertheless, this property could be of operational interest when retrieval algorithm based on the synergy between passive and active sensors are developed.

Paper 3 **SPATIO-TEMPORAL DOWNSCALING OF SOIL MOISTURE FROM PASSIVE MICROWAVE USING ACTIVE MICROWAVE**
10:50 *Sat Kumar Tomer, Ahmad Al Bitar, Centre d'Etudes Spatiales de la BIOsphère, France; Sekhar Muddu, Indian Institute of Science, India; Samuel Corgne, UMR 6554 CNRS LETG Rennes Costel, France; Yann Kerr, Centre d'Etudes Spatiales de la BIOsphère, France*

Soil moisture retrieved from SMOS (passive microwave) has a fine temporal resolution (approximately 3 days), but the spatial resolution is coarse (approximately 50 km) (Kerr, Y.H. et al., 2001). On the other hand, the active microwave satellites are capable of providing fine spatial scale (less than 100 m) products but with a poor temporal resolution (around 3 weeks) (Moran, M.S. et al., 2004). There is a potential to merge both the sensors to provide the soil moisture at a better spatial and temporal resolution, which would be helpful in various applications like agriculture, hydrology, atmospheric sciences etc. The current study presents a methodology for the spatio-temporal down-scaling of the soil moisture retrieved from the SMOS with the help of active microwave data (RADARSAT-2), and the methodology is tested in an experimental watershed, Berambadi, South India. First, a non parametric algorithm based on the CDF transformation was developed to retrieve the soil moisture from RADARSAT-2. This developed algorithm was validated using the 28 satellite images and field data collected in 50 agricultural fields spanning over 3 years. The developed algorithm provided a good estimate of the surface soil moisture with a RMSE of 0.05 (v/v). Then the surface heterogeneity (soil texture, land use and SMOS mean antenna patterns) was analysed by up-scaling and comparing the validated RADARSAT-2 soil moisture maps with the SMOS retrieved soil moisture. In the study area, it was observed that up-scaling based on the land use outperformed the others. Then by considering the significant effect of land cover on up-scaling, a methodology was developed to downscale the soil moisture from SMOS based on a combination of the statistical down-scaling of variance observed at large scale (Blöschl, G. et al., 2009) and spatial patterns obtained from the RADARSAT-2 derived soil moisture. The methodology was first calibrated using the 14 RADARSAT-2 images, and then was validated using the separate 14 RADARSAT-2 images and field data. The developed methodology showed the promising results with a RMSE of 0.07 (v/v).

Paper 4 **MODELING PASSIVE AND ACTIVE MICROWAVE SIGNATURES OF GRASS IN THE MAQU AREA OF THE TIBETAN PLATEAU**
11:10 *Laura Dente, University of Twente, Netherlands; Leila Guerriero, Paolo Ferrazzoli, University of Rome Tor Vergata, Italy; Zhongbo Su, Rogier van der Velde, University of Twente, Netherlands*

Emissivity and backscattering coefficient show a different sensitivity to surface and vegetation parameters and they can provide complementary information on the observed land surface. Research recently focused on the combined use of passive and active microwave information, but only few studies exploited discrete scattering models to investigate this topic. The main reason lies in the difficulty to obtain a detailed description of soil and vegetation needed as input by the models. However, this problem might be mitigated by using a single model to simulate both emission and backscatter, since the number of constraints in the model inputs should be increased. The main objective of this study was to evaluate the advantage of using a unique model, i.e. the Tor Vergata model, driven by a unique set of input parameters to estimate both emissivity and backscattering coefficient and to validate these estimates with AQUA AMSR-E and Metop ASCAT observations. Up to now, most applications of this model have been applied over different land covers by several studies, but to passive and active observations separately. The combined use of active and passive microwave signatures has the potential to improve the understanding of emission and scattering mechanisms over land. In this way, if the model is used to train a retrieval algorithm, the number of constraints on the retrieval process should be increased, thus leading to an improvement of the soil moisture retrieval accuracy. The investigation was carried out for the Maqu area, located along the upstream reach of the Yellow River (in the north-eastern part of the Tibetan Plateau), where measurements of soil moisture and soil temperature are continuously collected in several sites. The area of interest is flat and covered by homogeneous grassland with a thin litter layer over the soil surface. The analysis consisted of two main steps: the optimization of the model inputs, which was carried out over 2009 data, and the validation of the results over 2010 data. The average of soil moisture in situ measurements and the leaf area index obtained from MODIS Terra/Aqua 8-days LAI products were used as model inputs. Moreover, the surface temperature obtained from Ka-band AMSR-E data was used to compute the brightness temperature from the modeled emissivity. This allowed us to make the comparison with the satellite data. No measurements were available for other model inputs, such as surface roughness, litter biomass and vegetation structural parameters, therefore they were optimized to obtain the best match with both ASCAT and AMSR-E observations of 2009. The synergistic use of active and passive data was crucial at this step of the study, because it allowed us to find more realistic input values than in the case of using one kind of data only. The optimization over 2009 data led to obtain a good agreement between model outputs and satellite signatures for the active case, with a determination coefficient (R2) of 0.9 and a root mean square error (rmse) of 0.5 dB, and a slight overestimation for the passive case, with R2 of 0.8 and rmse of 6.3 K for H polarization and R2 of 0.5 and rmse of 5.9 K for V polarization. The validation results with 2010 data were slightly worse than the optimization ones (R2 of 0.8 and rmse of 1 dB for the active case and R2 of 0.5 and rmse of 8 K for the passive case). Different sources of uncertainties affected the results, such as our knowledge about litter moisture and biomass and the method for estimating the surface temperature.

Paper 5 **DEVELOPMENT OF THE SMAP RADIOMETER SOIL MOISTURE ALGORITHM USING SMOS OBSERVATIONS**
11:30 *Rajat Bindlish, Thomas Jackson, USDA ARS HRSL, United States; Steven Chan, NASA JPL, United States; Tianjie Zhao, Michael Cosh, USDA ARS HRSL, United States; Peggy O'Neill, NASA GSFC, United States; Eni Njoku, Andreas Colliander, NASA JPL, United States; Yann Kerr, CESBIO, France*

The Soil Moisture Active Passive (SMAP) mission will provide three Level 2 soil moisture products, each with a different spatial resolution. The 36-km gridded (~ 40 km resolution) SMAP soil moisture product (L2_SM_P) is derived using only the passive sensor and ancillary data and has heritage to other satellite-based soil moisture products. This paper contributes to the development of the SMAP L2_SM_P product by exploiting the heritage of the Soil Moisture Ocean Salinity (SMOS) satellite observations and products. SMOS observations provide us with the opportunity to develop a testbed for the evaluation of different SMAP L2_SM_P retrieval algorithm options. Microwave observations from the SMOS mission are reprocessed to simulate SMAP microwave radiometer observations at a constant incidence angle of 40o. This provides a brightness temperature (TB) data set that closely matches the observations that would be provided by the SMAP radiometer. The reprocessed SMOS brightness temperature data provide a basis for evaluating different SMAP L2_SM_P algorithms. In this investigation we examined: (a) Single Channel Algorithm h-pol (SCA-H), which is based on a zero-order approximation to the radiative transfer equation and uses the channel that is most sensitive to soil moisture (H-pol). Brightness temperature is corrected for the effects of temperature, vegetation, roughness, and soil texture using ancillary data sets. This is the current SMAP L2_SM_P baseline algorithm. (b) Single Channel Algorithm v-pol (SCA-V) – similar to SCA-H, but uses v-pol instead of h-pol observations. (c) Microwave Polarization Ratio Algorithm (MPRA) – a two-parameter retrieval model (soil moisture and vegetation opacity) based on the original Land Parameter Retrieval Model. It uses the microwave polarization ratio at 1.4 GHz and emissivity to parameterize vegetation opacity and estimate soil moisture. (d) Dual Channel Algorithm (DCA) – uses both radiometer polarizations to iteratively solve for soil moisture and vegetation opacity. The outputs of the candidate radiometer-only SMAP algorithms were compared to both in situ measurements and SMOS soil moisture products for a period of 4 years (2010-2013). The SCA-H is currently the SMAP L2_SM_P baseline algorithm and was the initial focus of this study. The global soil moisture spatial patterns obtained from SMOS TB and the SCA-H retrieval algorithm are consistent with geographical features. The SMOS soil moisture estimates using the SCA-H algorithm also compare well with the in situ observations over USDA ARS watersheds (RMSE=0.037 m3/m3, Bias=-0.016 m3/m3, R=0.745). The SMOS/SMAP SCA retrievals have a low bias and RMSE. The results from the SCA-V algorithm were comparable to the h-pol retrievals, although the study also suggested the need to have polarization dependent vegetation parameters in the SCA retrieval. The SCA in this study uses a 10-year MODIS-based vegetation climatology for vegetation correction which results in robust and stable soil moisture retrievals over the entire study period. In contrast to the SCA, the soil moisture retrieval performance was not as good with other algorithm options. The use of both polarizations in the other algorithms (MPRA and DCA) resulted in soil moisture retrievals with a positive soil moisture bias and greater dynamic range than the in situ observations. Algorithms that use both channels appear to be less robust and result in greater soil moisture error in the presence of noise in brightness temperature observations. Initial results indicate the SMAP L2_SM_P algorithms can meet the mission soil moisture target accuracy requirement of 0.04 m3/m3. USDA is an equal opportunity provider and employer.

Wednesday, March 26 — Calibration for L-band Radiometers — 13:00 - 14:40

Lecture Session — **Ramo Auditorium, Bldg 77**

Session Co-Chairs: David Le Vine, NASA - Goddard Space Flight Center; Darren McKague, University of Michigan

Paper 1 **PRACTICAL ISSUES ON SMOS SINGLE ANTENNA PATTERNS**
13:00 *Lin Wu, Israel Durán, Francesc Torres, Ignasi Corbella, Nuria Duffo, Universitat Politècnica de Catalunya, Spain; Josep Closa, Rodrigo Manrique, Quiterio Garcia, EADS CASA Espacio, Spain; Roger Oliva, Manuel Martín-Neira, European Space Agency, Spain*

SMOS is the acronym for the Soil Moisture and Ocean Salinity mission by the European Space Agency (ESA) designed to provide global maps of soil moisture over land and sea surface salinity over oceans [1]. Its single payload, the Microwave Imaging Radiometer using Aperture Synthesis (MIRAS) is a "Y" shape array that comprises 69 dual-pol antennas that was successfully launched in November 2009. After a six month Commissioning Phase devoted to characterize the payload, the sensor entered in its operational mode to produce a continuous flow of high quality brightness temperature images that have turned into significant findings regarding geophysical parameters over land, ocean and ice [2] [3]. SMOS single antennas were carefully characterized on-ground and assumed not to suffer any significant change in flight configuration. Antenna errors seem to be well within requirements and adequate for most SMOS applications. However, these errors are now assumed to be the dominant source of the so called "spatial bias" defined as the difference between the reconstructed brightness temperature image in a ocean reference area and that predicted by a complete geophysical model provided by the Laboratoire d'Oceanographie et du Climat (LOCEAN), France. Antenna errors have a different impact on "spatial bias" depending on the image reconstruction technique. This impact is large in the so-called Basic approach where the calibrated visibility samples are directly inverted to retrieve the image. On the other hand, the impact of antenna errors are very much mitigated in the so-called Model approach where a theoretical model of the Earth is removed at visibility level (before inversion) [4]. SMOS data offers an opportunity to better understand the nature and impact of antenna errors in aperture synthesis applications for improved performance and also to set design guidelines for SMOS future missions. In this work both the Basic and Model inversion approaches are combined to assess the accuracy of the ground antenna characterization and to go through several practical issues to be taken into account. [1] H. Barré, B. Duesmann, and Y. Kerr, "SMOS. The mission and the system," IEEE Transactions on Geoscience and Remote Sensing, vol. 46, no. 3, pp. 587–593, March 2008. [2] I. Corbella, F. Torres, N. Duffo, V. González-Gambau, M. Pablos, I. Duran and M. Martín-Neira. "MIRAS Calibration and Performance. Results From the SMOS In-Orbit Commissioning Phase". IEEE Transactions on Geoscience and Remote Sensing. Vol. 49, Num: 9, pp: 3147-3155. 2011. [3] Y. Kerr et al. "SMOS: significant findings after three years ans a half in orbit" .IGARSS, 2013, Melbourne, Australia. [4] A. Camps, M. Vall-llossera, I. Corbella, N. Duffo, F. Torres. "Improved Image Reconstruction Algorithms for Aperture Synthesis Radiometers". IEEE Trans. Geosci. Remote Sens., Volume 46, Issue 1, pp. 146-158, Jan. 2008.

Paper 2 **ADVANCES IN CALIBRATION OF THE SMOS ZERO-BASELINE RADIOMETERS**
13:20 *Andreas Colliander, Jet Propulsion Laboratory, California Institute of Technology, United States; Juha Kainulainen, Aalto University, Finland; Chun-Sik Chae, Jet Propulsion Laboratory, California Institute of Technology, United States; Francesc Torres, Ignasi Corbella, Universitat Politecnica de Catalunya, Spain; Roger Oliva, Manuel Martín-Neira, European Space Agency, Spain*

SMOS (Soil Moisture and Ocean Salinity) is European Space Agency's (ESA) satellite mission launched in November 2009 to make L-band brightness temperature measurements from Low Earth Orbit. The scientific objective of the mission is the global measurement of water content of soil surface, or soil moisture, and sea surface salinity (SSS) of the oceans. The calibration of the instrument of SMOS is essential for accurate soil moisture and SSS measurements. The instrument is called MIRAS (Microwave Interferometric Radiometer using Aperture Synthesis) and it uses interferometric technique to resolve brightness temperature images. In MIRAS the relative distribution of emission within the field of view is resolved using interferometer baselines while the absolute level of antenna temperature is measured with dedicated radiometer units, which from the interferometer perspective measure the zero-length baseline. Therefore, the calibration and performance of the zero-baseline radiometers is essential for the SMOS operation and studies of soil moisture and SSS. Over the course of the four-year mission several enhancements have been developed for the calibration of the zero-baseline radiometers. The reference radiometer units provided an overall stable antenna temperature for the SMOS measurements since the start of the mission, but after one year of operation an additional correction was developed to compensate for some drifts detected through the sky calibration procedures. Bi-weekly sky calibration procedures are the nominal basis for the calibration of the reference radiometer units. The calibration procedure assumes front-end loss parameters, which are nominally obtained from the ground characterization, and determines the noise injection level for antenna temperature retrieval. However, two novel methods were developed to determine the antenna loss parameter in orbit using the sky measurements. For the reference radiometers these methods have produced antenna loss values with about 0.3 dB difference (on average) to the nominal value. The uncertainties in these methods are being investigated; the accurate knowledge of the antenna loss is inherently important for stable operation of the radiometers. The antenna of the zero-baselines, as the regular receiver units, has a finite isolation between vertical and horizontal polarization. The technique to determine the cross-coupling effect was improved after launch and is now being resolved from the sky calibrations. In addition to polarization isolation, a tiny amount of the noise injection signal of the zero-radiometers leaks back to the direction of the antenna and can couple to the other channel causing correlated noise between channels. The compensation of this effect was also improved to enhance the measurement of third and fourth Stokes parameter in particular. Ocean surface is relatively well known target in terms of microwave emission. The Aquarius satellite is using a sophisticated model to estimate the brightness temperature of the oceans. This model was used to simulate the antenna temperature of the SMOS zero-baselines in order to estimate their performance and understand the similarities between SMOS and Aquarius. The simulator results agree very well with the measurements suggesting consistency between the missions, which has been observed elsewhere too (although some differences have been found as well). This paper will summarize the advances made so far regarding the calibration of the SMOS zero-baselines which has improved the quality of not only SMOS brightness temperature product but also soil moisture and sea surface salinity products. Acknowledgements The research described in this publication was carried out in part at the Jet Propulsion Laboratory, California Institute of Technology, under a contract with the National Aeronautics and Space Administration. The SMOS data was provided by the European Space Agency.

Paper 3 AIRBORNE L-BAND RADIOMETER MEASUREMENTS OF THE DOME-C AREA IN ANTARCTICA.
13:40 *Niels Skou, Steen Kristensen, Sten Søbjærg, Jan Balling, Technical University of Denmark, Denmark*

Our globe is presently being measured by two spaceborne L-band radiometers: SMOS and Aquarius. Such radiometer systems include internal calibration loops in order to provide stable and calibrated data. However, the antenna systems are outside the calibration loops, and these may also have their own uncertainties. Hence, there is a need for stable and well known external targets for calibration checks. Due to the wide antenna beams inherent at L-band, such targets must be of very extended size like hundreds of kilometers. One of the few feasible terrestrial targets that might live up to all expectations is the area around Dome-C in Antarctica. The basic idea is that the penetration depth in the ice at L-band is so large that a radiometer will basically sense a brightness temperature governed by the mean annual physical temperature. Analysis of existing radiometric data at C-band and higher indicates good stability and spatial homogeneity. Tower based L-band measurements at the Concordia station has proven excellent temporal stability, so the remaining question is: what about the spatial homogeneity at a SMOS sub-pixel scale? In January 2013 ESA launched the DOMECair campaign in which a 350 by 350 km area around the Concordia station was mapped by the EMIRAD radiometer system, mounted on a Basler airplane owned and operated by the Alfred Wegener Institute. The EMIRAD is an L-band, fully polarimetric, digital radiometer featuring advanced RFI detection systems, and the instrument was developed by the Technical University of Denmark for use in a range of SMOS related airborne campaigns around the World. The instrument features 2 antennas, one nadir pointing, one pointed sideways at 45° incidence angle. In addition to the mapping the 350 by 350 km area by 11 parallel lines plus one crossing line, wing wags were carried out for calibration purposes, and circle flights were performed in order to investigate possible azimuth signatures. The wing wags revealed the incidence angle signatures at horizontal and vertical polarizations, and they match very well those measured from the tower at Concordia. Circle flights were carried out at very different times during the day in order to mitigate the influence from the Sun, and indicated no azimuth signature in the surface brightness temperature. Based on the 11 + 1 straight flight lines 2-D brightness maps were generated. These maps (at nadir and 45° H and V) reveal significant brightness temperature variations within the 350 km scale: up to 15 K variations are found over the quite flat area. The variation are multi-scale ranging from slopes to wiggles, and the dynamics is illustrated by examples where the brightness temperature changes almost 1 K per km. By comparing with a map of the bedrock in the area, significant correlation between brightness temperature and bedrock elevation is noted. This is being investigated further. The Dome-C area is still being considered as a viable target for calibration and comparison between instruments, but careful planning of the exact location of footprints is mandatory.

Paper 4 A COMPARATIVE STUDY OF STOKES PARAMETERS FROM AQUARIUS AND SMOS MEASUREMENTS
14:00 *Chun Sik Chae, Sidharth Misra, Andreas Colliander, Shannon Brown, NASA JPL, United States*

Aquarius and SMOS have been successfully providing L-band brightness temperature (Tb) since 2009 and 2011, respectively [1, 2]. Since both missions provide Low Earth Orbit observation at the same frequency, comparison of brightness temperatures measured from these two missions has drawn attention. For a radiometer, stability testing and drift monitoring of measured brightness temperature are often performed by comparing measured Tb with estimated Tb using in-situ temperature measurement and higher frequency microwave observations. Therefore having one additional reference Tb measured by another radiometer will help characterize and calibrate a radiometer with higher accuracy and benefit both missions. Thus, SMOS L1C data (2010~2013) are reprocessed for the Aquarius-SMOS inter-comparison study. The data are designed to include both land and ocean for separated ascending and descending paths for all Stokes parameters. Incident angles are binned with 24 degree points. Spatial points are gridded with 0.25 degree bin which results in 1440 longitude and 720 latitude points. SMOS data products are: 1. Tb including raw RFI, 2. RFI-mitigated Tb [3], 3. mean RFI, 4. maximum RFI, 5. timestamp, 6. Azimuth angle. The presentation will include the comparison results using Aquarius and SMOS Th, Tv, and T3 data. Similarity and difference of these between the missions will be analyzed and accessed. The results will provide useful data and insights on the impact of error sources on the measurement using L-band microwave radiometers. Acknowledgements: The research described in this publication was carried out at the Jet Propulsion Laboratory, California Institute of Technology, under a contract with the National Aeronautics and Space administration. The SMOS data was provided by the European Space Agency. Reference 1. Y. H. Kerr et al., "The SMOS Mission: New Tool for Monitoring Key Elements of the Global Water Cycle," Proceedings of the IEEE, vol. 98, No. 5, May. 2010. 2. D. M. Le Vine et al., "Aquarius Third Stokes Parameter Measurements: Initial Results," IEEE Geosci. Remote Sens. Lett., vol. 10, No. 3 Jan, 2012. 3. S. Misra et al., "Analysis of Radio Frequency Interference Detection Algorithms in the Angular Domain for SMOS, " IEEE Trans. Geosci. Remote Sens., vol. 50, no. 5, May. 2012.

Paper 5 A METHOD TO INTER-CALIBRATE ORBITING L-BAND RADIOMETERS
14:20 *Francois Cabot, CESBIO, France; Eric Anterrieu, IRAP, France; Yann Kerr, CESBIO, France*

The SMOS mission, in orbit since November 2009, has been the first spatial instrument observing the earth at L-Band since the Skylab experiment in 1977. Since then, it has been joined by Aquarius in June 2011, and will be joined by SMAP in October 2014. Within these 4 years, earth observation at L-band has gone from historical curiosity to highly repetitive constellation. Still, since all these instruments do not share the same technology and even principle of acquisitions, direct comparison and synergistic use of their measurements is not straightforward. The objective of this paper is to propose a method to make them inter-comparable, down to a common reference. The proposed method uses SMOS as a transfer radiometer. This method can be applied over different types of surfaces: i) making use of a stable target to assess the consistency and stability of both data sets. This is done over the area surrounding Dome Concordia in Antarctica. After careful selection and filtering, statistics of the comparison are retrieved along with long term trends in both data sets. ii) Once every so often, satellites overpass the same area within a very short time period. Due to different inclinations these alignments occur essentially along the equator, but over different surfaces, giving access to wide dynamic range in brightness temperature. These collocation will be happening at about the same frequency for Aquarius and SMAP. After the selection of measurements, SMOS measurements is used in an innovative way - taking advantage of it accessibility to wide areas with a large range of incidence angles - to make it directly comparable to other instruments. Accounting for instrument characteristics such as real antenna patterns is also done at this step. This presentation will completely describe the method, along with examples of results when applied to compare SMOS and Aquarius measurements. Demonstration of use for SMAP will also be presented.

Wednesday, March 26 — Calibration Techniques and Methods — 14:40 - 16:00

Poster Session — Dabney Hall, Bldg 40

Session Co-Chairs: Francois Cabot, CESBIO; Alan Tanner, NASA JPL

Paper 1 INTER-CALIBRATION OF THE ADVANCED MICROWAVE SCANNING RADIOMETER2 (AMSR2) LEVEL-1B DATASET
Arata Okuyama, Keiji Imaoka, JAXA, Japan

The Global Change Observation Mission (GCOM) aims to achieve global and long-term monitoring of the Earth by using two polar orbiting satellite observing systems with three consecutive generations. GCOM-W1, the first satellite of the GCOM-W (water) series, was successfully launched on May 18, 2012. The Advanced Microwave Scanning Radiometer-2 (AMSR2) is a single mission instrument on GCOM-W1 satellite. Basic characteristics of AMSR2 is similar to that of a predecessor sensor, AMSR for the Earth Observing System (AMSR-E), to continue the AMSR-E observations, with several improvements including larger main reflector with 2.0 m diameter, additional channels at C-band frequency, improved calibration system, and the increase of reliability by adding a redundant momentum wheel. Since July 3, 2012, the instrument has functioned properly and accumulated measured brightness temperature (Tb) dataset and standard Tb products have been made available to the public since January 2013. Geophysical products have also been published since May 2013. Properly characterizing and calibrating observing sensors are the crucial issues in remote sensing. Keeping calibration consistency is a fundamental requirement to merge the information from multiple instruments and removing sensor drifts is a key in monitoring proper climate trend. The absolute calibration is not easy for microwave radiometers at this moment both pre- and post-launch because of the lack of the reliable absolute standard. This presentation reports characteristics of the AMSR2 Tb measurement through inter-calibration approach. During the initial calibration and validation period, Tb values are being evaluated and characterized through methodologies such as the inter-calibration among similar microwave radiometers including the Tropical Rainfall Measuring Mission (TRMM) Microwave Imager (TMI) with help of radiative transfer models. The inter-calibration is examined on both of cold and warm end of Tb, ocean and rainforest, and on both of ascending (daytime) and descending (nighttime) orbits. The inter-calibration results indicate that AMSR2 has calibration difference, 5K at most, compared with TMI and the relative biases of some channels depend on observed scene temperature. There is no apparent seasonal variation and no undesirable discrepancy between daytime and nighttime orbits on the AMSR2 Tbs. AMSR-E and AMSR2 are in the A-Train constellation orbit with same incidence angle and less observation time difference. Since AMSR-E observation channels are almost identical to the ones of AMSR2, the measured Tbs can be comparable without empirical correction. Indirect comparison of AMSR2 with AMSR-E was examined because AMSR-E stopped operational observation before the AMSR2 launch. The comparison shows that AMSR2 measured Tb has relatively positive bias for AMSR-E, which is reasonable because the AMSR-E Tb is empirically calibrated in reference to the TMI. Direct inter-calibration for AMSR-E is also underway to support investigation into the cause of the calibration difference. Thanks to the intensive efforts by NASA and JAXA operation teams, the resumption of instrument rotation with slow rotating speed of 2 revolutions per minute was realized and the data are available from December 2012. Further studies will be required in the near future since the data from this observation mode will provide independent inter-calibration results to increase the confidence.

Paper 2 CONAE MICROWAVE RADIOMETER (MWR) COUNTS TO TB ALGORITHM AND ON ORBIT VALIDATION.
Zoubair Ghazi, Andrea Santos-Garcia, Linwood Jones, María Marta Jacob, University of Central Florida, United States

A joint international science mission (Aquarius/SAC-D) between NASA and the Argentine Space Agency (CONAE) was launched on June 10, 2011. This paper presents the brightness temperature algorithm and on orbit validation results for the CONAE Microwave Radiometer (MWR) that operates at 23.8 GHz (K-band) H-pol and 36.5 GHz (Ka-band) H- & V-pol. MWR is a three state Dicke radiometer with two noise references (ambient temperature reference load and a pulsed noise diode), that provide radiometric calibration. The Central Florida Remote Sensing Lab (CFRSL), in collaboration with CONAE, have developed an algorithm to convert the radiometric counts to Tb for MWR.

This algorithm is based upon both pre-launch thermal vacuum radiometric calibration testing and on orbit inter satellite cross calibrations (XCAL) with the Naval Research Lab's WindSat radiometer, on board of Coriollis satellite. The MWR instrument is described and a derivation of the radiometric transfer function is presented. On orbit radiometric calibration XCAL results are presented for the newest version (V6) of the MWR counts to Tb algorithm that includes a correction for a small radiometer non-linearity. To establish a linear radiometer transfer function, we analyzed MWR on orbit Tb measurements that includes Cold Sky Calibration (CSC) and ocean and land observations to provide a wide dynamic range of brightness temperatures. The analysis procedure is described, which includes normalization of the on orbit gain changes due to physical temperature changes. XCAL validation results of the previous version (V5) and the new V6 algorithm are shown for one year of comparisons between MWR and WindSat.

Paper 3 RADIOMETRIC INTER-CALIBRATION OF SAPHIR USING THE MICROWAVE HUMIDITY SOUNDERS

Hamideh Ebrahimi, University of Central Florida, United States; Saswati Datta, Data and Image Processing Consultants, United States; Andrea Santos-Garcia, Linwood Jones, University of Central Florida, United States

The Microwave Humidity Sounders (MHS) on NOAA and MetOp satellites have been extensively inter-satellite cross-calibrated; thus these MHS radiometers serve as the radiometric calibration standards for other satellite sounder radiometers. Unfortunately, inter-satellite radiometric calibration (aka XCAL) between similar, but not identical, radiometers is not trivial. This paper explores the application of a "Double-Difference (DD)" XCAL technique to sounders, which has been successfully used for conical scanning microwave imagers. Specifically, the water vapor sounder Sondeur Atmosphérique du Profil d'Humidité Intertropicale par Radiométrie (SAPHIR) on the Megha-Tropiques satellite is inter-satellite calibrated using the MHS instruments on the NOAA-18, NOAA-19, and MetOp-A satellites. In the DD XCAL technique, the first step is to calculate observed "Single Differences (SD)" between the observed radiances (Tb's) and theoretical Tb's, which are calculated using an ocean radiative transfer model. This procedure normalizes the Tb observations to remove the effects of frequency and earth incidence angle (EIA) differences between radiometers. The final step is to calculate the double differences of the two single differences, which is the radiometric bias between channels. For previous XCAL inter-satellite comparisons with microwave imagers, observations were spatially and temporally collocated in 1° Lat/Lng boxes, and biases were performed on binned average Tb's that were heavily filtered to provide homogeneous clear-sky ocean scenes. However for cross-track sounders, this procedure was modified to include both comparisons at individual IFOV match-ups and binned averages over 1° boxes. Further, since SAPHIR & MHS are cross-track scanners, the DD bias determination is examined for scan-position dependent biases. Results are presented for two different methods; 1) Binned average and 2) IFOV matchup. Further each method is sub-divided into three different cross-over scenarios, namely: "Case A", where both SAPHIR and MHS EIAs are close to nadir; "Case B", where only MHS EIAs are close to nadir; and "Case C", where the absolute difference between their EIAs are matched within ± 5°. Also, conservative filters are applied to limit comparisons to clear sky oceanic observations by using a convection filter that removes samples with rain and heavy clouds. In addition to the EIA constraints mentioned above, the following filters are applied: 1) for 1° boxes the number of observations must be ≥ 10 and the time coincidence between satellites < ±1 hour; 2) for IFOV match-ups, temporal match-ups must be ≤ 30 min, and the spatial collocation ≤ 25 Km.

Paper 4 ESTIMATION OF TRMM MICROWAVE IMAGER ANTENNA TEMPERATURE DURING DEEP SPACE CALIBRATION MANEUVERS

Spencer Farrar, Linwood Jones, University of Central Florida, United States

In 1998, during on-orbit check-out period of the Tropical Rainfall Measurement Mission (TRMM) observatory, a set of special attitude maneuvers were performed for the calibration of on-board instruments (including the TRMM Microwave Imager, TMI). These maneuvers essentially put the spacecraft's attitude into an inertial hold, whereby the spacecraft's attitude position was locked to its inertial reference frame, which allowed the spacecraft to perform a 360 degree pitch rotation relative to the normal geodetic earth point mode. This caused the TMI main reflector beam to view a non-polarized homogenous scene (deep space) of ~ 2.7 K. TMI is a two-point externally calibrated total power radiometer; thus, at the warm calibration point, the feed horns view a blackbody target (warm load microwave absorber), and at the cold point, a secondary reflector, Cold Sky Reflector (CSR), is illuminated and forms a beam that views space. Unfortunately, during the majority of the Deep Space Calibration (DSC) maneuver, the CSR beam was rotated to intercept the earth; hence, the two-point calibration process was no longer valid. In 2001, Remote Sensing Systems (RSS) analyzed these maneuvers to perform an absolute radiometric calibration of TMI, but because of the CSR intersection of the earth, their analysis was restricted to less than 16% of the deep space view of the main reflector beam. This reduced period for analysis was an issue because of a variable Tb bias from the emissive main reflector that was cooling. It is highly desirable to have a longer time series of calibrated antenna brightness temperatures (TA) to resolve the emissive component of the TMI radiometric bias. To this end, the Central Florida Remote Sensing Lab (CFRSL) has developed a novel approach that permits TMI counts to estimate TA from only a single warm calibration point and a few ancillary physical temperature measurements. This approach establishes a complex correlation coefficient between the radiometer gain, offset and receiver physical temperature. This robust relationship is established during normal (geodetic) pointing mode as a function of the receiver physical temperature, which is cyclic over a single orbit. During the DSC maneuver, we use the warm load counts and physical temperature measurements, and other available temperatures to estimate the receiver linear transfer function and thereby reconstruct the TA. Results are presented from three DSC maneuvers that show the time history of receiver gain and offset and an estimate of the resulting reconstructed TA uncertainty.

Paper 5 MICROWAVE RADIOMETER (MWR) BEAM-POINTING VALIDATION FOR THE AQUARIUS/SAC-D MISSION

Bradley Clymer, Catherine May, Larry Schneider, University of Central Florida, United States; Felipe Madero, Martín Labanda, María Marta Jacob, Comision Nacional De Actividades Especiales, Argentina; Linwood Jones, University of Central Florida, United States

The Aquarius/SAC-D joint international science mission, a collaborative effort between NASA and the Argentine Space Agency, CONAE, was launched on June 10, 2011. The purpose of the Aquarius/SAC-D mission is to provide measurements of global sea surface salinity (SSS), which will be used to understand climatic changes of the global water cycle and how these changes influence the general ocean circulation. This paper concerns CONAE's instrument, the Microwave Radiometer (MWR), which is a three-channel Dicke radiometer operating at 23.8 GHz (H-Pol) and 36.5 GHz (V- and H-Pol). The instrument has two multi-beam parabolic reflector antennas in a pushbroom configuration with eight beams per frequency (looking both forward and aft). MWR's main purpose is to provide measurements that are simultaneous and spatially collocated with those of NASA's Aquarius radiometer/scatterometer. For this reason, knowledge of the MWR antenna beam footprint geolocation is crucial to mission success. Results of an on-orbit validation of the MWR antenna beam pointing - using calculated MWR instantaneous field of view (IFOV) centers - are presented. This procedure compares CONAE-calculated IFOV centers at land/water crossings with high-resolution coastline maps. MWR IFOV locations versus time are computed from knowledge of the satellite's instantaneous location relative to an earth-centric coordinate system (provided by on-board GPM receivers), and a priori measurements of antenna gain patterns and mounting geometry. Previous conical scanning microwave radiometer missions (e.g., SSMI) have utilized observation of rapid change in T_b to estimate the location of land/water boundaries, and subsequently to determine the antenna beam-pointing accuracy. In this paper, an algorithm to quantify the MWR beam center geolocation error based upon two-dimensional convolution between each beam's gain pattern and land-water transition is presented. Also, these analysis procedures have been validated with computer simulation and are applied to on-orbit datasets that represent good land-water boundaries. The goal of this research is to gain a better understanding of satellite radiometer beam-pointing error and thereby to improve the geolocation accuracy of past and future satellite microwave radiometer missions.

Paper 6 TOWARDS IMPLEMENTING SI-TRACEABLE MICROWAVE BRIGHTNESS-TEMPERATURE STANDARDS

David Walker, NIST, United States; Dazhen Gu, Derek Houtz, University of Colorado, United States; Edward Kim, NASA GSFC, United States

Microwave brightness temperature (Tb) observations by satellite sounders represent some of the most important input data for numerical weather prediction (NWP) models as well as providing vital records for climate trend detection. Each flight instrument, even if built to nominally identical specifications, has a unique calibration, typically based on the implicit assumption that the on-board black body target is well understood and characterized, but even more importantly that the transfer function between the Tb received at the antenna and the thermometry embedded in the target is well determined. NIST demonstrated an SI-traceable brightness temperature calibration for passive microwave radiometers in 2012 based on a method that determines the transfer function between the Tb collected at the antenna and the physical temperature of the on-board black body target, all with well-characterized uncertainty estimates. The initial demonstration was made in a laboratory environment. Since then, we have continued research on various aspects of Tb calibration to better understand the physics of black body targets, how these targets interact with the radiometer and its environment, ways to reduce our measurement uncertainties, and extending the frequency range of our Tb standards. Developing workable strategies for the practical transfer of a Tb reference calibration to a flight instrument is a primary goal of the project. A key aspect of NIST's Tb calibration method as applied to a satellite-borne radiometer is that it provides for transferring the pre-launch target calibration to an on-orbit calibration. The Advanced Technology Microwave Sounder (ATMS) instrument will be used as an example of how this could be implemented. In this talk, we'll describe our current plans, the tradeoffs involved, and the achievable uncertainties.

Paper 7 SOIL MOISTURE ACTIVE/PASSIVE (SMAP) RADIOMETER ANTENNA PATTERN CORRECTION (APC) ALGORITHM

Jinzheng Peng, NASA Goddard Space Flight Center /Morgan State University, United States; Jeffrey Piepmeier, Edward Kim, NASA Goddard Space Flight Center, United States

The SMAP radiometer is to measure Earth surface emission at L-band from space on the 6 AM/PM near-polar, sun-synchronous orbit for global soil moisture retrieval. Its antenna is an assembly of a shared single feedhorn and 6-m diameter parabolic mesh reflector with the L-band synthetic aperture radar. The radiometer measurement swath width is 1000 km by conical scan. While the radiometer measures the emission over a footprint of interest, unwanted emissions are also received by the antenna through the antenna sidelobes from the cosmic background and other error sources such as the Sun, the Moon and the galaxy. The unwanted emissions from the Sun/Moon/Galaxy not only enter the antenna directly but also are received through Earth surface reflection. So their contribution to the antenna temperature is varied with geolocation and antenna rotation angle and they need to be evaluated accurately. The SMAP radiometer L1B algorithm is to get the Earth surface emission from the radiometer measurements. The APC is the most complex algorithm in the L1B_TB processing since it involves the most ancillary data and sources of uncertainty. It is to derive the main beam apparent temperature at the top of ionosphere from the measured antenna temperatures for all 4 modified Stokes parameters. To accomplish this, the APC seeks to remove all the unwanted source contributions from the measured antenna temperature, ideally leaving nothing but the apparent temperature viewed by the main beam. In the APC algorithm, the contribution from the error sources (the Sun, the Moon, and the galaxy including the cold sky) entering the antenna directly and reflected by the Earth surface are modeled; the emission from the Earth surface in the antenna sidelobe region is corrected based on the correlation between adjacent area. Results show that the algorithm satisfies allocated error budget. In addition, the APC algorithm simplifies the process for correcting antenna temperature measurements to derive the apparent temperature above the ionosphere and it can significantly reduce computation.

Paper 8 SOIL MOISTURE ACTIVE/PASSIVE (SMAP) RADIOMETER L1 FORWARD BRIGHTNESS TEMPERATURE SIMULATOR

Jinzheng Peng, NASA Goddard Space Flight Center /Morgan State University, United States; Jeffrey Piepmeier, Edward Kim, NASA Goddard Space Flight Center, United States

The SMAP is one of four first-tier missions recommended by the US National Research Council's Committee on Earth Science and Applications from Space (Earth Science and Applications from Space: National Imperatives for the Next Decade and Beyond, Space Studies Board, National Academies Press, 2007) [1]. It is to measure the global soil moisture and freeze/thaw from space. One of the spaceborne instruments is an L-band radiometer with a shared single feedhorn and parabolic mesh reflector. While the radiometer measures the emission over a footprint of interest, unwanted emissions are also received by the antenna through the antenna sidelobes from the cosmic background and other error sources such as the Sun, the Moon and the galaxy. Their effects need to be considered accurately, and the analysis of the overall performance of the radiometer requires end-to-end performance simulation from

Earth emission to antenna brightness temperature, such as the global simulation of L-band brightness temperature simulation over land and sea [2]. To assist with the SMAP radiometer level 1B algorithm development, the SMAP forward brightness temperature simulator is developed by adapting the Aquarius simulator [3] with necessary modifications to incorporate SMAP specifications. These specifications include narrow antenna beamwidth with conical scan and land focus. It results in that more ancillary datasets and footprints. Simulation speed becomes critical for simulation application. The approaches of improving simulation speed in algorithm include 1) Use simplified atmospheric radiative transfer model; 2) Implement parallel computation; 3) Optimize simulation code efficiency. The other two major modifications are the incorporation of the Microwave Emission Model [4] for land and IGS TEC ancillary for Faraday rotation correction. The SMAP L1B forward TB simulator is a major risk-reduction asset in the SMAP L1B algorithm development. Its simulation result has been used for the modeling of the antenna temperature contribution from the Sun/Moon/Galaxy, and it will be used in the post-launch Cal/Val activities as well.

Paper 9 CHARACTERIZATION OF AUTOEMISSION REFLECTION AT MICROWAVE FREQUENCIES FOR PRECISE RADIOMETER CALIBRATION

Albin Gasiewski, University of Colorado at Boulder, United States; Derek Houtz, National Insitutute of Standards and Technology, United States; David Kraft, Vladimir Leusky, University of Colorado at Boulder, United States

The close coupling of antenna horns and pyramidal calibration targets is standard in the design of calibration systems for operational spaceborne radiometers. However, various radiometer front end architectures can allow radiation leakage (autoemission) out of the horn that can produce local oscillator standing waves and upper and lower sideband signals reflected back into the radiometer. Calibration targets are designed to minimize such reflections but the residual of these effects can still have a measurable impact on calibration error amplitudes that is important for radiometric studies of long term trends in climate. Front end RF isolators and low noise amplifiers (LNAs) can be unavailable or expensive at frequencies above ~90 GHz, in which case there is little protection against autoemission. This study investigates the standing waves resulting from pyramidal microwave calibration targets due to autoemission for representative sounding radiometers operating at both 50-58 and 183 GHz. The 50-58 GHz radiometer has a single upper sideband (USB) channel at 55 GHz and is configured either with or without an LNA and/or isolator. The 183 GHz radiometer has seven channels using a direct conversion double side band (DSB) architecture with RF offsets from the LO frequency ranging from 0.55 GHz to 16 GHz. No LNA or isolator was available for the 183 GHz radiometer. To measure autoemission a calibration target is stepped in distance while brightness temperatures are regularly sampled. By detrending gain variations and coherently averaging the measured brightness temperature scans a standing waveform is obtained. A Fourier transform is subsequently used to analyze this standing wave data in the spatial frequency domain. The standard deviation of the standing wave is statistically calculated and compared for a number of measurement cases. Contributing sources of the observed autoemission amplitude are identified as due to either local oscillator (LO) reflections or the reflected RF passband noise from one of the two sidebands of the DSB radiometer. Two candidate pyramidal targets were investigated at 4 alignment positions, including over the tip, valley, and combinations of these two cases. Standing wave results from the 55 and 183 GHz radiometers were compared for various cases of these targets and for a flat aluminum reflecting plate. Autoemission returns over the targets were commonly observed to be in the range of ~0.05-0.2K, depending on the presence or absence of an LNA and/or isolator. In addition, the standing wave phase depended on the location of the feedhorn axis with respect to the pyramid tip. The impact of these studies on operational sensor calibration sampling strategies along with a discussion of the nature of such autoemission amplitude and phase variations will be presented.

Paper 10 ASSESSMENT OF LONG-TERM ERRORS OF WET TROPOSPHERIC CORRECTION FOR ALTIMETRY MISSIONS: A MEAN SEA LEVEL ISSUE

Soulivahn Thao, Bruno Picard, Estelle Obligis, CLS, France; Laurence Eymard, IPSL/LOCEAN, France; Marie-Laure Frery, CLS, France

The assessment of long-term errors of altimeter sea level measurements is of crucial importance for studies concerning the Mean Sea Level (MSL) evolution. One of the main contributors to the long-term sea level uncertainties is the correction of the altimeter range from the wet troposphere path delay, which is provided by onboard microwave radiometers for the main altimeter missions. The first part of the study is dedicated to the wet tropospheric correction (WTC) estimated from microwave radiometers. Nowadays, water vapor products from microwave radiometers are rather consistent but important discrepancies remain. Understanding these differences can help us to improve the retrieval of water vapor and reduce at the same time the error on the mean sea level. Three radiometers are compared: Advanced Microwave Scanning Radiometer for EOS (AMSR-E), JASON-1 Microwave Radiometer (JMR) and ENVISAT Micro-Wave Radiometer (MWR). Water vapor products are analyzed both in terms of spatial and temporal distribution over the period 2004-2010, using AMSR-E as a reference. Overall, the study confirms the general good agreement between the radiometers: similar patterns are observed for the spatial distribution of water vapor and the correlation of the times series is better than 0.90. However, regional discrepancies are observed and a quantitative agreement on the trend is not obtained. Regional discrepancies are driven by the annual cycle. The JMR product shows discrepancies highly dependent on water vapor, which might be related to calibration issues. Furthermore, triple collocation analysis suggests a possible drift of JMR. MWR discrepancies are located in coastal regions and follow a seasonal dynamic with stronger differences in summer. It may result from processing of the brightness temperatures. These discrepancies explain why the operational ECMWF atmospheric model is usually used as a common reference for mean sea level studies. However, due to several major improvements on the processing, this model is not homogenous over the altimetry period (from 1993 onwards) preventing the detection of errors on radiometer wet tropospheric correction especially on first altimetry decade. The second part of this study aims at determining the quality of WTC provided by ERA interim atmospheric model reanalyzes (ECMWF) in comparison with ECMWF operational fields and also with reanalyzes derived from National Centers for Environmental Predictions / National Center for Atmospheric Research (NCEP/NCAR). Separating our analyses on several temporal and spatial scales, we demonstrate that ERA interim is the best model WTC for the altimeter sea level at climate scales. Overall, this work demonstrates the relevance of the feed-backs that the "altimetry" and "atmosphere" communities can bring to each other.

Paper 11 INFLUENCE OF ECMWF BACKGROUND ERROR COVARIANCES ON THE RETRIEVAL OF TEMPERATURE AND HUMIDITY BY THE HAMP RADIOMETER.

Emiliano Orlandi, University of Cologne, Germany; Elias Holm, ECMWF, United Kingdom; Mario Mech, Susanne Crewell, University of Cologne, Germany

Profiles of temperature (T) and humidity (Q) are fundamental for weather forecasting, climate monitoring as well as the interpretation of remote sensing instrument measurements. Radars, for example, rely on the accurate knowledge of T and Q profiles to calculate the attenuation of the emitted pulses and for the discrimination between liquid and solid targets. Since direct measurements of these variables by radiosondes and dropsondes are rather limited in space and time, passive microwave observations are routinely used to retrieve such profiles with improved temporal resolution and spatial coverage. Bayesian retrieval algorithms typically blend instrumental measurements and a-priori information into the most probable solution for the retrieved variable. For such algorithms the knowledge of a-priori and measurement errors plays a fundamental role. They govern the weight given to the measurements and to the a-priori information on the retrieved variable and thus they need to be properly assessed. In this work we present an 1-D variational assimilation algorithm to retrieve profiles of temperature and humidity for an AMSUA-MHS-like radiometer. ECMWF 3-hour forecast profiles of temperature and humidity are used as a-priori information. Vertical error correlation matrices and standard deviations of the a-priori profiles are derived from ECMWF ensemble data assimilation system using the method described by Holm and Kral (2012). The retrieval is applied to brightness temperatures collected during an aircraft campaign and validated against measurements from dropsonde launched during the flights. The information content added by the radiometer measurements to the a-priori profiles is assessed. In addition, a sensitivity study is performed on the dependency of the added information content with varying a-priori standard deviations. The radiometer used for the algorithm validation is the passive component of the HAMP instrument (Microwave Package for HALO, the High Altitude Long Range aircraft), which consists of a 36 GHz Doppler cloud radar and a 26-channel radiometer. The HAMP radiometers have frequencies along absorption lines (22, 60, 118 and 183 GHz) and in window regions, overlapping with those of AMSUA and MHS. HAMP flew during a test campaign over Germany in June and July 2013 and will participate in December 2013 and January 2014 in the dedicated remote sensing HALO mission NARVAL (Next-generation Aircraft Remote-sensing for VALidation studies). During the NARVAL campaign HALO will be flown over Northern and Tropical Atlantic, giving the opportunity to test the newly developed retrieval algorithm in different environmental conditions.

Wednesday, March 26	Oceans and Ice II	14:40 - 16:00
Poster Session		Dabney Hall, Bldg 40

Session Co-Chairs: Xiaolan Xu, NASA - Jet Propulsion Laboratory; Paolo de Matthaeis, NASA - Goddard Space Flight Center

Paper 1 RETRIEVAL OF SEA ICE THICKNESS FROM AQUARIUS DATA: INITIAL RESULTS

Paolo de Matthaeis, NASA/USRA, United States; Alexis Moyer, University of British Columbia, Canada; Cuneyt Utku, NASA/USRA, United States; David Le Vine, NASA, United States

Aquarius is a NASA instrument flown aboard the Aquarius/SAC-D spacecraft and operating at L-band. Its main goal is to measure global sea surface salinity with a spatial resolution of 150 km and a monthly RMS accuracy of 0.2 psu. The instrument package includes a set of three radiometers to measure salinity and one scatterometer that corrects for the ocean surface roughness. The scatterometer is time shared between the radiometers and monitors the same ocean pixels as the radiometers. This unique feature of combining co-located and simultaneous active and passive measurements can be exploited for studying the polar regions. Passive microwave measurements from the Soil Moisture Ocean Salinity (SMOS) mission, operating at the same L-band frequency, have recently been used to retrieve sea ice thickness with promising results [1]. In this work, Aquarius brightness temperature data are used to calculate sea ice thickness in the Arctic region. The method is based on the inversion of a radiative transfer model for ice-covered sea. Using this technique, the initial sea ice thickness values retrieved from Aquarius data are compared with the SMOSIce Preliminary Evaluation Data also and will be compared with estimates from NASA's Operation IceBridge laser and radar altimeter. The results show similar trends between the SMOS- and Aquarius-derived sea ice thickness, however the Aquarius estimates tend to be higher and noisier than the corresponding SMOS values. The accuracy of retrieved Aquarius ice thickness is possibly influenced by uncertainties in the ancillary input parameters and by coarser resolution of Aquarius beams compared to SMOS. The presence of a snow layer over the bulk of the ice was also not corrected in this study in contrast to the study done for SMOS. This is an initial attempt to retrieve sea ice thickness from Aquarius surface brightness temperatures. It is a starting point to explore the potential for exploiting the full active/passive combination capabilities of Aquarius. [1] Kaleschke, L., Tian-Kunze, X., Maas, N., Maekynen, M., and Drusch, M.: Sea ice thickness retrieval from SMOS brightness temperatures during the Arctic freeze-up period, Geophysical Research Letters, 39, 2012.

Paper 2 DESIGN, MODELING, AND IN-SITU VERIFICATION OF WIBAR AS SNOWPACK/LAKE ICE THICKNESS SENSOR

Hamid Nejati, Song Wong, Roger De Roo, Lin van Nieuwstadt, Anthony England, University of Michigan, United States

Wideband autocorrelation radiometer (WiBAR) enables us to measure the physical characteristics of layered media including snowpacks and freshwater ice. Due to multiple reflections occurring within the layered media, the autocorrelation response of the received signal demonstrates distinct peaks corresponding to the travel times of subsequent reflections. Since the Fourier transform of the autocorrelation response gives the power spectral density, monitoring the received power spectral data enables the extraction of physical characteristics of the layered media. We have successfully implemented WiBAR in the frequency range of 7–10GHz by connecting a 23dB gain pyramidal horn antenna to a wideband amplifier chain of nearly 60dB gain. The output is then monitored using a handheld spectrum analyzer. The sensitivity of the implemented WiBAR is tuned by setting the resolution and

video bandwidths of the spectrum analyzer. WiBAR adopts a simplified yet more robust calibration procedure compared to typical radiometers, since the absolute temperature measurement is not required in WiBAR. Our reverse thickness extraction technique is capable of removing the gain pattern of the WiBAR and enhances the thickness reconstruction in our system. An equivalent microwave circuit modeled, designed, and measured mimicking the multiple reflection process inside the layered medium. In the next step, we have performed several measurements of a setup consisting of a thin high-dielectric sheet hanged above water with an air gap in between. The airgap mimics the ice/snow layer and the thin dielectric sheet provides reflection at the top interface. We successfully reconstructed the thickness of the airgap using our algorithm. We gathered the H-polarized far field measurements of snow covered terrains/lake ice using our implemented WiBAR over several locations in Ann Arbor and Houghton, MI. This technique can reconstruct layer thicknesses even with incidence angles as high as 45 degree, so long as a good approximation of snow dielectric constant is achieved. The refractive index mixing formula using the ice density of the snow measured on site was employed to estimate the snow dielectric constant. The reconstructed snow thicknesses are in good agreement with in-situ physical depth measurements, with an accuracy of within 0.7cm.

Paper 3 ANALYSIS OF SMOS AND AQUARIUS L-BAND OBSERVATIONS OF SOIL FREEZING AND THAWING PROCESSES OVER ARCTIC REGIONS

Alexandre Roy, Université de Sherbrooke, Canada; Alain Royer, Benoit Montpetit, Alexandre Langlois, Universite de Sherbrooke, Canada; Ludovic Brucker, NASA, United States; Chris Derksen, Environment Canada, Canada; Arnaud Mialon, Yann Kerr, cesbio, France

In subarctic regions, the physical state of the soil (freeze versus thaw) affects the surface energy balance. Therefore, it is a key parameter in climate models, which needs to be monitored for climate studies. With the availability of L-band radiometric satellite missions, it becomes possible to monitor the soil freezing and thawing cycles over the high latitudes of the Northern Hemisphere lands, even in the presence of a snow cover. This constitutes a secondary mission objective of the current ESA's Soil Moisture and Ocean Salinity (SMOS) mission and the forthcoming NASA's Soil Moisture Active/Passive (SMAP) mission. Additionally, the L-band radiometric observations from the Aquarius/SAC-D mission can be used. In this presentation, we present an analysis over the Arctic tundra of a) Aquarius weekly-polar-gridded L-band brightness temperature (TB) observed at three different incidence angles (28.7, 37.8, and 45.6 deg); and b) SMOS daily reconstructed TB recently released by the French space agency (CNES) (www.catds.fr/sipad/). These data sets, covering the period August 2011 – present, are useful to characterize the freeze/thaw (FT) soil state, including in winter when a snow cover exists. Our study is conducted over three Artic tundra and subarctic sites over North Eastern Canada during two winters. As expected, a significant increase of several Kelvins as well as a depolarisation in both SMOS and Aquarius TBs occurs when the soil freezes. The amplitude of the variations depends on the viewing angle. TBs L-band satellite observations are compared to in-situ measurements of soil temperature and ground-based meteorological data. Moreover, optical and thermal infrared temperature data from the Moderate Resolution Imaging Spectroradiometer (MODIS) are used to determine either the soil FT state before snow accumulates, or the snow cover state (dry versus wet) during the winter months. Finally, variations of the observed SMOS and Aquarius TB are discussed against TB simulations using the recent Mironov's dielectric model for Arctic frozen soil.

Paper 4 WEEKLY-GRIDDED AQUARIUS RADIOMETER AND SCATTEROMETER PRODUCTS OVER THE POLAR REGIONS: CRYOSPHERIC APPLICATIONS

Ludovic Brucker, NASA GSFC / USRA GESTAR, United States; Emmanuel Dinnat, NASA GSFC / Chapman Uni., United States; Lora Koenig, NASA GSFC, United States

Passive and active microwave observations at 1.413 GHz (L band) from the Aquarius/SAC-D mission offer new capabilities to study and to monitor the Earth's polar regions. However, due to the lack of polar-gridded products, applications over the cryosphere are difficult. To offer an easy use of the Aquarius data over the polar regions, and to move forward our understanding of the L-band measurements of ice sheet, sea ice, permafrost, and polar oceans, we produce three weekly-polar-gridded products. Aquarius data recorded at northern and southern latitudes higher than 50 degrees were averaged and gridded into three weekly products of: a) Brightness Temperature (TB); b) Normalized Radar Cross Section (NRCS); and c) Sea Surface Salinity (SSS). Additionally, each grid cell contains sea ice fraction and the standard deviation of TB, NRCS, and SSS along with the number of footprint measurements collected during the seven-day cycle. These products are distributed on the version 2.0 of the Equal-Area Scalable Earth (EASE2.0) grid, with a grid cell resolution of 36 km. They are available since August 2011, with the first Aquarius measurements, and are updated on a monthly basis following the release schedule of the Level 2 data sets. In this presentation, we describe the new weekly-polar-gridded products of TB and NRCS, and present maps and time series of these Aquarius data over the Greenland and Antarctic ice sheets, and sea ice in both hemispheres. Of note, the presence of Radio Frequency Interference (RFI) substantially impacts the monitoring of the Greenland ice sheet, and the Beaufort sea. This is especially noticeable during descending orbits when the Aquarius' sensors are pointing toward the Distant Early Warning (DEW) line. Additionally, due to the anisotropy of the ice-covered surface, NRCS measurements recorded during the ascending and descending orbits must be studied separately. The largest differences appear over the Antarctic ice sheet and sea ice in both hemispheres. For the ice sheet, we highlight the effect of the 2012 summer melt event at Summit, Greenland which created a sudden TB variation including a drop larger than 15 and 20 K at vertical and horizontal polarization, respectively. This drop was observed during the Aquarius cycle 47 (July 12–19, 2012), and results from the refreeze of the surface snow. After the melt/refreeze cycle, the TB level remained ~5 K lower than before the event, revealing the significant impact that a refrozen snow layer can have on the L-band TB, and thus on the monitoring of long-term snow accumulation. Over sea ice, both TB and NRCS reveal strong seasonal cycles. TBs are the highest when snow on sea ice is melting, and decrease during the summer months when the sea ice cover is melting and more fractured, with wider leads exposing open water. NRCS has the lowest values (about -20 dB) when the sea ice cover is packed and snow covered. NRCS values increase in summer and reach their maximum (about -12 dB) in fall before snow accumulates.

Paper 5 EFFECT OF SNOW SURFACE CHANGE ON L-BAND OBSERVATIONS AT DOME C, ANTARCTICA

Ludovic Brucker, NASA GSFC / USRA GESTAR, United States; Emmanuel Dinnat, NASA GSFC / Chapman Uni., United States; Ghislain Picard, Nicolas Champollion, LGGE, Uni. Grenoble Alpes/CNRS, France

In addition to being a key element of the climate system, the Antarctic ice sheet is of interest for remote sensing applications and sensor calibrations. The Antarctic Plateau (eastern side of the ice sheet) is characterized by high elevations, low snow accumulations, weak winds, and low temperatures so that melt never occurs, and the evolution of snow and firn (i.e. aged snow) is usually slow. Thus, the Plateau presents ideal characteristics to study the relationship between microwave observations and snow/ice properties. It is also a promising target for radiometer calibration, and inter-calibration between sensors. Due to the low microwave dielectric loss of dry snow and ice, L-band (~1.4 GHz) radiation has a large penetration depth. The energy emitted at depth, up to hundreds of meters, propagates from the ice, firn, and snow toward the surface with little attenuation. L-band radiometric observations from the Aquarius/SAC-D mission are collected with a sensitivity of 0.15 K. Thanks to such a very good sensitivity, it is possible to understand subtle variations of brightness temperature (TB) with snow property changes. The objective of this presentation is to emphasize the impact of snow surface changes on the Aquarius L-band TB observations at Dome C (75S, 123E). Aquarius TB at Dome C during the two-year period of Sept. 2011 – Sept. 2013 is characterized by large summer-time variations, larger than 2 K at horizontal polarization. These variations typically happen summer between December and February, and are significant compared to the 0.15 K sensitivity of Aquarius' radiometers. Results show that these TB variations are correlated to changes in the snow properties at the very surface, which is observed by a surface-based near-infrared camera taking picture of the surface every hour. Specifically, and as identified at higher frequencies, increase in the ratio of TB observed at horizontal (H) and vertical (V) polarizations (TB H/V) is correlated with the formation of hoar on the surface. Therefore, evolutions of the snow properties near the surface, that usually change rapidly and irregularly, need to be precisely quantified to use the Antarctic Plateau as a calibration/inter-calibration target. Not taking into account the formation and disappearance of hoar on the surface may have great implications on the calibration (or inter-calibration) of the Soil Moisture and Ocean Salinity (SMOS), Aquarius, and the forthcoming Soil Moisture Active/Passive (SMAP) L-band radiometers.

Paper 6 MEASUREMENTS OF SNOW PHYSICAL AND RADIOMETRIC PROPERTIES DURING RAIN-ON-SNOW EVENTS (ROS) OVER EASTERN CANADA

Alexandre Langlois, Alain Royer, Benoit Montpetit, Alexandre Roy, Université de Sherbrooke, Canada

The first and strongest signs of global climate variability and change have been observed in the Arctic over the past three decades due to a variety of strong climate related feedbacks. Patterns in the spatial extent and mass balance of snow, sea ice and ice caps show a statistically significant trend towards negative anomalies. These patterns do have significant impact on how the cryosphere responds to climate change at various scales, as well as unveiling new challenges for northern communities that are now confronted with transport, health and economic issues arising from these changes. A direct consequence of warming temperature during winter is the increased occurrence of extreme events such as rain-on-snow (ROS) events. Strong linkages between surface temperatures and passive microwaves do exist, but the contribution of snow properties under winter extreme events such as rain-on-snow events (ROS) to the signal needs to be better understood. Among the challenges, spatial heterogeneity includes emission contributions from different surface features that affect the signal interpretation. A multi-scale approach becomes essential and, thus, in-situ validation of the satellite measurements must be conducted. In this paper, we present a ROS case study that occurred during winter 2012 in Sherbrooke, Canada. During the ROS event, coincident meteorological (including precipitation phase), snow and radiometric (at 19 and 37 GHz) measurements were taken. The data allowed the distinction between melt events solely driven by warm temperatures and ROS event using a decision tree based on the gradient ration between 19 and 37 GHz. An empirical detection method is proposed, and applied to AMSR-E in Nunavik, Canada. The validation using observed ROS in Nunavik in 3 different pixels suggest a detection precision of 57 to 89% and a maximum potential error in omission/commission of 2-11%.

Paper 7 A COMPARISON OF SNOW DEPTH FROM GPS-INTERFEROMETRY VS. AMSR-E/AMSR-2

Edward Kim, NASA, United States; Hemanshu Patel, Albert Wu, NASA/Emergent Space Technologies, United States; John Braun, UCAR, United States; Eric Small, Kristine Larson, Univ. of Colorado, Boulder, United States

The validation of snow data products from satellite microwave sensors such as AMSR-E on Aqua has perennially faced the key challenge of finding station data that is both widely distributed and possessing sufficient spatial density to provide accurate validation statistics. Point data from ground truth stations have been widely used despite the orders-of-magnitude scale mismatch as well as the insufficient spatial density; this has persisted mainly due to the lack of better alternatives. We evaluate a novel source of validation data that uses ground-based GPS networks, by comparison against snow data products from the AMSR-E sensor aboard the Aqua satellite and now the AMSR2 sensor aboard the GCOM-W1satellite. There are three advantageous features of this approach. First, the GPS networks already exist. Second, they are widely distributed spatially and have a higher spatial density than other stations currently used for snow validation. And third, the observed area of the GPS technique approaches 10,000 m2—much larger than other station observations (1 to 10 m2). Evaluating the new GPS approach along with the more well-known AMSR-E snow depth product will provide a baseline for exploiting this potentially large new validation data source in a variety of remote sensing science studies. This work is based on recent advances in data analysis techniques that have allowed geodetic quality GPS instrumentation to be used to measure changes in soil moisture (Larson, et al, 2008) and snow depth (Larson, et al, 2009) in the region surrounding GPS antennas. These retrievals relate observed changes in ground reflected GPS signals to changes in the either the soil conditions around the antenna or the depth of snow at the site. In this paper, we will focus solely on snow depth. While retrievals using individual GPS satellites sample the variability within an area surrounding the GPS antenna that approaches 10,000 m2, a retrieval using multiple GPS satellites can be used to create a single estimate for the entire area around the antenna—a much less variable estimate vs. traditional point measurements. When compared to in-situ measurements, these GPS retrievals will provide better spatial sampling characteristics for satellite products such as those produced by the AMSR-E or AMSR2 instruments with spatial resolution on the order of 10's of km. Suitable existing GPS networks in the USA, include thousands of stations. Of course, not all of these sites are suitable, but many will be, and it is the goal of this study to determine which types of sites are suitable for snow validation purposes. Observations from approximately 10 GPS stations from the Plate Boundary Observatory (PBO), operating in varied locations in the western United States will initially be used. These sites span a range of climates (especially precipitation cycles), soil types, vegetative characteristics, and snow pack conditions. They also have relevant in-situ data collected as part of ongoing studies, including hydrological and vegetation observations. We will use data from all of these sites, with the additional expectation that a subset of the 1000 existing PBO stations will be also be suitable for use, as a validation data set for AMSR-E data products. These stations will allow for regional and seasonal comparisons of AMSR-E data, providing a unique way to monitor land and cryosphere products throughout a broad range of climatological conditions. Comparisons will be presented of GPS-derived snow depth vs. AMSR-E/AMSR2 snow data products as well as vs. ground truth.

Wednesday, March 26	Oceans and Ice I	14:40 - 16:00
Poster Session		Dabney Hall, Bldg 40

Session Co-Chairs: Wendy Tang, NASA - Jet Propulsion Laboratory; Emmanuel Dinnat, Chapman University

Paper 1 APPLICATION OF THE AQ RAIN ACCUMULATION PRODUCT FOR INVESTIGATION OF RAIN EFFECTS ON AQ AND SMOS SEA SURFACE SALINITY MEASUREMENTS

Andrea Santos-Garcia, Hamideh Ebrahimi, University of Central Florida, United States; María Marta Jacob, Comisión Nacional de Actividades Espaciales, United States; Yazan Hejazin, Linwood Jones, University of Central Florida, United States; William Asher, University of Washington, United States

Sea Surface Salinity (SSS) is a sensitive tracer of ocean circulation and fresh water exchange between ocean and atmosphere, hence, it provides vital scientific observations for understanding the earth hydrological cycle and the effects of climate change. An analysis of Aquarius (AQ) and Soil Moisture and Ocean Salinity satellite (SMOS) SSS retrievals reveals that the spatial patterns of delta-SSS (differences between the Hybrid Coordinate Ocean Model (HYCOM) and remotely sensed SSS measurements) can often be associated with rainfall events. Therefore, it is important to understand the source of these observed differences to sort out real SSS changes due to seawater dilution by rain from remote sensing retrieval errors. This paper describes the development of an AQ Rain Accumulation (RA) product that provides the rainfall history for each AQ IFOV during the previous 24 hours to the observation time. The AQ RA product overlaps the AQ L-2 SSS science data, and it is derived from Tropical Rainfall Measuring Mission (TRMM) 3B42 rain product, which is a near-global rain rate dataset on a 0.25° grid that extends from ±50° latitude and produced 8 times daily at 0Z, 3Z, 6Z . . . and 21Z (3 hr windows). Results are presented from an intensive validation activity that uses independent WindSat rain retrievals (environmental data records, EDRs) over a significant set of collocated samples (within ± 45 min). The use of this AQ RA product facilitates the identification of instantaneous and prior rainfall accumulations, which will aid in the investigation of rainfall effects on the SSS measurements. Furthermore, comparisons of triple collocations, delta-SSS from AQ and SMOS with the AQ RA product, provide complementary information to explore several hypotheses. For example, we describe electromagnetic models that predict ocean surface brightness effects caused by: instantaneous roughening by rain (Splash Effect) and impedance matching by a surface rain layer (ponds) over seawater. These rainfall accumulation time histories are used with an empirical ocean diffusion models to examine possible rain freshening effects.

Paper 2 CLIMATE-QUALITY OCEAN WINDS FROM COMBINED RADIOMETER-SCATTEROMETER OBSERVATIONS AT L-BAND

Lucrezia Ricciardulli, Thomas Meissner, Kyle Hilburn, Frank Wentz, Remote Sensing Systems, United States

An L-band radiometer/scatterometer system is operating for the Aquarius mission designed to measure ocean surface salinity. The scatterometer operates at 1.26 GHz and the radiometer at 1.41 GHz. The NASA sensor was launched on June 10, 2011 aboard the Argentine CONAE SAC-D spacecraft and has been taking science data observations since August 25, 2011. Ocean surface wind measurements result as a byproduct of the salinity retrievals. Salinity retrievals need to be corrected for effects due to the sea surface roughness. For this purpose, an algorithm was developed to retrieve wind speed via a synergistic combination of measurements from various channels of the Aquarius L-band scatterometer (active sensor) and the radiometer (passive sensor). By using only backscatter measurements from the horizontal polarization (HH-pol) channel on the Aquarius scatterometer, the wind speed retrievals have a global accuracy of about 0.8 m/s at a 100 Km resolution. This matches the performance of wind speed retrievals from established missions such as WindSat, SSM/I, and QuikSCAT. The accuracy can be improved by including observations from the H-pol L-band radiometer channel into the wind algorithm, scaled by an appropriate weight. This active/passive channel combination improves the global accuracy of the wind speed retrievals by about 10%, with an even more significant improvement for cross-wind observations and at high winds. Our presentation will give an overview of the methodology of the combined active/passive L-band wind speed algorithm, and will describe the performance of the scatterometer alone versus the combined sensor wind retrievals. We will show results from validation studies of the combined wind speed retrievals, versus buoys, aircraft data, as well as compare the performance to other satellite retrievals from radiometers and scatterometers. Special attention will be devoted to validating retrievals at high wind speeds, by using model-analyzed wind data from the NOAA Hurricane Research Division. Finally we will discuss the role that these L-band measurements have for the construction of a Climate Data Record (CDR) of ocean vector winds, currently under development at Remote Sensing Systems. The 25-year CDR will result from a careful combination of measurements from C-band (ASCAT, ERS) and Ku-band scatterometers (QuikSCAT, NSCAT, OSCAT, and the future RapidScat mission), as well as the L-band measurements from Aquarius and the planned SMAP mission. Integrating all the measurements into a continuous and accurate timeseries suitable for climate analysis is a challenging task. An essential requirement for this purpose is the consistency among wind retrievals from different sensors at all wind speed ranges. Our approach consists in using a similar methodology for developing the wind retrievals from each scatterometer, and adopting for all of them a common calibration standard. One additional challenge is presented by the potential contamination of wind retrievals by rain signals. Rain affects both direct and backscattered signals, as well as the ocean surface roughness through a "splash" effect, and its impact is more relevant at higher frequencies. The rain impact can therefore be studied by comparing retrievals from Ku-band, C-band scatterometers and L-band scatterometers. Rain attenuation and backscatter are very small effects at L-band, and hence the Aquarius and SMAP scatterometers will provide the means to study the surface roughening effect due to splashing rain.

Paper 3 ASSESSMENT OF THE AQUARIUS SPACE-BORNE SEA SURFACE SALINITY RETRIEVALS IN POLAR OCEANS

Ludovic Brucker, NASA GSFC / USRA GESTAR, United States; Emmanuel Dinnat, NASA GSFC / Chapman Uni., United States; Guillaume Vernieres, Robin Kovach, NASA GSFC / SSAI, United States; Lora Koenig, NASA GSFC, United States

Ocean salinity and temperature differences drive thermohaline circulations. These properties also play a key role in the ocean-atmosphere coupling. With the availability of passive and active L-band space-borne observations, global-scale Sea Surface Salinity (SSS) can be retrieved. While SSS retrievals are performed with a reasonable accuracy and a low bias over the tropical and mid-latitude (warm) oceans, a thorough assessment of the satellite retrievals has not been performed yet in the polar (cold) oceans. To assess the Aquarius SSS retrievals in polar oceans, this study uses SSS a) measured during ship cruises in the northern and southern cold polar oceans, and b) simulated by the version 5 of the Goddard Earth Observing System (GEOS-5) assimilation and forecast model. In the southern hemisphere, cruises in the Austral Ocean between Hobart (Tasmania) and Terre Adélie (Antarctica) are used. In the northern hemisphere, cruises between Denmark and Greenland are used. These quality-controlled shipborne SSS measurements (more extensive than the Argo profiling floats which rare in the polar oceans) allow us to assess for the first time the seasonal and inter-annual polar SSS variability monitored by Aquarius since August 2011. Additionally, shipborne measurements include sea surface temperature (SST) to analyze the accuracy of the Aquarius SSS as a function of SST. SSS retrieval in the polar oceans is challenging. First, salinity retrieval is less accurate for very rough sea surfaces, which are frequent in the high latitudes of the southern hemisphere. In addition, polar ocean waters are cold and Aquarius observations are less sensitive to salinity in cold waters. Finally, the presence of sea ice and icebergs within the radiometer field of view adds complexity to the retrieval of accurate SSS. TB is highly sensitive to the presence of sea ice, and currently no correction in the SSS algorithm is considered. Therefore, the presence of sea ice increases TB and, if not identified accurately, is interpreted by the SSS-retrieval algorithm as a decrease of SSS. Using the GEOS-5 assimilation and forecast model in combination with a Feed Forward Artificial Neural Network, already used in global-scale SSS monitoring but here specifically trained in cold waters, we show that the difference between the cold-water Aquarius SSS retrievals and the shipborne SSS is reduced, especially in the Austral Ocean. Therefore, the use of Aquarius retrievals in conjunction with in-situ measurements, and a data assimilation/neural network system improve SSS retrievals in cold water. The refined SSS data set may be used to better constrain deep water formation, and to help monitoring SSS changes in the polar regions related to freshening (i.e. related to the melting cryosphere).

Paper 4 ENHANCED RESOLUTION FOR AQUARIUS SALINITY RETRIEVAL NEAR LAND-WATER BOUNDARIES

Cuneyt Utku, NASA/USRA, United States; David Le Vine, NASA, United States

The goal of the Aquarius instrument which was launched on June 10, 2011, is to map the surface salinity field of the global oceans with a spatial resolution of 150 km and a monthly RMS accuracy of 0.2 psu. Given the accuracy requirements for the salinity retrieval and the large footprint sizes of the Aquarius radiometers, salinity retrieval is restricted to the open ocean several hundred kilometers away from land, corresponding to several Aquarius footprints. At closer distances, radiation from land received through the antenna side lobes, biases the measurements and causes underestimation of the salinity field beyond the 0.2 psu accuracy requirement. A straightforward remedy to this land contamination problem is to estimate the land contribution and subtract it from the antenna temperature. This approach, however, requires accurate modeling of microwave emission from land and can be used with limited improvement over the current state of retrieval. Alternatively, a deconvolution type reconstruction scheme is used in this study to investigate the possibility of Aquarius salinity retrieval near land-water boundaries. The deconvolution approach in effect enhances the spatial resolution of the retrieved salinity field. The main advantage of this approach is that the need for an accurate land model is eliminated. However, the drawback is that deconvolution problems are ill-posed (unstable and no-unique solution). Consequently the retrieved salinity is generally not uniquely determined and is unrealistic. But, given some a-priori information about the nature of the solution, it is often possible to obtain a reasonable solution for the deconvolution problem. Simulations of the Aquarius salinity retrieval near land-water boundaries are performed in this study to demonstrate the feasibility and limits of this approach using a multi-order regularization scheme. For the simulations, Aquarius antenna patterns and HYCOM salinity fields as well as NCEP values for soil moisture and surface temperatures and ECOCLIMAP vegetation maps, are used in order to simulate realistic scenarios. For the regularization scheme, constraints such as smoothness of brightness temperature over ocean and proximity to initial estimates obtained from estimates of the mean values of salinity, soil moisture and surface temperatures, are used. With an assumed noise standard deviation of 0.2 K (Aquarius noise standard deviation is about 0.1 K) the technique currently yields salinity retrievals close to the 0.2 psu RMS accuracy requirement within a footprint of the land-water boundary. At its current state, the results are promising with sufficient room for further improvement and could lead to improved retrieval of salinity by Aquarius near coasts.

Paper 5 ACTIVE AND PASSIVE SATELLITE MEASUREMENTS OF THE EFFECTS OF SEA SURFACE RAIN ON RADAR CROSS SECTION AND BRIGHTNESS TEMPERATURE

David Weissman, Hofstra University, United States; Vladimir Irisov, NOAA/Environmental Research Laboratories, United States; William Plant, Applied Physics Laboratory, United States

The dual instruments onboard the Aquarius satellite provide a unique opportunity to engage in the development of a combined theoretical model for the sea surface spectrum applicable to active and passive sensing, at L-band. This study seeks joint predictions of the surface normalized radar cross section (NRCS) and brightness temperature (Tb), over a range of wind speeds and microwave frequencies. A special case of this subject is the effect that rainfall has on the observed values and how this effect could be introduced into the theoretical models. It is expected that spaceborne measurements will be subjected to the complications caused by inhomogeneous air-sea conditions associated with a weather event that contains rain. It is necessary to contend with a wide range of possible wind speeds, rainrates and inhomogenous beam filling that exist within the antenna footprints of the Aquarius sensors. Resources from JPL PO.DAAC and the Remote Sensing Systems, Inc now incorporate, in addition to the microwave quantities, auxiliary information on wind speeds and rainrates produced other spaceborne sensors. High spatial and time resolution of near surface rainrate is available from the NWS NEXRAD archives, when observing events in coastal regions. Preliminary results indicate that the brightness temperature is appreciably affected by rain, whereas the NRCS shows little or no sensitivity in this regard. Appreciable data is needed to support theoretical models. Efforts are also in progress to investigate the effect of rain on the C-band brightness temperature, using the AMSR-E radiometer that operates at 6.9 GHz. Both H-pol and V-pol are being studied, in conjunction with the high resolution rain information provided by the NEXRAD resources that span the U.S. coastline. Supporting wind and sea surface temperature data is available using the multi-platform data sets provided by the JPL PO.DAAC. Theoretical modeling is also of interest.

Paper 6 WHITECAP FRACTION OF ACTIVELY BREAKING WAVES FROM SATELLITE-BASED PASSIVE MICROWAVE OBSERVATIONS

Magdalena D. Anguelova, Paul A. Hwang, W. Erick Rogers, Naval Research Laboratory, United States

Oceanic whitecaps are the most direct surface expression of breaking wind waves in the ocean. Whitecap fraction W quantifies the breaking events and is thus a suitable forcing variable for parameterizing and predicting air-sea interaction processes associated with breaking waves. Satellites-borne microwave radiometers provide observations suitable to obtain the total whitecap fraction W, including foam generated during active wave breaking and residual foam left behind by these breaking waves. The total whitecap fraction W is important for predictions of sea spray aerosol production and heat exchange. However, the active portion WA, is necessary for evaluating processes such as turbulent mixing, gas exchange, ocean ambient noise, and spray-mediated intensification of tropical storms. It is thus pertinent to be able to separate WA from W. One possible way to make such a separation is to develop a scaling factor R = WA/W, which when applied to satellite-derived data for W will provide data for WA on a global scale. Theoretical basis for our approach is the Phillips (1985) concept which connects WA to the energy dissipation rate of breaking waves. We pursue our goal in two major steps, which involve calculations and comparisons of energy dissipation rates and WA from buoy and wave model data. We describe the principle of the W versus WA separation, identify the parameters that affect the accuracy of the approach, and present results for a scaling factor between WA and W. Comparison of energy dissipation rates from buoy data matched up with WindSat observations and wave model calculations provide basis for expanding the scaling factors from regional to global scale.

Wednesday, March 26 — Clouds and Precipitation — 14:40 - 16:00

Poster Session — **Dabney Hall, Bldg 40**

Session Co-Chairs: Boon Lim, NASA - Jet Propulsion Laboratory; Joe Turk, NASA - Jet Propulsion Laboratory

Paper 1 HURRICANE IMAGING RADIOMETER WIND SPEED AND RAIN RATE RETRIEVALS DURING THE 2010 GRIP FLIGHT EXPERIMENT

Saleem Sahawneh, Spencer Farrar, James Johnson, Linwood Jones, University of Central Florida, United States; Jason Roberts, Sayak Biswas, MSFC, United States; Daniel Cecil, NASA MSFC, United States

Microwave remote sensing observations of hurricanes, from NOAA and USAF hurricane surveillance aircraft, provide vital data for hurricane research and operations for forecasting the intensity and track of tropical storms. The current operational standard for hurricane wind speed and rain rate measurements is the Stepped Frequency Microwave Radiometer (SFMR), which is a nadir viewing passive microwave airborne remote sensor. This paper discusses the next generation of airborne sensor (Hurricane Imaging Radiometer, HIRAD), which will extend the nadir viewing SFMR capability to provide wide swath images of wind speed and rain rate, while flying from a high altitude aircraft. HIRAD was first flown in the Genesis and Rapid Intensification Processes, GRIP, NASA hurricane field experiment in 2010 and this paper reports on geophysical retrieval results and hurricane images from GRIP flights. HIRAD is a four-frequency, C-band, synthetic aperture radiometer with a 0.8m × 0.6m, stacked patch array antenna that provides a ± 60° swath. It flew on the NASA Johnson Space Center's WB-57 aircraft at 18 km altitude during GRIP over Hurricanes Earl and Karl, on September 1-2, 2010 and September 16, 2010, respectively. Simultaneously, NOAA Hurricane Research Division flights with SFMR provided under-flight passes that covered the entire HIRAD swath and allowed for comparison and validation of the HIRAD measurements. This paper will provide an overview of: the HIRAD instrument, the ocean emissivity radiative transfer model, and the wind speed/rain rate retrieval algorithm that uses maximum likelihood estimation statistical theory. Also results are presented for hurricane wind speed and rain rate images for Earl and Karl, which are compared to collocated SFMR retrievals for validation purposes.

Paper 2 AN ATTEMPT TO CLASSIFY THE TYPES OF CLOUDS BY A DUAL FREQUENCY MICROWAVE RADIOMETER

Laura Resteghini, Carlo Capsoni, Lorenzo Luini, Dipartimento di Elettronica, Informazione e Bioingegneria, Italy; Roberto Nebuloni, CNR-IEIIT, Italy

Clouds have a definite impact on the propagation of waves at frequencies above 30 GHz and their effect, in terms of path attenuation, cannot be underestimated. For example, the fade due to clouds at the zenith and for a yearly probability of 1% falls between 3 and 4 dB in the W band in Europe. The evaluation of water cloud attenuation AC up to approximately 200 - 300 GHz is facilitated, being AC proportional to the Integrated Liquid Water Content (ILWC) along the path, i.e. it does not depend on the Droplet Size Distribution (DSD) or, in other terms, on the cloud type. The situation is different if we move from microwave to optical wavelengths that are becoming the new frontier of the advanced telecommunication and space science systems. Indeed, the droplets size results to be much greater than the wavelength (0.8 to 1.5 micrometer) and the Rayleigh scatter approximation, typical for microwaves, does not hold any more. In this case, the Mie scattering up to its optical limit has to be used. Therefore, the DSD, which depends on the type of clouds, must be properly considered in the calculation of AC. This contribution addresses the topic of cloud classification. The databases used in this work are time-series of a dual-channel (23.8 and 31.6 GHz) radiometer collected at the experimental station of Spino d'Adda (Italy) for 7 years and high resolution radiosonde observations (RAOBS) launched from Milano Linate airport for 10 years. Both databases were combined to derive Integrated Water Vapor Content (IWVC) and ILWC through the application of the Salonen Uppala cloud detection algorithm and mass absorption models such as those proposed by Liebe and Rosenkranz. Using RAOBS data as reference, water clouds were catalogued according to their type (Status, Nimbostratus, Cumulus and Cumulonimbus), in dependence on cloud thickness and height above ground. Furthermore, looking at the scatter plot of the IWVC against the ILWC, the above classes turn out to correspond to different regions that are separated by straight lines. In our analysis, it is assumed that each RAOBS ascent represents a picture of a cloud situation. Time series of ILWC and IWVC derived from the radiometer were low-pass filtered with a moving average. Once the presence of a cloud is identified in the ILWC time series, it is catalogued according to the linear dependences of ILWC and IWVC provided that the threshold is overtaken for a given number of minutes. Results indicate that the cloud classification identified from RAOBS applies as well to the radiometric measurements as far as the subdivision of clouds into stratiform and cumuliform is concerned: the difference between the occurrence of the two datasets is in the order of a few percent. We also assessed that rain events are detected only in presence of cumulus and cumulonimbus, as expected.

Paper 3 SENSOR SYNERGY TO DETECT CLOUDS AND PRECIPITATION: RESULTS OF THE FIRST HALO-HAMP FLIGHT CAMPAIGN.

Emiliano Orlandi, Mario Mech, Susanne Crewell, University of Cologne, Germany; Felix Ament, Christian Klepp, University of Hamburg, Germany

Clouds and precipitation play an important role in the atmospheric water cycle and radiation budget. Unfortunately, the understanding of the processes involved in cloud and precipitation formation and their description in global and regional models are still poor. Not only models poorly describe such processes, also satellites retrievals often show discrepancies in surface precipitation estimates. To improve our understanding of these processes and to reduce model and retrieval uncertainties, new observation and retrieval techniques exploiting the synergy between active and passive sensors are needed. In this respect HAMP (Microwave Package for HALO, the High Altitude Long Range aircraft), consisting of a 36 GHz Doppler cloud radar and a 26-channel radiometer, is an ideal test-bed. HAMP radiometers have frequencies along absorption lines (22, 60, 118 and 183 GHz) and in window regions, overlapping with those of AMSUA and MHS. HAMP will participate in winter 2014 in the dedicated remote sensing HALO mission NARVAL (Next-generation Aircraft Remote-sensing for VALidation studies). During NARVAL, the HALO payload will include a water vapor lidar and dropsondes in addition to HAMP. The campaign consists of two parts: NARVAL South, which will take place over the subtropical Atlantic Ocean, with the aim of investigating shallow convection in the trade wind region; NARVAL North, focusing on post-frontal lows over the North Atlantic Ocean. In this work we present measurements collected during three test flights conducted over Germany during summer 2013 as well as those that will be collected during the NARVAL campaign. Preliminary data analysis will be illustrated, and examples of the synergistic use of active and passive sensors to detect, categorize and quantify hydrometeors will be given. The analysis will focus on precipitation forming west of cold fronts crossing the North Atlantic Ocean, where different satellite retrieval algorithms show discrepancies in surface precipitation, and on precipitation produced by shallow cumuli in the trade wind region, often underestimated because close to the detection limits of the current satellite sensors.

Paper 4 ON THE COMPUTATION OF THE PATH DELAY IN DEEP SPACE MISSIONS APPLICATIONS BY MEANS OF A SCALAR RADIOMETRIC–BASED INDICATOR

Ada Vittoria Bosisio, National Research Council of Italy, Italy; Vinia Mattioli, Università " La Sapienza", Italy; Alberto Graziani, Paolo Tortora, University of Bologna, Forlì (I), Italy

The discrimination of sky conditions is of importance for a variety of applications in atmospheric sciences, such as microwave remote sensing and satellite communications. In this framework, ground-based microwave radiometers proved their potential in the characterization of the atmospheric channel attenuation. Also, they were used for the accurate estimation of the path delay due to the water vapor to calibrate deep space observables, e.g. in the framework of the gravity science experiments carried out during the Cassini mission to Saturn. For this experiment, NASA-JPL developed an advanced media calibration (AMC) system, consisted in an ultra stable advanced water vapor radiometer (AWVR), a meteorological station and an atmospheric profiler [1]. Aim of AMC is to improve the accuracy of the tropospheric calibrations of the deep space observations with respect to the current one based on GPS observations. As the presence of liquid water in the atmosphere is a major impairment in deep space observables, when the AWVR data are flagged as in presence of liquid water, (clouds or rain) the path delay is estimated through GPS data. Since the accuracy of the GPS calibration is more reliable but less accurate with respect to AWVR, it is of interest to investigate the reliability of the tropospheric calibrations as given by radiometric observations. The authors aim at using a Status Sky Indicator (SSI) [2], a ratio between the brightness temperatures observed at different frequencies in the K band, to discriminate among sky propagation conditions and evaluate the AWVR path delay performances for the deep space application. The discrimination performances of SSI were already tested against different set of measurements using concurrent rain gauges as ground data [2]. A preliminary analysis was described in [3], addressing one month of radiometric data recorded at the NASA/JPL Deep Space Network (DSN) Goldstone Complex during the Cassini SCE1 experiment, to validate the SSI at different elevation angles. The proposed paper will describe the SSI computation on a larger dataset of measurements, collected at the two NASA/JPL DNS complexes of Madrid and Goldstone during the entire Cassini mission to Saturn. These measurements will be used to classify data according to the sky propagation conditions and to define the SSI thresholds for each complex. Since the radiometric data have been collected during tracking operations, the SSI will be computed as function of the elevation. Then, the SSI-discriminated data will be processed to assess the estimated path delay to be used in the Orbit Determination (OD) process. In particular, SSI could be considered as a quality index to check whether data are corrupted by rain or external interferences. The last section of the paper will also show the application of the SSI procedure in calibration data to be used in the OD process, in order to evaluate how the SSI-processed data will affect the observation residuals in terms of average and root mean square with respect to data fully calibrated with GPS observations. References [1] Tanner A.B., Riley A.L. Design and performance of a high-stability water vapor radiometer Radio Science, Vol. 38, No 3, 8050, doi: 10.1029/2002RS002673, 2003 [2] Bosisio A.V., Ciotti P., Fionda E., Martellucci A. - A sky status indicator to detect rain-affected atmospheric thermal emissions observed at ground, IEEE Trans. GRS, Vol. 51, No. 9, pp. 4643-4649, 2013 [3] V. Mattioli, A.V. Bosisio, A. Graziani, P. Tortora, L. Castanet, Analysis and Improvements of Methodologies for Discriminating Atmospheric Conditions From Radiometric Brightness Temperatures, Proc. of 7th European Conf. on Antennas and Propagation, EUCAP 2013, Goteborg (SW), April 2013.

Paper 5 A PRELIMINARY SITE-DIVERSITY ANALYSIS BY USING MICROWAVE RADIOMETERS
Vinia Mattioli, He Space Operations GmbH, Germany; Ada Vittoria Bosisio, National Research Council of Italy, Italy; Xavier Boulanger, Laurent Castanet, ONERA, France; Frédéric Lacoste, CNES, France

With the strong business demand for modern broadband services, future satellite communication systems are planned to operate in Ka-band for user links and in Q/V bands for feeder links to (between 18 and 50 GHz) get both the required bandwidth and data rate to offer multimedia services of chosen quality. The signal propagating at these frequency bands is limited by the tropospheric effects, whose impact could be reduced on feeder links by the implementation of gateways in site diversity configuration. CNES (F) and ONERA (F) are conducting a site diversity experiment to collect measurements at Ka-band and to extrapolate the channel behaviour at Q/V band. In this framework, a network of various equipment, ranging from satellite beacon receivers to radiometers (MWRs), including meteorological sensors such as rain gauges, has being deployed in the South of France, mainly in the Toulouse area. Specifically, a Radiometrics profiling radiometer, TP/WVP-3000, is deployed in Toulouse, three RPG-HATPRO radiometers are located in Le Fauga-Mauzac, Aire sur l'Adour and Salon de Provence, and an RPG-LWP dual frequency radiometer is installed in Aussaguel. In this work, a preliminary site-diversity study involving two among these MWRs is addressed, namely the Radiometrics located in Toulouse and the RPG dual-channel LWP based in Aussaguel. Both point towards ASTRA 3B satellite at an elevation angle of about 35°. From 26th June 2012 to 11th March 2013, the RPG at Aussaguel performed continuous observations in tip-cal configuration. The scanning procedure was implemented to evaluate the correlation between the slanted observations (along a direction pointing almost toward Toulouse) observed at Aussaguel and the scenario as seen from the Radiometrics in Toulouse, being the two site 16 km apart. A comparison was performed between the Radiometrics' measured TBs and the retrieved IWV, LWP, and the scanning observations from RPG dual-channel in Aussaguel. A fairly good agreement was observed between measurements and retrieved IWV collected at Aussaguel at the elevation angle of 160.2° and those collected in Toulouse. This comparison led to a preliminary analysis aiming at characterizing the spatial variations in water vapor between the two stations by using temporal data analysis, to study the spatial-temporal correlation of water vapor variations via the frozen flow model. Temporal variograms as RMS differences between observations from each radiometer will be calculated and temporal autocorrelation and cross correlation will be shown to give an indication of the temporal spectra of the water vapor fluctuations.

Wednesday, March 26 — Theory and EM Models — 14:40 - 16:00

Poster Session — Dabney Hall, Bldg 40

Session Co-Chairs: Ed Kim, NASA GSFC; Xiaolan Xu, NASA JPL

Paper 1 A MODEL BASED RADIOMETER DISAGGREGATION TECHNIQUE USING RADAR BACKSCATTER INFORMATION FOR SMAP
Ruzbeh Akbar, Mahta Moghaddam, University of Southern California, United States

By combining active and passive remote sensing techniques, the NASA Soil Moisture Active Passive (SMAP) mission aims to measure and detect global surface soil moisture estimates and address many of the current and pressing climate dynamics questions. To meet mission requirements and achieve unprecedented retrieval accuracy and spatial resolution, SMAP will integrate information from an L-band SAR along with an L-band radiometer system. Fundamentally, two issues must be addressed (1) the inherent spatial resolution disparity between the two instruments due to the real-aperture vs. synthetic aperture nature of radiometers and radars, respectively, and (2) how to combine active and passive measurements in a soil moisture estimation scheme, regardless of the resolution scale of each measurement. The spatial resolution disparity problem will be addressed in this work and a method will be presented to generate higher-resolution brightness temperature (TB) information from SMAP backscattering coefficient and TB measurements, '0 and TBsmap, respectively. To utilize current efficient soil moisture estimation techniques, the SMAP coarse resolution brightness temperature TBsmap (~36 km resolution) must be downscaled to a high-resolution product, TBd. This process is known as TB disaggregation. Since the L-band radar provides information on the fine scale heterogeneity contained in a given radiometer pixel, and since both the radar and radiometer are fundamentally sensitive to the same microwave properties of the scene under observation, it is possible to leverage the radar measurements to arrive at a higher-resolution TB product. We work on the premise that a single coarse scale TBsmap measurement corresponds to variations and heterogeneity of soil moisture, vegetation water content, and roughness at finer scales represented by the radar backscattering cross-section measurements. Over the dynamic range of the parameter space listed, a multi-dimensional mapping is generated, which links the expected emission and backscatter cross-section from a target. This mapping is created by evaluating the associated radar and radiometer forward models over the parameter space of interest and populating look-up tables such that for any high resolution '0 measurement obtained from SMAP an estimate of TBd is possible: TBd = f('0,TBsmap). Each TBd is generated using the appropriate forward model at the SMAP radar resolution and corrected by the grid average difference with respect to the coarse TBsmap measurement. Given that within a single TBsmap pixel multiple higher resolution radar measurements exist, the outcome of the disaggregation process yields a TBd map at the same scale as the radar. Results are presented to show the suitably of this method towards SMAP disaggregation and integration of this technique in an Active-Passive soil moisture retrieval algorithm. The performance of this disaggregation technique is assessed through numerical simulations to synthesize SMAP-like measurements, as well as application to available airborne data as reference "true" TBd. Disaggregation sensitivity to measurement noise is also investigated by examining the absolute disaggregation cumulative distribution error per pixel (cdf) of |TB¬d-TBi| per pixel, as well as comparing TBd spatial covariance with the corresponding radar spatial covariance. For nominal SMAP system noise characteristics, preliminary TB disaggregation over the complete range of soil moisture and VWC of interest indicates that 90% of disaggregated pixels have a 20K or less absolute error. Improvements to this current method are ongoing to achieve a more desirable (~ <10K) absolute error for most of the pixels under consideration.

Paper 2 SCATTERING BY LARGE PERIODIC ROUGH SURFACES: NOVEL NUMERICAL METHODS AND APPLICATIONS
Martin Maas, UBA-Conicet, Argentina; Oscar Bruno, Caltech, United States; Francisco Grings, UBA-Conicet, Argentina

We present novel numerical methods that enable efficient treatment of problems of scattering by realistic rough surfaces, including, for example, actual tilled agricultural soils containing complex geometrical features, as well as resonant problems – for which the wavelength is comparable to the rms height. As is known, efficient treatment of large/resonant periodic surfaces is necessary in order to accurately approximate the types of natural and man-made, possibly non-periodic, rough surfaces that arise in the field of remote sensing. The scattering produced by such surfaces can differ significantly from corresponding predictions that rely on well-known prototypical surfaces and/or approximate theories. A typical difficulty relates to polarization ratios in active microwave remote sensing: experiment contradicts existing theory that indicates that copolar backscattering coefficient ratio (HH/VV) cannot exceed unity for bare soils. An additional problem concerns Wood anomalies. Such configurations (at which one or more scattered waves propagate in a direction parallel to the scattering surface) present computational and theoretical issues. For instance, the classical periodic Green function is not even defined in such cases; furthermore, near Wood anomalies, the rough-surface integral equations become severely ill-conditioned. The problem becomes even more severe for large 2D and 3D surfaces, for which finely spaced sets of Wood anomalies appear throughout the spectrum – thus preventing accurate solution for virtually all frequencies unless the problem is adequately addressed. To tackle these issues we employ a range of novel mathematical techniques, including modified integral equations that can be solved uniquely even at and around Wood anomaly frequencies (on the basis of shifted rapidly-convergent Green functions) together with a novel acceleration technique, for both 2D and 3D problems, which is based on use of equivalent electromagnetic sources and Fast Fourier Transforms. The scheme is completed by means of a smooth windowing function and high-order quadrature rules for the resulting singular integrals. To our knowledge, this is the first approach that can accurately address the difficulties inherent in modeling of large periodic surfaces and associated Wood anomalies. We illustrate the accuracy and efficiency of our methodology by means of a variety of numerical results for active and passive microwave problems, including comparison with experimental data, that demonstrate, in particular, agreement with observations of HH/VV ratios provided by SAR data. Thus the new forward-model methodology impacts significantly on remote sensing problems such as soil moisture determination which rely heavily on polarization discriminated data.

Paper 3 RADIOMETER BASED MEASUREMENTS OF SLANT-PATH ATTENUATION IN THE V/W BANDS
George Brost, Kevin Magde, William Cook, AFRL, United States

The V/W frequency bands of 71-76 GHz and 81-86 GHz have been allocated for satellite communications. V/W offers the potential of wide bandwidth and available spectrum, but availability will be limited by tropospheric attenuation from clouds and rain. Extrapolation of existing models that predict attenuation statistics to these higher frequencies is unreliable. Unfortunately there is little data available that characterizes these aspects of the propagation channel for the V/W bands. Experimental distribution functions (EDFs) for attenuation with over 20 dB of dynamic range are needed to develop and validate prediction models. Ground-based radiometry offers the potential of a low cost means to provide the much needed slant-path attenuation statistics. In this paper we present data and analysis of slant-path attenuation in the V and W bands. Slant-path data was collected at Rome, NY with a multi-channel radiometer with receivers at 23.8, 31.4, 72.5 and 82.5 GHz. The main challenge is to invert the measured brightness temperature to obtain attenuation in a highly attenuating and scattering atmosphere. The scattering albedo for rain is about 0.5 for the V and W bands, depending on rain rate and drop size distribution. The usual estimates of the mean radiating or effective temperature are not adequate for these conditions. A model based approach applying radiative transfer theory provides a possibility to obtain the attenuation statistics with acceptable uncertainty. A backwards Monte-Carlo simulation was used to solve the radiative transfer equation (RTE). Current simulations use a 1-D (planar) atmospheric model. Extension to a 3-D model is planned. The goal of these simulations is to determine the relationship between attenuation and measured brightness temperature and surface temperature, pressure and relative humidity, and requirements for other meteorological parameters. The other way to perform radiometric based attenuation measurements utilizes the sun as source. Our radiometer provides sun-beacon measurements of slant-path attenuation with over 30 dB of dynamic range. These sun based measurements do not provide adequate statistics but can be used to validate and or determine an attenuation retrieval algorithm, since they measure both attenuation and brightness temperature.

Paper 4 CREATION OF A LAMBERTIAN MICROWAVE SURFACE FOR RETRIEVING THE DOWNWELLING CONTRIBUTION IN GROUND-BASED RADIOMETRIC MEASUREMENTS
Benoit Montpetit, Bruno Courtemanche, Alain Royer, Alexandre Roy, Université de Sherbrooke, Canada

Passive microwave in situ brightness temperature measurements are often made in complex environments. In such cases, the measured signal integrates contributions of many different sources. This complicates the study and analysis of specific targets such as snow and soil measured in situ. This is why tools need to be created in order to separate the multiple components of the measured signal. Here we present the different stages used to create a lambertian reflective surface to measure the downwelling contribution reflected at the surface of a target. First, using ray tracing to extrapolate the bidirectional reflectance distribution function (BRDF) of a surface with high reflectivity in the microwave spectrum, we characterized a surface that act as a near lambertian reflector at 37 GHz. An aluminum plate was then molded with a standard industrial wet sand technique to create this lambertian surface of 50 x 60 cm. The lambertian properties were then validated using ground-based radiometric measurements. An emissivity of 0.091 was found for the created plate. We also give guidelines to creating a lambertian surface at different frequencies and improving the conception of such a plate to take into account logistic issues for field work (size and weight). A field experiment was also conducted showing the usefulness of such a tool to measure the downwelling contribution of ground-based radiometric measurements in low downwelling radiative fluxes (clearings) and high downwelling radiative fluxes (forested areas). The emissivity of a stable soil sample was measured in these different areas and the standard deviation of the emissivity for 8 sites was 0.038 in horizontal polarisation and 0.006 in vertical polarization.

Wednesday, March 26	Theory and EM Models	16:00 - 18:00
Lecture Session		Ramo Auditorium, Bldg 77

Session Co-Chairs: Leung Tsang, University of Washington; Roger Lang, George Washington University

Paper 1 **PHYSICAL MODEL OF MICROWAVE RADIOMETRIC SIGNAL FROM WAVE BREAKING**
16:00 *Vladimir Irisov, NOAA, Zel Technologies, LLC, United States*

Microwave radiometry of the ocean is an important method of measurement such global parameters as near surface wind, sea surface temperature, and salinity. Understanding of microwave radiation from sea surface is essential for adequate interpretation of satellite data. It is understood that the wave breaking and associated foam patches are important for adequate modeling of sea surface radiation. We propose a model of wave breaking based on simple physical assumptions. We consider the sea surface as a Gaussian process described by power spectrum and study a statistics of areas with the local slope exceeding certain threshold. The value of excess gives us an estimate of breaker intensity and velocity. This way we are able to derive a distribution of breaking crest length versus breaker velocity – ′-function introduced by Phillips (1985). ′-function allows one to estimate integral foam coverage, energy dissipation, and other parameters associated with wave breaking. Comparison of the wind dependencies of the foam coverage, the peak breaker speed, and the peak of ′-function with empirical relations shows good agreement and allows us to define unknown parameters of the model. To calculate microwave radiation from an individual foam patch we treat a foam layer on a sea surface as multilayered media with air-water fractions changing with depth. Following Anguelova and Webster (2006) we use mixing formula to estimate effective dielectric constant of sublayers. We assume that the total thickness of the foam is decaying exponentially with time and we account for local tilt of the foam layer due to underlying long waves. Emissivity of the foam-free wavy surface is calculated using the small slope approximation. For comparison purpose we use empirical dependencies of ocean microwave emissivity obtained by Yueh et al.(2013) for L-band and by Meissner and Wentz (2012) for the frequencies from C-band to W-band. Our model azimuthally averaged brightness temperature contrast agrees quite well with empirical functions for all frequencies and wind speed from 3 to 25 m/s. The first and second azimuthal harmonics show some discrepancy. We would like to mention that the values of the first and second harmonics are about 10 times smaller than the typical value of azimuthally averaged brightness temperature contrast, so the value of the discrepancy is relatively small. We believe that further adjustment of the model parameters will help us to reduce the difference between our model and observations. References Anguelova, M. D. and F. Webster, 2006: Whitecap coverage from satellite measurements: A first step toward modeling the variability of oceanic whitecaps. J. Geophys. Res., 111, C03017, doi:10.1029/2005JC003158. Meissner, T, and F. Wentz, 2012: The emissivity of the ocean surface between 6 and 90 ghz over a large range of wind speeds and earth incidence angles. IEEE Trans. Geosci. Remote Sens., 50, N.8, pp.3004-3026. Phillips, O. M., 1985: Spectral and statistical properties of the equilibrium range in wind-generated gravity waves. J. Fluid Mech., 156, 505–531. Yueh, S, W. Tang, A. Fore, G. Neumann, A. Hayashi, A. Freedman, J. Chaubell, and G. Lagerloef, 2013: L-band passive and active microwave geophysical model functions of ocean surface winds and applications to Aquarius retrieval. IEEE Trans. Geosci. Remote Sens., 51, N.9, pp. 4619 - 4632

Paper 2 **EFFECT OF EXIT-HOLE FREQUENCY SHIFT AND WALL LOSS ON THE PERMITTIVITY MEASUREMENTS OF SEAWATER AT L BAND**
16:20 *Yiwen Zhou, Roger Lang, The George Washington University, United States; Cuneyt Utku, David Le Vine, Ocean Sciences Laboratory/Code 615 NASA Goddard Space Flight Center, United States*

The accuracy of the George Washington University's (GW) L-band cavity measurements of seawater is examined by measuring the effect of the capillary tube's exit hole on the resonant frequency and by performing a theoretical study of the effect of cavity wall loss on the perturbation equations. The purpose of this study is to confirm the accuracy of past seawater measurements. GW has employed a cavity technique to determine the complex permittivity of seawater at L-band (1.413 GHz). A capillary glass tube is installed in a brass cavity through a center hole in each endplate. Seawater is introduced into the cavity through the glass tube. By applying perturbation theory, the changes in the resonant frequency and in the cavity Q value can be used to determine the real and imaginary parts of the dielectric constant of seawater, respectively. Based on the measurement data, an accurate model function of seawater permittivity has been developed. In this paper, the effect of the exit hole on the cavity resonant frequency is studied by using a specially designed exit hole bushing. The bushing is made so that graphite can be inserted around the tube just after it exits the cavity. This graphite attenuates the fields as they exit the tube. Measurements are being made with and without the graphite to see the effect. Simulations that have been made by [1] have predicted that a small effect should be observed. In another test of the measurement's accuracy, the effect of cavity wall loss is studied. The naval brass construction of the cavity is more lossy compared to copper, silver or gold. It has been preferred however because it can be machined more precisely. A theoretical study is made to determine the effect of this loss on the accuracy of the perturbation equations. Exact modal equations are developed for the cavity without assuming that the loss in the cavity walls is small. These results are compared with the perturbation theory findings to test their accuracy. Initial results of the exit hole and wall loss effects appear to be small but further results will be reported at the meeting. [1] Per O Risman and Birgitta Wäppling-Raaholt 'Retro-modelling of a dual resonant applicator and accurate dielectric properties of liquid water from −20 °C to +100 °C', Meas. Sci. Technol. 18 959, 2007

Paper 3 **LAND SURFACE MICROWAVE EMISSIVITY DYNAMICS: OBSERVATIONS, ANALYSIS AND MODELING**
16:40 *Yudong Tian, University of Maryland, United States; Christa Peters-Lidard, NASA Goddard Space Flight Center, United States; Kenneth Harrison, University of Maryland, United States; Sarah Ringerud, Colorado State University, United States; Sujay Kumar, Science Application International Corp., United States*

The microwave emissivity from the Earth's surface is the critical signal for remote sensing of land surface parameters and is a noise for atmospheric variables. The dynamics of microwave emissivity over many types of the earth's surfaces is still not well understood, because the microwave emission from the earth's surface is a complex dynamical process. It depends on a wide range of physical parameters and their spatial and temporal variability associated with different types of surfaces. We studied the dynamical behaviors of the microwave emissivity over a very diverse sample of land surface types. Using seven years of satellite measurements from AMSR-E, we identified various dynamical regimes of the land surface emission in a judiciously selected two-dimensional phase space. Many of the regimes are well defined and distinct, and within each regime seasonality drives the dynamics into different regions. Within each region, the dynamics in turn shows differing degrees of complexity, reflecting the interplay of various seasonally dependent terrestrial processes. Many surfaces belonging to the same climate or ecology class do not necessarily occupy the same regime. In addition, we used two radiative transfer models (RTMs), the Community Radiative Transfer Model (CRTM) and the Community Microwave Emission Modeling Platform (CMEM), to simulate land surface emissivity dynamics. Both models have been widely employed for both retrieval and forward modeling applications, but their land surface emissivity components have not been extensively validated. In this study, we modeled land surface emissivity with both RTMs and evaluated their emissivity-modeling skills. With both CRTM and CMEM coupled to NASA's Land Information System, global-scale land surface microwave emissivities were simulated for five years, and evaluated against AMSR-E observations. It is found that both models have successes and challenges over various types of land surfaces. Among them, the desert shows the most consistent underestimates (by ~70-80%), due to limitations of the physical models used, and requires a revision in both systems. Other snow-free surface types exhibit various degrees of success and it is expected that parameter tuning can improve their performances. Various error sources, including from model physics, parameters and model input are discussed. Suggestions for improving emissivity modeling include the adoption of a better desert model, parameter tuning, and a microwave-based land surface classification scheme.

Paper 4 **LOCAL AND GLOBAL SCALE INVESTIGATIONS OF SNOW PROPERTIES BY MEANS OF MICROWAVE RADIOMETRIC MEASUREMENTS AND MODEL SIMULATIONS**
17:00 *Emanuele Santi, Marco Brogioni, Simonetta Paloscia, Paolo Pampaloni, Simone Pettinato, Enrico Palchetti, IFAC - CNR, Italy; Chuan Xiong, Institute of Remote Sensing Applications, China; Andrea Crepaz, ARPAV, Italy*

Monitoring of terrestrial snow on both local and global scales is a topic of ever increasing interest due to the crucial role that the snow plays in the climate dynamics. Moreover, snow cover information is extremely important for the water resource management, the energy production, and the avalanche risk prevention. In this framework, microwave radiometers operating from space are an important tool for snow monitoring and retrieving snow depth (SD) and water equivalent (SWE). Research enabling the retrieval of SD and SWE from multi-frequency radiometric data dates back to the late 1970's, when several investigations indicated the sensitivity of microwave emission to the snow cover characteristics. On the basis of satellite and ground based sensors, the key frequency channels in detecting the presence of snow on ground and estimating SD and SWE are Ku- and Ka-bands, and therefore most retrieval algorithms of snow parameters are based on these bands. However, the effect of each snow parameter, namely depth, density, number of layers, grain size and so on, on the measured brightness temperature at each frequency and polarization may affect the sensitivity to SD and SWE and needs therefore to be investigated and characterized. The analysis of the relationships between brightness temperatures, related indexes (i.e. Polarization Index (PI), Frequency Index (FI) and Spectral Polarization Difference (SPD)) and snow parameters was carried out by using data collected with IFAC ground based radiometers in several long term experiments from 2007 to 2011 in the Eastern Italian Alps. Continuous radiometric acquisitions on a protected area were carried out during each winter, while direct measurements of snow parameters (grain shape and size, liquid water content, density, water equivalent, surface roughness and hardness) were provided once a week, as well as every time the snow cover underwent significant changes, by the Avalanche Center of Arabba. For better understanding the mechanisms that drive the microwave emission from snow covered soil and therefore for interpreting the experimental measurements and characterizing the effect of each parameter on the measured brightness, the emission of snow was modeled by using a forward electromagnetic model. In particular, we considered a multilayer implementation of the dense-medium radiative transfer theory under the quasi crystalline approximation (DMRT-QCA) that accounts for the effects of snow layers on the emission of dry snow. Model simulations have been compared with radiometric measurements of snow collected during the ground based experiments with the twofold purpose of validating the model and interpreting some particular aspects of snow microwave emission. The good sensitivity of radiometric measurements to the snow parameters was confirmed and the model was able to simulate the measured data with a satisfactory accuracy. Comparison of experimental results and model analyses made it also possible the investigation of the polarizing effect of snow layering and the assessment of the sensitivity of PI, FI and SPD to the different snow parameters. This analysis was then extended to a larger scale by considering time series of AMSR-E acquisitions and corresponding ground truth provided by the available meteorological stations on some test areas located in Scandinavia and Siberia. These areas were selected as typical targets covered by winter snow and characterized by sparse vegetation (Tundra). Also in this case model simulations were considered for supporting the analysis, and the main findings of the ground based experiment were confirmed. An additional effort was finally carried out for evaluating the effect of forests on snow emission, by including in this analysis a test area in Russia, which is covered by dense coniferous forests.

Paper 5 **BICONTINUOUS/DMRT MODEL APPLIED TO ACTIVE AND PASSIVE MICROWAVE REMOTE SENSING OF TERRESTRIAL SNOW**
17:20 *Wenmo Chang, Leung Tsang, University of Washington, United States*

The Cold Regions Hydrology High-Resolution Observatory (CoReH2O) was one of the three candidate missions considered for the 7th Earth Explorer by ESA. As a part of feasibility studies for the mission, tower based measurements were conducted in Sodankyla, Finland, covering several winter seasons. The instruments is called SnowScat, owned by ESA. The tower based measurements include both microwave radiometry measurements and radar backscatter measurements. Brightness temperatures of dual polarization modes were observed at 1.4, 10.65, 18.7, 37 and 90 GHz, from 30-degree to 60-degree incident angles at a 10-degree interval. Radar backscatters of VV, HV, HH, VH polarizations were measured by a fully polarimetric scatterometer, operating at 10.2, 13.3, and 16.7 GHz, covering from 30-degree to 60-degree incident angles at a 10-degree interval, and a wide variety of azimuthal directions. In addition to the microwave measurements, extensive ground measurements were taken of the snow characteristics in northern Finland, including grain size, snow depth, fraction volume (or snow density), and specific surface area. In this paper, the bicontinuous/DMRT model is used to calculate both active and passive microwave signatures of snow. The bicontinuous random medium is used for the physical characterization of the microstructure of snow. An advantage of the bicontinuous random medium is that the computer simulated microstructures resemble that of real terrestrial snow. In the simulations, we use two size parameters to describe the probability distribution of wavenumbers of stochastic waves that are used for the bicontinuous random medium: ‘’’ and b, that correspond respectively to inverse size and clustering property. The phase matrix computed is then used in the DMRT equations to compute the brightness temperatures and the backscattering coefficients. Distinct features of the bicontinuous/DMRT model compared with Rayleigh scattering and Rayleigh phase functions are: (i) weaker frequency dependence, (ii) weaker size dependence, and (iii) strong forward scattering. The strong forward scattering is characterized by the mean cosine of scattering. These three features are consistent with the QCA/DMRT model and also with the empirical HUT model. A large mean cosine of scattering, assuming the scattering coefficients are the same, will have large brightness temperatures and less backscattering. In addition, the bicontinuous/DMRT has a fourth feature which is giving strong cross polarization. This feature is consistent with the results of the prior Foldy-Lax multiple scattering equations. In this paper, the bicontinuous/ DMRT theory is applied for data analysis of recent experimental measurements of brightness temperatures and backscattering collected by SnowScat instruments. In the simulations of radar backscatter and brightness temperature, we used the same bicontinuous parameters for a specific snowpit. We use ground measurements of grain size, densities and layering of snow cover as input for the theoretical models. The bicontinuous medium model is also characterized by correlation functions and Specific Surface Areas (SSA). The ground measurements of such quantities are also used. Fig. 1 shows the comparison between brightness temperature predicted by bicontinuous/DMRT model and that observed at IOA snowpit on Jan. 18, 2011. The theoretical results of brightness temperatures in dual polarizations are in good agreement with the observations at 10.65 GHz and 18.7 GHz, and four incident angles. In addition, bicontinuous/DMRT model is also applied to the prediction of radar backscatter. Fig. 2 shows the comparison between radar backscatter predicted by bicontinuous/DMRT model and that observed at IOA snowpit from Jan. 4 to Mar. 1, 2011. The theoretical results of co-polarization backscattering agree well with the observation of the scatterometer at 10.2, 13.3, and 16.7 GHz.

Paper 6 **COMPARISON OF RETRIEVAL ALGORITHMS FOR THE WET TROPOSPHERIC PATH DELAY**
17:40 *Soulivanh Thao, CLS, France; Laurence Eymard, LOCEAN, France; Estelle Obligis, Bruno Picard, CLS, France*

The ocean mean sea level (MSL) is a key indicator of the global warming. Its long-term survey is an issue not only for climate evolution study, but also for economic and social consequences of its elevation. The monitoring of the MSL has greatly benefited from the development of spatial altimetry missions since the nineties: satellites allow a nearly complete coverage of the ocean surface and data are provided in near real time. Microwave radiometers play a major role in those missions. They are used to provide a correction (the wet tropospheric correction) for the underestimation of the sea surface height (up to 50 cm) by the altimeter radar, due to the presence of water vapor in the troposphere. This correction represents currently one of the most important parts of the mean sea level error budget. Performance and stability requirements for those radiometers are stringent, especially in climate studies: any errors made on the wet tropospheric path delay directly impact the retrieval of the sea surface height. The uncertainty on this correction is nowadays around 1-cm rms (Ruf et al. 1994). The integrated water vapor content (wv) and the wet tropospheric path delay (dh), being nearly proportional to each others, are retrieved using similar methods. The relationship between dh (respectively wv) and the radiations measured by the radiometer is empirically established using a statistical regression. Three frequencies are generally used to build this relationship: around 18.7, 23.8 and 34.0 GHz. The main 23.8-GHz frequency, being close to the 22.235-GHz water vapor absorption line, is highly sensitive to water vapor. The 18-GHz and the 34-GHz channels are used to eliminate the sea surface and cloud contribution from the signal to be retrieved. For instance, this principle is used in altimetry missions such as TOPEX, Jason-1 and Jason-2, or with microwave imagers such as SSMI. However, some radiometers on board altimetry missions, such as ENVISAT or SARAL, only possess two channels around 23.8 and 34.0 GHz. In this case, the lack of a low frequency channel is partly compensated by the use of the altimeter backscattering coefficient in the retrieval algorithm. This paper will present the performances of several retrieval algorithms for the wet tropospheric path delay, including those used in the operational processing of altimetry missions. The algorithms are built and compared on the same learning and test databases to determine which regression method is more appropriate. The database is composed of atmospheric and oceanographic conditions taken from the European Centre for Medium-Range Weather Forecasts (ECMWF) analyses and the brightness temperatures are simulated with the UCL radiative transfer model. The importance of each input for the different algorithms is analyzed and the performances of the different algorithms are assessed in terms of error (bias and standard deviation) but also in terms of geographical distribution of the errors and correlation with other environmental variables. Our results show that the altimeter backscattering coefficient could not totally compensate the lack of channel at 18GHz which provide useful information of the sea surface temperature. However, the altimeter backscattering coefficient provides additional information on the sea surface wind speed which improves the retrieval when combined with the brightness temperature at 18GHz.

Thursday, March 27	Instrument Technology	08:00 - 09:40
Lecture Session		Ramo Auditorium, Bldg 77

Session Co-Chairs: Jeffrey Piepmeier, NASA - Goddard Space Flight Center; Todd Gaier, NASA - Jet Propulsion Laboratory

Paper 1 **A HIGHLY EFFICIENT AND COMPACT CROSS-CORRELATOR FOR SYNTHETIC APERTURE RADIOMETRY FROM GEO.**
08:00 *Erik Ryman, Anders Emrich, Omnisys Instruments AB, Sweden; Alan Tanner, Isaac Ramos, Jet Propulsion Laboratory, California Institute of Technology, United States*

The lack of data on temperature and moisture distributions within highly dynamic weather formations such as cloud formations has motivated efforts directed at deploying microwave radiometers in geostationary earth orbit (GEO). The cloud penetrating ability of microwave radiometers, as compared to optical instruments, as well as the high temporal resolution made possible by GEO could fill this gap. Aperture synthesis by interferometry has been suggested as a solution to the very large aperture needed for reaching required image resolution at the relatively long wavelengths and distance to earth from GEO. We present a cross-correlator for the purpose of sampling and cross-correlating the signals in such a space-borne interferometric imager. Two application specific integrated circuits (ASIC) were developed; an 8-channel comparator ASIC and a 64-channel digital cross-correlator ASIC. The comparator, used for digitizing of input signals, has features such as per-channel offset calibration, bias control pins, clock return and flip-flop sampling. The features are specifically useful in a cross correlator system where low power consumption is one of the main objectives targeted. The digital cross-correlator, which performs pair-wise cross-correlation between all inputs, also targeted low power/performance ratio. Eight comparator and one cross-correlator ASIC were integrated on a single printed circuit board (PCB) together with clock distribution, power conditioning, programmable offset calibration and readout & control logic. The board measures 136 by 136 mm and weighs 135 g. Both ASICs as well as the assembled PCB has been tested. The digital cross-correlator ASIC has shown a power/performance ratio of 0.13 mW/prod/GHz where top speeds of at least 2.5 GHz can be reached. Radiation testing hints at single event upset rates of around 1 upset/day in GEO and total ionizing dose tolerance of beyond 100 krad. The comparator shows crosstalk isolation in the -50 dB range and common mode rejection of around 30 dB. Sample rates of 4.5 GS/s with a power consumption of 48 mW/channel or 1 GS/s with a power consumption of 17 mW/channel have been demonstrated. The assembled board has been tested to perform cross-correlations and sampling at up to 1.6 GHz, currently limited by the clock distribution circuit. It has been tested within an interferometer system, successfully performing sun observations. The correlator sets a new standard for portability as well as power/performance ratio. Test results as well as the compactness of the design demonstrate that interferometric imaging from GEO has now become a real possibility. A next generation cross-correlator ASIC has already been designed, doubling the number of input channels, and is expected to further reduce power dissipation.

Paper 2 **ADVANCED ICE CLOUD IMAGER WITH POLARIMETRIC CAPABILITIES**
08:20 *Jean-Marc Goutoule, David Sanson, Patrick Crescence, Astrium, France; Catherine Prigent, LERMA, France; Laurent Grandsire, APC, France; Elena Saenz, ESA, Netherlands*

This paper presents and proposes an Advanced Ice Cloud Imager, a low earth orbit radiometer insuring a polarimetric imagery of the Earth atmosphere from millimetre waves up to nearly 1THz. It is focused on the characterization of ice clouds, convection and snowfall. It will extend the capabilities of the Ice Cloud Imager (ICI) thanks to enhanced polarimetry by: • Measuring both orthogonal polarizations in all 'window' channels • Measuring the full polarization vector for the lowest window channel, at 150GHz. • Including a 874 GHz channel to help bridge the gap between the millimetric and the far infrared measurements. The observation is based on a conical scan sub-millimeter wave instrument. The ground resolution is 12Km from 800Km altitude, on a "METOP-like" polar orbit. The full satellite is in the 500Kg/500W range. The channels frequencies range from 150GHz (with polarimetric capabilities) to 874GHz. The paper puts the emphasis on the impact of the polarisation measurement capability onto the instrument architecture, in particular the antenna: in a first approach the Offset antenna configuration has been explored, with one or two 157 GHz horns. Then a Cassegrain antenna has been preferred in order to meet the stringent cross polarisation requirement. Finally, for accommodation and antenna performance reasons, the antenna has been split in a Cassegrain antenna for low frequencies and a separate small offset antenna for the two upper ones. The calibration system, also split in two parts, is depicted and the overall instrument implementation is show. Finally the paper identifies the remaining technology steps needed to open the way to this highly accurate instrument: • Proof of actual low cross-pol horn (design, manufacturing, verification) • Wide band Stoke parameters acquisition, aiming at a "157GHz radiometer with digital backend" • Refinement of full Stoke parameters calibration

Paper 3 **CRYOGENIC AMPLIFIER BASED RECEIVER FRONT-ENDS FOR SUBMILLIMETER-WAVE RADIOMETER AND SPECTROMETERS**
08:40 *Goutam Chattopadhyay, Theodore Reck, Lorene Samoska, Andy Fung, NASA-JPL/Caltech, United States*

Radiometric and high-resolution spectroscopic studies at submillimeter-wave frequencies play a very important role in the Earth science, astrophysics, and planetary exploration. Its importance is underscored by the key role of heterodyne spectrometers in the ESA cornerstone Herschel Space Observatory, NASA's Microwave Limb Sounder (MLS) instrument on Earth Observation System (EOS) Aura satellite, NASA's Microwave Instrument on the Rosetta Orbiter (MIRO), as well as the ground-based Atacama Large Millimeter Array (ALMA), and airborne Stratospheric Observatory for Infrared Astronomy (SOFIA). Traditionally, where highly sensitive measurements are the prime requirement, superconductor-insulator-superconductor (SIS) mixer based receivers cooled to 4K temperature were used at the front-end of the submillimeter-wave radiometer and spectrometers. When cryogenic cooling is not an option, Schottky diode based receivers operating at the room temperature were the obvious choice for these applications as there were no amplifiers available at the submillimeter wavelengths. However, InP high electron mobility transistor (HEMT) based amplifiers and mixers are now available at these frequencies. At submillimeter-wavelengths, low noise amplifiers with substantial gain at the front-end will reduce noise contribution from mixers and intermediate frequency (IF) amplifiers. Moreover, power amplification available through these devices would significantly improve local oscillator (LO) efficiencies. Cryogenic cooling of these amplifiers to 20K provides sensitivity similar to SIS mixers. Although the noise temperature of the front-end HEMT amplifier cooled to 20 K might not be as close to the SIS mixers, however, the 20-30 dB gain it will provide at the front of the mixers and IF amplifiers will provide system noise temperatures similar to a SIS based system, without a 4 K cooling system. Moreover, the sensitivity to physical temperature is much less for amplifiers than SIS. The amplifier receivers would still work at higher temperatures, though at a bit higher system noise, unlike the SIS receivers. Moreover, the higher operating temperature makes these amplifier receivers better suited to planetary instruments and earth remote sensing suborbital platforms where available power is scarce. In the last few years, the development of transistor technologies with maximum device frequency (fMAX) over 1 THz has pushed operating frequencies of amplifiers well into the 700 GHz range. Northrop Grumman Aerospace Systems (NGAS) has developed an ultra-short-gate-length HEMT process which has produced InP HEMT amplifiers working at 700 GHz and beyond. We have evaluated several of these amplifiers in the 300 GHz and 650 GHz band and cooled them to 20K. The amplifier noise temperatures were reduced by a factor of 8 to 10 when cooled to 20K from room temperature. In this paper, we will discuss the science drivers and progress in the cryogenic HEMT amplifier based heterodyne receivers at submillimeter wavelengths and their potential for future spectroscopic and radiometric instruments. This work was carried out at the Jet Propulsion Laboratory (JPL), California Institute of Technology (Caltech), Pasadena, California, USA under a contract with National Aeronautics and Space Administration (NASA).

Paper 4 **MINIATURE LOW NOISE QUADRATURE RECEIVERS FOR TEMPERATURE AND HUMIDITY SOUNDING**
09:00 *Pekka Kangaslahti, Oliver Montes, Chaitali Parashare, Isaac Ramos, Alan Tanner, Bjorn Lambrigtsen, Todd Gaier, Jet Propulsion Laboratory, California Institute of Technology, United States; Victoria Hadel, Steven C. Reising, Colorado State University, United States*

Weather forecasting, hurricane science and atmospheric science applications depend on temperature and humidity sounding of atmosphere. Current microwave instruments provide these measurements from ground based, airborne and LEO satellites by measuring radiometric temperature on the flanks of the 183 GHz water vapor line or the 60 or 118 GHz oxygen line. We have developed miniature low noise receivers that will enable these measurements from a geostationary thinned array sounder that operates as an interferometer. This geostationary instrument is based on hundreds of low noise receivers that convert the millimeter wave signal directly to baseband in-phase (I) and in-quadrature (Q) signals for digitization and correlation. The developed receivers provided a noise temperature of 350 to 450 K and had a mass of 3 g while consuming 24 mW of power. These are the most sensitive broadband I-Q receivers at these frequencies that operate at room temperature, and are significantly lower in mass and power consumption than previously reported receivers. Further benefit is the low LO power requirement of 0 to +3 dBm, an important feature for large arrays providing significant DC power savings. These DC power savings are achieved from the reduced number of LO driver amplifiers needed. Currently we are in the process of assembling and testing hundreds of these receivers to demonstrate scalability of the receiver system. The receivers developed so far were demonstrated as an interferometer in laboratory tests and outdoor measurements of sun overpasses. Furthermore we will integrate the receivers into an airborne radiometer system currently under development.

Paper 5 **INNOVATIVE APPROACH TO LOCAL-NOISE-SOURCES & THEIR COUPLING NETWORKS, FOR MMW & THZ RADIOMETERS' INTERNAL CALIBRATION**
09:20 *Israel Galin, Northrop Grumman, United States*

There is a growing demand for local-noise-source (LNS) and its coupling network technologies, as local temperature-reference resident in millimeter-wave (MMW) and THz spaceborne radiometers. An LNS reference facilitates superior radiometric retrieval products, by accounting for radiometer nonlinearity [1] (vO=aTI2+bTI+c, with a≠0). In this case, the LNS embodies a third T3 reference, for 3-point (and 4-point) calibrations [2][3] – augmenting the common 2-point (references T1=TWARM-LOAD, and T2=TCOLD-SKY) spaceborne calibration practice. The 2-point calibration assumes a radiometer's linear transfer function, i.e., vO=aTI2+bTI+c, with a=0. In another case, a LNS embodies the sole critical internal TN reference, for calibrating non-scanning, i.e., push-broom, spaceborne radiometers [4]. LNSs past success in these roles - e.g., Global Precipitation Measurement (GPM) Microwave Imager (GMI) instrument, and on the Advanced Microwave Radiometer (AMR) on Jason-2 – is at frequencies below 100 GHz. Currently planned applications, e.g., the Surface Water and Ocean Topography (SWOT), underscore the challenges of similar technologies at 160 GHz and beyond. The common approach for implementing spaceborne radiometer calibration with internal LNS requires: 1. A LNS at the radiometer's input band 2. A coupling network, e.g., coupler, switch etc., in cascade to the radiometer's input. To date, LNS technology beyond 150 GHz is not readily available, requiring a significant and challenging development effort. Furthermore, the LNS's coupling network in cascade to the radiometers front-end input degrades considerably radiometer noise-figure performance. This paper presents a novel implementation for the LNS and its coupling to a heterodyne radiometer – forgoing the need for a LNS and a coupling network, at the radiometer's input band. The new approach features: 1. A LNS at lower frequencies than the radiometer's input band 2. A coupling network that does not penalize radiometer's performance The heterodyne radiometer's front-end mixer, operating as a multiplier, facilitates conversion of a MW LNS sub-harmonically related to the radiometer's MMW/THz input band – the multiplied LNS band is then mixed-down into the radiometer's IF band. The same radiometer's mixer ports, LO or IF, avail themselves as sub-harmonic LNS injection ports, without the introduction of loss damaging to the radiometer's sensitivity performance. The paper describes a demonstration of this novel approach as a 4-point calibration for a 183±8 GHz radiometer, as well as for a 280±8 GHz radiometer. Measured 4-point calibration data and nonlinearity calculations are presented and discussed for the 183 GHz radiometer. The paper also considers the opportunity afforded by a 4-point calibration for characterizing the radiometer's as a cubic transfer function, i.e., vO=aTI3+bTI2 +cTI+d, with a and b≠0. Finally the paper discusses considerations for selecting a preferred noise level TN magnitude – from the available range of 10K> TN >1000K to generate an optimized 4-point set, i.e., T1, T2, T1 +TN, and T2 +TN for calibration. References [1] SW Bidwell, et al, "The Global Precipitation Measurement (GPM) Microwave Imager (GMI) Instrument: Role, Performance, and Status", IEEE International Geoscience and Remote Sensing Symposium IGARSS, July 2005. [2] N Skou, "Microwave Radiometer Linearity Measured by Simple Means", IGARSS, June 2002, Vol-6, P 3664-3667. [3] D McKague, "Microwave Radiometer four Point Calibration", Seoul. Korea IGARSS, July 2005,. [4] P Kangaslahti, et al, "Radiometer Testbed Development for SWOT", JPL TRS 1992+, 2010

Thursday, March 27	Small Satellite Instruments and Missions	10:10 - 11:50
Lecture Session		Ramo Auditorium, Bldg 77

Session Co-Chairs: Bill Blackwell, MIT Lincoln Laboratory; Ed Kim, NASA - Goddard Space Flight Center

Paper 1 **THE COMPACT OCEAN WIND VECTOR RADIOMETER: A NEW CLASS OF LOW-COST CONICALLY SCANNING SATELLITE MICROWAVE RADIOMETER SYSTEM**
10:10 *Shannon Brown, Paolo Focardi, Amarit Kitiyakara, Frank Maiwald, Oliver Montes, Sharmila Padmanabhan, Damon Russell, James Wincentsen, Jet Propulsion Laboratory, United States*

The paper describes the design and development of the Compact Ocean Wind Vector Radiometer (COWVR) which is currently being designed, built and tested by the Jet Propulsion Laboratory for an Air Force proof-of-concept technology demonstration mission planned for launch no earlier than 2016. COWVR is a low-cost, low-mass, low-power fully-polarimetric imaging radiometer system operating at 18.7, 23.8 and 34.5 GHz and based on the Jason-2/3 Advanced Microwave Radiometer (AMR) design. The fully-polarimetric observations enable retrieval of ocean surface wind vector, as well as other key environmental parameters such as precipitable water vapor, cloud liquid water, precipitation rate and sea ice. The measurement of ocean surface vector winds using a polarimetric microwave radiometer was first demonstrated by the Naval Research Laboratory WindSat radiometer (launched in 2003). Because this was a first-of-its-kind measurement, the system minimized use of new technology to ensure successful demonstration of the new measurement technique (Gaiser et al., 2005) and consequently had a large mass and power (380 kg and 350 W). The COWVR system utilizes a novel design to reduce the system complexity which in turn significantly reduces the cost, mass, power and volume from the heritage WindSat sensor, yet is predicted to maintain the same wind vector retrieval accuracy. The enabling features include the use of a single multi-frequency feed horn permitting a simple antenna rotating about the feed axis, as opposed to having to spin the entire radiometer system; internal calibration sources which enable fully polarimetric calibration and eliminate the need for an external warm load and cold sky reflector simplifying the mechanical design and enabling a complete 360 degree scan; and a compact highly integrated MMIC polarimetric combining receiver implementation, lowering the system mass and power which in turn makes the system well suited for deployment on smaller class, lower cost satellites. This paper will give a description of the COWVR system and an overview of the technology demonstration mission. We will discuss the unique processing techniques required for this system, including Electronic Polarization Basis Rotation to transfer the polarimetric measurements from the instrument frame to the Earth frame and describe how this actually improves the sensor calibration compared to the more traditional sensor design approach. We will also discuss the wind vector retrieval performance improvement enabled by the two-look (fore and aft) observations from the 360o scan. The performance of the sensor will be discussed and compared to the more traditional conical sensor design.

Paper 2 **PREPARATION FOR THE MICROMAS CUBESAT MISSION**
10:30 *Bill Blackwell, MIT Lincoln Laboratory, United States*

The Micro-sized Microwave Atmospheric Satellite (MicroMAS) is a 3U CubeSat (30x10x10 cm, ~4kg) hosting a passive cross-track-scanning microwave spectrometer operating near the 118.75-GHz oxygen absorption line. MicroMAS aims to address the need for low-cost, mission-flexible, and rapidly deployable spaceborne sensors. The focus of the current MicroMAS mission is to observe convective thunderstorms, tropical cyclones, and hurricanes from a near-equatorial orbit. As a low cost platform, MicroMAS is a core element of a new observing system comprising multiple satellites in a constellation that can provide near-continuous views of severe weather. The existing architecture of few, high-cost platforms, infrequently view the same earth area thus potentially missing rapid changes in the strength and direction of evolving storms leading to degraded forecast accuracy. MicroMAS is a scalable

CubeSat-based system that will pave the path towards improved revisit rates over critical earth regions, and achieve state-of-the-art performance relative to current systems with respect to spatial, spectral, and radiometric resolution. The current MicroMAS mission will demonstrate the viability of CubeSats for high fidelity environmental monitoring and space control that would provide profound advances by reducing costs, by at least an order of magnitude, while increasing robustness to launch and sensor failures. The MicroMAS radiometer is housed in a 1U (10 x 10 x 10 cm) payload section of the 3U (10 x 10 x 30 cm) CubeSat. The payload is scanned about the spacecraft's velocity vector as the spacecraft orbits the earth, creating crosstrack scans across the earth's surface. The first portion of the radiometer comprises a horn-fed reflector antenna, with a full-width at half-maximum (FWHM) beamwidth of 2.4º. Hence, the scanned beam has an approximate footprint diameter of 17 km at nadir incidence from a nominal altitude of 400 km. The antenna system is designed for a minimum 95% beam efficiency. The next stage of the radiometer consists of superheterodyne front-end receiver electronics with single sideband (SSB) operation. The front-end electronics includes an RF preamplifier module, a mixer module, and a local oscillator (LO). The RF preamplifier module contains a low noise RF amplifier and a weakly coupled noise diode for radiometric calibration. The mixer module comprises a HEMT diode mixer and an IF preamplifier MMIC. The LO is obtained using a 30-GHz dielectric resonant oscillator (DRO) and a resistive diode tripler to obtain a 90-GHz LO frequency. A key technology development in the MicroMAS radiometer system is the ultra-compact intermediate frequency processor (IFP) module for channelization, detection, and analog-to-digital conversion. The antenna system, RF front-end electronics, and backend IF electronics are highly integrated, miniaturized, and optimized for low-power operation. The payload also contains microcontrollers, one of which is used in the payload interface module (PIM), to package and transmit radiometric and housekeeping data to the spacecraft bus. A voltage regulator module (VRM) was also designed for the payload to convert the input bus voltage to the required voltages for the payload electronics.

Paper 3 MICROWAVE ATMOSPHERIC SOUNDER ON CUBESAT (MASC)
10:50 *Sharmila Padmanabhan, Shannon Brown, Pekka Kangaslahti, Damon Russell, Richard Cofield, Robert Stachnik, Boon Lim, Jet Propulsion Laboratory, United States*

We are currently developing a prototype version of the microwave atmospheric sounder that would enable measurements of temperature and humidity profiles from a CubeSat. The MASC would use the 6U CubeSat form factor, providing the distinct advantages of sufficient power, sufficient volume for the instrument scanning reflector and blackbody calibrator and platform stability, all with the necessary margin to maintain a low mission risk. The 6U bus uses avionics and spacecraft hardware developed for, tested and proven on multiple 3U CubeSats. Millimeter-wave MMIC-based radiometers developed under extensive NASA ESTO funding would be employed in the proposed MASC, providing state-of-the-art performance in a compact package. MASC would enable low cost, compact radiometer instrumentation at 118 and 183 GHz that would fit in a 6U Cubesat with the objective of mass-producing this design to enable a suite of small satellites to image the key geophysical parameters that are needed to improve prediction of extreme weather events. In this paper, we will describe the design and implementation of the 118 GHz temperature sounder and 183 GHz humidity sounder. It uses super-heterodyne receivers to sample frequencies near the 118 GHz oxygen line and 183 GHz water vapor line. IF filters are used to define the frequency channels at 1, 3, 5 and 7 GHz. MASC would be a nadir-viewing, cross-track scanner. A summary of radiometer calibration and retrieval techniques of temperature and humidity will be discussed. The successful demonstration of this instrument on the 6U CubeSat would pave the way for the development of a constellation sampling tropospheric temperature and humidity with fine temporal and spatial resolution.

Paper 4 POLARCUBE: A CUBESAT 118 GHZ MICROWAVE SENSOR TO DEMONSTRATE GLOBAL FLEET-BASED WEATHER FORECASTING
11:10 *Albin Gasiewski, Lavanya Periasamy, Brian Sanders, Glenda Alvarenga, David Gallaher, University of Colorado at Boulder, United States*

The importance of acquiring meteorological data at high spatial and temporal resolution which has been emphasized in the U.S NRC Decadal Survey's Precipitation, Atmospheric, Temperature and Humidity (PATH) mission requirements, arises from a need for weather forecasting to cope with rapidly evolving weather patterns. The positive impact of passive microwave observations of tropospheric temperature, water vapor and surface variables on short term weather forecasts has been clearly demonstrated in recent error growth studies. The development of a fleet of such passive microwave sensors especially at V-band and higher frequencies in low earth orbit using 3U and 6U CubeSats can help accomplish the aforementioned objectives at low system cost and risk as well as provide for regularly updated radiometer technology. The University of Colorado's PolarCube satellite is intended to serve as a demonstrator for such a fleet of MMW and higher frequency passive sounders and imagers. PolarCube is a 3U CubeSat based on an existing bus design (CU ALL-STAR) supporting an eight channel, double sideband 118.7503 GHz passive microwave sounder. The mission is focused primarily on sounding in Arctic and Antarctic regions with the following key remote sensing science and engineering objectives: (i) Collect coincident tropospheric temperature profiles above sea ice, open polar ocean, and partially open areas to develop joint sea ice concentration and lower tropospheric temperature mapping capabilities in clear and cloudy atmospheric conditions. This goal will be accomplished in conjunction with data from existing passive microwave sensors operating at complementary bands; and (ii) Assess the capabilities of small passive microwave satellite sensors for environmental monitoring in support of the future development of inexpensive Earth science missions and (possibly) operational satellites supporting the NRC PATH and Aerosol/Cloud/Ecosystem (ACE) goals. The design details and latest status of PolarCube spacecraft, sensor, and mission will be presented. The instrument's performance for temperature profiling in clear air conditions will be demonstrated with data obtained from laboratory roof top measurements, and the PolarCube mission, design, and concept of operations will be discussed.

Paper 5 RACE - THE RADIOMETER ATMOSPHERIC CUBESAT EXPERIMENT
11:30 *Boon Lim, JPL, United States*

The Jet Propulsion Laboratory (JPL) is developing the Radiometer Atmospheric CubeSat Experiment (RACE) - a water vapor radiometer integrated on a 3U (30cm x 10cm x 10cm) CubeSat platform. RACE will measure 2 channels of the 183 GHz water vapor line utilizing 35 nm Indium Phosphide (InP) high electron mobility transistors (HEMT) for the low noise amplifiers (LNA) and a novel amplifier based internal calibration subsystem. The 3U spacecraft will be provided by the University of Texas at Austin's Satellite Design Laboratory. The radiometer utilizes a direct detect topology to reduce power draw. Each amplifier only draws ~12 mW of power (not including conversion losses). The complete payload electronics draws ~1.2 W, with the majority of power utilized for payload command and data handling (C&DH). Internal calibration consists of a coupled amplifier-based noise-source and a Dicke switch to a matched load. During operations on orbit, cold sky and other vicarious scenes will also be utilized for calibration. The integrated system noise figure has been measured to be approximately 10.5 dB, driven primarily by the performance of the Dicke switch. The typical noise figure of the LNAs is < 4.5 dB. Across the expected temperature range, the gain of the system changes by 0.06 dB/K. The LNA noise source adds ~100 K of noise depending on the channel. Characterization tests are ongoing, and results from the system fully integrated with the CubeSat are expected by early 2014. RACE was selected for launch by the NASA CubeSat Launch Initiative (CSLI) in 2012 and is expected to be launched in Q2 2014. RACE will advance the technology readiness level (TRL) of the 183 GHz receiver subsystem from TRL 4 to TRL 6 and a CubeSat 183 GHz radiometer system from TRL 4 to TRL 7.

Thursday, March 27	RFI and Spectrum Management	13:00 - 14:40
Lecture Session		Ramo Auditorium, Bldg 77

Session Co-Chairs: Niels Skou, Technical University of Denmark; Sidharth Misra, NASA - Jet Propulsion Laboratory

Paper 1 SKAR – SIGNAL CHARACTERIZING KA-BAND RADIOMETER
13:00 *Justin Bobak, David Dowgiallo, Yunghsin Chen, Glendon Frick, Douglas Carssow, Naval Research Laboratory, United States*

The corruption of environmental microwave radiometer data by RFI is a growing problem, both from the global proliferation of emitters and the increased availability of inexpensive hardware at higher, previously uncontaminated frequency bands, including now the portion of the spectrum near 18-19 GHz. Detection of contamination in data, with subsequent removal of contaminated data from retrievals is a necessary reactive step. However, if more and more data is lost to contamination, environmental sensors will be less and less useful in measuring geophysical parameters. If, however, contaminating signals can be characterized, and the offending emitters classified, proactive steps can be taken to prevent or mitigate future disruptions. The Remote Sensing Division has developed the Signal Characterizing Ka-band Radiometer (SKaR) to test different methodologies for detecting and parameterizing sources of radio frequency interference (RFI). The Ka-band was chosen to begin with a relatively RFI-free band, and to be able to monitor the encroachment of systems into the radiometric band as a function of the proliferation of emitters. The system is a digitizing radiometer, allowing more access to the details of the contaminating signal. The system and its concept of operations are designed to find the best methods to retrieve parameters of the transmitter (polarization, power, pattern) and signal (carrier frequency, duty cycle, modulation) to improve the chance of identifying the system that is the source of the RFI and to assist in understanding the changing environment so that mitigation strategies can evolve. SKaR is being used to develop and demonstrate the capability to parameterize the RFI in such a way, while simultaneously operating as a microwave radiometer with good radiometric accuracy. NRL's efforts in identifying RFI in radiometer data are briefly discussed as context. The design and operation of SKaR are presented, including radiometric performance metrics. The results of laboratory and field experiments are presented. These experiments involve observations of both uncontaminated and contaminated scenes and demonstrate the capability to detect and parameterize a contaminating signal in a radiometric background. For field experiments, coincident measurements with a powerful spectrum analyzer allow us to present highly quantified ground truth data. Finally, results from a field experiment involving a real world system are presented. The ability to not only detect the presence of corrupting RFI in microwave data, but to determine the parameters of the emitter and signal characteristics, will be key to mitigating the growing impact of RFI, and will, in turn, help to protect the ability to make reliable measurements of environmental parameters. *presenting author; Justin.bobak@nrl.navy.mil

Paper 2 A WIDE-BAND AND FLEXIBLE ON-BOARD RFI MITIGATING DIGITAL BACK-END SYSTEM FOR PASSIVE MICROWAVE RADIOMETERS
13:20 *Sidharth Misra, Keizo Ishikawa, Robert Jarnot, Andre Tkacenko, JPL - CalTech, United States; Suraj Gowda, University of California, Berkeley, United States; Shannon Brown, JPL - CalTech, United States*

Recent passive space-borne microwave observing systems operating below 40GHz have shown an increase in the amount of man-made interference corrupting incoming natural thermal emissions (McKague et al., 2010). Many radiometer systems operate in bands (e.g. 18.7GHz) that are shared with space to ground-transmissions. Other space-borne systems (e.g. Aquarius, Soil Moisture Ocean Salinity – SMOS) operate in protected radio bands to avoid RFI (Radio Frequency Interference) (Misra et al., 2008; Oliva, R et al., 2012). Measurements from these missions have shown that RFI still persists even in protected bands. The RFI environment has forced many radiometer systems to operate in narrower bands than usual. This directly impacts the radiometric noise and instrument design, which in turn impacts the necessary fidelity required for retrieving the EDRs. Based on these issues, there is a need for developing wideband microwave radiometer systems that can co-exist with a harsh RFI environment. The following talk will present the work undertaken by the Jet Propulsion Laboratory, to develop an agile wideband digital backend system that can operate in and adapt to any RFI environment. The digital backend system needs to be capable of implementing a flexible digital signal processing system that can detect and mitigate RFI contaminated spectrum regions. The goal of the digital backend is to incorporate all necessary processing in the backend to take a corrupted spectrum and produce a single RFI mitigated output value with a minimal data rate. The first portion of the talk will focus on the intermediate RFI detection algorithms that were compared and contrasted with each other in terms of algorithm performance and backend implementability. The algorithms are compared with respect to various RFI parameters such as duty-cycle, power, spectral width, number of sources etc. We utilize innovative evaluation techniques and performance metrics to compare the different algorithms. The algorithms are also tested using real airborne data measured during the Soil Moisture Active/Passive Validation Experiment (SMAPVEX) field campaign of 2012. An optimal version of the kurtosis detection algorithm and an innovative "squrtosis" algorithm with crossfrequency is implemented. A brief description of these algorithms will be presented. The final aspect of the talk will focus on the firmware implementation of the above algorithms. The algorithms are implemented on a Reconfigurable Open Architecture Computing Hardware (ROACH) -2, a Xilinx Virtex 6 stand-alone FPGA board. We will present results on the initial implementation as well as initial results based on lab-generated RFI signals. Further work based on the obtained results will also be discussed. References: [1] McKague, D, Puckett, J.J., and Ruf. C.S., "Characterization of K-band radio-frequency interference from AMSR-E, WindSat and SSM/I", 2000 IEEE International Geosci. and Remote Sens. Symposium (IGARSS), Honolulu,HI [2] S. Misra and C. S. Ruf, "Detection of Radio-Frequency Interference for the Aquarius Radiometer," IEEE Trans. Geosci. And Remote Sens.,, vol. 46, pp. 3123-3128, 2008. [3] Oliva, R. ; Daganzo, E. ; Kerr, Y.H. ; Mecklenburg, S. ; Nieto, S. ; Richaume, P. ; Gruhier, C., "SMOS Radio Frequency Interference Scenario: Status and Actions Taken to Improve the RFI Environment in the 1400–1427-MHz Passive Band", IEEE Trans. Geosci. And Remote Sens., vol. 50, no. 5, p.p. 1427-1439, Feb, 2012

Paper 3 **EVALUATING RFI DETECTION ALGORITHMS FOR THE SMAP RADIOMETER**
13:40 *Omar Salama, The Ohio State University, United States; Priscilla Mohammed, Morgan State University, United States; Jeffrey Piepmeier, NASA's Goddard Space Flight Center, United States*

SMAP (Soil Moisture Active Passive) is a mission to be launched by NASA to measure soil moisture of the Earth's land surface. The SMAP radiometer operates in the L-band protected spectrum (1400-1427 MHz) that is known to be vulnerable to radio frequency interference (RFI). Radiometric observations show substantial evidence of out-of-band emissions from neighboring transmitters and possibly illegally operating emitters. SMAP faces large levels of RFI and also significant amounts of low-level RFI equivalent to 0.1 K to 10 K of brightness temperature. Such low-level interference would be enough to jeopardize mission success without an aggressive mitigation solution. A decision has been made to employ an advanced digital microwave radiometer, the first of its kind for spaceflight, for use on SMAP. The mission takes a multi-domain approach to RFI mitigation utilizing an innovative on-board digital detector backend with DSP algorithms to detect and filter out harmful interference. Four different baseline RFI detectors are run on the ground and their outputs combined for a maximum probability of detection to remove RFI within a footprint. The SMAP radiometer outputs the first four raw moments of the receiver system noise voltage in 16 frequency channels for measurement of noise temperature and kurtosis as well as complex cross-correlation products for measuring the third and fourth Stokes parameters. Evaluating each of the four individual RFI detection algorithms is essential to ensure the highest efficiency produced by the maximum probability of detection. Receiver operating characteristic (ROC) curves are generated for each of the different detectors to evaluate performance. ROC curves graph the probability of detection versus false alarm rate. The optimum case would correspond to the highest probability of detection (PD) and lowest false alarm rate (FAR). A given threshold for the RFI algorithms would produce a corresponding (PD, FAR). The rest of the line curve is graphed by varying threshold from a minimal value to a maximal value. The ROC curves are performed on all different RFI algorithm detectors which include time-domain, cross-frequency, kurtosis, and polarization detectors. Each detector operates differently and behaves differently under different injected RFI. Different injected RFI include pulsed and sinusoidal at different frequencies, amplitudes, and power. The focus of the study is to optimize each of the given RFI detectors given any RFI signal. For example, since the cross-frequency algorithm uses only frequency resolution and no time resolution, its performance should be best for RFI that is localized in frequency. Since continuous wave (CW) RFI are localized in frequency by definition, as expected, the cross-frequency detector performed very well against CW RFI relative to other detectors. The RFI detection performance that is ultimately achieved will be a function of the threshold (that returns the highest PD versus lowest FAR), the nature of the RFI encountered, and radiometer system parameters such as the number of frequency channels and the integration period.

Paper 4 **RFI DETECTION AND MITIGATION FOR AMSR-E OCEAN RETRIEVALS**
14:00 *Kyle Hilburn, Chelle Gentemann, Marty Brewer, Lucrezia Ricciardulli, Frank Wentz, Remote Sensing Systems, United States*

Radio frequency interference (RFI) is a rapidly growing source of error for passive microwave measurements. The bandwidths of microwave channels used for Earth-observation are typically much wider than the very limited protected bands allocated for microwave remote sensing. Thus microwave instruments can receive RFI from nearby approved communication frequency bands. The Advanced Microwave Scanning Radiometer on Aqua (AMSR-E) provides measurements used to retrieve several geophysical parameters over the ocean, including: sea surface temperature (SST), surface wind speed, precipitable water vapor, cloud liquid water, and surface rain rate. During the last decade, the number of RFI sources and their spatial coverage has increased dramatically. The primary source of RFI for AMSR-E is television broadcasts from geostationary satellites. Strong signals are broadcast to very specific markets, resulting in large regional errors. The severity of the errors depends not only on RFI characteristics and RFI glint-angle relative to AMSR-E, but it also depends on ocean surface roughness – a highly variable quantity in time. The lower frequency channels (6.9, 10.7 and 18.7 GHz) are most severely affected, and errors have been observed in all the aforementioned geophysical parameters. The geometry is such that RFI from geostationary sources only affects the descending orbit segments of AMSR-E. However, both ascending and descending passes are affected by ground-based RFI, also a growing problem. Simply removing all data affected by RFI is no longer practical. We will present detailed descriptions of both our detection and mitigation algorithms. Detection involves a two part approach. The first part is identification of probable RFI based on its radiometric signature. This uses closure analysis of measured AMSR-E brightness temperatures against a state-of-the-art radiative transfer model. The analysis provides information on the strength and microwave frequency of the potential RFI. The second part is to confirm that the viewing geometry is consistent with RFI. For geostationary RFI, this involves confirming that the reflection of AMSR-E boresight off the ocean surface intersects geostationary altitude at a location consistent with known RFI sources. For ground-based RFI, this involves confirming it fits the location of known RFI activity. Once RFI is detected, we then use a suite of channel-adaptive algorithms to retrieve geophysical parameters without the RFI affected channels. The estimates from different algorithms must be blended appropriately depending on the probability of RFI to avoid introducing artificial seams in the data. The use of channel adaptive algorithm for 10.7 GHz works very well at removing space-borne RFI, especially around Europe. In the absence of RFI, AMSR-E SST retrievals have a standard deviation relative to in situ observations of 0.65°C. When RFI is present, the standard deviations can be 5°C or greater. We will present examples before and after the use of RFI mitigation, and present validation statistics. We will include examples of RFI at 10.7 GHz and its impact on SST near Europe, and examples of RFI at 18.7 GHz and its impact on wind speed around North America. We will estimate the magnitude of spurious trends from RFI and compare against regional climate trends. The RFI-mitigated data highlighted in this presentation will be publicly released as a new Extended AMSR-E dataset.

Paper 5 **THE SCIENCE IMPLICATIONS OF CHOOSING AN OPERATING POINT ON THE ROC CURVE FOR RFI DETECTION**
14:20 *Christopher Ruf, David Chen, University of Michigan, United States*

The RFI detection algorithm used by the Aquarius microwave radiometer operates in the time domain. The finest time resolution of 10ms provides samples significantly more often than that required for Nyquist spatial sampling as determined by the antenna footprint size and spacecraft orbital velocity. This permits short duration radar pulses to be more easily detected. A pulse blanking mitigation algorithm is applied after the detection. The RFI-flagged samples are discarded and the remaining samples within a Nyquist sampling interval are averaged together to produce RFI-filtered antenna temperatures. The detection algorithm includes adjustable parameters that determine where it operates on the Receiver Operating Characteristic (ROC) curve. The operating point determines the false alarm rate of the algorithm – the probability that RFI will be detected when it is not present. This statistic can be readily computed from the ROC operating point because the statistics of RFI-free data samples are generally well known. In principle, the operating point on the ROC curve also determines the probability of missed detection of RFI that is present. However, in practice, this statistic is much more difficult to estimate because the statistics of data samples in the presence of RFI are dependent on properties of the RFI that are generally not well known. For this reason, decisions about where to operate on the ROC curve are most often based on false alarm rate considerations. In the case of Aquarius, false alarms will reduce the number of sub-Nyquist samples that are averaged together to produce the antenna temperature data products at the Nyquist sampling interval. This, in turn, degrades the precision (the NEDT) of the composite antenna temperatures. Since the NEDT of individual antenna temperature samples is not a driving source of error in the Aquarius salinity measurements, it is not the best metric by which to set the operating point on the ROC curve. One driving source of error is the bias in antenna temperature calibration, which is directly related to the probability of missed detection. This, or a related function of it, is a more relevant metric to use to set the operating point on the ROC curve. We propose as a figure-of-merit for setting the ROC operating point the following statistic: the expected value of undetected RFI. This statistic more directly translates into an impact on science performance than does the conventional probability of missed detection. In order to determine the expected value of undetected RFI, an estimate is needed of the likelihood of occurrence of RFI as a function of its amplitude. We present an approach to construction of such an RFI amplitude PDF, then apply it to the problem of setting a suitable ROC curve operating point for the case of Aquarius.

Thursday, March 27	**Snowfall Retrieval Algorithms and Snow Modeling**	15:30 - 17:30
Lecture Session		Ramo Auditorium, Bldg 77

Session Co-Chairs: Frank Marzano, Sapienza University of Rome; V Chandrasekar, Colorado State University

Paper 1 **ADVANCES IN MELTING LAYER SIMULATIONS FOR SATELLITE-BASED PASSIVE MICROWAVE REMOTE SENSING OF SNOWFALL**
15:30 *Benjamin Johnson, University of Maryland Baltimore County Joint Center for Earth Systems Technology and NASA Goddard Space Flight Center, United States; Gail Skofronick-Jackson, William Olson, NASA Goddard Space Flight Center, United States*

Satellite-based passive microwave remote sensing of atmospheric ice-phase precipitation presents a unique set of challenges. Snow exhibits a wide variety of spatial and temporal variations, at both the cloud scale and at the microphysical scale. Individual snowflakes exhibit a wide-variety of shapes and sizes, even if normalized by the water content. This is in contrast to rainfall, where there is relatively little variation of shapes or sizes for a given liquid water content, lending itself to a more direct relationship between observed TBs Even if one has accurate models of snowflake sizes and shapes, the problem of transitioning from snow to rainfall through the melting layer has been largely oversimplified, despite being radiometrically significant. In this research, we describe our approach to characterizing the microphysical description of snowfall, and in particular, we focus on recent advances in modeling the melting-layer for use in passive microwave remote sensing applications. A heuristic melting model is applied to a wide variety of snowflake sizes and shapes. The scattering and extinction properties of these randomly-oriented melting flakes (ranging from pristine crystals to complex aggregates) have been computed using the discrete dipole approximation. These properties are then integrated over a specified size distribution to obtain an ensemble-averaged set of scattering and extinction properties, and populate a thermodynamically driven melting-layer model, similar to that of Mitra et al. (1990). Finally, a forward radiative transfer model, with full polarization, is used to compute the top-of-the atmosphere brightness temperatures for a few selected cases. We examine, on a normalized basis, the brightness temperature sensitivity to physical variations in the melting layer properties, and describe how this impacts precipitation retrievals. One key finding is that the physical distribution of melt-water on a snowflake, all else being equal, has a strong impact on its radiometric properties, and consequently, on simulated top-of-the-atmosphere brightness temperatures. This result in general agreement with previous studies that have used ersatz spherical snowflakes in their simulations, and with remote sensing observations of melting precipitation using ground-based observations. This sensitivity, consequently has an important influence on physically-based retrievals of precipitation when melting is present. These findings and other results of our research will be incorporated into passive-microwave precipitation retrieval algorithms under development for the Global Precipitation Measurement mission (GPM: http://pmm.nasa.gov/).

Paper 2 MULTI-PLATFORM RETRIEVAL OF VOLCANIC ASH CLOUD: SYNERGY OF MICROWAVE RADIOMETERS WITH GROUND RADARS.

15:50 *Frank Silvio Marzano, Mario Montopoli, Sapienza University of Rome, Italy; Domenico Cimini, IMAA CNR, Italy; Luigi Mereu, Sapienza University of Rome, Italy; Errico Picciotti, Center of Excellence CETEMPS, Italy*

Volcanic ash clouds are now widely recognized as a significant hazard to aviation and to population. As a result, there is a considerable effort being expended by scientists to mitigate this hazard. This effort involves remote sensing of volcanic clouds by many ground-based and satellite sensors. One of the main challenges is to provide near real time quantitative estimates of ash properties close to volcano vent in order to better constrain the ash dispersion models and then to improve the ash forecasts. Ground-based radars systems have been shown to be useful during and for up to few hours following volcanic eruptions. However, most volcanoes are very often out of range of modern radar systems which are deployed near cities. Satellite-based ultraviolet sensors are used to study volcanic gas clouds and infrared sensors are used to track and characterize volcanic ash clouds in the atmosphere for up to several days after an eruption. However, near the volcanic vent, many volcanic ash clouds are opaque in the infrared region and appear similar to meteorological clouds. As a result, visible-infrared sensors aboard low-Earth-orbit (LEO) and geosynchronous Earth orbit (GEO) satellites, migth be of limited use in determining the particle size distribution and mass of these opaque volcanic ash clouds. Thus, there is an increasing interest in developing multi-platforms and multi-sensors approaches which allow to overcame the limitations in the use of single sensors. In this work the potential of satellite passive microwave sensors to provide quantitative information about near-source volcanic ash cloud parameters is assessed using reference information from the ground-based microwave weather radar. Radar and radiometer information are used together with forward-model simulations. The latter are based on 2-D simulations with the numerical plume model Active Tracer High-Resolution Atmospheric Model (ATHAM), in conjunction with the radiative transfer model Satellite Data Simulator Unit (SDSU) that is based on the delta- Eddington approximation and includes Mie scattering. The study area is the Icelandic subglacial volcanic region. The analyzed case study is that of the Grímsvötn eruption in May 2011. Consistency between ATHAM/SDSU forward-model simulations and Special Sensor Microwave Imager/Sounder (SSMIS) observations are found in terms of ash brightness temperature versus ash cloud columnar contents. The correlation coefficients of the comparisons between observations are encouraging and they are found to vary from −0.37 to −0.63 for SSMIS channels from 91 to 183 ± 1 GHz, respectively.

Paper 3 SNOWFALL RATE RETRIEVAL USING NPP ATMS PASSIVE MICROWAVE MEASUREMENTS

16:10 *Huan Meng, National Oceanic and Atmospheric Administration, United States; Cezar Kongoli, Nai-Yu Wang, Jun Dong, University of Maryland, United States; Ralph Ferraro, Banghua Yan, Limin Zhao, National Oceanic and Atmospheric Administration, United States*

Satellite snowfall rate retrieval is an emerging topic in satellite remote sensing. Passive microwave measurements at certain high frequencies are sensitive to the scattering effect of snow particles and can be utilized to retrieve snowfall properties. Some of the microwave sensors with snowfall sensitive channels are Advanced Microwave Sounding Unit (AMSU), Microwave Humidity Sounder (MHS) and Advance Technology Microwave Sounder (ATMS). ATMS is the follow-on sensor to AMSU and MHS. Currently, an AMSU and MHS based land snowfall rate (SFR) product is running operationally at NOAA/NESDIS. Based on the AMSU/MHS SFR, an ATMS SFR algorithm has been developed recently. The algorithm performs retrieval in three steps: snowfall detection, retrieval of cloud properties, and estimation of snow particle terminal velocity and snowfall rate. The snowfall detection component utilizes a logistic regression model and a combination of temperature and water vapor sounding channels to detect the scattering signal from falling snow and derive the probability of snowfall (Kongoli et al., 2013). In addition, a set of NWP model based filters is also employed to improve the accuracy of snowfall detection. Cloud properties are retrieved using an inversion method with an iteration algorithm and a two-stream Radiative Transfer Model (Yan et al., 2008). A method developed by Heymsfield and Westbrook (2010) is adopted to calculate snow particle terminal velocity. Finally, snowfall rate is computed by numerically solving a complex integral. This algorithm has been validated against radar and gauge snowfall products. The validation results have shown the robustness of the algorithm for various snowfall events.

Paper 4 RADAR-RADIOMETER SYNERGISTIC INFERENCE OF PREVAILING SNOWFLAKE GROWTH MECHANISMS

16:30 *Dmitri Moisseev, University of Helsinki, Finland; Chandrasekar V Chandra, Coloardo State University, United States; Susanna Lautaportti, University of Helsinki, United States; Pablo Saavedra, University of Bonn, Germany*

Weather radar-based quantitative precipitation estimation in snowfall is a challenging problem. Dual polarizations radar observations have been able to provide indirect evidence of snow growth mechanisms. Dual-polarization radar observations of snow depend on size, orientation and density of the snow particles. For example Bechini et al (2013, Bechini, R., L. Baldini, V. Chandrasekar, 2013: Polarimetric Radar Observations in the Ice Region of Precipitating Clouds at C-Band and X-Band Radar Frequencies. J. Appl. Meteor. Climatol., 52, 1147–1169), showed that specific differential phase signatures in stratiform precipitation can be used to speculate the growth mechanism of dendritic crystals. Variability in these physical properties is one of the major uncertainty sources in quantitative snowfall estimation with radar. Microwave radiometer retrievals, on the other hand, depend on a priori knowledge of precipitation profile, for example presence and location of super cooled water. Liquid water is one of major factors determining prevailing snowflake growth processes, i.e. vapor deposition, riming and aggregation. Snow growth processes, on the other hand, are determining physical properties of ice particles. The goal of this study is two fold. Firstly, we are using microwave radiometer observations of liquid water path to help identify radar observations that correspond to different snow growth processes. Secondly, we are using radar observation to identify layers where liquid water is potentially present. For this study data collected during the Light Precipitation Validation Experiment (LPVEX), which took place in Helsinki in the fall of 2010 and winter 2011, is used. During the experiment a large number of winter storms were sampled by dual-polarization weather radars, scanning microwave radiometer (ADMIRARI), and surface sensors. The LPVEX data is used to show the synergistic inference of snow growth mechanisms.

Paper 5 PRE-LAUNCH PERFORMANCE EVALUATIONS OF FALLING SNOW USING THE GLOBAL PRECIPITATION MEASUREMENT (GPM) RADIOMETER RETRIEVAL ALGORITHM

16:50 *Gail Skofronick-Jackson, Stephen J. Munchak, Benjamin Johnson, NASA Goddard Space Flight Center, United States*

Retrievals of falling snow from space represent an important data set for understanding the Earth's atmospheric, hydrological, and energy cycles. Estimates of falling snow must be captured to obtain the true global precipitation water cycle, snowfall accumulations are required for hydrological studies, and without knowledge of the frozen particles in clouds one cannot adequately understand the energy and radiation budgets. While satellite-based remote sensing provides global coverage of falling snow events, the science is relatively new and retrievals are still undergoing development with challenges remaining. This work reports on the development and pre-launch testing of retrieval algorithms for the Global Precipitation Measurement (GPM) mission Core Observatory satellite, to be launched in early 2014. (most likely just prior to the MicroRad meeting). In particular, we will report on GPM Microwave Imager (GMI) radiometer instrument algorithm performance with respect to falling snow detection and estimation. Estimates of falling snow from ground and space based sensors have been difficult due to the physical characteristics of snowflakes including their complex shapes, sizes, fall patterns, melting fractions, and densities; and their radiative characteristics including weak falling snow signatures with respect to background (surface, water vapor) signatures for passive sensors over land surfaces. While these challenges remain, knowledge of their impact on expected retrieval results is an important key for understanding falling snow retrieval estimations. Our earlier work in this field has shown, through both theoretical and observational studies, that falling snow rates of approximately 0.5 mm/hr (melted) can be detected from GMI (Skofronick-Jackson, et al., 2013, Munchak and Skofronick-Jackson, 2013). Using the 0.5 mm/hr threshold of detection rate, this work provides evaluations of and enhancements to the pre-launch falling snow detection and estimation algorithm components for the GMI radiometer instrument. Throughout 2013, the at-launch GMI precipitation algorithms, based on a Bayesian framework, have been revised and delivered to the GPM data processing center. The Bayesian framework for GMI retrievals is rather dependent on the a priori database used in the algorithm and how profiles are selected from that database. Our work has shown that knowing if the land surface is snow-covered, or not, can improve the performance of the algorithm. Recently, improvements were made to the algorithm that allow for daily inputs of ancillary snow cover values. We evaluate the final algorithm, a priori database, and subsetting of that database using NMQ data sets as the truth.

Paper 6 RECENT ADVANCES IN THE EVALUATION OF WATER PERMITTIVITY MODELS IN SUPERCOOLED CLOUDS.

17:10 *Maria Cadeddu, Argonne National Laboratory, United States; Stefan Kneifel, Stephanie Redl, Emiliano Orlandi, Ulrich Löhnert, University of Cologne, United States; David D. Turner, National Atmospheric Oceanic Administration, United States; Ming-Tang Chen, Academia Sinica Institute of Astronomy and Astrophysics,, Taiwan*

Accurate quantification of remotely-sensed supercooled water in clouds and snow from satellite and ground-based data is limited by the uncertain knowledge of the dielectric properties of supercooled water in the microwave and millimeter-wave spectral region. We present a review of recent (2010-2013) advances in the evaluation of models of the dielectric properties of supercooled water at microwave and millimeter-wave frequencies. Some initial results for the frequencies of 90 and 150 GHz were presented at Microrad 2010, and a full analysis was published in 2011 (Cadeddu and Turner, 2011). The study used data from multiple ground-based remote sensors located in Oklahoma and Alaska and showed that in the 23-180-GHz frequency range, the Stogryn, 1995 model provided the best fit to the observations at frequencies at and above 90 GHz. In a more recent study Kneifel et al., 2013 (submitted) added a recently published model by Ellison (2007), and used multiple datasets collected by instruments located in Germany, and Greenland. This second study showed that the Stogryn and Ellison 2007 models provide the best fit to the observations at higher frequencies, with slightly better results provided by the Ellison model at frequencies larger than 90 GHz. Although the studies use different methodologies and independent datasets they provide a consistent picture of the behavior of dielectric models at low temperatures. They both point out to the inadequacy of the Liebe 91 model, a model still widely used in the remote sensing community, and show that the use of this model at higher frequencies can lead to a substantial underestimation of liquid water path at temperatures below –20o C. In the low-frequency range 23-30 GHz the results are consistent with a previous study by Mätzler et al., (2010). We describe the details of the two methodologies and of the datasets, discuss the results and provide recommendations for a suitable dielectric model.

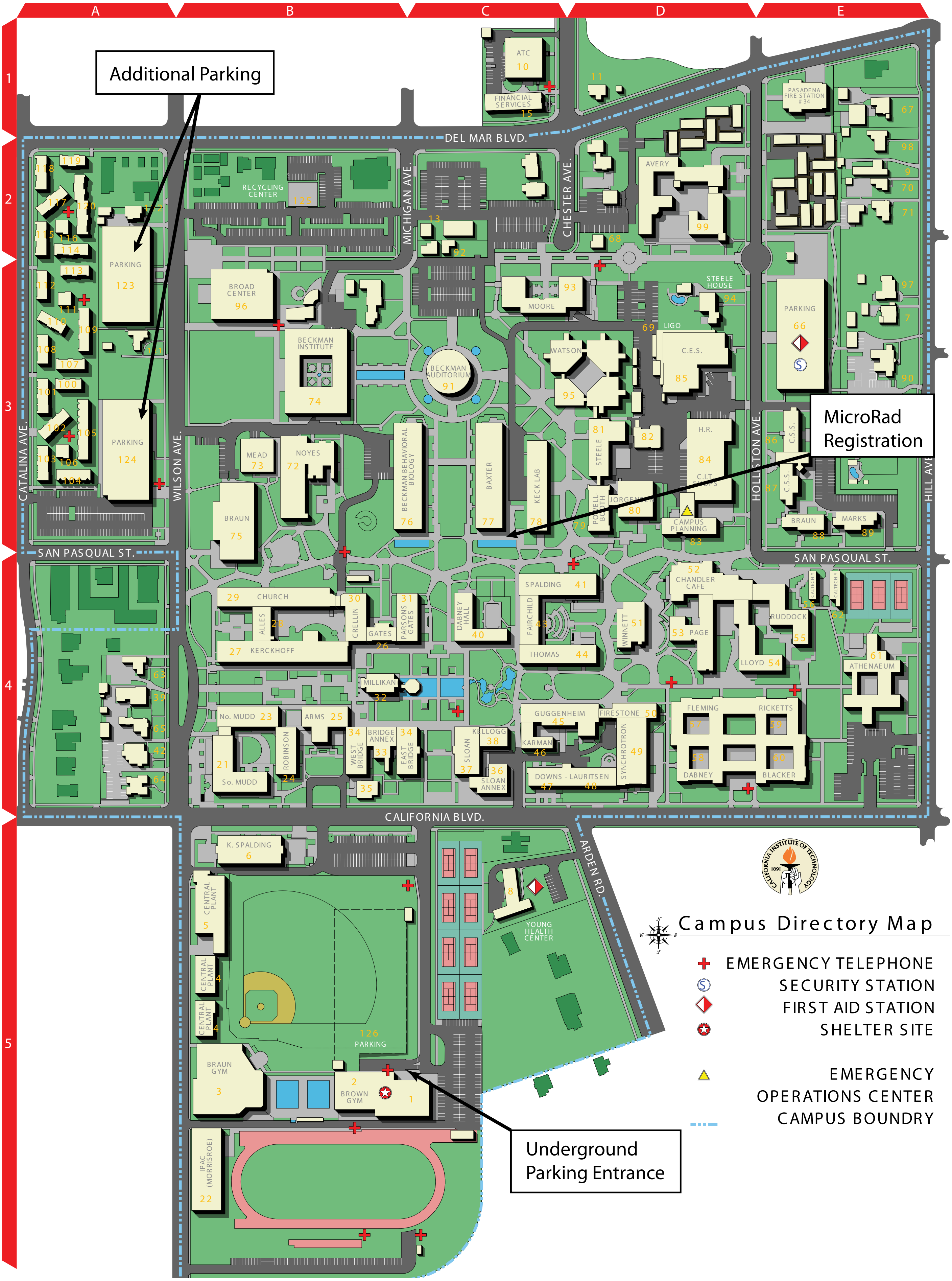
Additional Parking
MicroRad Registration
Underground Parking Entrance
Campus Directory Map
EMERGENCY TELEPHONE
SECURITY STATION
FIRST AID STATION
SHELTER SITE
EMERGENCY OPERATIONS CENTER
CAMPUS BOUNDRY
A
B
C
D
E
1
2
3
4
5
DEL MAR BLVD.
CALIFORNIA BLVD.
SAN PASQUAL ST.
CATALINA AVE.
WILSON AVE.
MICHIGAN AVE.
CHESTER AVE.
HOLLISTON AVE.
HILL AVE.
ARDEN RD.
PARKING 123
PARKING 124
PARKING 66
126 PARKING
RECYCLING CENTER
BROAD CENTER 96
BECKMAN INSTITUTE 74
BECKMAN AUDITORIUM 91
MOORE 93
STEELE HOUSE 94
LIGO
WATSON 95
C.E.S. 85
AVERY
ATC 10
FINANCIAL SERVICES 15
PASADENA FIRE STATION # 34
MEAD 73
NOYES 72
BRAUN 75
BECKMAN BEHAVIORAL BIOLOGY 76
BAXTER 77
KECK LAB 78
STEELE 81
H.R. 84
C.I.T. 82
JORGENSEN 80
POWELL-BOOTH 79
CAMPUS PLANNING 83
C.S.S. 86
C.S.S. 87
BRAUN 88
MARKS 89
CHURCH 29
ALLES 28
CRELLIN 30
PARSONS GATES 31
GATES 26
KERCHKOFF 27
DABNEY HALL 40
SPALDING 41
FAIRCHILD 43
THOMAS 44
WINNETT 51
CHANDLER CAFE 52
PAGE 53
RUDDOCK
LLOYD 54
ATHENAEUM 61
MILLIKAN 32
No. MUDD 23
ARMS 25
BRIDGE ANNEX 33
WEST BRIDGE 34
EAST BRIDGE 34
ROBINSON 24
So. MUDD 21
35
KELLOGG 38
SLOAN 37
SLOAN ANNEX 36
GUGGENHEIM 45
KARMAN 46
FIRESTONE 50
SYNCHROTRON 49
DOWNS - LAURITSEN 47 48
FLEMING 57
RICKETTS 59
DABNEY 58
BLACKER 60
K. SPALDING 6
CENTRAL PLANT 5
CENTRAL PLANT 4
BRAUN GYM 3
BROWN GYM 2
YOUNG HEALTH CENTER 8
IPAC (MORRISROE) 22

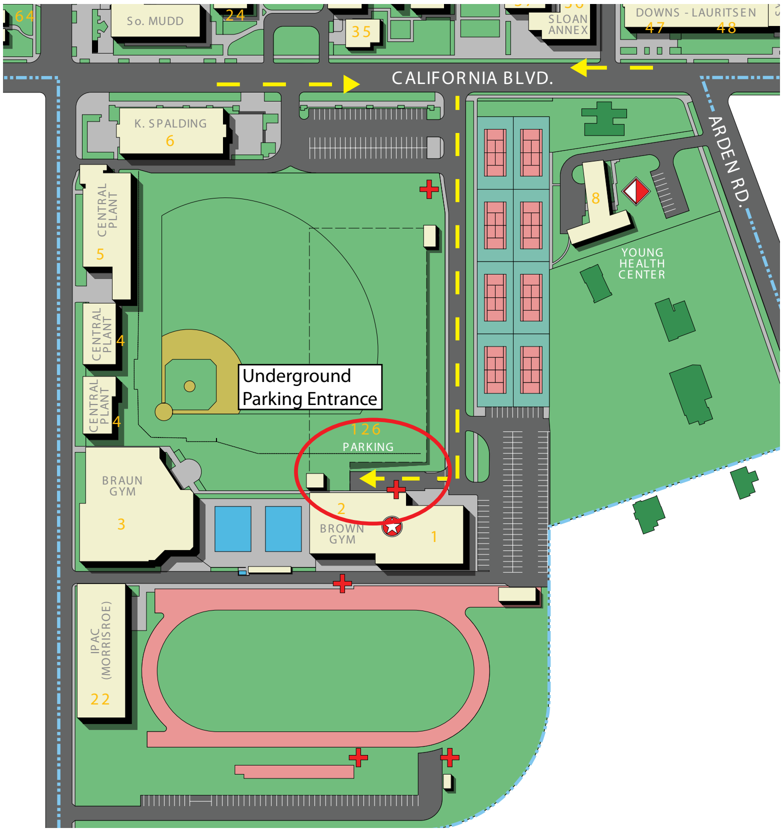
So. MUDD
SLOAN ANNEX
DOWNS - LAURITSEN
CALIFORNIA BLVD.
K. SPALDING
6
ARDEN RD.
CENTRAL PLANT
5
8
YOUNG HEALTH CENTER
CENTRAL PLANT
4
CENTRAL PLANT
4
Underground Parking Entrance
126 PARKING
BRAUN GYM
3
2
BROWN GYM
1
IPAC (MORRISROE)
22


BECKMAN AUDITORIUM
91
WATSON
95
C.E.S.
85
90
81
82
STEELE
H.R.
84
C.I.T. SHOPS
HOLLISTON AVE.
86
C.S.S.
87
C.S.S.
HILL AVE.
BECKMAN BEHAVIORAL BIOLOGY
76
BAXTER
77
KECK LAB
78
79
POWELL-BOOTH
JORGENSEN
80
CAMPUS PLANNING
83
BRAUN
88
MARKS
89
SAN PASQUAL ST.
Oral Session
Lunch/Coffee
SPALDING 41
52
CHANDLER CAFE
CALTECH Y
56
CALTECH Y
62
31
PARSONS GATES
GATES
26
DABNEY HALL
40
FAIRCHILD
43
WINNETT 51
53 PAGE
RUDDOCK
55
61
ATHENAEUM
Poster Session
THOMAS 44
LLOYD 54
MILLIKAN
32
GUGGENHEIM
45
FIRESTONE 50
FLEMING
57
RICKETTS
59
BRIDGE ANNEX
34
33
KELLOGG
38
KARMAN
46
SYNCHROTRON
49
58
60
Banquet
SLOAN
37
36
SLOAN ANNEX
DOWNS - LAURITSEN
47
48
DABNEY
BLACKER
Parking
35
CALIFORNIA BLVD.